MICROTOPOGRAPHICAL STUDIES
ON
NATURAL AND SYNTHETIC QUARTZ CRYSTALS

THESIS PRESENTED FOR THE DEGREE OF
DOCTOR OF PHILOSOPHY
IN THE
UNIVERSITY OF LONDON
BY

MANUBHAI SURYARAM JOSHI

NOVEMBER, 1959.

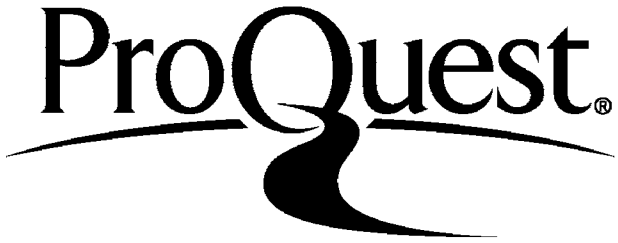

To facilitate the comparison of
the figures with the text, this thesis
has been bound in two separate volumes.
Volume I contains the text, and Volume II
the figures.

A B S T R A C T

Phase contrast and multiple-beam interferometric techniques have been applied to the study of surface structures of natural and synthetic quartz crystals. A summary is given in a tabular form of the observations of growth by spiral mechanism recorded during the years 1949 - 1959. An improved thin-film collodion technique has been worked out and applied to the study of extremely irregular crystal surfaces. The merits of this technique are assessed, and it is shown that with the help of this technique step heights less than 10 Å. can be detected and measured.

Spiral patterns on the basal planes and rhombohedral faces, and the vertical striations on the prism faces of synthetic quartz crystals are illustrated and described.

A mechanism of growth of synthetic quartz crystals is proposed, and it is shown that all the results obtained support this proposed mechanism. The curved nature of the profile of spirals on the basal planes, recorded for the first time, is established with the help of the improved thin-film collodion technique. The mechanism of the formation of such a profile is described. Very strange tadpole-shaped features observed on synthetic quartz are described and interpreted.

Properties of the growth pyramids on the faces of natural quartz crystals and the information available therefrom about gradients and the direction of flow of mother liquid are given. Also described are associated growth of other crystals, replacement of other minerals by quartz, natural etch figures, surface structures of red quartz etc.

The first clear evidence of the growth of natural quartz crystals by spiral mechanism is given. A new approach to the twinning problem is described and Sunagawa's newly proposed mechanism of 'twin formation by a kind of fault' is established for quartz.

The surface structures of trigonal bipyramidal faces are briefly dealt with and a study made of the surfaces of four samples of fused quartz. Finally the effects of a crack produced by an explosion, at a pressure of 24,000 atmospheres, inside a diamond bomb are examined.

C O N T E N T S

PART I

THEORIES OF GROWTH

PART I

THEORIES OF GROWTH

C H A P T E R I

Theories of Growth of Perfect Crystals

An account of theories of growth of crystals is given in two chapters. This chapter deals with the growth of perfect crystals and the next one with the growth of imperfect crystals. In general the theories of crystal growth can be divided into two main groups, one of which stresses the importance of the environment which surrounds the crystal during its growth, and also the arrival of the material at the growing face, while the other lays importance on the structure of the crystal itself.

In general there are three ways in which crystals are formed. Crystallization of most substances takes place when they are allowed to solidify (a) from solutions, or (b) from liquid melts, or (c) from a state of vapour. Crystals may also be formed in any one of these three ways when a substance originates from the combination or decomposition of other substances.

The early theories were not based on the atomic models, and hence growth by layer deposition was not thought of. According to Bentivoglio (1927) the form of a crystal is influenced by three main factors: (i) its internal structure, (ii) the nature of the solvent and (iii) a variety of external factors not easily subjected to exact study, such as the crystals proximity to the walls of the vessel or to other crystals and the effects of diffusion or concentration gradients.

The first quantitative theory for the study of crystal growth was given by Gibbs (1878) on thermodynamical grounds. In 1885 Curie gave the theory of growth which takes into account the effect of surface energy on the growth of a crystal. Wulfe (1901) and others followed it. The work of Noyes and Whitney (1897) was concerned with the part played by diffusion in crystal

growth. As regards the growth of the ideal perfect crystals, the main contribution has come from Volmer (1922, 1939), Kossel (1927, 1928), Stranski and his co-workers (1928, 1949), Becker (1949), Becker and Döring (1935) and Frankel (1945, 1946). On the other hand, Burton, Cabrera and Frank (1949, 1951) are the pioneers in introducing the concept of dislocations in crystals to explain the growth of imperfect crystals. A discussion of the various aspects of theories of crystal growth is given in a series of papers in the Disc. Faraday Soc., 5 (1949). A review of the historical development of theories of crystal growth has been given by Wells (1946) and Buckley (1951).

Only a brief account of theories of growth of perfect crystals will be given. Emphasis will be laid on those parts of these theories which have a bearing on the later theory of imperfect crystals in which dislocations play such an important role, as it is this theory which concerns some of the experimental observations to be presented in this present work.

The idea that the growth of crystals is a discontinuous process was suggested by Gibbs (loc. cit.) as early as 1878. It was only in 1922 that Volmer (loc. cit.) for the first time enunciated the idea that growth takes place by the spreading of layers. This concept of layer spreading was further amplified by Brandes in 1927.

Experiments by Cockroft (1928) and Volmer and Eastermann (1921) indicated that the flow of molecules over the crystal surface plays an important role in the rate of crystallization. These experiments indicated that appreciable surface migration of the adsorbed molecules takes place before they return to the vapour phase or get incorporated in the lattice, and hence the growth of a molecular layer will take place primarily by the

diffusion of adsorbed molecules towards the edge. According to Mott (1950) the direct current of molecules to the edge from the vapour is relatively unimportant. The fact that atoms undergo activated diffusion along the surface has been clearly demonstrated by the experiments of Becker (1929) on barium and other metals coated on a tungsten filament. The same is also illustrated by experiments of Volmer and Adhikari (1926) on surface flow of benzophenone on glass, and Kowarski (1935) on p-toluidine obtained from vapour.

Kossel (loc. cit.) was the first to give the theory of crystal growth which makes use of an exact atomic model. Similar to Kossel's theory is the Stranski's theory (loc. cit.) which was published in 1928, but according to Desch (1934, p.37) it was originally published in the Bulgarian language in 1927, independently of Kossel. The assumption underlying the theory of growth of perfect crystals was that the crystal builds itself up by the continuous deposition of the atoms at the kinks in the steps on the surface. Thus once a layer or a step has been started, it will spread rapidly and get completed by this process. Hence the rate of crystal growth will depend on the chance of an atom finding a site on a completed flat surface, rather than upon the rate at which subsequent atoms are adsorbed at the layer which is thus started.

The growth from solution, of simple ionic and homopolar crystals has been considered by Kossel (loc. cit.). According to his calculations of the yield of energy of an ion or an atom on getting attached to various positions on a face of a crystal, the greater the yield of energy on attachment, the greater is the stability of the ion or atom. An atom on a corner of a face, or on an edge some distance from a corner or on a completed

lattice plane away from corner or edge, will have only one nearest neighbour. Such cases and also the cases in which an atom has two or three nearest neighbours were considered by Kossel. From his considerations of the energies of attachment of single atoms at different sites on a completed layer, Kossel showed that in the case of homopolar crystals the chance of the site of the first atom to a completed lattice plane being at a corner is least, but is greater at the edge, and is greatest at any other point on a face. On the other hand, in the case of ionic crystals, Kossel showed that the chance of starting a new layer is highest at a corner, smaller at an edge and least at a point on a face remote from edges and corners. Kossel's belief was that a single atom could constitute a layer nucleus. Brandes and Volmer (1931) arrived at similar results. They calculated the preference for starting a new layer on the (100) face of rock salt, by finding the specific edge-energy the work released when the two-dimensional seed is formed, stable enough to survive at very slight supersaturation. In 1945 it was pointed out by Frankel (loc. cit.) that vicinal faces with very high indices ought not to be regarded as planes of high specific free energy. According to him vicinal faces consist of steps, the flat portions of which are planes having low indices. Thermal fluctuations will give rise to a series of vicinal faces. It is considered that the growth of a crystal face is a result of the random deposition on it of particles. Some of these particles get attached to the vertical steps bounding the atomic terraces, and move along until they get firmly attached at kinks, because it is the kinks where the growth actually begins. With the progress of growth the face becomes a low index plane, and when the crystal is bounded by such planes, it is difficult for it to grow. Thereafter the initiation of a new layer may take place according to Kossel - Stranski model.

Stranski (loc. cit.) considering the growth of ionic crystals from their vapour, suggested that until a certain critical size is reached a layer nucleus is unstable. Thus in this respect, Stranski's suggestion differs from Kossel's given above. As regards the growth of ionic crystals, Stranski's conclusion was the same as that of Kossel.

From the ideas stated above it is clear that for a perfect crystal to grow bounded by its principal faces, a nucleus is required to be formed on its surface. Such a nucleus will have a critical size, for a given degree of supersaturation. If the nucleus is smaller than this size it will evaporate. Burton and Cabrera (1949) have shown that below a certain critical supersaturation, the probability for the formation of such a two-dimensional nucleus is negligible. Above the critical size deposition will take place more rapidly than evaporation, so that the two-dimensional nucleus will grow, spreading the unimolecular layer across the crystal face. The nucleation rate is shown to be a very sensitive function of supersaturation. The temperature and the degree of supersaturation are the two factors on which the critical size of the nucleus depends, the critical size decreasing as the temperature and the supersaturation increase.

In the case of perfect crystals kinks are essential for growth. Such kinks can only be produced under high supersaturation conditions. Thermodynamical fluctuations at low supersaturations will not be able to produce such kinks.

For homopolar crystals a simple theory of growth has been given by Buerger (1947). It takes into account the views put forward by Bravais (1866) and Kossel (1927). According to Kossel growth takes place by the deposition and spreading of layers. Buerger suggested that once a layer is initiated it will spread with the same speed on any face. The ease with which

the new layers are formed on different forms accounts for the difference in the growth velocities. All the theories of growth of perfect crystals assumed that the crystal is ideal, and that it has geometrically perfect lattice planes.

Studying the rate of growth of iodine crystals in slightly supersaturated vapour at 0°c., Volmer and Schultze (1931) found that the rate of growth was proportional to the supersaturation down to 1%. From the above work, for this supersaturation, no growth should occur at all, which is in contradiction with the experimental observation of Volmer and Schultze. In general there are crystals which grow at rates proportional to supersaturation down to a supersaturation much lower than the theoretical critical supersaturation required by the surface nucleation theory.

It is found from the mechanical properties of solids that no crystal has the theoretical strength of the perfect crystal, but this is not surprising as it has been proved by X-ray diffraction experiments that most real crystals are imperfect. The concept of dislocation is the result of the study of mechanical behaviour of crystalline solids. Taylor (1934), Orowan (1934), and Polanyi (1934) were the first to use this concept of dislocation to explain deformation of crystals.

The first experimental evidence of growth by deposition and spreading of layers on crystal faces was reported by A. Marcelin (1918). He observed the spreading of growth layers in the case of p-toluidine from alcoholic solutions. The plates were thin enough to exhibit Newton's colours in reflection, and thereby the simultaneous observation of growth in depth and surface area was made possible. He found that as growth proceeds, coloured bands having definite geometrical boundaries spread on the surface at regular speeds. At any time during growth there will be a

series of regularly spaced bands of different colours with parallel edges. The colour of each band was found to remain constant as it spreads along the face, the difference in the tint of different colours being attributed to different thicknesses of the layers. In one case he was able to observe a layer only three molecules thick. From his observations, he concluded that growth takes place by deposition and spreading of layers, whose thickness approaches molecular dimensions.

Kowarski (loc. cit.) carried out similar experiments on the same substance, and found that layers were in general initiated at the edge of the face, and in particular at the point of intersection of the edge with a neighbouring crystal. The layers were found to be circular near the centre of initiation but became more and more irregular as they proceeded across the face. The rate of advance of thinner layers was greater than that of the thicker ones, and so the former usually overtake the latter whose thickness thus increases further. The same conclusion was arrived at by Volmer (1922), and Bunn and Emmett (1949). Bunn and Emmett ascribed this to an increase of energy with decrease of step height. According to Frank (1949) the initial bunching of unimolecular layers is due to fluctuations in concentration at the initiation point. He gives other reasons for further thickening of growth layers. The bunching of closed loops of unimolecular layers initiated by pairs of screw dislocations could also possibly be due to one or more of these factors. Factors affecting the visibility of growth layers in the case of beryl have been studied closely by Griffin (1951).

Marcelin and Boudin (1930) observed growth layers on several organic crystals including napthalene. Thin layers were observed by Volmer (loc. cit.) on lead iodide crystals. He also succeeded in observing growth layers on cadmium iodide crystals deposited electrolytically and on crystals of mercury grown from

the vapour. By means of their crossed-fringe multiple-beam technique Tolansky and Wilcock (1946) were able to produce evidence for growth by layer deposition in the case of diamond. Tolansky (1946) demonstrated that equilateral triangular shaped pits found on some diamond crystals are probably formed by the intersection of growth sheets advancing across the surface of the crystal in three directions inclined at 60° to each other. Multi-molecular layers in the case of Urotropine, grown at temperatur-es above 170°c., have been observed by Stranski (1949).

Bunn and Emmett (1949) have carried out an extensive study of growth by layer deposition and spreading in the case of many different crystalline substances, both ionic and non-polar. They placed a drop of warm saturated solution on a warm microscope slide, covering it with a thin cover-slip, and this was observed under the microscope while the solution was cooling. The minimum height of the edges of the growth sheets obtained by this method was of the order of 1000 Å. In the case of sodium chloride the thickness of layers was 300 - 700 unit cells, and in the case of cadmium iodide the thickness was 3000 to 5000 Å.. They also observed multimolecular growth layers on potassium dihydrogen phosphate, lead nitrate, sodium nitrate in the presence of lead nitrate, potassium sulphate, potassium chromate, alum, ferrous ammonium sulphate, mercuric chloride, magnesium nitrate, sodium formate, sodium diethyldithiocarbonate, sodium phosphate, urea, acetamide and pyrocatecol, the last six substances being grown from aqueous solutions. On the other hand, no layers were observed by them on some inorganic compounds, nor on some twenty or more organic compounds grown from aqueous, alcoholic or benzene solutions. The main conclusions of their experiments were:

(1) The centres of initiation of growth layers are in general at points on face away from corners and edges, rather than at corners or edges.

(2) As the layers proceed away from the growth centre they become thicker and thicker.

(3) If the rate of growth is rapid, the growth fronts are more irregular, but as the rate of growth becomes slow they become more and more regular conforming the symmetry of the face.

(4) Growth sheets are visible only in the case of ionic crystals.

The first conclusion mentioned above is not in agreement with Kossel's theory of crystal growth. Bunn found that in the case of growth of crystals of sodium chlorate, the concentration of the solution around the crystal was higher at the corners than at the face centres but that the diffusion process delivered more solute at the face centres than at the corners. According to him diffusion flow can initiate growth layers and thus the initiation at face centres was accounted for. The spreading of layers on many crystals, during growth, is shown clearly in some very remarkable films produced by Emmett.

According to Bunn and Emmett (loc. cit.) a high index surface is constituted by a series of uniformly spaced molecular layers. If the layers get split up into several groups, each group forming a thick layer, the new layers will in general be of low index, and there will be a decrease in surface energy per unit height of layer.

According to Kaischew and Stranski (1935), and Becker and Döring (1935) the general tendency of the bounding faces is to be faces of low indices. High index faces are less stable as surfaces, and presumably their surface energy is higher than that of low-index faces. High-index faces created by spreading layers will tend to split up into comparatively large steps so that the bounding surfaces will have low indices. In most cases the edges

of the steps are regarded as surfaces having high indices; the direct evidence for this view being derived by them from their observations on sodium chloride.

Bunn and others firmly believe that growth of real crystals can be satisfactorily explained on the basis of two-dimensional nucleation theory, according to which only one layer will be seen spreading on a face at any one time. A layer will spread over the face before the next one is initiated. On the other hand, according to the experiments by Marcelin, Kowarski and Bunn, at any time during growth a large number of growth layers can be seen spreading across the crystal surface. Their experiments give the interpretation of vicinal faces as a succession of uniformly spaced edges of growth layers.

Berg (1938) and Humphreys Owen (1949) also found that in the case of growth of sodium chlorate from solution the supersaturation of the solution in contact with the crystal is highest at the face centres. Small amounts of impurities adsorbed at the face centres may perhaps possibly be taken as the cause of initiation of layers at face centres, but it is unreasonable to suppose that impurity would not be adsorbed at the corners and edges of the crystal face.

Bunn and Emmett (loc. cit.) studied the effect of addition of soluble impurities to the solution on the thickness of growth layers, and found that in some cases the thickness remains the same while in others it either increases or decreases. In some cases the shape and habit of growth layers were affected by impurities but in most cases they were not.

On theoretical grounds, it has been accepted that growth takes place by spreading of unimolecular layers. Two-dimensional nucleation theories and also the screw dislocation theory of Frank (1949) suggest the same mode of crystal growth. With the

exception of Marcelin (loc. cit.) and Volmer (loc. cit.), other workers could observe multimolecular layers only. Bunn and Emmett (loc. cit.) from their experimental observations of multimolecular layers on a large number of substances, during growth, concluded that this mode of growth is quite common or perhaps even normal. Seager's observations (1952) on crystals after growth support this view.

Horn, Fullam and Kaspar (1952) have reported growth layers about 200 Å. thick on Al B_2. Wyckoff produced the photograph taken with an electron microscope of a protein crystal. This was the first evidence of unimolecular layers, and was communicated privately to Bunn (see Bunn and Emmett 1949 p.130).

Owing to the difficulties of resolution with an optical or electron microscope, it was not possible to observe the molecular growth fronts in the majority of crystals. The edges of growth layers are too small in vertical height to be detected with an electron microscope, and are too closely spaced to be laterally resolved with an optical microscope.

Growth fronts observed by Bunn on the crystals which he studied were found to be invariably closed, but this could hardly be an argument against the growth by dislocation mechanism, because the edges of the growth layers were not monomolecular but multimolecular.

Forty, Verma, Amelinckx and other workers have found that polymolecular growth fronts of spiral shape can and do occasionally develop on crystals, including CdI_2 which was one of the crystals studied by Bunn. Details of these spirals will be given in a later chapter. That such growth fronts can also develop on natural quartz crystals has been put on record for the first time by the author in this present work (chapter XII). Growth by spiral mechanism on sythetic quartz is also clearly illustrated in chapter VI of this work.

C H A P T E R II

Growth of Imperfect Crystals

2·1. Introduction:

That an important difference in the properties of crystals is related to the distinction between ideal and real crystals was first pointed out by Smekal (1933). He classified the properties of crystals into two distinct groups; (i) structure-insensitive properties which are essentially independent of crystal defects, and (ii) structure-sensitive which depend upon the presence of defects. Elasticity thermal expansion and compressibility, specific heat, diamagnetism, paramagnetism etc. are properties of the first kind, while the ionic and electric conductivity, the internal photo-effect, crystal strength, plasticity etc. are of the second.

Imperfections are in general of three different types: (a) crystal defect which consists of lattice flaws where foreign atoms have taken up the normal positions of the atoms in the crystal lattice; a vacant site may be said to be a special case of this; (b) crystal defect which consists of either foreign atoms or atoms of the crystal material, outside the regular geometrical arrangement of the crystal lattice, and known as interstitial atoms; (c) flaw which is called a dislocation; it consists of purely geometrical faults in the crystal lattice. It is only the dislocation which has any effect on the lattice at distances greater than a few interatomic spacings. Seitz (1952) has given a synthesis of different imperfections in crystals. There are two standard types of dislocation, the 'edge' and the 'screw' dislocations, with a series of intermediate cases which consist of various combinations of these two standard types. An excellent account of the theory of dislocations has been given by Cottrell (1949) and Read (1953).

There is a school of thought which deals with crystals having imperfections in their surfaces. Frank (1949) explained distorsions of the perfect lattice in terms of dislocations. From the point of view of crystal growth the most important of these dislocations are screw dislocations. Burgers (1939) and Kohler and Loos (1941) have worked out the mathematical theory of growth of imperfect crystals. This theory was further developed by Mott and Nabarro (1948) and Frank (1949a). Reviewing dislocation theory, Cottrell (1950) gave the definition of screw and edge dislocations. According to Burton, Cabrera and Frank (1949a, 1951) a crystal having screw dislocations emerging on its surface does not require a surface nucleation process provided that the distance between a pair of dislocations or a dislocation and the boundary is greater than the size (diameter) of the critical nucleus of the surface nucleation theory for the corresponding degree of supersaturation. Screw dislocations are distorsions of the lattice with a screw component perpendicular to the crystal face. It has been established experimentally that the mechanical strength of good crystals is, at best, only about one per cent. of the theoretically expected value. This difference between the experimental and theoretical values of the mechanical strength is attributed to the presence of dislocations.

Now on the basis of two-dimensional nucleation theory of crystal growth, once a three-dimensional nucleus is formed from the vapour phase, it would require, for growth to continue, a supersaturation of vapour of about 50%. From some of the experimental observations on the critical supersaturation necessary for growth, the value is found to be below about 1%. According to Frank (1949b, 1950a) and Mott (1950b) at high supersaturations high-index stepped surfaces will disappear, and then the crystal will continue to grow by two-dimensional nucleation by a new molecular layer on unstepped surfaces circumscribing the initial

crystal. Growth of crystals at low supersaturation can only be explained by recognizing the fact that such crystals are imperfect. The theoretical value (viz. 50%) of supersaturation of vapour necessary for two-dimensional nucleation has been accepted by the dislocation theory, but it still maintains that, at least at low supersaturations, growth does not take place by two-dimensional nucleation. High supersaturation will be required for two-dimensional nucleation to take place on a perfect completed lattice plane. To get rid of this difficulty the interpretation must be such that it will provide the surface with a step required for growth, thereby making two-dimensional nucleation unnecessary. In fact the dislocation theory states that the screw dislocations are present in the case of real crystals, and that they terminate at the surface with a screw component. They give rise to ever-present steps on the surface of the crystal, and deposition can take place on these steps. At ordinary supersaturation growth will take place by deposition of molecules along the ledge created by the dislocation terminating on the surface. The point on the crystal surface where the screw dislocation terminates is called the axis. Now the molecules in the crystal no longer lie on planes but on screw surfaces about the axis. As the molecules get deposited on the ledge, it rotates and a spiral is created. The general assumption is that dislocations of opposite signs exist on crystal faces. If the distance between two screw dislocations of opposite signs is less than the critical size (diameter) of the two-dimensional nucleus no growth will occur. On the other hand, if the distance between them is greater than this they send successive closed loops of steps. According to Burton, Cabrera and Frank (loc. cit.) the growth of unsaturated faces (e.g. (111) faces of sodium chloride or any face of high index) is independent of dislocations

or two-dimensional nucleation.

A single screw dislocation emerging on a crystal face will produce a growth pyramid, the edges of the layers of which will be of a spiral form. If growth is independent of crystallographic orientation, a circular spiral will be formed. On the other hand, if growth depends on crystallographic direction the spirals will be polygonal. In either case the ultimate fate is the formation of low growth pyramids whose sides are vicinal faces. Growth from the vapour or from solution is explained by the dislocation theory. It does not deal with growth from the melt.

A full account of the experimental evidence of crystal growth by screw dislocation is given in chapter IV, the first being given by Griffin (1950a) who by a remarkable coincidence produced a photograph of a spiral on beryl at the same meeting where Frank read his paper on screw dislocations. Spirals were observed by Verma on silicon carbide crystals even before the existence of the dislocation theory. Menzies and Sloat (1929) had observed spirals on silicon carbide as early as 1929, but in the absence of any theory no significance was attached to their observations. Buckley (loc. cit.) who also observed spirals on silicon carbide even before the birth of the dislocation theory attributed them to some macroscopic events taking place in the vapour in the vicinity of the surface at the moment of solidification.

A dislocation is a line of discontinuity which must either form a closed loop within the crystal or end on its surface. If a dislocation lies in a slip plane in the crystal it can be defined as the line separating the part of the material that has slipped from that which has not. It is characterized by Burgers vector, which represents the distance through which the slip has occurred.

2·2. Edge Dislocations:

This type of dislocation was first introduced by Taylor (1934), Polanyi (1934) and Orowan (1934). In this case the dislocation line and the slip vector are at right angles. Fig. 1 shows the slip process in terms of which an edge dislocation can be represented. Slip has occurred over the area PQRS in the direction of the slip vector, the rest of the plane remaining unslipped. The line PQ is the internal boundary of the slipped area and therefore by definition a dislocation. The exact arrangement of atoms along PQ is not known, however, an arrangement which is probably a good approximation is shown in figs. 2 (a) and (b) for a simple cubic case, looking along PQ. The atoms in the lower part are extended while those in the upper part are compressed. This type of dislocation could be regarded as being formed by the addition of an extra plane of atoms above the slip plane or by the removal of a plane from the lower half of the crystal in such a way that the edge of this plane coincides with the dislocation line. There must be one vertical plane of atoms coming from above and terminating on the slip plane. The imperfection along PQ is called an edge dislocation since it constitutes the edge of an extra plane. Taylor (loc. cit.) showed that the motion of a dislocation line of the edge type across the slip plane, produces a shear displacement of an amount equal to the Burgers vector of the part of the crystal above the slip plane relative to that below that plane (Mott. 1951). This is its main property which characterises it when introduced into the theory of plastic flow.

Dislocations can also exist which are the inverse of the type shown in figs. 1 and 2, where there is an extra plane coming from below and terminating on the dislocation line. These two types are called positive and negative edge dislocations. Since,

by inverting the crystal a positive dislocation can be transformed into a negative one the distinction between them may appear superfluous. However, this distinction is necessary since two like dislocations repel each other while conversely two unlike attract.

2·3. Screw Dislocations:

This type of dislocation was first introduced by Burgers (1939). In this case the dislocation line and the slip vector are parallel. This may again be illustrated by a crystal model. A cut PQRS is made in the crystal, fig. 3(a), and the crystal material to the right is pushed down by one molecular diameter. The result is shown in fig. 3(b). A step has now been created on the surface of the crystal such that on the left hand side, the plane of the crystal surface is higher and on the right hand side it is lower. The step does not extend throughout the surface of the crystal but extends only from the point P to the edge of the crystal. This line PQ is the boundary line between the right and left parts of the crystal which have slipped by unequal amounts, and hence is the dislocation line. In the case of a dislocation line meeting the surface of the crystal at right angles, the arrangement of molecules is illustrated by the model of fig. 4, the atoms being represented by cubes. The structure of a screw dislocation is shown in fig. 5, dotted lines and circles represent the molecules to the left of the slip plane of fig. 3(b), whereas the molecules to the right of the slip plane are represented by full lines and circles. In this case the dislocation line PQ is parallel to the slip direction.

Screw dislocations are of two types, right - and left - handed. In the latter type, moving along the Burgers circuit from a higher level to a lower level, the route is anti-clockwise, whereas in the former type it is clockwise. The right-handed screw dislocation will be obtained when the crystal material to

the right of the cut PQRS in fig. 3(a) has been pushed down with respect to that on the left; the inverse operation will create a left-handed screw dislocation. This distinction between the left - and right - handed screw dislocations is trivial but arises out of the forces exerted between two dislocations.

The strength of the dislocation may be defined as the difference between the slip vectors on the slip plane on either side of the dislocation line. A route may be considered on any lattice plane of the crystal along a line drawn through the nearest neighbouring atoms in such a way that it forms a closed loop. Such a line is called the Burgers circuit, and could be used to define the strength of the dislocation. If when tracing a line, corresponding to a circuit in a perfect lattice, it does not form a closed loop then the area enclosed by the line contains a dislocation. The vector required to complete the loop is called the Burgers vector. It can be seen that the Burgers vector in the case of the screw dislocation illustrated by fig. 3 is equal to the slip vector. A more detailed description of the general behaviour of the Burgers circuit has been given by Frank (1951a) and Read (1953). Since the Burgers circuit can be continuously displaced along the dislocation line without change in its Burgers vector, a dislocation cannot terminate within the crystal.

The screw dislocation can move in the slip plane in a direction perpendicular to the screw-axis, and also perpendicular to the slip plane. Both these processes take place without activation energy. However, a screw dislocation cannot move through diffusion of lattice sites. An account of the experimental evidence of the movement of screw dislocations will be given in Chapter IV.

2·4. Role of Screw Dislocations in Crystal Growth:

The dislocations taking part in the growth of a crystal are of the screw type. As mentioned above, a screw dislocation emerging on the surface of a crystal produces a step on the surface, which connects the end of the screw dislocation line with the edge of the crystal. This step is self-perpetuating in the sense that when one, or two or any number of layers of atoms have been laid down on the crystal surface, the step remains. The step provided by a screw dislocation will have kinks, and when the atoms are adsorbed on the crystal surface they will diffuse to the step and finally to the kinks where they are adsorbed for the building up of the crystal; and thus the step advances. However, it can never grow out so as to produce a completed surface since the upper surface of the crystal is a spiral ramp. In the case of a perfect crystal the step would extend all the way across the crystal surface so that it would advance parallel to itself, thereby completing a new layer. On the other hand, if the step provided by a screw dislocation extended all the way across the crystal surface, although it would advance parallel to itself, all points moving with constant velocity, the end point of the dislocation where the step terminates remains fixed, and hence the step tends to rotate round the dislocation somewhat like the hands of a clock. At a particular supersaturation each point on a straight step will advance with the same speed, therefore, the section of the step near the dislocation will have a higher angular velocity for the same linear velocity, and consequently make a larger number of revolutions in a given time than the sections farther out. Thus the step winds itself in a spiral form. Several stages in the development of the spiral are shown in fig. 6. The spacing between successive loops of a spiral is proportional to the size of the critical nucleus for the growth on a perfect crystal, and is inversely proportional to the supersaturation.

Strictly speaking, the theory outlined above applies only to the growth of crystals from the vapour, but it is clear that it will also apply in principle to growth from solution. The main difference is that in general in growth from vapour $x_s > x_o$, while in solution $x_o > x_s$. The observations of growth spirals on crystals grown from solution, a brief account of which is given in Chapter IV indicate that the above theory of growth of an imperfect crystal is applicable also to the growth of crystals from solution.

These considerations first put forward by Frank (1950, 1951), and Burton, Cabrera and Frank (1951) predict that on the surfaces of crystals which have grown by this mechanism, flat molecular spiral pyramids should be observed. The faces of these pyramids will be the vicinal faces, and the occurrence of such faces is naturally explained by the theory. An ideally long annealing would get rid of these dislocations, but in practice some may always be expected to remain.

2·5. Circular Spirals:

The simplest case is that in which the rate of growth is independent of crystallographic orientation. The rate of advance of a straight step is given by the equation:

$$v_\infty = 2(\sigma - 1) x_s \nu e^{-W/kT}$$

where σ = saturation ratio, p/p_o (p = actual pressure of vapour, p_o = saturation value);

x_s = mean distance of adsorbed molecules = the average distance a molecule wanders on the crystal surface between the time it hits the surface and the time it evaporates,

ν = frequency factor (it is of the order of atomic frequency of vibration $\sim 10^{13}$ sec^{-1} in the case of monoatomic substances),

W = evaporation energy,

k = Boltzmann constant, and

T = absolute temperature.

Such conditions are likely to occur in growth from vapour so that the rate of advance, v_∞ , of a straight step does not vary with the orientation in the crystal face. Under these circumstances $x_s >> x_o$ even for orientations of closest packed directions.

Mean distance between kinks on a step $= x_o = \frac{1}{2} \exp(\phi/2kT)$

$$x_s \sim a \exp(3\phi/2kT)$$

where, ϕ = nearest neighbour interaction and
a = interatomic distance.

In such cases the molecules will have a high probability of adhering to the step if adsorbed near it, irrespective of the orientation of the step. Therefore, the rate of advance of the ledge will be independent of crystallographic orientation, and a rounded spiral will result, the shape of which can be calculated under the assumptions, given by Burton, Cabrera and Frank (1951).

A ledge which forms a portion of the spiral and has a radius of curvature ρ , will advance with a velocity v_ρ given by,

$$v_\rho = v_\infty (1 - \rho_c/\rho)$$

provided the supersaturation is not too high.

$$\rho_c = a\phi/(2kT \log \alpha)$$

The spacing between the successive arms of the spiral will be constant and will be given by $\delta h = 4\pi\rho_c$.

2·6. Polygonal Spirals:

When the rate of advance of a growth front depends on its orientation, polygonal spirals will result. When the step is parallel to a close-packed direction it is obvious that this may influence the rate of advance. The step will then have relatively few kinks, the kink energy being high. Therefore, if the condition $x_s >> x_o$ is no longer true, so that the kinks are few

and far between and the distance moved by the adsorbed molecule is small, polygonal spirals will result, the edges of the steps becoming straight in a direction at right angles to the directions of minimum growth. But in general true straight step lines are not to be expected (Frank, 1952). These growth spirals which become polygonal will exhibit the degree of symmetry of the crystal face. According to Frank (1950b) the dependence of growth rate upon crystallographic orientation can therefore be represented by a two-dimensional polar diagram.

2·7. Properties of growth fronts and interaction of growth spirals:

When the advancing growth fronts meet an obstruction they can propagate round corners; in fact it might be said that this point behaves like a secondary source of growth fronts. Verma (1953) has obtained 'fish like' obstructions on silicon carbide crystals.

Sometimes amongst the dislocations emerging on a crystal face, one may dominate the rest. This will happen if the supersaturation at one centre is slightly greater than at other centres. The growth pattern originating from the weaker sources will continually shrink and if conditions remain constant, ultimately only one growth pyramid will be seen. The weaker screw dislocations play little part in growth, and merely pass on the growth fronts received from the dominant screw dislocation with a slight delay and in a slightly modified form.

2·8. Growth pattern for two screw dislocations:

(a) Two screw dislocations of the same sign:

If two screw dislocations of the same sign emerge on a crystal surface in such a way that the distance between them is less than $2\pi\rho_c$ (ρ_c = radius of the critical nucleus), they will generate a pair of non-intersecting growth spirals. In such a case the spiral is doubled, and if the members are strictly

parallel, the two dislocations may be said to co-operate with one another, and will behave like one dislocation of double strength. On the other hand, if the distance between them is greater than $2\pi\rho_c$ the ledges originating from one will intersect the ledges from the other, and the resultant growth pattern will be as shown schematically, in full lines, in fig. 7, where the two dislocations D_1 and D_2 are assumed to be of equal strength. Fig. 8 shows the resultant growth hill in three dimensions.

(b) Two screw dislocations of opposite sign:

When the screw dislocations of opposite sign emerge on the face of the crystal a ledge will run between them as shown in fig. 9. Growth will start if the supersaturation is raised to such a value that the size of the critical nucleus is less than the distance between them. When the critical nucleus is not circular, this will be equivalent to a correctly oriented critical nucleus passing between the two dislocation points. As long as the supersaturation is kept above this value, adsorbed atoms will join the step and therefore the step tends to spiral around both dislocations. Fig. 10 is a schematic representation of this, looking down from above. However, as the step doubles back on itself (fig. 11 (d)) the two points M and N which are at the same level will become joined up by atoms filling in the lower level C to form a bridge. This stage is shown in fig. 11 (e). The parts E and F of the step grow very rapidly since the curvature is negative, that is to say the length of the step decreases as the step advances. Thus a closed loop will be generated, and in the final stage the step will return to its original position, and is thus ready to start the cycle again. This mechanism is similar to the Frank-Read source (1950). Therefore, as successive loops are developed the surface of the crystal becomes a pyramid, composed of sheets or molecular layers.

2·9. Growth pattern for a large Number of Dislocations:

Quite complicated growth patterns result when a large number of dislocations emerge on the surface of a crystal. The successive arms of the spirals originating from any two dislocations can join with each other if the two dislocations are of the same strength. Conversely if successive steps from two dislocations join and fuse together, without leaving a fault surface, it can be concluded that the step heights of the two spirals are equal. It has been concluded by Verma (loc. cit.) that in any one region of the crystal, the dislocations are of the same sign and have the same strength, at least on Si C, but recent experiments (Sunagawa, 1959) have disproved this conclusion.

2·10. Density of Dislocations:

The density of dislocations varies widely on different crystals of the same substance. Verma has found that on Si C crystals the density of dislocations is $\sim 10^4$ or 10^5 screw dislocations per sq.cm. of the crystal surface. Dawson and Vand (1951) have reported a density of dislocations $(1{\cdot}6+2\times10^6 A_{001})$ where A_{001} is the area in sq.cm. of the paraffin crystal face (001).

Forty and Frank (1953) found that in the case of Ag crystals, grown from vapour, the density of observable dislocations is quite low; usually one or two screw dislocations emerge on a face 0·1 sq.mm. . On the other hand, the density of dislocations for metal crystals grown from melt is quoted at $\sim 10^8$ per sq.cm. . The great difference in these values may possibly be due to the much greater perfection of Ag crystals grown from vapour. In general all those crystals on which growth by spiral mechanism has been studied seem to be nearly perfect.

2·11. Groups of Dislocations:

Quite often groups of dislocations arranged in different ways

emerge to the crystal surface and the growth patterns take complex geometrical shapes. If a spiral system of s branches is generated by a group of some n dislocations of the same sign arranged along a line of length L, the resultant activity of the group is given by

$$(1+s)/(1+L/2\pi\rho_c)$$

times that of a single dislocation (Burton et alia 1951).

2·12. Some Information about the Conditions of Growth:

From the microscopic observations of the spirals, information about the conditions of growth like the size of the critical nucleus, the supersaturation and the temperature can be derived.

$$\delta r = 4\pi\rho_c$$

Hence measuring δr, ρ_c can be evaluated.
Using the relation

$$\rho_c = a\phi/(2kT\log\alpha)$$

the supersaturation can be calculated, provided ϕ/kT can be estimated. For this estimation Trouton's rule may be used according to which

$$\phi/kT = (3\cdot5)(T_b/T)$$

where T_b is the boiling point in ^{o}K. At an absolute temperature of 0·6 of the boiling point of the material $\phi/kT \sim 6$.

Verma (loc. cit) has found that Si C crystals grow at a very low value of supersaturation $\approx$ 0·2 per cent.. Griffin (1951b) has calculated that the beryl crystals which he studied grew at a supersaturation of about 0·5 per cent.

2·13. Dislocations of Multiple Strength:

The step formed by the emergence of a screw dislocation onto the crystal surface will have a step height corresponding to the difference in the amounts of slip between the neighbouring regions

of the crystal. In addition to the elementary spirals having step heights equal to the height of the X-ray unit cell, spirals having large step heights are also seen on some crystals. Such spirals usually have high visibility and can often be seen simply with a microscope using bright field illumination even without silvering the crystal. Such a spiral results from a dislocation of multiple strength, the Burgers vector being a multiple of the X-ray unit cell. A brief review of such spirals observed on different crystals is given in Chapter IV.

2·14. Dissociation of Steps:

According to Frank (1951b) the rate of advance of a multiple step of a spiral will be controlled by the deposition rate at the bottom of the step, and as long as the bottom of the step is not priviledged with respect to the diffusion from the gas, the multiple step will not dissociate into its component steps. Dissociation of steps in the case of Si C crystals has been observed by Verma (loc. cit.). He found that the edges of the steps are not close-packed. Fizeau fringes passing over the steps were observed to be continuous right over the edges, which indicates that the edges are not vertical. Again the crystal face between successive edges was also found to be not close-packed, since upon them some faint step lines were observed.

Cabrera (1953) has considered the stability of a multiple step of a growth spiral. In the case of growth from solution, e.g. in CdI_2 crystals, the fact that the top of the step is under a higher supersaturation than the bottom (Seegar, 1953) seems to be sufficient to maintain the multiple step as a unit. A possible explanation of this fact for the corresponding case of growth from vapour, for crystals which grow in layers separated by stacking changes, e.g. Si C crystals, has been given by Cabrera (loc. cit.). He has shown that for the hexagonal Si C crystals with Zhdanov symbol (33), (22) etc. the multiple step will have the same minimum supersaturation for growth as the unit step, and

will therefore tend to separate into its components. The situation is, however, different in the rhombohedral Si C crystals, which have the general Zhdanov symbol $[(33)_n 32]$ with (2n+1) stacking changes. In this case the multiple step will tend to remain intact.

2.15. Fault Surfaces:

Three cases will arise in considering the interaction of two dislocations of unequal strength:

(a) When two series of steps, originating from two screw dislocations, advance towards one another and meet, if the two step walls are identical, they will fuse together forming an unbroken crystal surface.

(b) If the two step walls of the growth layers advancing towards one another consist of the same repeat unit but have different step heights, since the structure of the step walls is identical, they will fuse with one another but since their step heights are unequal, they will leave a step of height equal to the excess of the repeat unit of one over the other.

(c) When the two screw dislocations are of different strengths and also have different structures the two step walls of the layers from these dislocations will consist of different numbers of layers, which will also be arranged differently. In this case, the two steps cannot fuse with one another in a perfect way, crystallographically. A surface of lattice discontinuity will extend from every imperfect dislocation. Step lines terminating on imperfect dislocations therefore mark out fault surfaces and cannot move as easily as steps extending from perfect dislocations.

A geometrical configuration, due to Frank (see Forty 1952a), for the interaction of a smaller dislocation group with dominating growth layers is shown in fig. 12. Such a pattern will reproduce itself after each cycle of rotation of the dominating spiral, if the approximately radial steps advance more slowly than the main spiral step. This is possible only if the dominated

dislocation is an imperfect dislocation of the structure resulting from the dominating one, so that the radial steps approximately follow the trace of the fault surface in the crystal. The hindrance to the passage of a growth step over a fault surface will depend on the degree of misfit at the fault surface. Fig. 13(a) shows the configuration in the extreme case when the hindrance is complete. If the supersaturation on either side of the fault surface is different the configuration will be as shown in fig. 13(b). If as growth proceeds the fault tries to heal itself, it will leave a large sized dot on the step lines on either side of the fault surface. Such dots, as observed by Verma (1953) on Si C crystals, reveal the past history of the extermination of faults.

When growth fronts advance into the loop formed by the line of misfit, it can be said that the crystal material inside the loop is crystallographically perfect though elastically strained, and may be termed a 'good crystal'. According to Frank (1951a,b) and Read and Shockley (1952) a good crystal is defined as a region in which the strains, and density of atomic defects are small enough to allow the unmistakable correspondence to the ideal lattice.

Different dislocations in any one region of a crystal may have originated from one dislocation with a large Burgers vector. According to Frank (1951b) the step associated with the large Burgers vector will not terminate abruptly, but macroscopically speaking will taper away. It will actually break into discrete dislocations and most likely into dislocations of unit Burgers vector; these component dislocations thus broken up will be of the same sign, and due to repulsion between each other, they will tend to spread apart as growth proceeds.

Interlacing of spirals also takes place in some cases. These have been observed and explained by Verma (loc. cit.) in

the case of Si C crystals.

2·16. Polytypism:

According to the theory of Burton, Cabrera and Frank, the spiral form is obtained when during the process of growth, the inital ledge formed on the crystal face by the emergence of the screw dislocation, winds itself into that shape. Thus a crystal growing by this mechanism is not composed of an indefinite number of layers stacked upon each other, but of a finite number of interleaved helicoids, where each helicoid axis is a dislocation. The structure necessarily repeats with a period corresponding to the pitch of the screw. The X-ray unit cell, which is equal to the step height, becomes the crystal building unit giving rise to different polytypes.

2·17. Origin of Dislocations:

Frank (1952a) suggests that Si C crystals may initially grow into plates by surface nucleation mechanism. These plates will become self-stressed, through non-uniform distribution of impurities or through thermal stresses due to partially screened intense radiation, ultimately up to its theoretical yield stress, when the thin plate will buckle and shear. This will raise terminated steps on the crystal face, and if the shear is by a uniform amount terminating fairly abruptly, a ledge will be exposed. Growth will take place on this ever present step, and growth spiral will result. Vand (1951) has also given an explanation on similar lines. An accidental stacking fault in the exposed ledge will afford an alternative explanation of polytypism.

Korndorffer, Rahbek and Sultan (1952) have described an interesting experiment which throws much light on the creation of dislocations by mechanical deformation in an otherwise seemingly perfect crystal of CdI_2. They indented such thin crystals with the help of a glass rod drawn into a fine point. It was found that by bringing the indentor in contact with the 'dead' crystal, it began to grow rapidly again, increasing both in extension and

in thickness, and on some of these crystals spiral steps could clearly be resolved. It is clear that the stress produced by the indentor would facilitate the buckling and slip mechanism, and thus the experiment provides simple, direct experimental evidence of this mechanism.

According to Seitz (1950) dislocations may be formed by the condensation of vacant lattice sites as the crystal is cooled, some confirmation of which is obtained in the experiments of Teghtsoonian and Chalmers (1951) when metals grow from melt. Frank (1952) suggests another possibility for the origin of dislocations. He suggests that either the crystal begins to grow on a foreign solid, which may already be dislocated, or if the early mode of growth is dendritic the arms of the dendrite will probably meet each other imperfectly and so produce dislocations. There will be a natural selection of suitably dislocated crystals as growth proceeds at low supersaturation. This will account for the emergence of one or a few dislocations near the centre of the growing face. The fact that, in the majority of crystals, dislocations occur more or less throughout their volume may be attributed principally to the deformations caused by impurities. A convincing evidence of the existence of dislocations comes from the observation of Hedges and Mitchell (1953), who have succeeded in getting polytypic silver to separate out along dislocation lines in a transparent AgBr crystal.

In addition there are cases in which growth is promoted by the persistent re-entrant angles in the surface provided by twinned crystals. Good examples are provided by fluorite and calcite (Frank, 1949 a,b). Dawson (1952) studying the growth of n-hectane crystals obtained lath shaped crystals, in addition to the features conforming to the spiral mechanism. These laths themselves are always twinned having a re-entrant angle on one of

the narrow faces. This provides an indestructible step at the twin boundary so that growth in the one direction is greatly accelerated.

2·18. Movement of Dislocations:

Griffin (1952) in his observations of the static growth features on beryl crystals has observed certain anomalies in the layer structure near the dislocation. This was inexplicable in terms of either growth or dissolution, and he attributed it to the movement of a dislocation in some stage of the history of growth.

Taylor (loc.cit.) has calculated the forces exerted between two edge dislocations and Nabarro (1952) has given a general treatment for these forces in different cases. According to Eshelby and Stroh (1951) the force between two screw dislocations emerging normally in thin plates falls off exponentially with the distance between them. Peierls (1940) was the first to calculate the constraining force anchoring a dislocation to its equilibrium position between the lattice rows. According to him (loc. cit.) and Nabarro (1947) the force depends on the elastic constants of the medium. At a certain distance of separation between two dislocations of opposite sign, the attractive and anchoring forces will balance each other. During the process of growth of the crystal the two dislocations will draw towards one another, and will finally coalesce, joining to form a common centre, unless the distance of separation is greater than the above equilibrium value.

Mott (1953) has explained the example of such a case reproduced in a photograph by Anderson and Dawson for a paraffin crystal. He states that the crystal has grown on two screw dislocations of opposite sign and after the growth has been completed, the dislocations have moved together under their mutual attraction, and annihilated one another. Experimentally

dislocations of opposite sign are seldom observed.

Anderson and Dawson (1953) have produced a series of micrographs of n-nonatriacontane (C_{39} H_{80}) crystals grown from solution, which demonstrate very clearly the mechanism of the growth of the crystal by the creation of a dislocation ledge and the subsequent movement of dislocation. According to Anderson and Dawson in the last stage of growth when the solvent evaporates, the crystal will become subject to stress, and will collapse on the supporting film; the imprint of the line of rupture will be transmitted to the upper surface, raising there a ledge which will be opposite in sense to the initial ledge that has spiralled itself. This stage is schematically shown in fig. 14 (c). In general, it can be said that there will always be an interaction and fusing of the steps due to subsequent growth, thereby producing a row of kinks (fig. 14(d)), if the ledge created by the rupture is an integral multiple of the growth step. Indeed the order difference between the steps fusing with one another on either side of the line of rupture will give its height as a multiple of the growth step. If the ledge due to rupture is not an integral multiple of the growth step it will leave a fault surface.

Alternatively it can be said that the collapse of the crystal is actually the movement of the dislocation in its own glide plane, from its original point of emergence to the edge of the crystal. This will obviously raise a step between the two positions of the dislocation, and subsequent growth will lead to a growth pattern exactly as before. Anderson and Dawson do not agree with Mott's interpretation of the annihilation of two dislocations of opposite sign. They suggest that the two dislocations have actually moved under the action of the force imposed from without by the collapse mechanism. The annihilation of dislocations of opposite sign leads to symmetrical closed

growth sheets without any dislocation at the centre. If the slip occurs after the growth has ceased, no interaction of the slip step and growth step would take place.

Forty and Frank (1953) from their observations of the growth patterns on silver crystals grown from vapour in vacuo have concluded that all the growth and slip steps are equal and monatomic, and hence the slip step is a unit slip step, but no measurements of step heights have been made.

2·19. Holes in Crystals and Hollow Dislocations:

Various workers have shown that dislocations are generally the centres for chemical etching. If a thin crystal in which a screw dislocation extends perpendicularly right through from one face to the opposite one, is etched for a long time a hole right through the crystal will result. That such is the case has been shown by Verma (1953) in the case of Si C crystals.

Frank (1951c) has shown that for a dislocation whose Burgers vector exceeds a critical value, of the order of magnitude 10 Å., there exists a state of equilibrium in which the core of the dislocation is an empty tube. Taking a simple case of a material with isotropic elastic constants, Frank has examined the condition that a dislocation should have less energy when the core is hollow than when it is filled with strained material. It has been found that the dislocation will be hollow only if Burgers vector exceeds about 20 Å., although Frank has estimated 10 Å., to be a more reliable value. For a Burgers vector as large as 100 Å., for a typical dislocation in equilibrium, a hollow core of the order of 1000 Å. in diameter may be expected. A dimple or a crater at the point of emergence of a screw dislocation on a free surface is also attributed to the same cause. According to Frank, if the surface energy is independent of orientation, the dimple will be shallow in form but of infinite volume and depth

except at a natural habit crystal face where it is of finite depth or may even be totally absent. In a photomicrograph of spirals the hollow dislocation, if any, will appear as a black dot at the centre of the spiral. In Si C crystals Verma (1953) found that a crater had a flat bottom. In the case of a group of like dislocations, Burton, Cabrera and Frank (loc. cit.) have suggested that a pit may be developed on the crystal face if the growth fronts have difficulty in penetrating the group itself. Verma observed on some crystals of Si C spots of different sizes on step lines giving them a kinked appearance, and also spots unattached to step lines. Frank suggested that these may be ends of edge dislocations. In some cases even if the Burgers vector is much greater than 20 Å., the dislocation may not be hollow. The reason for this, according to Frank, is that a complete dislocation is readily dissociated into a cluster of weak partial dislocations. Holes at the centre of spirals on Si C were found to be hexagonal conforming to the symmetry of the crystal.

The mechanism of growth by dislocation rather than by two-dimensional nucleation has been favoured by topographical study, on molecular scale, which has been carried out in the case of only a few crystals. It is of interest to note that many features connected with crystal habit, habit modification and oriented overgrowth cannot be explained by either of the theories. Hence an open mind must be kept as regards the applicability of any particular theory of growth in an attempt to interprete the observations of the microtopagraphy of quartz given in the present work.

P A R T II

PROPERTIES OF QUARTZ

AND

PREVIOUS OBSERVATIONS

C H A P T E R III

QUARTZ

3·1. Introduction:

There is such a vast literature on quartz that it is very difficult to give a brief account of quartz. However, a humble effort is made in the following few pages. Properties of quartz have been described at length by Sosman (1927), and briefly by Davey (1934), Heising (1945), Mason (1949) and Vigoureux and Booth (1950). A general description of quartz family minerals is given by Dake, Fleener and Wilson (1938).

In the entire mineral kingdom, no species is more abundant, wide-spread, or beautiful than quartz. Owing to its wide dissemination in nature and the unsurpassed beauty of its crystalline forms, quartz has been admired by man since remote antiquity. A full understanding of quartz minerals is truly a prerequisite to the study of mineralogy and geological sciences. Quartz also occupies a rather unique and prominent position in the field of semi-precious stones.

In view of their number, general distribution, and attractive qualities, it is not surprising to learn that quartz crystals were among the very first to be seriously examined and analyzed by man. In fact, quartz crystal has received more attention than any other mineral form, and it was this mineral with which the renowned geologist Steno (1669) established the "Law of constancy of crystal angles". As early as 1885, its crystallography was fully investigated.

3·2. Occurrence:

Quartz is found in great many varieties in the rocks of all ages and of nearly every type, including igneous, sedimentary and metamorphic. Granite rocks and granite pegmatites are favourite

places for the formation of large single quartz crystals. Quartz minerals are found widely distributed throughout the entire world. India has been the source of beautiful stones of the quartz family for many centuries, and early in the seventeenth century, Cambay (India) became the leading centre for the cutting of these semi-precious stones. The crystalline quartz minerals generally have their home in volcanic rocks, or are closely associated with them. Crystals of remarkable size have been found in the Alps, Brazil, Japan, Madagascar, however, good crystals are also found in Herkimer county and Alaska. Clear, brilliant, well developed quartz crystals from Herkimer county in New York are called 'Herkimer diamonds'.

3·3. Crystallization:

Crystallization of quartz by the process of sublimation is by far the rarest or most uncommon but observations have proved that it does actually occur at times. This mode of crystallization may account for, or at least play some important part in, the formation of "high temperature quartz". Crystallization can also take place by fusion. If the cooling of the magma is slow good crystals result, otherwise amorphous quartz is obtained. The most common and important mode by means of which quartz crystals are formed, is their crystallization out of solution.

3·4. Synthetic Quartz:

Quartz can be prepared artifically in the laboratory, the temperature for preparation being between 250°c.to 450°c.. The earliest experiment of this kind on record was by Schafhautle in 1845. To him falls the credit of having been the first to prepare quartz artifically. Spezia (1905, 1906) was the first to succeed in growing large synthetic quartz crystals by using a solution of sodium metasilicate in a silver-lined bomb. In the upper part of the bomb, where the temperature was 330°c. , a

silver basket containing fragments of broken quartz was kept while just below it, where the temperature was 200°c. the seed crystals of natural quartz were suspended. The quartz fragments dissolving at the higher temperature re-deposited on the seed crystals at a slightly lower temperature, the rate of growth being about 1 cm. in 100 days.

Woosters (1946) have described an isothermal process for growing large quartz crystals. During the period 1939-45 Nacken developed, independently, similar techniques using vitreous silica, with the help of which it was possible to obtain growth under isothermal conditions by producing a solution which is undersaturated with respect to vitreous silica and supersaturated with respect to the seeds of natural quartz. The rate of growth is at first rapid; but then decreases and eventually falls to zero. For this reason the temperature gradient method is generally preferred. Progress in this direction has been reported by Praagh (1949), Walker and Buehler (1950) and Brown and co-workers (1951).

Brown et alia (loc. cit.) have used a temperature-gradient method and found difficulties in an attempt to prolong the growth cycle beyond a day due to the divitrification of the silica glass. Hale (1948) found it convenient to reverse the arrangement used by Spezia, i.e., to use an autoclave heated from its base, the temperature decreasing upwards. Hale (1949) and Walker and Beuhler (loc. cit.) mostly using seeds cut parallel to a rhombohedral face succeeded in growing fairly suitable crystals of quartz. According to them growth on a cut c-face is of poor quality until pyramidal caps are complete, but thereafter quartz of sound quality is deposited on the newly formed rhombohedral faces.

The temperature-gradient method used by Brown et alia was more or less similar to that described by Walker. They used a

cylindrical steel autoclave which was charged with an acqueous solution of sodium carbonate, with crushed quartz placed loosely in the bottom and the seed crystal suspended from the lid. The autoclave was heated from the base which was resting on a hot plate and the temperature drop was 40°c. over the entire length of the autoclave. Sufficient liquid was put in the autoclave to produce, at the working temperature of 360° - 400°c. , a pressure between 1000 and 2000 atmospheres. They have produced good quality quartz at the rate of 0·5 mm. per day on each (0001) face, and have found that although the main growing face is not planar and is much more rough than other faces (see chapter VI) quartz prepared by them were of as good quality as the best Brazilian quartz. The synthetic crystals grown by them on seed plates parallel to (0001) were found to have habit which is suitable for the economical fabrication of oscillator plates. In general, such crystals were found to be completely free from cracks, inclusions and twinning, and their refractive index was found to be equal to that for best natural quartz crystals. From their experiments they found that mass of quartz which can be deposited in a given time increases with the area of the seed plate but this area is naturally limited by the size of the autoclave. In preparation of quartz in an autoclave, usually a solution of sodium carbonate is used but sometimes to it are added solutions of sodium hydroxide and sodium chloride.

3·5. Chemical Composition:

Quartz is described by the chemist as silicon dioxide SiO_2. It crystallizes in hard, brittle, glass-like six-sided prisms with pyramidal terminations. It seems unbelievable, though nevertheless true, that the two elements, Si and O, entering into the quartz molecule, make up 75% of the surface material of the earth.

3·6. Physical Properties:

The specific gravity of purest quartz is 2·65, while for

other varieties it ranges from 2·5 to 2·8. Its melting point is 1750°c., and its physical hardness is 7, on the Moh's scale. Crystalline quartz is unstable at temperatures above 800°c. Quartz, under atmospheric pressure, below 573°c. is called α-

-quartz or low-temperature quartz; above this temperature it is called β-quartz or high temperature quartz, the designations α & β- quartz being first introduced by Mügge in 1907. Subjecting quartz to temperatures above 573°c. produces a rearrangement of its molecular or atomic structure. Vein quartz and the huge crystals in pegmatite dikes generally form at lower temperatures, while the granite quartz crystallizes at higher temperatures.

Quartz is insoluble in ordinary acids but dissolves in hydrofluoric acid and in hot alkalis. It is soluble to some extent in water at high pressures and temperatures, and to a much larger extent if sodium hydroxide is present. It does not exidise readily.

At ordinary temperatures, quartz is a very poor conductor of heat, but at temperatures near its melting point it becomes as good conductor of heat as copper is at ordinary temperatures. Thermal conductivity of quartz is maximum along its principal axis.

The piezoelectric property of quartz and other minerals was discovered by Pierre and Jacques Curie in 1880. Quartz crystals were the first piezoelectric crystals to receive wide application, and because of their excellent mechanical properties they are still the most widely applied piezoelectric crystals. Quartz exhibits double refraction and is optically active, c-axis being the direction of the optic axis.

A study of the origin and deposition of quartz has led to numerous important conclusions in the field of geology, mineralogy,

and ore deposits. Quartz has rightly been referred to as a "geological thermometer".

When a quartz crystal is heated gradually an abrupt change in the values of most of its physical constants occurs at a well defined temperature approximately 573°c., which is the conversion temperature of α-β varieties.

3·7. Smoky Quartz and Milky Quartz:

(a) Smoky Quartz: This is a variety of crystal quartz characterized by a smoky-yellow to dark smoky brown; however crystals of all colour gradations from a mere tinge of colour to some so dense as to be practically opaque are not uncommon. The colour of most smoky quartz can be removed by heating it to about 350°c. to 450°c. . It has been thought that the smoky colour is due to colourless crystals having been exposed for long periods of time to radium emanations from the surrounding rocks.

(b) Milky Quartz: This is a transluscent to opaque variety of massive quartz. The white colour is not due to any colouring matter but to millions of fluid enclosures.

3·8. Symmetry, Form and Habit:

No more instructive example exists of the principles of crystalline symmetry, both geometrical and physical, than quartz.

The basic form of quartz is the hexagonal prism terminating in rhombohedron. An ordinary quartz crystal, when doubly terminated, resembles a combination of a hexagonal prism and a bipyramid as shown in fig. 15. Sometimes the form is a simple bipyramid. In fig. 15 faces marked m are prism faces, which are of the form $\{10\bar{1}0\}$ while at either end, the hexagonal prism is terminated by six rhombohedral faces, which consist of two sets of three alternate faces. One set, the members of which are usually more developed and more bright is designated as positive or major rhombohedron and the other which are usually less developed and less bright or rather dull is designated as negative or minor rhombohedron. The first set is symbolized as R and the second as r. They are of the form $\{10\bar{1}1\}$.

Naturally in a doubly terminated quartz crystal each prism face will have a positive rhombohedron at one end and a negative rhombohedron at the other. Sometimes, e.g., from Hungary and Brazil, quartz crystals are found terminated at each end by only one set of three positive rhombohedra.

Some natural quartz crystals have small trapezohedral faces adjoining the lower right hand corner of the major rhombohedral faces, while others have these same small trapezohedral faces situated to the left. These two types of crystals are called right-handed and left-handed respectively. These faces are symbolized as ' x ', and have the form $\{51\bar{6}1\}$ and $\{6\bar{1}\bar{5}1\}$ for the right- and left- handed crystals respectively. In much the same way, some quartz crystals have small trigonal bipyramidal faces at the right and left hand corners of positive rhombohedral faces in the case of right- and left- handed crystals respectively. They are symbolized as 's', and are of the form $\{11\bar{2}1\}$ for right-handed and $\{2\bar{1}\bar{1}1\}$ for left-handed crystals. The two types with ' x ' and 's' faces are shown in fig. 16. The right- or left-hand nature of quartz can be ascertained by (a) position of ' x ' face, (b) direction of the zone 'r s x m', or (c) direction of the striae on 's' face.

The existence of enamtiomorphous growth forms on quartz was first observed by Herschel in 1821; however it was also independently discovered by the crystallographer Weiss in 1836.

α- quartz crystallizes on space-group D_3^4 or D_3^6 depending on whether it is left-handed or right-handed. It has three molecules per unit crystal. α- quartz possesses one axis of three-fold symmetry which is vertical and coincides with the c-axis pointing the upper and lower ends of a doubly terminated crystal. It has three axes of two-fold symmetry passing through the pairs of opposite prism edges, but has no plane of symmetry and no centre of symmetry. In α- quartz the three horizontal axes are polar, and it belongs to the trigonal trapezohedral class (32) of the hexagonal system.

On the other hand, β- quartz belongs to the hexagonal trapezohedral class of the hexagonal system. It has one axis of six-fold symmetry and six axes of two-fold symmetry perpendicular thereto, and separated by angles of 30°; it has no plane of symmetry and no centre of symmetry. When a fragment of low-quartz inverts at 573°c. into high quartz the axis of three-fold symmetry remains fixed in direction, while the three two-fold axes of low quartz change into three of the six two-fold axes of high quartz. Finally, all of the plane faces on the low-quartz remain as plane faces on the high quartz.

Crystals whose growth takes place in fissures will present a definitely greater number of irregular and 'rare planes' than those occurring in closed cavities. Smoky crystals are also likely to present rare planes.

Occasionally the chemical nature of the solutions from which quartz crystals grow may change to such an extent as to create 'capping' layers and etchings upon crystal faces, and at times the passing solution may even change to a solvent, in which case instead of a continuation of deposition of the material, portions of the growing crystals may be actually dissolved away. ~~Leaving hopper-faced crystals. The shape of the nucleus on which growth starts and~~ The presence of impurities in the silica solution and environment are the two important factors which influence the shape of a crystal forming in a solution.

It is a fact that the apparent hexagonal pyramids are really combinations of two rhombohedrons, while the apparent hexagonal prisms are combinations of two three-sided prisms; the terminal faces are, therefore, called rhombohedrons and not pyramids.

Fig. 17 is a diagram of a quartz crystal showing different faces with their indices, but it should be mentioned that the face (0001) is a cut face, because such a face is seldom or never found on a natural quartz crystal.

3·9. Mechanical Flaws:

Twisted quartz apparently seems to consist of a single warped crystal, but it is in reality composed of many individuals, each turned through a small angle, so as to produce a spiral effect. A common fault is caused by cracks due to strain set up either directly by mechanical shock or indirectly by thermal gradients in the crystal.

3·10. Prism Faces:

One of the distinguishing characters of quartz is the presence of horizontal, parallel striations which occur on prism faces, these faces being rectangular in outline. According to English striations upon crystal faces represent a sort of conflict waged between two nearly balanced forces - one striving to produce a crystal of a certain type and the other trying to produce another type, - the result being an arrangement of minute, sometimes microscopic faces, called 'the oscillatory combination'. The horizontal striations on prim faces of quartz crystals show plainly the oscillation between the growth of prism and terminal rhombohedral faces.

Angle between R and m faces is $141^{\circ}-47'$.

" " r " m " " $141^{\circ}-47'$.

Angle between alternating faces at the apex of the pyramid is $94^{\circ}-14'$.

3·11. Phantoms:

Plants and animals assimilate their food inwardly and increase their size or growth from within; on the other hand, crystals grow definitely by the accretion of material from without. It would be too much to expect that all crystal growth, from beginning to end, would be a continuous process and in fact it is not; we can, therefore, safely assume that in the formation of some crystals, there were many pauses or periods

when growth ceased altogether, due to lack or scarcity of the required material. Many of these pauses leave traces or marks which one cannot fail to see, and from which a skilled crystallographer can easily read the life history of the crystal. In the case of quartz these pauses are revealed in various manners and habits. In the most casual form, the type of material of which the crystal is composed is homogeneous throughout, and each phase or stage of growth is shown by more or less faint mirror or ghost-like outlines or images called "phantoms". Generally they are but faint, feathery traceries most clearly observed when the crystals are turned at certain angles to the light.

Phantoms may be smoky, blue, white or bubbly in texture and they may occur in groups, clusters or a succession of forms, where the process is repeated again and again, resulting in a series of internal cappings. Occasionally, these cappings are separated by foreign material. That phantoms are closely related to disturbed growth conditions is apparent from their close relationship to crystal faces.

3·12. Inclusions:

Since quartz is usually nearly the last mineral to crystallize during the process of solidification of a rock magma, it may include within it crystals of any other minerals which have crystallized previously or at the same time with it. Inclusions may be of solid, liquid, and gaseous material; individual inclusions may vary in size from sub-microscopic to those easily visible with naked eye, and may be isolated, or arranged in lines, or planes or curved surfaces. When inclusions are sufficiently small and closely grouped, they give a bluish cast to the group, but when they are larger, the group appears white. When bubble inclusions occur in organized groups, the group is referred to as a bubble phantom, or bubble veil.

From analysis it has been found that cavities in quartz

contain carbon dioxide, water, salt solutions, and other substances that might have been present during growth. Occasionally, the liquids included are hydrocarbons, oily petroleum-like substances; however in many rocks the imprisoned liquid was carbon dioxide in the liquid state. These liquid inclusions seldom completely fill the cavities, a condition which permits the liquid to move about from place to place and to be seen as a bubble. All prolific quartz localities afford liquid inclusions of some kind.

According to E. Mitchell Gunnell, in many instances there is a definite orientation of the liquid inclusions in quartz crystals. In his opinion this is bound to be so, because these liquid inclusions are merely occupying the oriented cavities in skeletally developed crystals. Though this may not always be true, it was often found to be so in his observations.

Needle inclusions appear as long, thin, lines or needles, which may be straight or curved, blue, white or otherwise. Needles visible without concentrated illumination, are likely to be inclusions of crystalline material, such as rutile (brown), tourmaline (black) etc.

3 ·13. Pseudomorphism:

Quartz readily responds to replacement process and is often found masquerading in many unexpected crystal forms. The word pseudomorph is used to indicate a mineral that has replaced another of entirely different form and composition. A pseudomorph is a body possessing the form of one substance and the chemical composition of another. Quartz gives unique facilities in the formation of its pseudomorphs, assuming the crystal form of no small number of minerals which it is capable of replacing. Silica often forms pseudomorphs after other minerals, such as calcite and fluorite, usually replacing them by quartz. Besides replacing other minerals, quartz itself may be replaced, but such pseudomorphs are less common than the

obverse type. Wood turned to stone, is one of the most common forms of organic pseudomorphs.

3·14. Twinning:

Crystals of many minerals have an occasional habit of intergrowth, as a result of which it may appear as if two crystals were trying to occupy the same space at the same time. This tendency of crystals is called twinning. Twinning is an abnormality of growth, in which an apparently homogeneous crystal is not actually of the same handedness, electrical sense or orientation throughout. Low quartz exhibits two principal types of twinning, Dauphiné or electrical and Brazil or optical twinning.

In the Dauphiné type the two portions of the crystal are of the same hand, but one is rotated 180° about the principal axis with respect to the other; the twinning axis is the c-axis and the twinning plane is a face of the first order hexagonal prism; R faces of one coincide with r faces of the other; electrical polarity is reversed; and the crystal is electrically and elastically inhomogeneous although optically homogeneous.

In Brazil twinning, the two crystalline individuals are of opposite hands, one being left-handed and the other right-handed; there is no rotation of twinned portion; R and r faces of one coincide with R and r faces of the other; polarity gets reversed; there is no twinning axis; a face of the trigonal prism of the second order $\{11\bar{2}0\}$ is the twinning plane, and the crystal is optically and electrically inhomogeneous although elastically homogeneous.

Sometimes a combination of Dauphiné and Brazil twins is found present in quartz crystals. In such a type, called Compound twin, the twinned portion is rotated 60° (or 180°) about the Z-axis with respect to and is of the opposite hand as compared with the untwinned portion; R faces of one coincide with r faces of the other, and although there is no reversal of

piezoelectric activity, the crystal is elastically and optically inhomogeneous.

The Dauphine', Brazil and compound twins are illustrated in fig. 18(a), (b), (c) respectively. It should be stressed that the idealized form of twinning, shown in fig. 18, is not found in practice, but the twinning boundaries are usually much more irregular. Experience with many thousands of crystals has shown that almost all crystals are twinned to some extent, and that while electrical and optical twinning are very common, compound twinning is extremely rare.

A less common twin of the orientational type is the "Japanese twin", in which the two portions are symmetrical with respect to a trigonal bipyramid of second order viz. $\{11\bar{2}2\}$ on a right-handed crystal of the pyramid $\{2\bar{1}\bar{1}2\}$ on a left-handed crystal.

Any type of twinning is usually difficult or impossible to detect from the exterior form of the crystal. The best method of detecting twinning is by etching the surface with hydrofluoric acid.

3·15. Etching:

Hydrofluoric acid and hot alkalis are used as etching agents for quartz. Dilute hydrofluoric acid acts first upon the rhombohedrons without attacking other faces. Of the two rhombohedrons, negative rhombohedrons are the more readily attacked; becoming mat in appearance because of the great number of small pits, while on the positive rhombohedrons there are fewer and bigger pits. Of all the simpler planes of low quartz the plane (0001), perpendicular to the c-axis, shows the greatest diversity in etch figures, Etch figures with hydrofluoric acid are particularly variable, however, and etch hills in place of etch pits are the usual form on this plane.

Imperfect natural etch patterns are sometimes found on the crystal faces, but the perfect form for an untwinned right-handed quartz crystal are as shown in fig.19. Natural etch patterns which are frequently observed on m, R and r faces of a crystal indicate the presence of one or both twinning varieties. Simple etching technique is used universally whereby the presence of twinning is permanently recorded on the test specimen, whether natural crystal, cut slab or plate. Etch pits on alternate three rhombohedral faces are similar, which confirms the symmetry. Study of etch pits is a powerful tool in determining crystal symmetry.

A detailed account of etching of quartz is given by Ichikawa (1915) and a lucid description of etch pits and their interpretation, for minerals in general, is also given by Honess (1927).

3·16. Cracks:

Many quartz crystals contain cracks, which are not readily seen by casual surface examination. All types of quartz commonly contain one or more cracks, especially when badly twinned or full of inclusions. Some of these cracks may be due to rough handling, but others are due to growth conditions, or result from temperature changes after growth. Every visible crack may be considered to extend beyond its visible range, and some actual cracks will not be visible at all.

3·17. Gliding:

When subjected to stresses due to unequal cooling or to direct non-uniform pressure low-quartz exhibits gliding-planes parallel to the primary positive and negative rhombohedrons and to the hexagonal prism. No other gliding planes have been observed.

3·18. Cleavage:

The character of the cleavage is a qualitative property which states the relative ease with which a given cleavage can be produced mechanically, perfect and imperfect being the usual distinctions. The cleavage of low-quartz is not distinct in any direction. When broken by shock or stress, the crystal usually breaks with a conchoidal fracture. It can be said that it has a partial cleavage parallel to rhombohedral faces, because when plane surfaces of separation have been observed, they have nearly always been parallel to the primary positive or negative rhombohedron or to the hexagonal prism. The occasional plane surfaces of separation may be only the result of gliding planes, as suggested by Lehmann and by Judd. Separation parallel to the hexagonal prism or to the base is much less distinct than either of the rhombohedrons.

According to the experience of Japanese quartz workers, fracture surfaces sometimes occur not only parallel to rhombohedrons and hexagonal prism, but also the common trigonal pyramid and trapezohedrons. This has been shown by etching by Ichikawa (loc. cit.). Very rarely there is also an imperfect cleavage parallel to the second order prism $\{11\bar{2}0\}$. The fracture of quartz perpendicular to the principal axis is more irregularly conchoidal than that in other directions.

3·19. Structure:

From X-ray studies, Bragg and Gibbs (1925) and Wyckoff (1926) have shown that quartz has a complicated structure.

(a) Structure of β-quartz:

On account of greater symmetry of β-quartz, its structure is much simpler than that of α-quartz, Fig.20 illustrates the position of silicon and oxygen atoms in β-quartz. The oxygen planes are not coincident with the silicon plane but are situated at distances lying between 0·6 Å. to 0·9 Å. on either side and it is inferred with certainty that the diagonals of the oxygen

hexagons are not parallel to the diagonals of the silicon hexagons but are in perpendicular directions. Fig.21 illustrates the position of oxygen atoms in β-quartz showing their distance from the nearest side of the silicon hexagon. Here 'h' indicates the height of atom A above the plane of the figure and 'c' is the length of unit cell in the direction of C-axis.

(b) Structure of α-quartz:

The diffraction pattern of α-quartz is that of a single triangular lattice. The side of the equilateral triangle is $a_o = 4{\cdot}903$ Å. . The height of the unit prism is $c_o = 5{\cdot}39$ Å. , giving an axial ratio c = 1·10.

Quartz crystal is composed of three interpenetrating simple triangular lattices. The symmetry of the crystal leads us at once to believe that the unit triangle of each of the basal (0001) plane may be derived from those of the plane below by a rotation of 120° together with a vertical shift of c/3 along the Z-axis. It is necessary to assume that, although the quartz is made up of three interpenetrating lattices equally spaced along the Z-axis, yet these are differently situated with respect to each other along the X- and Y- axes than they would have been if the crystal were rhombohedral.

Bragg's values for the parameters of quartz are:

$$a_o = 4{\cdot}89 \text{ Å.} \; ; \qquad c_o = 5{\cdot}375 \text{ Å.}$$

Gibbs (1925) from a consideration of the diffracted beams from the (0001) planes assumed each basal plane to be split up into three others:

A plane of Si^{++++} sandwitched between two planes of O^{--}. According to him these planes are so spaced that the Z-axis of the unit cell is divided into approximately equal parts. Such an arrangement of basal planes would have the effect of

lifting all the three O^{--} of each cell and depressing all the other three of each cell or vice versa.

In quartz each Si^{++++} has two O^{--} which are slightly closer to it at room temperature than to any other Si^{++++}, so that the molecule of SiO_2 has a real existence in the quartz crystal. Such a crystal is a molecular crystal. At elevated temperatures it is to be expected that this slight inequality in spacing will be overcome from instant to instant for individual ions because of their increased freedom of motion. This means that at elevated temperatures quartz changes from a molecular compound to an ionic compound and should become electrically conducting. It is a matter of ordinary laboratory experience that this is indeed the case.

α-quartz has three molecules per unit crystal and its molecular symmetry requires a two-fold axis of symmetry perpendicular to $\{11\bar{2}0\}$. The molecule of quartz is shaped like a bent arm with the silicon at the elbow and an oxygen at the hand and at the shoulder. A line bisecting the angle of the elbow is, in every case, perpendicular to some member of the $\{11\bar{2}0\}$ form. The bisector is a two-fold axis of symmetry for the SiO_2 molecules.

Fig.22 shows positions of silicon atoms in α-quartz projected on a plane perpendicular to the C-axis, the three directions marked X X indicating the three two-fold axes of symmetry. The distance between the silicon and oxygen planes is 0·63 Å. and Gibbs (loc. cit.) assumes that the oxygen atom lies in a plane perpendicular to and bisecting the line $\overset{\frown}{a\ b}$. Fig.23 illustrates arrangement of Silicon and Oxygen atoms projected on a plane perpendicular to the C-axis, while fig.24 shows that projected on a plane perpendicular to electric axis (Gibbs, 1926).

The silicon atoms lie on three interpenetrating hexagonal lattices which have in the vertical direction a spiral arrangement with respect to each other. The oxygen atoms are apparently grouped in a tetrahedral manner about the silicon atoms. The unit cell contains three silicon atoms, and since a silicon atom has a half-share of each of its four surrounding O_2 - atoms, the Si - O_2 ratio is obeyed.

TABULAR SUMMARY

OF

OBSERVATIONS ON SPIRAL GROWTH

DURING THE YEARS 1949 - 1959

C H A P T E R I V.

Review and Record of Previous Observations.

One of the important observations presented in the present work is spiral patterns on natural and synthetic quartz crystals. Ever since the birth of the dislocation theory various workers in different laboratories have studied growth problems and surface structures of various substances, both metallic and non-metallic, but until now there has been no evidence of spiral growth on quartz. Most of the workers have, in general, obtained spirals only on one form of a particular crystal under study, and in all cases the profile of a spiral has always been flat with abrupt steps. The significant points of the spirals described in the present work are:

(a) spirals observed for the first time on quartz crystals, both natural and synthetic,

(b) some spirals have ripple shaped convex profile, unobserved before, and have no abrupt steps,

(c) spirals are obtained on two different forms, basal and rhombohedral faces,

(d) some spirals are eccentric, and

(e) giant dislocations, movement of dislocation, slip during growth, interlaced spirals, snail shaped and shooting star-shaped spirals, hollow dislocations, closed loops due to Frank-Read source, cooperating spirals etc., etc., are obtained.

Taking into consideration the above-mentioned points, the author felt that a consolidated summary of observations made on spiral growth during the decade since the birth of the dislocation theory would provide a useful overall picture and a ready source of reference. Such observations, including their references, are

given in a tabular form below. For lack of space observations of spiral growth in the case of metal crystals, theoretical discussion on the subject, and observations on revealing dislocations by etching are not included in this table. Abbreviations used in the table are as follows:

Metl. Mic.	Metallurgical Microscope (using bright-field illumination).
Elec. Mic.	Electron Microscope.
Phase. Con.	Phase contrast Microscope.
Ult. Mic.	Ultra Microscope.
M.B.I.F.	Multiple beam interference Fizeau fringes.
Feco	Fringes of equal chromatic order.

Year	Author	Crystal and face	Shape of spiral	Step height	Method used	Other details and remarks	Reference
1951	Amelinckx, S.	Si-C (0001)	hexagonal (circular after two turns)	up to 35 A°.	Metl. Mic. M.B.I.F.	steps of some spirals probably unimolecular; no exact measurement reported	Nature, 167 939
1951	Amelinckx, S.	Si-C (0001) Type II " 6H	triangular	7±2A°.	Metl. Mic. M.B.I.F.	step height is half-unit cell; double growth spiral having two components at 180° orientation w.r. to one another; two successive layers not identical	Nature, 168 431
1952	Amelinckx, S.	Mica (muscovite)	no spiral but a step terminating on the surface	140A° to 0 A°.	Metl. Mic. M.B.I.F.	step equal to 7 unit cells.	Nature, 169 580
1952	Amelinckx, S.	Apatite yellow fluor (1010)	polygonal; razor-blade	10±2A°	Metl. Mic. M.B.I.F.	Growth layers unimolecular; straight edge of spiral parallel to c-axis; photographs taken slightly off focus	Nature, 169, 841

Year	Author	Crystal and face	Shape of Spiral	Step height	Method used	Other details and remarks	Reference
1952	Amelinckx, S.	Apatite; tabular colourless crystals	polygonal	140±20A° (for main growth-fronts)	Metl. Mic. M.B.I.F.	crystals grown from solution; locality - Sulzbachtal, Austria; interlacing occurs in one direction; co-operating spirals also observed	Nature, 170, 760
1952	Amelinckx, S.	Gold; tabular crystals; (111) faces on (110) NaCl	triangular & hexagonal	of the order of 400±100A°	Metl. Mic. thin film technique	crystals obtained by precipitation; photo-graphs taken slightly off -focus; hollow dislocation at the centre of the spirals; first proof of dislocation in metals; growth fronts not smooth but kinked; large amount of misfit (25%) between the gold lattice and the host lattice is also responsible, at least partly, for the creation of dislocations	Phil.Mag., 43, 562

Year	Author	Crystal and face	Shape of Spiral	Step height	Method used	Other details and remarks	Reference
1952	Amelinckx, S.	Biotite	polygonal	-	Metl. Mic. M.B.I.F.	crystals from Vesuvius; interlacing also observed	C.R. Acad. Sci., Paris, 234, 971
1952.	Amelinckx, S. Grosjean, C. and Dekeyser, W.	Gold, (111)	triangular	-	Metl. Mic. M.B.I.F.	method of preparation of gold crystals described	C.R. Acad. Sci., Paris, 234, 113
1953	Amelinckx, S.	Salol, (phenyl ester of salicylic acid)	polygonal spiral growth-pits	from 400 to 18000 A^{o}.	Metl. Mic. two-beam interference;	assymetry of the diffraction pattern at an edge when going off-focus was useful in determining the character of the spiral; hopper faced crystals from solution and from melt; similar growth features observed also on citric acid crystallized from alcohol; Thymol also exhibits such growth features	Phil. Mag., 44, 337

Year	Author	Crystal and face	Shape of Spiral	Step height	Method used	Other details and remarks	Reference
1956	Amelinckx, S.	rock-salt single crystals	hexagonal, square; lozenge-shaped net-works; sets of parallel lines	very great	Ultra Mic. and decoration by means of Na-metal	density of decorating particles is a function of the orientation of the dislocation line w.r. to its Burgers vector; screw dislocations are not decorated; nodes of a net-work are decorated preferentially; emergence points of dislocation lines correspond to the centres of the etch pits produced by methyl alcohol etch	Phil.Mag. 1, 269

Year	Author	Crystal and face	Shape of Spiral	Step height	Method used	Other details and remarks	Reference
1957	Amelinckx, S. Bontinck, W. Dekeyser, W. and Seitz, F.	CaF_2	"	spacing between successive turns of helix large compared to the Burgers vector	-	factors influencing the development of helical dislocations are discussed; helical dislocations should be generated in many materials under a wide variety of circumstances in which climb occurs; such dislocations are, in principle at least, capable of generating whiskers when they occur sufficiently near the surface	Phil.Mag., 2, 355.
1957	Amelinckx, S. Bontinck, W. and Dekeyser, W.	fluorite (111)	helical dislocations and spiral etch pits	—	decoration	under certain conditions the etching of a helical dislocation gives rise to a spiral etch pit of the kind observed on germanium and silicon crystals	Phil.Mag, 2, 1264.

Year	Author	Crystal and face	Shape of Spiral	Step height	Method used	Other details and remarks	Reference
1955	Amelinckx, S.	n-alcohol crystals $C_{22}H_{45}OH$; $C_{24}H_{49}OH$ $C_{26}H_{53}OH$	polygonal	$H=d_{001}$ bimolecular	Phase con. Elec.Mic. M.B.I.F.	crystals grown from solutions in benzene and xylene; crystals of β-form (monoclinic); crystals exhibit a remarkable polytypism due to spiral growth and to the presence of stalking faults; interlaced spirals; some crystals contain more than two bimolecular layers in the unit cell; here polytypism is not due to imperfect dislocations.	Acta Cryst., 8, 530 C.R. Acad. Sci., Paris, 237, 1726

Year	Author	Crystal and face	Shape of Spiral	Step height	Method used	Other details and remarks	Reference
1956	Amelinckx, S.	n-alcohol $C_{22}H_{43}OH$; $C_{24}H_{49}OH$; $C_{26}H_{53}OH$	polygonal	bimole--cular	Phase con. Elec. Mic. M.B.I.F.	the influence of the presence of imperfect dislocations on the growth pattern discussed; single, double and four-fold interlaced spirals; growth patterns due to growth round perfect dislocations in the presence of imperfect dislocations; polysynthetic and contact twins	Acta Cryst., 9. 16
1956	Amelinckx, S.	paraffin (monoclinic) $C_{34}H_{70}$; benhic acid; n-alcohols $C_{34}H_{37}OH$	polygonal	—	Phase con. Elec. Mic. M.B.I.F.	interlaced patterns; it is found that in crystals of tetratriacontane and benhic acid successive growth layers can be turned through 180°, and that this kind of stacking fault is responsible for the growth of polytypic crystals; growth round imperfect dislocations in (contd.)	Acta Cryst., 9, 217

Year	Author	Crystal and face	Shape of Spiral	Step height	Method used	Other details and remarks	Reference
						(contd.) benhic acid does not produce polytypes; first example of doubly interlaced pattern	
1953	Anderson, N.G. and Dawson, I.M.	stearic acid $C_{17}H_{35}$-COOH	polygonal	47± 10 A°. bi-molecular;	Elec.Mic. shadow casting; Metl. Mic.	crystals prepared by re-crystallization of a solution in petroleum ether; silicon monoxide replica of stearic acid crystals used; retardation of growth by impurity particles; movement of dislocation; dissociation of steps; both substances are found polymorphic	Proc.Roy. Soc., A 218, 255
		paraffin n-nonatriacontane	" "	45±10 Å. uni-molecular			

Year	Author	Crystal and face	Shape of Spiral	Step height	Method used	Other details and remarks	Reference
1955	Anderson, N.G. Dawson, I.M.	n-propyl n-penacto-ntanoate, $n\text{-}C_{53}H_{106}O_2$	polygonal; closed loops; twin lath-like growth	75±12Å.	Elec.Mic. Ni-Pa shadow casting (15°)	(a) growth arises from sheet nuclei consisting of small condensed monomolecular films; screw dislocations arise at the edge of these sheets through the condensation of molecules in positions of incomplete register; (b) these crystals frequently occur with a twist boundary parallel to (0001) face; this twist boundary is penetrated by a screw dislocation or a group of dislocations	Proc.Roy. Soc., A 228, 539

Year	Author	Crystal and face	Shape of Spiral	Step height	Method used	Other details and remarks	Reference
1957	Bontinck, W.	Fluorite synthetic	helical dislocations; rows of closed loops	-	decoration process; Ultra Mic.	rows of closed loops and special features described and discussed; double rows of etch pits identified with the emergence points of the parts of helical dislocations obtained by cleaving through helices; axes of helices are at small angles with <110> direction	Phil. Mag., 2, 561
1957	Bontinck, W. and Amelinckx, S.	Fluorite synthetic	helicoidal dislocation lines; closed dislocation lines	very large	decoration process	thermal treatment at 1100°c; decorated helix shaped lines form when a dislocation of mixed character climbs as vacancies condense on it	Phil. Mag., 2, 94

Year	Author	Crystal and face	Shape of Spiral	Step height	Method used	Other details and remarks	Reference
1958	Dash,W.C.	Silicon (deformed)	dislocation jogs; polygonal spirals	-	decoration and etching	trails behind dislocations moved by plastic deformation; trails arise from non consecutive motion of jogs causing injection of vacancies in the crystal; trails sometimes zigzag suggesting alternate gliding and climbing	J.Appl. Phys., 29, 705
1953	Dekeyser,W. Amelinckx,S. Votata, E. and Vandermeersscha, G.	Zn S (111)	-	-	Elec.Mic.	sets of etch channels, observed; they were made up of individual pits; pits represent sites of dislocations along slip lines	Phil. Mag., 44,1142
1952	Dawson,I.M.	paraffin n-hectane $n\text{-}C_{100}H_{202}$	Polygonal; closed loops	125±5Å.	Elec.Mic.	step height equal to x-ray value of the chain length along c-axis; spiral dislocations on lath-shaped crystals	Proc. Roy. Soc.,A 214,72

Year	Author	Crystal and face	Shape of Spiral	Step height	Method used	Other details and remarks	Reference
1951	Dawson, I.M. and Vand, V.	long chain n-paraffin; n-hexatriacontane; $C_{36}H_{74}$; basal planes	polygonal		Elec.Mic.	small crystals grown from a solution in petroleum ether were shadow-cast with palladium; spirals due to dislocations of unit and multiple strength observed; photographs of unimolecular spirals shown	Nature, 167,476
1951	" "	"	"	"	45±5Å.	"	step height equal to size of X-ray unit cell ~~(47-~~ (47.51Å.)	Proc. Roy.Soc., A.206, Roy 555
1957	Dawson, I.M. and Watson, D.H.	n-pentacontanol-1 $C_{50}H_{101}OH$	polygonal lath shaped crystals formed	molecular and bimolecular	Elec.Mic.	a series of polar and non-polar solvents used; growth from polar solvents - monomolecular steps; growth from non-polar solvents - mostly bimolecular steps; and some monomolecular steps; step height is determined by the size of the associated group of molecules in (contd.)	Proc. Roy. Soc.,A 239, 349

Year	Author	Crystal and face	Shape of Spiral	Step height	Method used	Other details and remarks	Reference
						(Contd.) solution; twin growth occurs more extensively from non-polar solvents than from polar solvents; habit modification observed; only one of many crystals examined showed existence of polytypism	
1957	Ellis, S.G.	Silicon and (100) & (110) faces of germanium	Spiral etch pits	1000Å.	-	crystals grown slowly from melt; it was assumed that the lateral rate of etching is constant and that the point of nucleation moves in a circle	Phil. Mag., 2, 1285
1951	Forty, A.J.	CdI_2; (during growth); (0001); tabular crystals	polygonal; closed loops; triangular	750±100Å.	Metl. Mic. M.B.I.F.	crystals growing from acqueous solution; high visibility; visibility considerably increased by using a narrow illuminating pencil of light; spiral growth on both unpurified and re-crystallized CdI_2 crystals	Phil. Mag., 42, 670

Year	Author	Crystal and face	Shape of Spiral	Step height	Method used	Other details and remarks	Reference
1952	Forty, A.J.	Cd I_2; (0001); during growth, from acqueous solutions	hexagonal; two co-operating triangular (circular at the centre)	several hundred Å; sometimes over 1000Å.	vert. bright field illumination; Metl.Mic. Phase con. double transmission	growth layers not monomolecular; giant dislocations; even multiples occur with slightly greater frequency than odd multiples; different stages of growth shown by a sequence of photographs; kinking of step lines due to interaction of screw dislocation groups of different strengths; growth patterns similar to those on sic; hence CdI_2 could be polytype; hollow dislocations; cross laced patterns; co-operating spirals; formation of closed loops	Phil. Mag., 43, 72

Year	Author	Crystal and face	Shape of Spiral	Step height	Method used	Other details and remarks	Reference
1952	Forty, A.J.	Cd I_2	polygonal	several hundred Å.	Phase con. int. interference; metal shadowing	step structure on both surfaces of crystal plate, centred on same dislocation group	Phil. Mag., 43, 377
1952	Forty, A.J.	Cd	circular	very thin layers; step height thought to be 5Å.	Phase con. decoration by plasticine	crystals grown from their vapour in vacuo or in an inert atmosphere; step height estimated from their visibility; growth steps probably monomolecular; co-operating spirals observed on Mg crystals; growth steps decorated; no measurement of step height made	Phil. Mag., 43, 949
		Mg	circular	monomolecular;			
		Zn	no evidence of spiral growth;	probably 5 Å.			
		(0001)	closed loops only				

Year	Author	Crystal and face	Shape of Spiral	Step height	Method used	Other details and remarks	Reference
1953	Forty, A.J. and Frank, F.C.	Ag cubo-octahedron; cube faces; octahedron faces	polygonal closed loops; circular	thought to be uni-molecular	Phase con. decoration with plasticine	crystals were grown from their vapour in vacuo or in inert gas atmosphere inside a furnace; unit slip lines observed; slip by movement of dislocation, density of dislocation very low; 1 or 2 dislocations emerge on a face $1/10$ mm. sq.; crystals much more perfect	Proc. Roy. Soc., A 217, 262
1952	Forty, A.J.	Mg (0001) thin hexagonal flakes	circular	less than 20 Å.	Metl.Mic. Phase con. M.B.I.F. decoration; thin film technique	crystals obtained by sublimation; step height estimated to be either one or two atoms in thickness	Phil. Mag., 43, 481

Year	Author	Crystal and face	Shape of Spiral	Step height	Method used	Other details and remarks	Reference
1950	Griffin, L.J.	Beryl, $(10\bar{1}0)$	razor blade	$8 \cdot 5 \pm 1$ Å.	Metl.Mic. bright-field illumi--nation	photographs taken slightly offfocus; step height equal to X-ray value (7·9Å.) of repeat distance; unimolecular steps; no kink in Fizeau fringes; loops of layers and pair of unlike screw dislocations; 100 dislocations in an area of $7 \cdot 6 \times 10^{-3}$ sq.cm; in some parts no sign of screw dislocation in several sq.cm. area	Phil. Mag., 41, 196
1951	Griffin, L.J.	Beryl, $(10\bar{1}0)$	razor blade	-	Metl.Mic. Barakat's method	maximum visibility obtained with N.A. laying between 0·45 and 0·15	Phil. Mag., 42, 775
1952	Griffin, L.J.	"	"	"	Metl.Mic.	slight anomalies in the layer pattern interpreted as due to movement of the dislocation over a short distance; limited slip zones explained in terms of the generation of dislocations by Frank-Read sources	Phil. Mag., 43, 827

Year	Author	Crystal and face	Shape of Spiral	Step height	Method used	Other details and remarks	Reference
1951	Griffin, L.J.	Beryl. $(10\bar{1}0)$ Nat. & Syn.	razor blade	-	Metl.Mic.	dislocation theory also true for ionic crystals (e.g. beryl) with complex molecules and grown from solution; propagation of growth fronts past a dislocation group explained; complex topography discussed; lineage boundary; limited slip zones; behaviour of growth fronts at obstacles; super-saturation = 0·5%	Phil. Mag., 42, 1337
1952	Horn, F.H. Fullam, E.F. and Kasper, J.S.	AlB_2 artificially prepared; thin hexagonal	hexagonal	200 Å. and also small steps	Metl.Mic. M.B.I.F. Elec.Mic.	crystal etched; this produced one hole which was remarkably round; diameter of hole 1 - 20 μ.	Nature, 169, 927

Year	Author	Crystal and face	Shape of Spiral	Step height	Method used	Other details and remarks	Reference
1952	Horn,F.H.	Graphite	hexagonal; some with curved edges at the centre	500 Å. much larger for other spirals	Metl.Mic. M.B.I.F.	density of dislocations $\sim 10^4$ per sq.cm.; graphite may be poly-type; co-operating spirals also	Nature, 170,581
1952	Horn,F.H.	Si-C	circular and polygonal	not measured	Metl.Mic. bright field and dark field illuminat-ion; replica technique	crystals etched in fused alkali carbonate mixture k_2CO_3 : Na_2CO_3= 3:1 at 1000°c; screw dislocat-ions, etch figures and holes observed; holes attributed to the prefer-ential chemical attack at a screw dislocation; holes result from rapid dissolution; under such conditions of rapid etching the etch figure may be used to identify the centre of a spiral or more particularly to iden-tify the position of a (contd.)	Phil. Mag., 43, 1210

Year	Author	Crystal and face	Shape of Spiral	Step height	Method used	Other details and remarks	Reference
						(Contd.) screw dislocation; holes when small are round; when large they become hexagonal	
1951	Kalb and Wittborg	Si-C	Spiral lines observed	not measured	-	-	Naturwiss. 38, 156
1952	Korndorffer, A. Rahbek, H. and Sultan, F.S.A.	Cd I_2 growing in thin plates	hexagonal	-	Metl.Mic. reflection and transmission	crystals grown from solution; a drop of solution placed on a microscope slide; this was placed on C.T.S. microscope; crystals subjected to mechanical deformation by an indentation process, which leads to growth by spiral mechanism	Phil Mag., 43, 1301

Year	Author	Crystal and face	Shape of Spiral	Step height	Method used	Other details and remarks	Reference
1952	Mason, B.J. and Owston, P.G.	Ice crystals grown from vapour; $(10\bar{1}0)$; and (0001)	hexagonal (unusual spiral form)	-	-	incomplete hexagonal prisms with 'hopper' development of both prism faces (rectangular) and basal faces (hexagonal); this is not an example of crystal growth by spiral dislocations, for the crystals are made up of successive two-dimensional spiral layers and not one continuous three dimensional spiral	Phil. Mag., 43, 911
1954	A.M.Abdou (Méléka)	Zn highly pure grown from melt	-	-	Metl.Mic.	crystals when left in atmosphere: corrosion etch pits rapidly developed on the surface and their positions can be distinguished along slip lines and at random; when etched with 20% chromic acid: for rapid attack, etch pits group themselves along slip lines; on prolonged etching existing etch pits on slip lines are (contd.)	Phil. Mag., 45, 105

Year	Author	Crystal and face	Shape of Spiral	Step height	Method used	Other details and remarks	Reference
						(Contd.) deepened, while new ones develop at random	
1956	Méléka, A.H.A.	Zn highly pure	growth spirals ($hape?)	-	-	indexing dislocations by the presence of etch pits; crystals etched in 1% iodine in alcohol; assumed that every pit represents a site of a single dislocation of unit strength	Phil. Mag., 1, 803
1924	Mellor,J.W.	Si C	-	not measured	-		A comprehensive treatise on inorganic and theoretical chem., 5, 879
1929	Menzies, A.W.C. and Sloat,C.A.	Si C basal planes	spiral markings observed	no measurements made	-	spirals could be seen even with a hand lens; because of absence of any theory no explanation given	Nature, 123, 348

Year	Author	Crystal and face	Shape of Spiral	Step height	Method used	Other details and remarks	Reference
1958	Miller, G.T. and Lawless, K.R.	cuprous oxide formed on cu-single crystals	polygonal (circular at the centre)	100-200 Å.	Elec.Mic; Metl.Mic; shadow casting	spirals were present in most cases only on (111) and not on (100) & (110) faces; usually complex spiral patterns; dislocations of large Burgers vectors occur, perhaps being made stable by impurities; spirals usually appear on large and not on small oxide crystals, which indicates that they originate when two crystals of small disorientation collide with each other during growth	J.Appl. Phys., 29, 863
1949	Padurow, N.B.	Si C	polygonal	-	-	-	Neues Fb. Min. Geol. Palaont. A 9, 203

Year	Author	Crystal and face	Shape of Spiral	Step height	Method used	Other details and remarks	Reference
1953	Reynolds, P.M. and Verma, A.R.	stearic acid; basal planes; $CH_3(CH_2)_{16}COOH$	Polygonal; evaporation spirals	45±5Å. 46·1±0·9Å. (note in proof)	Phase con. M.B.I.F. int. reflection	step height equal to height of unit cell; step height odd half integral observed; tabular crystals produced by slow evaporation of a drop of the solution placed on a clean cooled microscopic slide; circular spirals obtained by rapid evaporation of a drop of solution upon a warmed glass plate	Nature, 171, 486
1958	Reynolds, D.C. and Greene, L.C.	CdS grown from vapour phase; (0001)	polygonal; (circular at the centre)	-	-	growth patterns, chemical etch patterns and vaporization patterns observed; single and interlaced spirals; collapse of lattice after growth was completed	J.Appl. Phys., 29, 559
1952	Seager, A.F.	Pyrite; cube faces	polygonal and closed loops	steps thought to be multimolecular	Metl.Mic.	surfaces not silvered, step height estimated from visibility; thick layers appear to separate into thin ones in some places	Nature, 170, 425

Year	Author	Crystal and face	Shape of Spiral	Step height	Method used	Other details and remarks	Reference
1952	Steinberg, M.A.	Titanium; hexagonal flakes; (0001)	hexagonal (after few turns)	240±100Å., 100 Å. in some cases even less than 100 Å.	Metl.Mic. bright field illumination; M.B.I.F.	crystals produced electrolytically (electrolysis of fused salt); also closed loops due to two dislocations of opposite sign observed	Nature, 170, 1119
1958	Sunagawa, I.	Haematite; (0001)	triangular	2·3 Å.	Phase con. M.B.I.F.	step height equal to 1/6 unit cell; saw tooth structure triangular layers and piled up triangular layers observed and step heights measured; possibility of polytypism suggested; crystals must have grown under high surpersaturation conditions	Journ. Miner. (Japan) 3, 543
1958	Sunagawa, I.	Haematite; (0001)	triangular; triangular / circular / irregular; irregular (contd.)	2·3 Å. 14 Å. high step 20-1000 Å. (contd.)	Phase con. M.B.I.F. Feco.	etching and growth mechanism discussed; explanation for the mechanism of twin formation is proposed; depression spiral; spiral (contd.)	Publ. from Geol. survey of Portugal (in Press)

Year	Author	Crystal and face	Shape of Spiral	Step height	Method used	Other details and remarks	Reference
			(contd.) etch spiral	high; no exact measure-ments		(contd.) growth from misfit boundary, misoriented crystal etc. discussed	
1958	Sunagawa, I.	Si C (0001)	triangular; hexagonal; circular	5, 10, 15, 140, 160 380, 1300 Å.	Phase con. M.B.I.F. Feco	interlaced star shaped spirals; Frank-Reed source; movement of dislocation; co-operating spirals	Private Communication
1956	Van der Vorst, W. and Dekeyser, W.	Rock salt with AgCl as an addition	decorated dislocation lines; net composed of hexagonal and lozenge shaped cells	-	Ultra Mic.	Nacl-Ag system used; specimens treated at 500°c; decoration poor at lower temperature; method very reliable for the production of visible dislocation net-works	Phil. Mag., 1, 882
1959 (17-10-'59)	Talansky, S. and Sunagawa, I.	Synthetic Diamond; cube face.	polygonal	estimated to be a couple of hundreds Å; (less than 1000 Å.)	Phase con.	very tiny crystals; grown in the usual way of the synthesis of artificial diamonds; crystals being very small no interferometric work could be carried out; step height estimated from the width of white fringe in the positive phase-contrast micrograph;	Nature, (in Press).

Year	Author	Crystal and face	Shape of Spiral	Step height	Method used	Other details and remarks	Reference
1951	Verma, A.R.	Si-C; (0001) type I	circular		Phase con. M.B.I.F. Feco	density of dislocation varies widely on different specimens, ranging from a few to 10^4 per sq.cm.; radius of the nucleus $\sim 2\mu$; supersaturation $\sim 0{\cdot}2\%$; on any one crystal dislocations are predominently of one hand	Nature, 167, 939
		type II	hexagonal (interfaced)	15·1 Å. (unit cell high)			
1951	Verma, A.R.	Si-C basal planes			Phase con.		Nature, 168, 430
		15 R	-	12±2 Å.		step height = $\frac{1}{3}$ lattice parameter of unit cell referred to the hexagonal axes;	
		33R	-	28±2 Å.	M.B.I.F.		
		159 R	hexagonal (circular at centre)	130 Å.		step height = a_{rh} of rhombohedral cell; step height = a_{rh} = giant unit cell	

Year	Author	Crystal and face	Shape of Spiral	Step height	Method used	Other details and remarks	Reference
1951	Verma, A.R.	Si-C	hexagonal 7 groups; hexagonal; (circular after few turns)	-	Phase con.	interlaced spiral and grouping of steps; spots on edges of steps; these spots may be end of edge dislocations	Nature, 168, 783
1951	Verma, A.R.	Si-C basal planes; 6H; 15R	circular and hexagonal -	14·1 to 15·3 Å. → 17·1 Å. → -	Phase con. M.B.I.F. Feco. -	impurity increases visibility of steps; co-operating spirals; interlaced spirals with 'spider-web' structure; fish-like obstruction; radius of nucleus $\approx 2\mu$; super saturation $\approx 0{\cdot}2\%$; density of dislocation varies from a few to 10^4 per sq.cm.; steps one unit cell high	Phil. Mag., 42, 1005
1952	Verma, A.R.	Haematite (Fe_2O_3) basal planes	triangular (become hexagonal)	16±3 Å.	Phase con. M.B.I.F. Feco	core of spiral not hollow; closed loops generated due to two dislocations of opposite sign	Nature, 169, 540

Year	Author	Crystal and face	Shape of Spiral	Step height height	Method used	Other details and remarks	Reference
1952	Verma, A.R.	Si-C	hexagonal; circular; hexagonal loops	620 Å. 120 Å.	Phase con. M.B.I.F. Feco.	dissociation of steps in three different directions; growth steps are multiple of X-ray unit cell; dislocation of multiple strength; two unlike dislocations give rise to closed loops with no trace of dislocation at the centre; groups of dislocations arranged in a line or in an elliptical hole give rise to spiral steps	Phil. Mag., 43, 441
1952	Verma, A.R.	Haematite; basal planes	triangular hexagonal; etch spiral pit	12·4 —16 Å. 11·5 Å. 100 Å. total depth 1000 Å.	M.B.I.F. Feco	hexagonal closed loops; very close spacing of two spirals indicate that growth of these pyramids took place at quite a high supersaturation; density of (contd.)	

Year	Author	Crystal and face	Shape of Spiral	Step height	Method used	Other details and remarks	Reference
						(contd.) etch pits $\sim 10^7$ per sq.cm.; etch pits started at end of dislocations; triangular pyramids with broken and irregular steps of heights of a few microns with a flat triangular top with rounded corners	Proc. Phys.Soc, B~~65~~, 806
1953	Verma,A.R. and Reynolds,P.M.	stearic acid; $CH_3(CH_2)_{16}COOH$	Polygonal and leaf-shape	46.3±0·8 Å. for elementary spirals	Metl.Mic. Phase con. M.B.I.F. thin film technique int. int~~f~~	crystals grown from solution; steps unit cell high; also steps half integral and multiples of unit cell found; shape of innermost steps do not correspond to [110] direction; this may have resulted due to some kind of movement of dislocation after growth had ceased	Proc. Phys. Soc., B 66, 414, and 989

Year	Author	Crystal and face	Shape of Spiral	Step height	Method used	Other details and remarks	Reference
1955	Verma, A.R.	palmitic acid crystals; $CH_3(CH_2)_{14}COOH$	hexagonal	integral multiples of X-ray repeat distance also half integral multiples; $1\frac{1}{2}$ bi-molecular unit	Metl. Mic. M.B.I.F. int. interference fringes	crystals grown from dilute solutions at approximately $0^{\circ}C$; two polymorphic forms; interlaced and co-operating spirals; dissociation of steps along diagonals; exhibit polytypism; large dislocations, their movements macroslips and cleavage illustrated	Proc. Roy. Soc., A 228, 34
1953	Votava, E. Amelinckx, S. and Dekeyser, W.	Zn-S; (111)	polygonal (not well developed)	about 500 Å.	Metl.Mic. Phase con. M.B.I.F.	step heights judged from visibility, no exact measurements made; extensive substructure and cross linking of growth fronts explained by movement of dislocation	Physica, 19, 1163

Willis (1952) has carried out an extensive study of growth pyramids on natural and synthetic quartz crystals, and has shown that these pyramids are produced by the spreading of multimolecular growth sheets from several initiating centres. He established that the gradient of the pyramid increases near the summit, and evaluated the size of the critical nucleus. He also observed a slip line, terminating at both its ends, on a major rhombohedral face; its step height was from 0 Å. to 950 Å.. Griffin (1950) and Willis (loc. cit.) found growth cones two to three light waves high on some quartz crystals; some of these cones had a protuberance. According to Willis, growth initially starts from a number of nuclei ($\sim 10^4$ per. sq.cm.) but as growth proceeds most of them become inactive and growth mainly takes place from only a few growth centres. Circular growth fronts were found on some Brazilian quartz crystals.

Tetrahedral growth pyramids were observed by Praagh and Willis (1952) on some prism faces, and according to them growth of prism faces is faster in a direction perpendicular than parallel to the triad axis. They found that the steep side (in the rhombohedral zone) of the vicinal hillocks causing the horizontal striations on the prism faces of quartz crystals had inclinations up to 15° from the prism faces.

Tolansky (1945) has shown, by virtue of the sensitivity of multiple beam interference fringes, that quartz vicinal faces are not truly plane, but possess a slight cylindrical curvature with a radius of curvature of 20 - 60 meters.

Kalb (1930, 1933, 1934) studied the interfacial angles of a large number of crystals from several different localities by means of a reflection goniometer. He discovered that the vicinal faces on any given habit face occurred in sets of three, although in certain special cases one or two of the set were absent, and each set constituted the three sides of a low growth pyramid.

The angles between the vicinal sides of the pyramids were of the order of five minutes of arc.

Seager (1952) has published a photograph which illustrates the ease with which layers on prism faces of quartz completely surround particles of impurity on the surface of the crystal. On the R face of a quartz crystal from the iron mines of Cumberland he found remarkable regularity of spacing of the layer edges which seems to indicate a rhythmic process of layer initiation. He has also given the various permutations and combinations of the rate of initiation and rate of spreading of growth layers which lead to plane, concave, convex or complex profiles of crystal surfaces. He observed that although in some cases of quartz crystals, layers appear to have spread round and engulfed solid particles of an impurity with no indication of hindrance, there were cases in which layers passed the particles of impurity and left growth shadows.

P A R T III

SPECIAL TECHNIQUES

C H A P T E R V

Special Techniques

5·1. Introduction:

Interferometry is a well established technique, and has been accepted as a powerful tool in studying a range of problems connected with the surface examination of materials, an authoritative account of which is given by Tolansky (1948). The particular importance of interferometry in crystal growth problems has long been recognized because it has enabled precise measurements of the thickness of growth layers to be made and without this information the mechanism of crystal growth would have remained unexplained. The interpretation, manipulations and calculations obtained from multiple beam interferograms depend upon the quality of the fringes in terms of definition, resolution, and contrast, and these in turn depend upon the interferometric gap; the narrower it is the sharper the fringes and the greater the precision of measurement. For a small interferometric gap, the surface under examination and the reference surface must be very close together, and this can only be obtained if the former is flat. The surface to be studied may not always be sufficiently flat, and may, sometimes, be quite uneven. At times a specimen may have a flat surface but may be so thin that in an attempt to obtain a narrow interferometric gap, the optical flat may be pressed too hard against the specimen, and the latter may break. Various difficulties have arisen in the past in interferometric work but each time solutions have been found for each particular problem. At times crystals were required to be studied, during the actual process of growth (Bunn 1949), and interferometric methods had

to be suitably adopted. Verma (1955), Forty (1952 a,b) and Verma and Reynolds (1953) used internal reflection interference fringes, Verma (1951, 1952) utilized fringes of equal chromatic order to determine the step height of spirals in some cases, while Willis (1952) exploited Fizeau fringes at geographic dispersion to study the properties of growth pyramids on natural quartz.

Tolansky and Omar (1952) used a thin film technique, where a drop of canada balsam was placed on a crystal surface, and then drawn in the form of a thin film with the help of cedar wood oil. They applied their method to flat surfaces since they were not faced with the problem of interferometric work on irregular surfaces. This was a technique which in practice was erratic. They obtained fringes which are not considered sharp in comparison with those obtained and illustrated in the present work, despite the complex and irregular nature of the surfaces dealt with here. One can readily compare their interferograms with those presented here, and appreciate the importance and usefulness of this improved technique, which makes use of a solution of colladion.

The problem, in the present case, was to obtain fringes on some pieces of quartz with extremely irregular faces. One specimen was a piece of natural quartz reclaimed from an autoclave after only five hours running and observations thereon are described and illustrated in chapter X. The remainder were basal planes of synthetic quartz, all of which were covered with a number of mole-hills, or spiral growth pyramids, and these are illustrated and discussed at length in chapter VI. It was difficult to find a flat area, even a small one, on these faces, and the few found were located in awkward positions beyond the reach of an optical flat or even a microflat. The irregularity of these surfaces demanded some special interferometric technique, and a suitable one has been developed, and found to

give surprisingly good results.

With the help of this improved technique, the author has been able to push high resolution technique to extreme limits, obtaining superb interferometric definition even at a magnification as high as X 2000.

Conditions which must be satisfied for the formation of high-definition multiple beam interference fringes are:

(i) The surface under examination must be coated with a film which has reflectivity as near unity as possible and yet has simultaneously a low absorption.

(ii) This film must contour the surface microtopography to within molecular dimensions.

(iii) The two surfaces between which multiple beam interference is produced must be very close to one another, particularly so for the higher microscopic magnification.

(iv) The reference surface against which the surface under study is to be matched must itself be free from structure.

(v) Optical collimation must be exact.

Tolansky and Bhide (1956) have established that a correctly deposited thermally evaporated silver film has surprisingly faithful contouring properties.

5·2. Improved Collodion Thin Film Technique:

The Surface to be studied is first thoroughly cleaned, and then coated with a silver film about 700 to 1000 Å. thick using a vacuum coating unit. A very dilute solution of collodion in acetone or amyl acetate is then poured on to it, and whilst it is wet another but thicker solution of collodion is quickly poured on top, after which the crystal is allowed to drain. Immediately after draining, the surface is viewed, in reflection, in the light from mercury arc lamp. The gradual change in the thickness of the film can be followed from the coloured reflection fringes, and by judicious inclination a straight wedge can be produced in

a desired direction.

The first coating of thin collodion will not only contour the microtopagraphy which it contacts on its lower surface (that in contact with the crystal) but in drying, the upper surface also tends to follow the lower. There is then a marked tendency for the formation of a film of more or less uniform thickness following the crystal microtopography. The second, the thicker one, forms a reasonably flat top surface, at least in the small regions in which we are interested. When completely dry it is coated with another silver film of such a thickness as to give about 70 per. cent. reflectivity. In this way a very small interferometric gap is obtained between two silver films, which will give high definition multiple beam interference fringes in reflection. If the crystal is transparent, and if fringes in transmission are desired, since they can give more information than reflection fringes, the second silver film should be of such a thickness as to give about 90 per cent. reflectivity. It should be noted that both the solutions of collodion should be applied very quickly and in such a way that they spread over the whole crystal face quite smoothly and that the second must be applied whilst the first is still wet. Every care should be taken to avoid wrinkling the collodion films, by tilting the crystal to obtain uniform spreading of the collodion, particularly over the area of interest, and ionic bombardment should be avoided in the vacuum coating unit prior to coating the crystal with the second silver film. Suitable concentrations of the two solutions, which should of course be free from dirt, can with experience be worked out. A correct thickness of the second silver film gives high contrast fringes and a correct thickness of the collodion film between the two silver films gives high dispersion sharp fringes.

Irregularities in the surfaces of these crystals prevented the use of an ordinary optical flat, and although especially

prepared microflats could be used with some advantage, and also could be used to confirm the results obtained with this improved thin film technique, nothing surpassed the latter. Limitations to the use of microflats will be referred to in a later section.

The advantages of this system are:

(i) The upper surface of collodion film is perfectly smooth (in terms of extension of the optical microscope).

(ii) It is completely rigid and hence thicker silver films than normal can be tolerated, and as there is no fear of creeping longer exposures can safely be used.

(iii) Collodion film is thin enough to permit the use of high numerical aperture objectives and thus full resolution of the optical microscope can be exploited. It also creates ideal optical conditions for localized multiple beam interference fringes.

(iv) Curvature of the top surface of collodion film is quite negligible, at least over the small regions encompased by the high power microscope, and the contouring of the crystal surface is faithful.

(v) The refractive index of collodion is 1·400 and since the fringes are formed in this medium, the fring separation is no longer $\lambda/2$ but $\lambda/2\mu$, and for green mercury it is 1940 Å. instead of 2730 Å. . This means there is about 40 per. cent. gain in sensitivity.

5·3. <u>High Definition Multiple Beam Interference Fringes with High Lateral Magnification and Resolution</u>:

The quite remarkable interferometric resolving power obtained from this thin film collodion technique is illustrated in fig.25, a multiple beam interferogram for a piece of quartz, the structures of which are described in chapter X. Even at a high magnification (X2000) the fringe definition is surprisingly good, the contrast is excellent, and this is perhaps one of the best multiple-beam interferograms to be recorded. This

interferogram taken with a good 4 mm. objective, N.A. 0·95, gives high lateral magnification with high resolution, and repetition with a different film proves that the contouring by the lower film is effectively perfect. For each repetition the dispersion and direction of the fringes are different, but this does not invalidate the conclusion arrived at as to the close fidality of contouring, because the former is only a matter of chance orientation and thickness of the film-wedge formed. Owing to the thin character of the collodion film, high resolution results and owing to the correct thickness of the second silver film on the top of the first, high contrast and definition are also obtained.

Kinks in the fringes reveal microstructures on the crystal surface. Each kink corresponds to a rut mark which is revealed by the microscope. Fringes are $1/7$th mm. apart on the crystal face. On the print they are 280 mm. apart and since this corresponds to a real height difference of 1940 Å. the magnification in depth within the fringe pattern has the remarkably high value of about 1,450,000.

The fringe-width on the print is appreciably less than 2 mm. i.e., less than $1/140$th of an order separation. From a careful estimation the fringe-width is found to be about $1/200$th of an order separation which means that it occupies only 10 Å..

The displacement at the point marked by the arrow A is very nearly equal to the fringe width, indicating that the rut is 10 Å. deep. Still smaller displacements are measurable and it will not be an exaggeration to claim that there are a few shifts which correspond to about 2·5 Å. elevation or depression. The resolution is much higher than that formerly claimed by this school of interferometry.

Let us now find out the smallest volume element resolvable

in this way. Such an element can be resolved in depth down to $2{\cdot}5 \times 10^{-8}$ cm. and in lateral extension down to 7×10^{-5} cm. , and thus the volume element resolvable is

$$(2{\cdot}5 \times 10^{-8}) \times (7 \times 10^{-5})^2 = 1{\cdot}75 \times 10^{-17} \text{ c.c.}$$

Another example of the great resolution in depth obtained by this technique is illustrated by the rut marked by the arrow B which has a measured depth of 50 Å. .

5·4. Evaluation of step Height from a Single Fringe:

Because of the only crude control of the wedge angle, the local conditions and accident dispersion may create a situation in which only one fringe is obtained in the field of view; of course it will be an exceptionally sharp fringe. In such cases there is no other fringe to compute fringe dispersion. Use of fringes of equal chromatic order is one solution to this difficulty, while another is to exploit the known fringe width as a measure of dispersion; or one can proceed as follows.

Obtaining an exceptionally sharp fringe passing over a number of features in the region of interest, the shift in the fringe due to each feature is measured in turn. Using a glass microflat, of suitable proportions, a second interferogram is obtained from which the height (or depth) of the largest of the selected features is calculated in the usual way. This interferogram will of course be at a lower magnification and the fringes will not show any measureable shift for very small structures which are clearly defined by single sharp fringe in the previous interferogram. Using this value as a reference datum, heights (or depths) corresponding to small shifts in the single sharp fringe can be calculated. Under good experimental conditions step heights of 10 Å. and probably less can be measured.

Fig. 26 illustrates such a case. The fringe passes through a number of tiny triangular structures. Magnitudes of depths

of each of these will be given in chapter X.

5·5. Fringes on Spirals:

The success, importance and usefulness of this improved collodion thin film technique were realized in the study of the basal planes of synthetic quartz.

Fig. 27, an interferogram of a spiral on a basal plane of synthetic quartz, clearly brings out the nature of the surface profile, where the fringe definition is fairly good. It was found impossible to run fringes across growth fronts and over the summit of a spiral hill with the help of a special microflat of glass or perspex, the method of preparation and use of which are given in sections 6 and 7 of this chapter. Another similar example is shown in fig. 53 in chapter VI.

Furthermore, fringes at geographic dispersion over a spiral growth pyramid on such an irregular face were not very difficult to obtain with this technique, one illustration of which is shown in fig. 28. Obtaining fringes at low but uniform dispersion over such an uneven face was also proved to be a possibility as shown in figs. 29 and 30 for spiral patterns shown in figs.39 and 40 (chapter VI) respectively.

All these interferograms at high magnifications, ranging from x 175 to x 2000, exhibit good quality fringes and prove that this technique can be exploited fully, but if collodion solutions are not of the correct concentration or if their films are not of the right thickness, nothing will be achieved. Vigilance at each stage is absolutely necessary.

5.6. Plano-Concave Glass Microflats:

A fairly rough estimate of the radius of curvature of different spiral growth hills on basal planes of synthetic quartz was made, and a number of plano-concave lenses having this order of magnitude of radius of curvature were selected. After protecting both surfaces of the lenses with plane glass plate and

watch glass of suitable radius of curvature a microflat was cut out from the central part of each lens using a copper tube as a boring rod, and carborundum and water as cutting medium. The sides of the microflat were then ground in the shape of a cone, with a suitable semi-vertical angle and its generating surface was polished. After removing the two protecting pieces of glass the microflat obtained is a miniature plano-concave lens, and can be used with advantage.

Fig. 31 a multiple beam interferogram, obtained using a glass microflat, prepared as explained above, for one of the spiral growth pyramids on a basal plane of synthetic quartz clearly shows that the surface between successive turns is not flat but convex, without abrupt steps, and this confirms the results obtained from the thin film technique. These results are described and discussed in detail in section 12 of chapter VI. One disadvantage with such a microflat is that high dispersion fringes could not be obtained, only fringes at geographic dispersion or very nearly so. The main factor responsible for this is that such a microflat has a perfectly spherical surface while a spiral growth pyramid has something between a cone and a hemisphere. There is no solution to this difficulty except to use a special microflat whose surface is a replica of the surface of the growth pyramid under consideration, which would be very expensive and not easy to produce either.

Another limitation to the use of a glass microflat is the radius of curvature, because plano-concave lenses with different radii of curvature, particularly for small values, are not readily available. This difficulty could, however, be overcome by using perspex microflats, where a wide selection of radius of curvature is possible, and at practically no cost.

5·7. Perspex Microflats:

A thin perspex rod is cut into small pieces each of which is shaped in the form of a cone, and then mounted in a conical brass jig specially prepared for the purpose. Supporting, at the top end, a ball bearing of required radius but having an extremely smooth surface, and a piece of pyrex glass at the base of the jig, the whole assembly is kept well pressed between the jaws of a clamp, and after heating it, in an oven, to about 160°c. allowed to cool slowly. Perspex becomes soft in the range 140°c. to 180°c., and hence the cone used will take the shape of a plano-concave lens, the curvature and quality of the spherical surface of which will, of course, depend on those of the ball bearing used. Such a microflat could be used for interferometric work on a surface covered with growth hills. A similar experiment was tried using marbles of different radii instead of ball bearings.

Cleaning the surface of a perspex microflat with hydrogen peroxide or soap solution or even by ionic bombardment is not advisable because it has been found that in doing so the surface is attacked, which means that such a microflat could be used only once with advantage. A few microflats were successfully prepared in this way. It should be remembered that sudden cooling strains perspex, and would render the microflat useless.

Fig. 32 illustrates Fizeau fringes, obtained using a perspex microflat, for a spiral shown in fig.35 (chapter VI).

As with a glass microflat, difficulty with dispersion does arise, and a way was thought out and tried but proved unsuccessful in this case. The crystal under study was heated to about 160°c. , and a perspex thin rod was maintained pressed against one region, say a spiral growth pyramid, and then the whole assembly was allowed to cool slowly, keeping the perspex rod pressed against the crystal throughout the whole process.

The end of the perspex rod in contact with the crystal takes exactly the same shape as the spiral pyramid, and hence a microflat cut from this rod can be expected to give fringes at the desired dispersion, i.e., high dispersion fringes running across the growth fronts of a spiral. But in this case an unavoidable difficulty arose in that the spiral turns produced a similar ridge on the surface of the microflat so that in spite of the smoothness and the right sort of curvature of the surface, it could not be used; polishing the surface made matters even worse. Although this method of preparation was not fruitful in the present case, it undoubtedly had its merits.

P A R T IV

GROWTH FEATURES ON SYNTHETIC QUARTZ

C H A P T E R VI

Spiral Patterns on Basal Planes of Synthetic Quartz

6·1. Introduction:

A Microtopographical study of over five hundred rhombohedral and prism faces of natural as well as synthetic quartz crystals was carried out, as a result of which a wide variety of interesting features were observed. One of the more outstanding observations was the presence of spiral patterns on both types of quartz, and this is the first clear evidence of the growth of quartz crystals by spiral mechanism. Perhaps it would not be out of place to mention here that a great deal of experimental evidence in favour of the dislocation theory of crystal growth has come from this laboratory, because it was here that Griffin (1950) obtained the first evidence of spiral patterns on beryl, Verma (1951, 1952) obtained a variety of patterns connected with spirals on silicon carbide and haematite, and very recently unbelievable though nevertheless true, growth layers only 2·3 Å. thick have been observed by Sunagawa (1958). The visibility of such small features is probably the limit of resolution for an optical microscope. To this record a contribution is made in the present work in the form of observations of spirals on quartz.

A very interesting and striking feature of the spirals observed on the basal planes of synthetic quartz crystals is that unlike spirals observed by Griffin, Verma, Amelinckx, Forty and others, these spirals have rippled convex profiles without abrupt steps. This is the first observation of its kind, in that the surface profile of these spiral growth pyramids is quite dissimilar to those previously observed, the surface between successive turns of a spiral being convex and not flat. This is

established by means of multiple beam interference fringes obtained with the help of an improved collodion film technique especially developed for the purpose. In the present chapter spiral patterns observed on the basal planes of synthetic quartz will be described and discussed, while those on natural quartz will be considered in chapter XII.

6·2. Specimens and Methods of Observation:

One of the specimens examined was a slice showing a natural C-face cut out from a Y-bar crystal which had been grown, in a run, on a seed crystal in the form of a bar in the Y-direction with about a 3 mm. square cross-section. Although the crystal was fairly transparent its surface was covered with a large number of mole-hills very difficult to deal with by interferometry. Each of the mole-hills was found to be a spiral growth pyramid, though in some cases it was very difficult to resolve growth fronts near the summit. The other synthetic quartz crystals examined were grown in a similar manner, but unfortunately no information was available about the size of the seed plates.

The phase contrast microscope was unsuitable for the study of the basal planes of synthetic quartz, because the faces were not sufficiently flat, and hence only a metallurgical optical microscope was used. Since the basal planes were invariably covered all over by a large number of hillocks of different heights and slopes it was very difficult in some cases to get uniform illumination in the field of view. As a result, some photographs were taken with aperture wide open, while some were taken with oblique illumination. In addition, some photographs were taken slightly off-focus because this increases the visibility of thin layers which otherwise could not have been traced.

Crystal faces were thoroughly cleaned, and then coated with silver films 500 to 700 Å. thick, using a vacuum coating unit.

These surfaces were then examined under a microscope visually or interferometrically. The large number of randomly distributed spiral growth hills of various heights and slopes prevented the use of an ordinary optical flat for interferometric work, and hence special techniques were evolved and used successfully. These include a thin film technique and the use of special micrflats of glass and perspex, a full account of which is given in chapter V.

6·3. Simple Spirals:

Fig. 33 is a photomicrograph showing one of the most beautiful triangular spirals observed on the basal planes, the step height of which is found, with the help of multiple-beam Fizeau fringes, to be about 5000 Å. . Fig. 34 illustrates another example of a triangular spiral where it should be noted that although its outer turns give an impression of a single spiral, close examination near the initiating centre shows three spirals originating from a close group of dislocations. This point will be referred to in section 12, at the end of the chapter. Although most of the spirals observed on the basal planes of quartz are triangular, some irregular, fig. 35, and some circular, fig. 47(a), spirals have also been observed, the latter will be dealt with in detail in section 8 of this chapter.

6·4. Co-operating Spirals:

Fig. 36 illustrates two spirals originating from a point with their arms strictly parallel to one another. Such spirals have been observed by Verma (1955) and Forty (1952). Fig. 37 provides another example of this kind but in this case the arms are not parallel. Growth fronts tend to bunch together in certain directions thereby increasing the visibility. The horizontal black line passing through the centre is a scratch on the crystal face.

6·5. Closed loops generated by Frank-Read Sources:

If two unlike screw dislocations having equal strength terminate on a crystal face growth will take place and closed loops of growth fronts will be formed if the distance between the points of emergence of the dislocations is greater than the size (diameter) of the critical nucleus (Frank and Read, 1950). If the distance of separation is less than this critical value no growth will take place. Fig. 38 is a photo-micrograph showing two unlike screw dislocations of equal strength forming closed loops. Fig. 39 provides another example of the formation of closed loops due to a Frank-Read source. Although there is no evidence of dislocation at the centre it would be absurd to attribute them to growth by two-dimensional nucleation because a number of spirals are distributed all over the crystal face and, in fact, there are about six spirals in the immediate vicinity. The two dislocations forming the loops must have annihilated. Similar cases of closed loops of growth fronts without any trace of dislocation have been reported and explained by Forty (1952), Anderson and Dawson (1953) and Verma (1952).

Fig. 40 also illustrates closed loops, formed in a similar way, but the inner ones are circular and the outer ones triangular, while a tube-like structure is visible near the centre which changes direction at three points, each time turning through 60°. It is evident from the figure that the growth fronts are affected wherever the tube crosses them. It is suggested that some kind of liquid impurity may have originally formed this tube, or alternatively that this is a result of the movements of two dislocations during growth. Unfortunately no evidence could be obtained in favour of either suggestion, because the crystal was on loan and no etching or indentation experiments could be carried out.

6·6. Interlocked Spirals:

An interesting example was found in which one spiral was interlocked with another, and this is illustrated in fig. 41(a). In addition to the main growth fronts of a triangular spiral some faint lines are also visible which are in fact the thin growth fronts of another spiral. This is shown more clearly in fig. 41(b) which is a photomicrograph of the same spiral taken slightly off-focus thus increasing the visibility of the thin growth layers (Griffin, 1950; Amelinckx, 1952, a,b.). Although the growth fronts of these spirals do not cross each other, sharp corners of the thin spiral do touch the growth fronts of the thick one and at these points kinks in the thicker one are observed. This means that both the spirals were growing simultaneously with their respective Burgers vectors, the thicker one having rounded corners while the thinner one having sharp corners. Both the spirals are multi-molecular. Interlaced spirals have been observed by Verma (1954), Forty (1952) and Amelinckx (1952, 1956, a,b).

A polytype crystal would show interlaced spirals but observation of an interlaced spiral need not necessarily be taken as evidence for polytypism. To determine whether this crystal is a polytype or not, 15° oscillation X-ray diffraction photographs were taken, from which the following observations were made:

$$a'^{*} = \frac{2\lambda}{a} \qquad \text{and} \qquad c^{*} = \frac{\lambda}{c}$$

Here $\lambda = 1{\cdot}54$ Å. ; $a = 4{\cdot}9$ Å. ; $c = 5{\cdot}39$ Å.

$$a'^{*} = \frac{2 \times 1{\cdot}54}{4{\cdot}9} = 0{\cdot}6250 \text{ R. U.}$$

$$c^{*} = \frac{1{\cdot}54}{5{\cdot}39} = 0{\cdot}2857 \text{ R. U.}$$

(Take 1 R.U. = 10 cms.)

C	R.U.	Cms.	a	R.U.	Cms
1	0·2857	2·857	1	0·6285	6·285
2	0·5714	5·714	2	1·2570	12·570
3	0·8571	8·571	3	1·8855	18·855
4	1·1428	11·428	4	2·5140	25·140
5	1·4285	14·285	5	3·1425	31·425
6	1·7142	17·142	6	3·7710	37·710
7	1·9999	19·999	7	4·3995	43·995

Using these values of 'C' along X-axis and those of 'a' along Y axis, a reciprocal net was drawn, and is shown in fig.42, which is reduced to $1/_5$th of the original.

For zero, second and fourth layers point O_1 was taken as origin (i.e., the axis of rotation passes through point O_1), and for first, third and fifth layers point O_2 was taken as origin. Observations are given below.

Crystal face parallel to incident X-ray beam;

Reading on the scale ..... 228° - $42'$.

Crystal turned through 30° towards incident X-ray beam;

Reading on the scale ..... 198° - $42'$.

Crystal allowed to oscillate through 15°: 198°-$42'$ —— 213° - $42'$. .

Layer	Point on net	X-ray spot	Height above zero level R.U.	Horizontal distance from centre	Indices
	O_1				000
	A				$\bar{1}20$
Zero	B				$\bar{2}40$
	C				$\bar{3}60$
	D				480
		1	0·00	0·86	003
		2	"	1·56	$\bar{1}25$
		3	"	1·90	245
	O_2				-
	A				010
	B				$\bar{1}30$
First	C				$\bar{2}50$
	D				370
		4	0·18	1·18	014
		5	"	1·46	015
		6	"	1·72	$\bar{1}35$
		7	"	1·94	254
	O_1				100
	A				020
	B				$\bar{1}40$
Second	C				$\bar{2}60$
	D				380
		8	0·36	0·57	102
		9	"	0·86	103
	O_2				-
	A^2				110
Third	B				030
	C				$\bar{1}50$
	D				270
		10	0·55	1·18	114
		11	"	1·72	035
	O_1				200
	A^1				120
Fourth	B				040
	C				$\bar{1}60$
	D				280
		12	0·72	1·31	120

In the X-ray photograph, fig. 43, there is only one set of spots indicating the presence of one stacking order only. If there had been additional spots very near to those in the photograph they would have indicated the presence of another stacking order. The total absence of such spots, near the main ones, rules out the possibility of any other additional stacking order and from this it may be concluded that the crystal is not a polytype.

Fig. 44 provides another example of this kind where three spirals originate from a very close group of dislocations, and the steps tend to bunch together in certain directions thereby increasing the visibility. This tendency of thin layers to bunch together in certain directions was also shown in fig. 37.

6·7. Interaction of Spirals:

As already mentioned above, the basal planes of quartz are covered over with a number of mole-hills, each being a spiral growth pyramid, interaction between spirals in such cases is neither uncommon nor unexpected. Fig. 45 shows a spiral, the growth fronts of which meet, in the lower half of the figure, seven dislocations, seen as black dots, which being comparatively weaker are dominated by the former. If these black dots were impurities they would cast shadows as the growth fronts move past them (see chapter VII), and the tadpole-like features seen in fig. 45 should have been depressions, but by using the light profile technique (Tolansky 1952) it was established that these features are in fact elevations. Domination of weaker dislocations by stronger ones has been observed by previous workers. Fig. 46 illustrates a similar case where candle-shaped features in the lower half of the figure are elevations. As a result of interaction between two or more spirals, growth forms may take quite a variety of strange shapes. Two illustrations have already been given in figs. 45 and 46, and two

much more interesting examples in the shape of a 'snail', are given in figs. 47(a) and 48(a), and described and discussed below.

6·8. Snail-shaped features:

Out of the many spirals examined on the basal planes of quartz, only a couple of cases of circular spirals were found. One of these is illustrated in fig. 47(a), where the outer turns are covered over by growth from other initiating centres giving it the shape of a 'snail'. It is evident that the rate of advance of the growth steps is independent of crystallographic direction, at least in this case. The turns of the 'snail' appear to be very nearly parallel to each other giving an impression that they all belong to one spiral only, but close examination indicates that the outer turns are not strictly parallel to each other suggesting thereby that they may belong to different spirals.

It should be noted that three independent members are seen to emerge from the centre of innermost turn, but only one of them seems to rotate to form the spiral, while the other two seem to become inactive very soon after the start, of course at the end of growth. Since most parts of the spiral have been covered over, it is difficult to say whether all the turns belong to one member, or to two or three members. Fig. 47(b) is a diagram showing the 'snail' as if it were a part of a circular spiral.

Fig. 48(a) illustrates another 'snail' which is a triangular spiral partly covered over by growth layers from other initiating centres (see fig. 48(b)).

6·9. Slip during growth:

Fig. 49, a photomicrograph, in fact shows a single spiral with a slip line passing very near its initiating centre, although the central region being somewhat scratched right at

first sight gives an impression of two independent growth centres. Due to some kind of stress, the crystal had slipped during growth and a step was formed. The fact that there is a layer to layer correspondence on either side of the slip line along its entire length indicates that growth steps on both sides of the slip line belong to one and the same spiral, and not to two independent spirals.

A similar case is illustrated in fig. 50 where two independent initiating centres are clearly seen and yet there is still a layer to layer correspondence on either side of the slip line, except possibly at the centre where it is difficult to trace growth fronts. Strict correspondence between the outer growth layers could be accounted for by growth from a close group of dislocations which, before the end of growth, was divided into two by the slip line, each group thereafter forming growth fronts of its own for which of course no strict correspondence could be expected. A similar form of growth may have occurred in the case shown in fig. 49 but the region at the centre being scratched precludes conclusive analysis.

6·10. Hollow Dislocations:

A black dot is distinctly visible at the initiating centre of the spiral shown in fig. 51 and similar dots are also visible though less distinctly, in some of the other spirals presented here. These, it is suggested, are hollow dislocations because according to Frank (1951) the core of a dislocation whose Burgers Vector exceeds 10 Å. may be an empty tube. As most of the spirals presented here are due to giant dislocations it is possible for their cores to be empty tubes, although such dislocations without empty cores are not uncommon.

6·11. Nature of Surface of Spiral Pyramids:

Surfaces between successive turns of spirals observed by previous workers were flat and this is also the case for the

spiral observed on a natural quartz crystal, which is illustrated and described in chapter XII. The profile of such a spiral growth pyramid is shown schematically in fig. 52(a), and may readily be compared with fig. 52(b), which is a schematic representation of the profile of a spiral growth pyramid observed on the basal planes of synthetic quartz. The latter diagram indicates that the surfaces between successive turns of the spiral are not flat but convex. Fig. 53, a multiple beam interferogram, obtained using the new thin film technique (see chapter V), for one of the spirals on a basal plane of synthetic quartz clearly brings out the nature of the surface of the spiral pyramid. The convex nature of the surface between successive turns is very well established by the curved fringes which would otherwise have been straight, and since the fringes run continuously while climbing over the edges of the growth layers it can be concluded that there are no abrupt steps in the spiral. The profiles of all the other spirals on the basal planes of quartz are similar. This is the first observation of a spiral with such an unusual profile since the birth of the dislocation theory ten years ago, and is more fully discussed in the following section.

At this stage, it should be made clear that the step height refers in such cases to the total vertical height between successive turns although there may be a number of growth layers, in between, which are unresolved.

6·12. Discussion:

1. Profile of Spiral Growth Pyramids:

As already mentioned, the surfaces between successive turns of all the spirals observed up till now on a variety of crystals have been flat, and this is also the case for spirals observed on a natural quartz crystal, described in chapter XII. On the other hand, surfaces between the successive turns of spirals on the basal planes of quartz are convex, which being the first

observation of its kind requires an explanation. Such a surface profile could come into being as a result of one of two mechanisms: (a) Etching or (b) Bunching.

(a) Etching: It is possible that the basal planes were first covered by growth spirals and after growth had finished, etching may have taken place during the cooling of the autoclave. Etching would proceed two-dimensionally and finally round off the corners, leading thereby to the formation of convex surfaces between successive turns. However, the absence of any strong evidence of etching in any part of the crystals, and the remarkably uniform nature of the spiral growth fronts and smoothness of the surfaces of some of the spirals leads one to conclude that this mechanism is unlikely to be responsible for such a profile.

Undoubtedly the surfaces of some of the spirals presented here are mottled, which might lead one to suspect etching, but no strong evidence of etching was obtained in any part of the crystal faces. The mottled nature of the surface may be due to deposition of quartz during the last stage of growth. This suggestion is substantiated by observations given in chapters VII and IX.

(b) Bunching: In the majority of spirals observed on basal planes the outer turns give the impression that they are singular, but close examination near the initiating centre shows that there is more than one component starting from the centre which can only be traced in the central region. Such observations suggest that each step is composed of a group of growth fronts bunched together in such a way that each group forms a convex surface between successive turns, but the growth fronts are so closely spaced that it is difficult to resolve them individually.

Frank (1958) has theoretically worked out the profile of surfaces, for both cases of etching and growth, and has also discussed the bunching phenomenon, which confirms the explanation given above for the profile of spiral growth pyramids presented here. It can therefore be stated conclusively that bunching and not etching is responsible for the observed rippled convex profile in the present case. The author admits that etching can produce convex profiles.

. 2. Mechanism of Growth:

From the detailed study of a large number of faces of natural and synthetic quartz crystals it is found that dislocations and well developed spirals are much more frequently found on the basal planes of synthetic quartz than on the rhombohedral faces of either type. Furthermore, the basal planes of synthetic quartz are invariably covered all over with randomly distributed mole hills of different heights and slopes. All this can easily be accounted for. A c-face is never or seldom found on natural quartz, while, an artificial crystal is often prepared from a cut c-plate which is used as a seed crystal on which growth is forced to take place. Here it is important and interesting to note that surfaces of such a cut c-plate are made quite rough by scratching or preferably by etching, prior to use as a seed plate. This provides a large number of growth nuclei, the majority of which are probably in the form of exposed ledges, which promote growth by spiral mechanism; once growth has been initiated in this way it does not require fresh nucleation and will continue indefinitely, subject of course to supersaturation conditions. For a variety of reasons growth of artificially prepared quartz crystals is carried out rapidly, although it is not theoretically desirable, and this is achieved by using roughened surfaces.

In the beginning the c-face is large, but gradually, as growth proceeds, rhombohedral faces tend to develop and the crystal tries to take the habit of natural quartz, i.e., c-faces tend to terminate into pyramidal ones, so that if growth were allowed to take place for a sufficiently long period no c-face would be left on a synthetic quartz crystal even though it originally grew on a c-plate. From this it can be said that a basal plane in quartz is a transitional face, and it may be considered a somewhat metastable one, on which, therefore, one would expect a large number of projections.

As mentioned above, a seed plate used for growing quartz crystals is usually scratched or preferably etched, and the exposed edges are screw dislocations in character with generally large Burgers vectors. Growth will start at these randomly distributed screw dislocation type ledges, which play the role of giant dislocations, and spirals with large step heights are formed. Since fresh nucleation is no longer required, growth continues and because the rate of growth in the direction of the c-axis will be much greater than in the direction perpendicular to it, spiral hills with steep gradients are formed on the basal planes. There is ample observational proof of this. As growth proceeds rhombohedral faces gradually develop while the basal planes tend to diminish in area and the axes of screw dislocations on the basal planes will meet the rhombohedral faces and may even become normal to them. One would, therefore, expect to find spirals on the rhombohedral faces with screw dislocation axes normal and in some cases inclined to the face. On rhombohedral faces, therefore, spiral patterns are to be expected and so also circular or irregular growth fronts with several, one or occasionally no initiating centre. Observations presented in chapter VII endorse the proposed mechanism.

Under these circumstances, therefore, a synthetic crystal may develop some extra faces which are not habit faces of quartz, and in fact such faces have been found on artificial crystals (see chapter VIII).

Furthermore, since in such cases the main growth takes place on the c-plate, and only subsequently on the rhombohedral faces, the rate of advance along the c-axis is much greater than in any other direction. Prism faces of such crystals could be considered to be developed as a result of the growth of basal planes and hence the striations normal to the c-axis will not be expected to be on them as those found on prism faces of a natural quartz crystal. Prism faces of a synthetic quartz crystal grown in this way should show traces of boundaries of interaction of several spiral pyramids and, since growth is predominent along the c-axis, these traces should appear as more or less vertical striations nearly parallel to the c-axis. That this is really the case is proved from the observations on prism faces fully described and illustrated in chapter IX.

However, this should not be considered to be the only way in which prism faces of synthetic quartz are formed; it is one of the possible ways in which they can and do come into being. It is quite likely that growth may take place on prism faces as well, in which case one would expect growth pyramids on prism faces also, and it would not be surprising if spirals are found on them. That such growth pyramids can and do occur on prism faces is proved by the observations described in chapter IX.

C H A P T E R VII

Topography of Rhombohedral Faces

7·1. Introduction:

In the present investigation about forty rhombohedral faces of synthetic quartz crystals were examined. Although most of these faces were bright, some exceptionally so, about half a dozen minor rhombohedral faces were found to be rather dull. About half a dozen faces were remarkably plane, while the remainder were uneven. Two faces were covered with a number of 'mole-hills' of different sizes and slopes giving them an appearance very similar to those on the basal planes. On some of the faces shooting-star shaped structures were observed and some showed the presence of impurities on them. A number of cases of growth round misorientated crystals were also found. Evidence of spiral patterns was also obtained.

7·2. Localisation of Centres of Initiation of Growth:

It is interesting to note that circular growth fronts were observed on all the faces without any exception. The number of growth centres on different faces varied widely but the tendency was to low numbers, and in fact on some faces there was only one initiating centre. Another striking observation was that the growth centres on any face were almost always near the end of the face which was farthest from the pyramidal termination, i.e. the growth fronts were convex when seen from the pyramidal termination. All these points of interest will be dealt with in section 7 of this chapter.

Fig. 54 is a photomicrograph illustrating circular growth fronts on a major rhombohedral face. Growth layers near the initiating centre are probably very thin and hence are not visible.

Because of the bunching of thin layers, those farther away from the centre of growth are fairly thick and are therefore visible. A similar case is illustrated in fig. 55. In the lower right half of the figure an almost vertical black line is visible, and there is a strict layer to layer correspondence on either side of this line. It indicates a step which, it is suggested, was formed by some kind of stress during the process of growth. Some boundaries of interaction of different growth hills are also visible in the upper part of this figure.

7·3. Growth round Misorientated Crystals:

A number of cases were found in which misorientated crystals played the roll of nuclei of growth on rhombohedral faces, and a couple of examples of these will now be described.

Fig. 56 is a positive phase-contrast micrograph illustrating a misorientated crystal on a major rhombohedral face, where circular growth fronts formed as a result of growth round this crystal are visible. Another example of this kind is illustrated in a positive phase-contrast micrograph, fig. 57, where a number of growth fronts are visible with a misorientated crystal at the centre. The surface surrounding the misorientated crystal was not sufficiently flat, and hence all parts were not properly phase contrasted resulting in uneven illumination in the micrograph. Fig. 58, a photomicrograph, shows growth round three misorientated crystals, which are not far away from each other. There is possibly a fourth misorientated crystal, which has given rise to the growth fronts which are visible in the central part of the top edge of the figure. Growth round misorientated crystals, settled on prism faces of a host crystal, will be described in chapter IX.

The observations described above suggest that some, if not all, rhombohedral faces were formed as a result of growth round misorientated quartz crystals. In some cases these misorientated crystals drop out at some stage of growth leaving cavities,

while in others they remain as projections on the faces of the host crystals. The observations described above and in section 5 of this chapter are of the latter type, while those described in section 4 of chapter IX are of the former.

7·4. Bubble-like Structures:

On a few rhombohedral faces bubble-like features were observed, all of which were found to be elevations having different magnitudes of height ranging from a few tens of angstroms to a couple of light waves. They were found in isolated areas as well as in a dense aggregate. Although the small ones looked almost elliptical, the bigger ones were in fact bean-shaped, while a few had shapes something between that of a bean and an egg.

Fig. 59, a positive phase-contrast micrograph, illustrates two bean-shaped features with their tips orientated in the same direction, while fig. 60 illustrates a similar case where a shooting star shaped structure is visible with a closely packed group of small bubble-like structures at its narrow end. In fig. 61, another positive phase-contrast micrograph, a large number of these features are visible both in isolated places and in aggregate. A feature which looks very much like a tadpole is illustrated in a photomicrograph, fig. 62, and some circular lines are clearly visible inside it.

Interpretation of all these features (figs. 59 to 62) will be deferred until the next chapter.

7·5. Spirals on Rhombohedral Faces:

Two rhombohedral faces of a synthetic quartz crystal, which in appearance were very similar to the basal planes of synthetic quartz (see chapter VI) in that they were covered with a number of 'mole-hills', showed the presence of spiral patterns. Fig. 63, a positive phase-contrast micrograph, illustrates a number of such small spiral patterns and figs. 64 and 65 are two

more illustrations of growth by spiral mechanism. In each of these figures there is a misorientated crystal, growth around which has given rise to some of the spiral patterns, illustrated here. The growth layers in these cases are so thin that it is very difficult to trace them, and because of the uneven nature of the surfaces the complete area in these photographs was not properly phase-contrasted.

7·6. Role of Impurities:

About a dozen faces showed the presence of impurities both scattered and in aggregate. Although most of the faces were covered with impurities scattered here and there, one face was very much more densely covered over the whole surface as shown in fig. 66, a positive phase-contrast micrograph. Fig. 67, another positive phase-contrast micrograph, illustrates the manner in which growth fronts behave when they advance past an impurity, while fig. 68, the corresponding multiple beam interferogram, shows the nature of the surface which is formed in such cases. That it is in fact a valley that is formed due to growth layers spreading past an impurity is made clear in fig. 69 which shows fringes of equal chromatic order, corresponding to the displacement in the left half of fig. 68. From these interferograms it is evident that although the surface between two valleys is more or less flat, the outside surface has a convex cylindrical curvature.

Fig. 70 is a positive phase-contrast micrograph illustrating a series of valleys formed by growth layers spreading past a row of impurities. The nature of these valleys and the crystal surface in between neighbouring valleys are defined in fig. 71 which shows fringes of equal chromatic order for this region. Here the fringes are reasonably sharp with a good contrast.

7·7. Discussion:

The mechanism of the growth of quartz crystals grown on

c-plates has already been described at length in section 12 of chapter VI, where it was mentioned that spirals and circular growth fronts are to be expected on the rhombohedral faces of such crystals. The observations presented in this chapter prove the existence of such growth patterns on rhombohedral faces, and thereby endorse the proposed mechanism. As mentioned earlier, the basal planes are large at the beginning of growth but the rhombohedral faces gradually tend to develop and in doing so will meet the axes of dislocations on the basal planes. This will occur at some points farthest away from the pyramidal terminations, because in these cases the crystals develop from the central parts towards the pyramidal terminations. These points therefore are responsible for the growth on rhombohedral faces, at least in the early stage of growth. That this is indeed the case for the majority of faces is proved by the observations described in this chapter.

As growth proceeds, more and more centres of initiation are to be expected on rhombohedral faces, but all of them will not remain active throughout the process of growth; in fact most of them become inactive because the weaker ones are dominated by the stronger. In the present investigation it was found that the rhombohedral faces have much more impurity atoms adsorbed on them than the basal planes or the prism faces.

The observations of a number of cases of growth round misorientated crystals, described above, suggest that at some stage of growth small quartz crystals can and do settle down, in any misorientated position, on rhombohedral faces and act as growth nuclei. This strongly supports the view put forward in section 12 of chapter VI that the mottled nature of the surfaces of some of the spirals on the basal planes is due to the deposition of quartz and not due to etching. Another fact which supports this interpretation will be given in section 6 of chapter IX.

C H A P T E R VIII

Tadpoles on Rhombohedral Faces

8·1. Introduction:

Out of the total number of rhombohedral faces of synthetic quartz crystals examined, only one showed peculiar orientated tadpole-like features. It was a small portion of a minor rhombohedral ($01\bar{1}1$) face of a quartz crystal grown in an autoclave from a solution of sodium carbonate at a low supersaturation, at a temperature of 350°c. and a pressure of 1000 atmospheres. The seed used in this case was a rectangular plate 5 cm. by 3·5 cm. with the c-axis perpendicular to it, and a diad parallel to its breadth. The rate of growth was 0·5 mm. per day on each of the two faces of the seed-plate. The crystal face was very smooth and quite flat and therefore well suitable for interferometry.

8·2. Characteristics of Tadpoles and Other Related Features:

Fig. 72, a positive phase-contrast micrograph, shows two tadpole shaped features both of which have the same crystallographic orientation. That these features are elevations is clear from fig. 73 which shows fringes of equal chromatic order for one of these features. The crystal face was covered with a number of similar tadpole-like structures which although unevenly distributed all had the same orientation. This was found to be at 30° to the extinction position, when examined under a polarizing microscope.

In addition to tadpoles, bean-shaped features were also observed on this face, but their density was very low; only seven were found on the whole face (about 2 sq.cm.), and these were located in isolated regions. One of these is illustrated in

fig. 74, a positive phase-contrast micrograph, while fig. 75, a multiple beam interferogram in transmission, using the green and yellow doublets of mercury as incident light, shows that one of these features is about one and a half light waves high. Although all seven features of this type were of different heights ranging from about one to five light waves, they were all orientated in the same direction as the tadpoles. That the tails of the tadpoles and the tips of the beans point in the same direction is shown clearly in fig. 76, a positive phase-contrast micrograph of another region on the face. Fig. 77, a multiple beam interferogram in reflection shows the structure of the bean-shaped feature, while fig. 78, an interferogram in transmission using three wave-lengths (one green and two yellow), reveals the nature of the tadpole and here the fringe definition is particularly noteworthy. That these bean-shaped features are elevations is demonstrated in fig. 79 which shows fringes of equal chromatic order.

Besides tadpoles and beans, some egg-shaped elliptical features were also observed on this face, and as illustrated in a positive phase-contrast micrograph, fig. 80, these are also orientated in the same direction as the tadpoles and beans. The identity of the orientation of the tadpoles and these elliptical features is also very well brought out in fig. 81, a multiple beam interferogram in transmission, using three mercury lines, where once again the fringe definition is particularly good and the contrast excellent if one keeps it in mind that the yellow doublet is unresolved. These elliptical features were also found to be elevations ranging from about 150 Å. to about two light waves. It was found that the elliptical features are much more abundant than the tadpoles, while the bean shaped features are very few compared with the latter.

8·3. Tadpoles on Basal Planes:

A couple of tadpole-shaped structures were also observed on

a basal plane of a synthetic quartz crystal, and the author thought it better to incorporate them in this chapter rather than in chapter VI, because it may help in interpreting the observations described above.

Fig. 82, on ordinary photomicrograph, illustrates two tadpoles on a basal plane of a synthetic quartz crystal. It is clear that, unlike those observed on a minor rhombohedral face (see section 2 above), these tadpoles have no strict crystallographic orientation. It should be mentioned that these tadpoles are elevations, and the crystal face is covered with a large number of growth patterns connected with the spiral mechanism.

8·4. Structures on Non-Habit Faces:

As mentioned in chapter VI, synthetic quartz crystals occasionally develop some extra faces which are not the habit faces, and hence surface structures on such faces may be quite different from and perhaps more complex than those on the habit faces, viz. R, z, m, x and s faces. The crystal referred to in section 1 of this chapter had a small face in the form of a narrow strip which, in fact, was a part of a non-habit face of the main crystal. Fig. 83, a photomicrograph, illustrates some strange surface structures in the form of elliptical and circular discs on this face, each one of which was found to be a depression.

8·5. Discussion and Conclusion:

No irregularity was observed on the crystal face referred to in section 1 of this chapter, and even with the help of a phase-contrast microscope no growth layers could be traced and no kinks in Fizeau fringes were obtained. No evidence of the presence of growth layers on this face was obtained. The tadpoles, bean-shaped and elliptical features appear to have the same origin and although their interpretation is somewhat difficult the

following alternative suggestions are made.

Four possible explanations of these features will be discussed:-

(i) Inclusions.

(ii) Further growth on the cavities which presumably were formed due to orientated bubble inclusions blown off at some stage of growth.

(iii) Result of interaction of growth forms due to dislocations.

(iv) Local lattice disorder.

Since the crystal face under consideration was a natural (uncut) habit face of a synthetic quartz crystal, the question of polishing marks does not arise.

Because the features have bubble-like shapes let us assume that they were due to orientated inclusions. If they were included long before the end of growth they should have been overgrown and would not have appeared as elevations, but they would of course have been visible in the body of the crystal. It is possible that these features may be inclusions which were partly overgrown, and thus formed elevations on the surface. In the case of inclusions the material inside the bubbles could be water, carbon dioxide or something similar. When the crystal was examined in transmitted polarized light, no difference was found in the refractive index inside and outside these features. It is possible that the water or liquid carbon dioxide trapped in the bubbles may have been converted into the gaseous state and then escaped leaving hollow bubbles, in which case the refractive index inside and outside these bubbles would be the same. To investigate this possibility a number of these bean-shaped features were indented with a pyramidal diamond indentor, and it was found that they were solid and not hollow. Fig. 84 (a), a positive phase-contrast micrograph, illustrates two bean-shaped

features, where the right one was indented right across while the left one was not. This may be compared with fig. 59 which shows the same two features as they were originally. All the crystal faces which showed the presence of these features were then etched in the vapour of hydrofluoric acid, and it was found that they are not hollow (see fig. 84 (b)). No preferential etching was found to take place either along the boundaries or the tips of these features. Different stages of etching are illustrated in figs. 85 (a) & (b).

The fact that all these features are solid means that they are not bubbles now; at the same time, this does not preclude the possibility that they once were. They do in fact have the shapes of bubbles and when the unsilvered crystal is gradually racked down towards the objective of a microscope the inner side of each of them is found to be very similar to the top and has almost the same curvature. Fig. 86 (A) represents schematically different successive stages (a, b, c, d, e) when the crystal is racked down towards the microscope-objective.

This leads us to the second alternative that these features were orientated inclusions, and at some stage of growth they were blown off forming orientated cavities. The formation of the tails of the tadpoles and the tips of the bean-shaped features can readily be explained by the direction of flow of solution. Further growth takes place and because these cavities are quite large kinks the rate of adsorption of atoms will be much greater in the cavities than on the general crystal surface outside. Not only will the cavities be filled up rapidly but also a bump will be produced having about the same curvature as the surface of the original cavity inside the crystal. A further question then arises, viz. 'How is a bump formed after the cavity is filled up to the general level of the crystal surface?' In this case since

there is a discontinuity at points such as P and Q (see fig.86(B)), where the surface of the cavity meets the crystal surface, atoms which are adsorbed between P and Q cannot migrate to the general surface outside, and the rate of adsorption being greater for the cavity, continues to be so even after filling up the cavity, thus an elevation is formed. Different stages of growth, the decrease of curvature of the surface inside the cavities, its change of sign and finally the formation of an elevation are schematically represented (stages 1, 2, 3, 4 and 5) in fig. 86(B). From careful observations it was found that the under-sides of these features were appreciably further below the general crystal surface than their top sides were above it; e.g., the bean-shaped feature illustrated in fig. 74 has a lateral extension (on the crystal face) of about 0·25 mm. , its elevation above the crystal face is about 0·008 mm., while the distance of its lower surface from the crystal surface is about 0·7 mm. This means that the greater portions of the bubbles were covered over, and if they were not blown off they soon would have been completely overgrown and incorporated inside the crystal leaving no sign of elevations. If this is correct the profiles of the tadpoles, beans and the elliptical features should be as shown in figs. 87 (a), (b) and (c) respectively.

Fig. 62 (chapter VII) illustrates a feature very much like a tadpole; it is the only one of its kind on which the edges of the growth layers were observed. Whether or not these layers belong to a spiral pattern it is difficult to say because on the crystal face (major rhombohedral) no evidence of spiral patterns was obtained. Nevertheless this particular feature and the observation of two tadpoles, fig. 82, on a basal plane of another synthetic quartz crystal suggest that these features may have something to do with dislocations.

Let us now, therefore, consider the third alternative. In the case of the basal planes there are many 'mole-hills' which

are spiral growth pyramids; in addition one or two spiral growth fronts are visible, starting at the tips of the tadpoles which may be the centres of initiation. The formation of tadpoles as a result of interaction between several spiral growth pyramids is illustrated schematically in Fig. 88. Interactions between the growth pyramids due to dislocations 2, 3 and 4 form the tail of the tadpole, while those between 1 and others (not shown in the figure) form its body. This interpretation appears to be quite convincing for the two tadpoles (fig. 82) on the basal plane for which there is ample evidence of spirals, dislocations and a large number of spiral growth hillocks. On the other hand, tadpoles (figs. 72, 76, 78, 80 and 81) observed on the minor rhombohedral face referred to in section 1 of this chapter cannot be explained in this way unless there is some evidence of dislocations on this face. In fact no growth layers at all are visible and furthermore the surface is exceptionally flat.

Growth fronts visible on a tadpole-like structure (fig.62) on a major rhombohedral face could only be the edges of circular growth layers filling the cavity and then forming an elevation, because on this face circular growth fronts are clearly visible (see fig. 54) and there is no evidence whatsoever of spiral patterns.

The fourth alternative is as follows.

Due to some kind of stress during growth, a local disorder in the lattice may have been produced forming a misfit boundary (see fig. 89), and further growth might have resulted in the formation of these structures. An elevation, in such cases, is a possibility because the rate of growth in the misorientated part will be greater than elsewhere. This final explanation does not however seem very likely.

Having examined the merits and demerits of the four possible interpretations, the author feels that the tadpoles and similar features on the rhombohedral faces are best explained by the second alternative, while those on the basal plane fit in best with the third.

C H A P T E R IX

Topography of Prism and Trapezohedral Faces

(A) Prism Faces:

9·1. Introduction:

Prism faces of natural quartz crystals are characterized by horizontal striations perpendicular to the triad axis, and in fact such striations are of great assistance in orientating quartz crystals. These striations are considered to be a result of oscillatory growth between rhombohedral and prism faces (Dake, Fleener and Wilson, 1938). Praagh and Willis (1952) have observed tetrahedral growth pyramids on prism faces of natural quartz crystals, and according to them the rate of advance of the growth layers of these pyramids is greater in a direction perpendicular to the triad than in a direction parallel to it, and the longer edges of these layers appear as striations. In the present investigation typical horizontal striations are observed on prism faces of natural quartz crystals, and are described and illustrated in chapter XIII. On the other hand, vertical striations almost parallel to the c-axis are observed on prism faces of synthetic quartz crystals, and this, being the first observation of its kind, requires an explanation. These observations are described and illustrated below. Growth pyramids formed due to growth on prism faces are also described and illustrated. The mechanism of the formation of prism faces of synthetic quartz crystals is discussed in section 6 of this chapter.

9·2. Striations:

Fig. 90 a photomicrograph, shows vertical striations on a prism face of a synthetic quartz crystal, where the line AB is the trace of the basal plane, CD represents the edge between adjacent prism faces, and AE the trace of a rhombohedral face. Fig.91 illustrates a similar case for a prism face of another

synthetic quartz crystal having a small basal plane, trace which is visible in the top part of the figure. Here, vertical striations are intercepted in some places by horizontal irregular lines.

Fig. 92 shows the central part of a prism face of another synthetic quartz crystal where the edge between two neighbouring prism faces may be seen at the extreme right, with the trace of a rhombohedral face in the upper right half of the figure. From this photomicrograph it is quite clear that striations in the central part of a prism face are very closely spaced and irregular but in the upper part of the picture, near the pyramidal termination, there are relatively few striations, which are smooth and regular with fairly smooth surfaces in between. All these observations are accounted for in section 6 of this chapter.

9·3. Growth Pyramids:

On most of the prism faces of synthetic quartz crystals examined, striations almost parallel to the c-axis were observed and occasionally these striations were found crossed by some horizontal step-like structures perpendicular to the c-axis. However, on two prism faces of a synthetic quartz crystal growth pyramids having their growth centres very near the edge of intersection with the neighbouring prism face were observed.

Fig. 93, a photomicrograph, illustrates a growth pyramid on a prism face $\{2\bar{1}\bar{1}0\}$. At the growth centre of this pyramid there appears to be something which might have acted as a growth nucleus. It is of interest to note that the pyramid has a hexagonal boundary and that the line AB is the intersection of this face with the neighbouring prism face while BC is that with an ' x ' face which is visible as a triangle in fig. 93. Surface structures on this ' x ' face are described in section 5 of this chapter. A similar growth pyramid on another prism face $\{\bar{1}\bar{1}20\}$ of the same crystal is illustrated in fig. 94, where

once again the growth sheets comprising the pyramid are hexagonal. At the centre of initiation a cavity, having hexagonal outline, is visible. Two similar hexagonal depressions are also visible a little on the right of the summit of the pyramid.

From these observations it can be concluded safely that during some stage of growth small crystals of quartz must have got attached to the prism faces, and further growth must have taken place around such crystals forming thereby pyramids having hexagonal outlines. These crystals must have then dropped out at some later stage of growth, and thus hexagonal cavities are formed. On these two prism faces about ten unorientated hexagonal depressions of different sizes and depths were observed. This observation not only endorses the above given interpretation for the formation of hexagonal growth pyramids but also substantiates the suggestion given in section 12 of chapter VI that the mottled nature of surfaces of some of the spirals on the basal planes of synthetic quartz crystals is due to deposition of quartz (probably after switching off the furnace) and not due to etching. Existence of small mis-orientated crystals which were probably the growth nuclei for some of the rhombohedral faces of synthetic quartz has already been reported in chapter VII.

9·4. Negative Crystals on Prism Faces:

Fig. 95 is a photomicrograph showing two black patterns having hexagonal outlines; and fig. 96, a positive phase-contrast micrograph, illustrates a similar case where the pattern is nearly hexagonal. The internal structure of the hexagon in the left half of fig. 95 is shown in fig. 97, a positive phase-contrast micrograph. The patterns are depressions having different magnitudes of depths, and are randomly orientated and distributed. It can be said conclusively that these are

negative crystals, and were formed due to other small quartz crystals getting attached to this face with their c-axis either perpendicular or inclined to it, and then dropped out at a later stage of growth leaving thereby cavities having hexagonal boundaries.

9.5. Surface Structures on a Trapezohedral Face:

Only one synthetic crystal showed the presence of a trapezohedral face. It was a left handed crystal. Fig. 98 is a photomicrograph showing the trapezohedral face, where the line AB is the intersection of this face with the prism face $\{2\bar{1}\bar{1}0\}$, BC is that with the prism face $\{10\bar{1}0\}$ and AC is that with a major rhombohedral face. It is clear that the face is crossed by striations which are parallel to the edge AB. At about four or five isolated regions growth pyramids are visible. These pyramids are very much extended laterally in a direction parallel to the edge AB than at right angles to it, and have their longer edges very nearly parallel to AB. From these observations it can be said that the rate of advance of the growth layers constituting these pyramids is much greater in a direction parallel to AB than that perpendicular to it.

9.6. Discussion:

Mechanism of Growth of Prism Faces:

From the observations described in this chapter two possibilities arise about the development of prism faces:

(a) Unless there is an evidence of independent growth on them, prism faces could be considered to have been formed as a result of growth mainly on the basal planes and at a later stage on rhombohedral faces. As already mentioned in chapter VI these crystals were grown on cut c-plates, previously roughened by scratching or etching. Because of a large number of growth nuclei on such a seed plate growth starts rapidly, mostly by

spiral mechanism. Very soon a large number of growth hills develop and as growth proceeds interaction between layers from different growth centres is bound to take place. In the beginning the c-face is large, but gradually rhombohedral faces tend to develop as well as prism faces. Boundaries of interaction between different spiral growth hills manifest themselves as striations on prism faces, and since a c-face is the main growth face on which the rate of advance in the direction of the c-axis is very much greater than that at right angles to it, striations should be parallel to the c-axis or very nearly so (figs. 90, 91 and 92). In the early stages there are many growth centres and so there will be many such boundaries and hence closely spaced irregular striations appear in the central portion of a prism face (fig. 92). As growth proceeds, weaker dislocations are dominated by stronger ones, causing more and more growth centres to become inactive, and hence there will be fewer and smoother striations on prism faces near the pyramidal terminations (figs. 90 and 91).

Prism faces are not perfectly flat, in fact the area between two striations has a small cylindrical curvature, and this may be understood readily if one remembers that growth fronts on the basal planes are slightly convex. At some places, where growth layers on the basal planes do not extend laterally right to a prism face, a step is formed which appears as a practically horizontal striation on the prism face (fig. 91). At least some, though not all, prism faces of a synthetic quartz crystal can and do develop by this mechanism particularly when a large seed-plate is used. Some of the crystals examined were in fact grown on large seed plates and the cross-sections of the fully grown crystals were not much bigger than those of the seed plates. Furthermore, seed plates are usually rectangular while the cross-section of a quartz crystal is

hexagonal and hence development of prism faces by independent growth on them is quite expected or rather common.

(b) In the early stage of growth prism faces are developed as a result of growth on basal planes, and at a later stage growth may take place on prism faces as well. In the latter case, there will be some evidence of independent growth on prism faces, and the cross-section of such a crystal will be greater than that of the seed plate. Growth on prism faces may occur either by two dimensional nucleation or by spiral mechanism, depending upon the type of nucleus available. Exposed ledge of a screw character, impurities, misoriented crystals etc., can and do act as growth nuclei.

Observations described in this chapter endorse both the possible modes of development of prism faces.

It is very interesting to note that prism faces $\{2\bar{1}\bar{1}0\}$ and $\{\bar{1}\bar{1}20\}$ are never found on natural quartz crystals. This is for the first time that surface topography of such rarely occurring faces has been investigated and put on record.

P A R T V

GROWTH FEATURES ON NATURAL QUARTZ

C H A P T E R X

Topography of Rhombohedral Faces

10·1. Introduction:

In the present investigation rhombohedral faces of quartz crystals were found to be covered with orientated growth pyramids which were built up by the spreading and piling up of triangular growth sheets. Properties of such growth layers, associated growth of other crystals, natural etch patterns, dissolution figures, surface structures of red quartz etc. are described in this chapter, while the problem of twinning will be dealt with in the next one. Evidence of growth of natural quartz crystals by spiral mechanism will be given in chapter XII.

10·2. Centres of Initiation of Growth:

(a) Number:

The summits of the growth pyramids are the centres of initiation of growth layers. Although the growth of different faces of a crystal starts from a number of nuclei, all of them may not remain active throughout the growth of the crystal. In fact, most of the initiating centres become inactive in a relatively short time in the history of growth of the crystal, and the growth of each face is governed by a very small number of growth centres. This was found to be the case for most of the rhombohedral faces studied because, for most of them, about two or three initiating centres per face were found to remain active until the end of growth. It should be noted that about sixty faces were found with only one growth centre.

On a minor rhombohedral face of a quartz crystal, about ten big pyramids were found, one of which is illustrated in fig.117 but they became inactive and were partly covered over by growth

layers from only two closely spaced initiating centres.

(b) Localisation:

In a large majority of cases growth centres were found to be in the central part of a face, away from an edge or a corner. This is to be expected because these crystals grew by the two dimensional nucleation mechanism and according to Kossel (1927) the energy of formation of a two-dimensional nucleus is least at the centre of the face. Also according to Frank (1949,b) dislocation lines are under tension and tend to emerge normal to the face, i.e., towards the face centre. In fact the centres of initiation of spirals observed on a natural quartz (see chapter XII) and also those on the basal planes of synthetic quartz (see chapter VI) were at the face centres, far away from an edge or a corner. However, about twenty cases were found in which the initiating centre was on an edge and about ten cases in which the initiating centre was at a corner of a face.

Fig. 99, a photomicrograph, illustrates a minor rhombohedral face having the centre of initiation on the r - m edge. It is evident that (i) there is no other growth centre, (ii) thick layers have been formed, at regular intervals, due to bunching of thin ones and (iii) the gradient of the growth pyramid suddenly increases near the initiating centre. Another interesting case is illustrated in fig. 100 where three initiating centres are on different edges. The initiating centre on the left-half bottom of the figure may possibly be on a broken edge, but that on the right-half bottom is on the R - m edge, while the one on the right top is on the edge between the two neighbouring rhombohedral faces. It is suggested that the three pyramids built up by growth layers from these three centres developed at a later stage of growth on the pre-existing growth layers.

Fig. 101(a) is a photomicrograph of a minor rhombohedral face for which the centre of initiation is on the edge between this

face and the adjacent major rhombohedral face; Fig. 101(b) is the corresponding multiple beam interferogram which reveals the nature of the growth fronts. A similar case is illustrated in fig. 102, a multiple-beam interferogram for a minor rhombohedral face where fringes are set at a geographic dispersion. From this interferogram it is evident that the growth fronts are remarkable in being uniformly thick and regularly spaced. The position of the centre of initiation at a corner of a face is illustrated by the interferogram shown in fig. 103.

None of the cases of edge and corner nucleation described above can be explained by either the two-dimensional nucleation theory or by the dislocation theory. They can, however, be explained by considering the effect of adsorbed impurities on the growth process. Such impurity molecules may either be pushed along the face by the advancing growth layers, or grown over by the layers and get incorporated in the lattice as impurities. Cases of the latter type are not uncommon, while in the former type the impurity molecules will be pushed to the edge of one face where they become trapped by the growth layers spreading from the adjacent face. But even in this trapped position they can still behave as nuclei for fresh growth. Also, if these impurity molecules are pushed along the edge to a corner, corner nucleation can occur. It should be mentioned at this stage that all the faces which showed the existence of edge or corner nucleation were in fact found to have some impurities on them.

It is very interesting to note that about forty cases were found in which the centre of initiation of growth layers was very near to but not exactly on an edge or a corner. From these observations it seems that the centre of initiation of growth layers has a definite tendency to be very near an edge or a corner of a crystal face.

10·3. Gradient of Growth Pyramids and Flow of Mother Solution:

Tolansky (1945) using sensitive multiple beam interference fringes found that the gradient of a growth pyramid increases near the summit of the pyramid. His observation was made only on one major rhombohedral face of a natural quartz crystal and no explanation for it was given. In the present investigation, barring one case, no such increase in the gradient near the pyramid summit was observed; on the contrary, the gradient near the summit of many growth pyramids was found to be less than that away from it. A further interesting point in the present investigation was that on about forty rhombohedral faces one side of the growth pyramids was much steeper than the other two although, in such cases, there was no sudden increase in the gradient near the summit. To study this in greater detail five crystals were selected, and some of the observations on one of the crystals will now be illustrated and described.

All the growth pyramids on the natural quartz crystals examined were formed due to spreading and piling up of triangular growth layers. Each pyramid has, therefore, three directions of minimum growth - say α, β and γ as shown schematically in fig. 104. In all these cases the side in the direction of α or β was steep but never in the direction of γ. For the crystal under consideration let the three minor rhombohedral faces be denoted by r_1, r_2 and r_3, and the three major rhombohedral faces by R_1, R_2 and R_3. It was found that growth pyramids on r_1 and R_1 had steeper sides in the α - direction than in the β and γ directions, while the pyramids on r_2, R_2, r_3 and R_3 had steeper sides in the β - direction than in the α - and γ - directions.

Fig. 105 is a multiple beam interferogram for a growth pyramid on the r_2 face, wherein the fringes are set at a geographic dispersion. The fringes are more closely spaced in

the β - direction than in the α - and γ - directions, indicating that the right-hand side of the pyramid is steeper than the left and the bottom. Fig.106(a) is a similar interferogram for a growth pyramid on the face R_1, while fig.106(b) illustrates, at a lower magnification, multiple beam Fizeau fringes for about half of this face. Both these interferograms, set at a geographic dispersion, indicate that all the growth pyramids on this face, (about eight growth centres are revealed in fig.106(b) have their left-hand side steeper than the right and bottom. In figs.106(a) and (b) the fringes are more closely spaced in the α - direction than in the β - and γ - directions. Fig. 107 illustrates multiple beam Fizeau fringes for a growth pyramid on the face R_2, while fig. 108 shows an interferogram for a growth pyramid on the face r_1. In both these interferograms the fringes are again set at a geographic dispersion. In fig. 107 the fringes are more closely spaced in the β - direction than in α - and γ - directions indicating that the right-hand side of the pyramid is steeper than the left and the bottom, while the reverse is the case in fig. 108 for the face r_1. Fig.109 shows an interferogram for a growth pyramid on the face r_3, while fig.110 is for that on the face R_3; both interferograms were set at a geographic dispersion. From these interferograms it is clear that the right-hand side of both these pyramids is steeper than the other two. It was found that the steepness of the left-hand side of the pyramids on faces R_1 and r_1 decreases in the order R_1, r_1, while that of the right-hand side of the pyramids on the remaining faces of the crystal decreases in the order r_2, R_2, r_3, R_3. Thus if the crystal is held with the c-axis vertical and the edge between r_2 and R_1 facing the observer, the faces R_1 and r_1 on his right will have pyramids with their left sides steep, while the faces r_2, R_2, r_3 and R_3 on his left will have pyramids with their right sides steep. The face R_3 will of course be away from the observer, but since the pyramid on this face has the growth centre at the extreme right part of the

face, it can be considered to be on the left of the observer .

The gradient at the side of a growth pyramid is dependent on the spacing between the edges of the growth sheets, the smaller it is, the steeper will be the gradient. Thus pyramids on the faces R_1 and r_1 have more closely spaced growth fronts in the α - direction than in the β - and γ - directions, while the pyramids on the faces r_2, R_2, r_3 and R_3 have more closely spaced growth fronts in the β - direction than the α - and γ - directions. Now the spacing between successive growth fronts depends on the rate of advance of the growth fronts, the faster it is, the smaller will be the spacing. The rate of advance of growth fronts in turn depends on the number of molecules adsorbed at the steps, the greater it is, faster will be the rate of advance of the growth fronts. In the case of vein quartz the solutions supplying the silica were at one time flowing from one direction to the other. From these observations it is suggested that in this case the solution which supplied the material for growth of this crystal must have been flowing to the edge between the faces r_2 and R_1, where it then divided into two parts, one part flowing to R_1 and then to r_1, and the other to r_2, R_2, r_3 and then to R_3. This accounts very well for the steepness in the α - direction for the pyramids on R_1 and r_1, and, in the β - direction, for the pyramids on r_2, R_2, r_3 and R_3.

Such a flow may bring with it crystals of other minerals which would have most effects on faces they meet first, and least on those they meet last. In fact, the number of triangular, square, and hexagonal features having the boundary depressions, described in section 8 of this chapter, is a maximum for the face r_2, while their density decreases from R_1 to r_1 on the right, and also decreases in the order r_2, R_2, r_3, R_3

on the left of the observer facing the edge between r_2 and R_1. The systematic variation in the density of these features from one face to the other therefore endorses the interpretation given above.

More or less similar results were obtained for the steepness of one side of the growth pyramids on the other four crystals. The results are summarised as follows:-

crystal no. 3:

Face	r_1	R_1	r_2	R_2	r_3	R_3
steep side of the pyramid	left	left	right	right	?	right

Solution flowing to the edge between R_1 and r_2.

crystal no. 7:

Face	r_1	R_1	r_2	R_2	r_3	R_3
steep side of the pyramid	right	?	?	left	left	left

Solution flowing to the edge between r_1 and R_3.

crystal no. 8:

Face	r_1	R_1	r_2	R_2	r_3	R_3
steep side of the pyramid	right	?	right	?	right	left

Solution flowing to the edge between r_1 and R_3.

crystal no. 10:

Face	r_1	R_1	r_2	R_2	r_3	R_3
steep side of the pyramid	left	nil	right	left	left	left

Solution flowing to the face R_1.

Variation in Gradient of a Growth Pyramid:

In all the interferograms illustrated in figs. 105 to 110 fringes were set at a geographic dispersion i.e., parallel to the edges of growth sheets which compose the growth pyramids. Successive fringes indicate points which are at a difference of level of half a light wave (in this case 2730 Å. , mercury green light being used), so that the closer the fringes are, the steeper will be the region and vice versa. In all these cases, the fringe spacing decreases very gradually as one proceeds from the edge of a pyramid, ~~but~~ which indicates a gradual increase in the gradient. But near the summit of each pyramid the fringes are more widely spaced than in the lower parts which shows that there is definitely no sudden increase in the gradient of the pyramids near their summits. The greater spacing between successive fringes near the summit than away from it is very well seen in all these interferograms particularly in those illustrated in figs. 106(a), 107, 108 and 110.

10·4. Splitting up of Thick Growth Layers:

Bunching of thin growth layers is quite common in many minerals, particularly so in quartz. Just the reverse case was found on a major rhombohedral face of a natural quartz crystal, the growth fronts being very irregular. In three or four isolated areas on this face some thick growth layers were observed to have split up into groups of thin layers which again join together forming the corresponding thick layer in Fig.111. This photomicrograph shows the growth fronts on the major rhombohedral face; in the right half of the figure some ten layers are seen split up each into a few (3, 4 or 5 etc.) thin layers which re-join to form a thick one once more. This temporary splitting up of thick growth layers could possibly be due to some local variation in the supersaturation conditions

existing at the time of growth, although there is no real evidence to support this.

10.5. Interlacing:

An explanation of interlacing of the spiral step lines has been given by Frank (1951b). The interlacing arises from the dependence of the growth rates on crystallographic directions and the change of the growth rate of the monolayers in different orientations of the crystal. The slowest growing monolayer in one orientation may not remain the slowest growing in another orientation inclined to the first. Any change in the velocities of growth layers in different directions leads to interlacing of the growth steps and is illustrated schematically in fig. 112, where F indicates the fastest growing layer while S the slowest. (Intermediate monolayers between these two, having intermediate rates of growth are not shown in the figure). Verma (1951) and Amelinckx (1951) have observed interlaced spirals and interpreted them in this way.

Interlaced growth fronts were observed on a major rhombohedral face of a natural quartz crystal and are illustrated in fig.113. This pattern cannot be due to spiral-growth mechanism because all the growth layers on this face belong to different pyramids which grew by the two-dimensional nucleation mechanism. The angle between the two main sets of growth fronts is about 145°. If two growth layers inclined to one another at 145° have different velocities they may well produce interlaced patterns. This appears to be so in the present case.

10.6. Development of Prism Faces on Rhombohedral Faces:

Fig. 114 shows a minor rhombohedral face of a natural quartz crystal where, in addition to a large number of growth pyramids, about half a dozen black lines are seen clearly across the face.

At first one may think that these are slip lines but is not likely for the following reasons.

When incident light is perpendicular to the rhombohedral face these lines appear black on the white (bright) background of the face as shown in fig.114. On the other hand, when the crystal is turned through 142°, so that incident light, still falling on this face, is perpendicular to the prism face these black lines appear as white (bright) strips on the black background of the face. This proves that each of these black lines is a small prism face. Furthermore, the fact that each of these lines is strictly parallel to the r - m edge substantiates this interpretation. It should be mentioned that from some four hundred rhombohedral faces examined only two minor rhombohedral faces showed such a structure.

10·7. Percussion Marks:

In the present study it was found that the large majority of quartz crystals examined had received some kind of percussion, this being shown by percussion marks on the crystal faces all having a more or less similar character. Fig. 115, a photomicrograph, illustrates a percussion mark on a minor rhombohedral face of a natural quartz crystal. A similar case is shown in fig.116 for a major rhombohedral face of another crystal where indentation has taken place along a line giving rise to a series of percussion marks. The extent to which the resultant cracks extend along the surface and in the interior of a crystal depends on the load and is therefore different in different cases.

10·8. Replacement of Other Minerals by Quartz: (Pseudomorphism):

Out of all the crystals examined only two crystals showed unorientated triangular, square, and hexagonal features which will now be described and interpreted.

On all the faces of one natural quartz crystal unorientated square, triangular, and hexagonal features were observed but

their density was not the same for all the faces, one face being covered with a bundred or so while the others had only about ten or even a smaller number of these features. Even on one face their distribution was quite uneven.

Fig. 117 shows a big growth pyramid on a minor rhombohedral face of a natural quartz crystal. Small unoriented features of all the different shapes mentioned above are visible all around this pyramid and also on its top surface. Fig. 119(a) illustrates, on a higher magnification, some of these features. Since they all have different shapes and do not have the same orientation they could not be etch figures; nor could they be indentations by other cubic crystals growing along with quartz, which later became detached, since for both these suggestions the features should have been flat bottom depressions which they are not.

Fig. 118 is a multiple beam interferogram showing Fizeau fringes passing over some of these features on the top surface of the growth pyramid illustrated in fig. 117, while fig. 119(b) illustrates, at a higher magnification, multiple beam Fizeau fringes running over a triangular feature. Fringes of equal chromatic order illustrated in fig. 120 reveal the profile of a square-shaped feature, while those in fig. 121 show the profile of a triangular one. From fig. 120 it is clear that the suqare-shaped features have boundary depressions and the surfaces inside and outside the square features are on the same level. On the other hand, fig. 121 proves that although the triangular features also have very deep boundaries the surface within is irregular and lower than that outside. Fig. 122 illustrates two squares, one inside the other, with diagonal lines joining their respective corners.

These structures can be explained as follows. The solutions supplying the material for building up this crystal must have carried along with it a number of small crystals of

cubic habit (like fluorite). Some of these crystals then became attached at random on different faces of the growing quartz crystal. As growth proceeded quartz replaced wholly or partly the cubic crystals that had become attached to it. Subsequently the cubic crystals were dissolved away and since the boundary between a host and a guest crystal is a region of weakness, etching will take place preferentially along the boundaries which results in the formation of boundary depressions of the square-shaped features. In cases where the dissolution rate was faster than the replacement, an irregular surface would be formed (see triangular features). Such an irregular surface is in fact found to be lower than the general crystal face. Formation of one square inside the other (fig. 122) is the result of replacement of a cubo-octrahedral crystal by quartz. Variation in the density of these features on different faces of the crystal has already been referred to in section 3 of this chapter.

10·9. Growth of Other Minerals in Quartz:

Although most of the natural quartz crystals examined were free from overgrowth, about half a dozen crystals showed growth of other crystals along with quartz, all such examples being unorientated growths; not a single case was found of an orientated overgrowth. Of these crystals all showed a fairly low density of associated growths, except for one which exhibited a very large aggregate of closely packed overgrowths.

Fig. 123(a) is a photomicrograph showing a portion of a major rhombohedral face of this particular crystal, while figs. 124 and 125 show some portions of a minor rhombohedral and a prism face respectively. From these photographs it is quite clear that all the faces of this crystal are densely covered over by other crystals so much so that very small areas of faces of the parent crystal are left uncovered. That these small irregular features are depressions has been verified with the help of fringes of

equal chromatic order and also light profile.

The crystal had three trigonal trapezohedral (x) faces in addition to six rhombohedral and six prism faces. Each of the three x faces being at the left bottom corner of the respective R face, it can be said that the crystal was a left-handed one. When the unsilvered crystal was examined with a hand lens or under a microscope very small pieces of crystals, green in colour were found in some of the cavities. Such remnant crystals were more abundant on x faces than on any other face of the crystal. The green colour suggests that chlorite crystals had grown along with quartz, and were then partly dissolved away forming cavities on the crystal faces. [Chlorites are silicates of magnesia (or iron) and alumina, containing also about 12 per. cent. water. They are monoclinic (pseudo-hexagonal) and are generally aggregates of small scales. They are dark green and have perfect basal cleavage .] The chlorite crystals were perhaps dissolved away in sulphuric acid which does not affect quartz, and some of the very small pieces left undissolved can be seen by careful inspection on the x faces, fewer on R and r faces and less still on m faces. The difference in the amounts of undissolved chlorites on the different faces may possibly be due to the different solubility of the crystals on the different faces.

It should be mentioned that due to surface irregularities a very small interferometric gap between the optical flat and the crystal face could not be obtained; hence all the attempts to get high dispersion sharp Fizeau fringes failed (see fig. 123 (b)).

Cleavage lines and hexagonal boundaries in figs. 123(a), 124 and 125 endorse the interpretation given above.

10.10. Natural Etching:

From the large number of rhombohedral faces examined about two dozen faces showed the presence of etch figures due to natural etching. Some of these observations will now be described.

(a) Orientated Pentagonal Etch Patterns:

Fig.117 shows a large growth pyramid on a minor rhombohedral face of a natural quartz crystal. At a low magnification no structure is seen on its left sloping side which appears only as a black strip. Examination at a higher magnification reveals pentagonal-shaped orientated features, as illustrated in fig.126(a). Similar pentagonal structures were observed along the entire left sloping side of this pyramid (see fig.126(b)) and it was found that all these pentagons have their apexes pointing in a direction parallel to the left edge of the pyramid. Fig. 127 is a multiple beam interferogram over these pentagonal features, while Fig. 128 illustrates fringes of equal chromatic order proving that these features are flat bottom depressions. From the orientation, shape and nature of these features it can be concluded that they are a result of natural etching.

In the extreme left of the fig. 126(a) square-shaped features with strict correspondence between the growth fronts inside and outside the squares can be seen. The nature of these square-shaped features has been described in section 8 of this chapter.

(b) Orientated Triangular Etch Patterns:

In the present investigation two crystals were found to have received pronounced natural etching and all the faces of both the crystals were covered over with a large number of triangular depressions oppositely orientated with respect to the growth pyramids. Fig. 129, a photomicrograph, illustrates a minor rhombohedral face showing natural etch figures oppositely orientated with respect to the face itself, while fig. 130 shows some of the etch figures at a higher magnification. Natural etch figures on the other faces of both these crystals had more or less similar characteristics.

(c) Preferential Etching along Edges of Growth Layers:

An interesting case of preferential natural etching was observed on two major rhombohedral faces of a natural quartz crystal. Fig. 131, a photomicrograph, illustrates a growth pyramid the edges of the layers of which have received natural etching. Triangular etch pits are visible all along the edges of the growth layers, and it is evident that as etching proceeds small pits extend along the surface and meet neighbouring pits thereby forming larger etch figures. It should be mentioned that etching not only spreads two dimensionally along the surface but also in the third dimension perpendicular to the crystal face. Etching probably extends a few unit cells in depth.

Fig. 132, a positive phase-contrast micrograph, illustrates a similar case for another major rhombohedral face of the same crystal. Both these photomicrographs show that the edges of growth layers are the sites for initiation of etching, as are impurities and other flaws on the surfaces of crystals.

10·11. Dissolution Patterns on Natural Quartz:

Although in the present investigation most of the faces examined were the habit faces of natural and synthetic quartz, one crystal had a strange history and showed some interesting features. The crystal was a piece of natural quartz reclaimed from an autoclave after running it for five hours. It was one of the feeding crystals kept at the bottom of the clave and was definitely not a seed crystal. The whole crystal was highly irregular having almost convex surfaces meeting in irregular ridges and some very small broken flat areas (grid-like in appearance) at different heights and different inclinations; none of its surfaces were plane.

Fig. 133, a photomicrograph, shows the structure of a curved part of this crystal, which was found to be covered with a large

number of extremely small orientated triangular features. Fig. 134 is a multiple beam interferogram, obtained using the new thin film technique described in chapter V, for another region of the same crystal. One may perhaps think that these triangular features are growth pyramids, but fringes of equal chromatic order, illustrated in fig. 135, clearly show that each of these features is a flat bottom depression. Their depths are found to range from a few hundred Å. to less than 10 Å.

A method to measure depth (or height) less than 10 Å. has been described in chapter V . The triangle marked A (fig. 134) has a measured depth of 50 Å. . From the magnitudes of the shifts produced in this single fringe by the other triangular markings B, C, D, E, F, G and H their depths are found to be 100 Å. , 22 Å. , 13 Å. , 23 Å. , 80 Å. 43 Å. and 28 Å. respectively.

Now the feeding material used for growing quartz crystals in a laboratory is usually broken pieces of quartz (or quartzite). Quartz has a conchoidal fracture and hence the crystal under consideration would have conchoidal surface before it was introduced into the clave. When it came in contact with the solvent dissolution commenced, which resulted in the formation of a very large number of triangular flat-bottom depressions. At first very tiny triangular features would be formed which gradually get bigger and intergrew with their neighbours. This would result in highly irregular surface markings, such as those seen in fig. 133 and in the interferogram shown in fig. 25 (chapter V). The initiation of such dissolution patterns on an irregular surface is illustrated in fig. 136.

10.12. Topography of Red Quartz:

Two very small crystals of red quartz were examined, surface structures on which will now be described. Both the crystals were fully developed and were doubly terminated, having all the

rhombohedral faces of almost equal size. Both crystals were of practically the same size; the distance between the pyramidal terminations was 7 mm. ; all the prism faces were of almost equal size. The uniform red colour of these crystals is probably due to the presence of haematite. The haematite present in these crystals must be in the crystalline form, and it is likely that the haematite was being continually and uniformly supplied along with the silica throughout the whole period of growth. Alternatively the red colour may be due to the presence of some other oxide of iron.

Fig. 137 shows a major rhombohedral face of one of these crystals, from which it is clear that it is covered with a large number of tiny triangular features all of which are oppositely orientated with respect to the face itself. All the twentyfour rhombohedral faces of these two crystals showed similar surface structures. Fig. 138 is a photomicrograph showing, at a higher magnification, some of these triangular structures on a minor rhombohedral face of the other crystal, the horizontal line at the bottom indicating the r - m edge; fig. 139 is a multiple beam interferogram for some other region of the same face. With the help of phase-contrast microscope and the light profile it was confirmed that these triangular features are depressions. Figs. 138 and 139 also show that the triangular depressions are oppositely orientated with respect to the rhombohedral face. These features are very similar to the natural etch patterns on the natural quartz crystals described in section 10(b) of this chapter and illustrated in figs. 129 and 130. It can be concluded that these features are also natural etch patterns. They are of various sizes and depths; very small ones may be about 100 Å. deep or even less while the bigger ones may be about two or more light waves deep. Unfortunately, since the faces were densely covered with innumerable pits, all attempts to obtain smooth fringes failed and so no advantage could be taken of

'feco' for measuring precisely the depths of the small features. At higher magnifications it was found that some areas are almost devoid of these triangular features; these areas are no doubt formed by intergrowth of many neighbouring etch pits.

Finally, it is suggested that each minute particle of haematite may have acted as a site for dissolution. On the other hand, growth of these crystals might have taken place by the reverse process, each haematite particle acting as a growth nucleus.

10·13. Phantoms:

Two crystals showed the presence of 'ghost-crystals' or 'phantoms' inside their bodies. One of them had very long prism faces, about 12 cms. long, and showed a large number of 'ghosts'. To facilitate the counting and taking the photographs, two of its prism faces were polished. Fig. 140 illustrates a series of phantoms inside this crystal. Although it is very difficult to photograph all the 'ghosts' present, by careful inspections it was found that there are twentyfive or more ghost-crystals inside this crystal. Fig. 141 illustrates another example of this kind. By careful inspection with a hand-lens, about twenty ghost-crystals can be counted in this case. In both these illustrations the pyramidal and prism faces of the ghost-crystals are remarkably parallel to the corresponding rhombohedral and prism faces of the main crystals. These ghost-crystals indicate different stages at which the crystal stopped growing for some time due to the lack or scarcity of the material. In a way, phantoms reveal the history of growth of the crystal.

C H A P T E R XI

Slip-Lines, Faults and Twin-Boundaries

11·1. Introduction:

For all minerals in general the phenomenon of twinning is very common and rather universal in quartz. It is not an exaggeration to say that almost every quartz crystal is a twin-crystal. Thus although as a phenomenon there is nothing unusual about twinning in quartz, a separate chapter is devoted to it in the present work because, the method of approach and the explanation of the mechanism of the formation of twin crystals to be described here are quite new in the literature on twinning problems. This new approach lies in the study of surface structures of crystals.

11·2. The Old Theories of Twinning:

Although fairly satisfactory explanation of the genesis of the mechanical twin, annealing twin, transformation twin and repeat twin have been given no satisfactory interpretation of contact twin and penetration twin, the most common among natural minerals, exists. In a review paper Cahn (1954) has treated all the aspects of different types of twinning. For contact-twin the widely accepted consideration is that a twinned crystal is a result of joining of two single crystals, in twin-position, during growth. This consideration is based on several experimental facts. On the other hand, as regards the formation of penetration twin it is believed that a minute twinned nucleus appears spontaneously and the two individuals grow at roughly equal rates, thus forming a twinned crystal. Both these explanations are unsatisfactory.

11·3. The New Approach to Twinning

From an exhaustive study of the surface structures of a very large number of haematite crystals from different localities Sunagawa (1959) was convinced that the contact twin of haematite crystals can by no means be explained on the basis of older theories, and hence a new way must be thought of. He is of the firm opinion that a study of surface structures of minerals would be of immense help in revealing the mechanism of the formation of contact twin. From his observations he has proposed a new explanation which will now be described briefly.

Sunagawa's Proposed Explanation of Contact-Twin:

His observations of twin-boundaries on haematite crystals can be summarised as follows:-

(i) A twin-boundary is not always a straight line parallel to the m $(10\bar{1}0)$ face, but often curved having irregular bends, and sometimes it has a very complicated form.

(ii) Thick layers spread evenly all over the crystal surface. No clear evidence of growth taking place independently on both sides of a twin-boundary was available.

(iii) Kinks are formed on growth fronts when they meet a twin-boundary.

(iv) There is always a level-difference at the twin-boundary.

(v) Further growth after the formation of a twin-boundary, is often observed.

(vi) The triangular patterns of thin growth layers had opposite orientations on the two sides of the twin-boundary.

From these observations he concluded that

(a) the discontinuity line is a twin-boundary,

(b) the twin-boundary is formed during growth and then further growth takes place,

(c) the twin-boundary is formed on a growing single crystal and not by the joining of two individuals in twin-position,

(d) the twin-boundary is formed by a fault and

(e) the amount of fault is such that the step is not completely filled up by later growth; although such a step may be filled up by the later growth a small part of it is almost always left unfilled.

The above-given characteristics of the twin-boundary do not fit in with the older belief according to which two single crystals join together in twin position while they are growing, and hence the twin-boundary should always be a straight line parallel to the m face, two independent growth patterns should exist on opposite sides of a twin-boundary and ridges and ruts rather than steps are to be expected at the twin-boundary. In addition, since growth of haematite mainly takes place as layers parallel to the basal plane and not on the prism face, one can expect twin-formation by this mechanism on the basal plane, and not on the prism plane.

Although the twinning in quartz is the penetration twin, different in character ~~than~~ as compared with the contact twin, the arguments of the newly proposed mechanism of the formation of the latter are given in this chapter in a greater detail because it will be some time before they will be published. It will be proved that like the contact twin in haematite, penetration twin in quartz is also formed by some kind of fault during growth.

11·4. Slip-Lines and Faults:

Figs. 142 is a photomicrograph illustrating four slip lines on a major rhombohedral face of a natural quartz crystal; each of these lines is found to be strictly parallel to the R - m edge. Fig. 143 is another example of this kind in which the slip line is parallel to the edge between the neighbouring rhombohedral faces.

Highly irregular and complex slip lines are not uncommon in

quartz. Four such cases are illustrated in figs. 144(a), 145, 146 and 147.

As a result of some kind of stress during growth, a certain portion of a crystal drops down or projects up with respect to the remainder and thus forms a fault. Such faults may be quite irregular in their outline and may be of different sizes. The level-difference of the surface of such a faulted crystal and that of the remainder may vary along its boundary. Examples of this kind are illustrated in figs. 148(a), 149(a) and 150(a). More often than not a fault takes place in such a way that the faulted crystal acquires a shape of a creature. For example, figs. 151 and 152 illustrate two faulted crystals which have the appearance of a fish in the former and the head of a tortoise in the latter. The extension of the discontinuity lines from one face to the other is illustrated (for one crystal) in fig. 150(b).

It is very important to note that in each of the cases cited above there is always a level-difference at the boundary of the fault or the slip, and that there is a strict layer to layer correspondence on both sides of the discontinuity lines. Interferograms illustrated in figs. 144(b) and 149(b) show the level difference for the cases referred in figs. 144(a) and 149(a) respectively. This suggests that these faults took place during growth, and that the growth layers on both sides of the discontinuity lines (or within and outside a faulted crystal) belong to the same initiating centre. Kinks are always produced at the discontinuity lines.

11·5. Twin-Boundaries:

Having realized the merits of the new approach to the problem and Sunagawa's newly proposed interpretation of the mechanism of the formation of the contact twin in the case of haematite crystals, it was thought that some such approach and some similar explanation should be applied to quartz also. After studying

the slip lines and faults in the three selected crystals (these are described in the previous section), they were etched in the vapour of hydrofluoric acid, and as a result it was found that these discontinuity lines are in fact twin-boundaries. This therefore is the key to the explanation of the mechanism of the formation of the penetration twin in quartz.

11·6. Explanation of the Mechanism of the Formation of Penetration Twin in Quartz:

At first a quartz crystal grows as single crystal. Some kind of fault or slip takes place during growth and produces discontinuity lines with level difference along these lines. Steps formed in this way are partly filled up by later growth. A fault is a result of some kind of stress and thus the nature and extension of the discontinuity lines will depend upon the magnitude and the distribution of the stress. The strict layer to layer correspondence and the level difference at the twin-boundaries endorse the new interpretation that the penetration twin is formed by some kind of fault during growth, in an originally single crystal. Although from the point of view of surface structures this explanation is convincing, it is not very easy to realize how such a fault gives rise to right - and left - handed nature to the two components of the twinned crystal. The answer to this needs careful consideration.

C H A P T E R XII

Spiral Patterns on Natural Quartz

12·1. Introduction:

Ever since the birth of the dislocation theory of crystal growth spiral patterns have been observed on a wide variety of crystals, a detailed account of which is given in chapter IV. Quartz is one of the minerals most studied but no clear evidence of the existence of spiral patterns has been put on record up till now. Willis (1952) obtained a slip line on a major rhombohedral face of a natural quartz crystal, and this was claimed as evidence of a screw dislocation. He stated that he also observed spirals but there is no evidence to that effect.

In a detailed study of the surface structures of some 400 rhombohedral and about 100 prism faces of quartz crystals, about eight faces of synthetic quartz showed a variety of spiral patterns which have been described and discussed at length in chapter VI, and about six faces of natural quartz showed clear evidence of triangular spirals and the formation of closed loops due to a Frank-Read source. This is the first clear evidence of growth spirals on natural quartz. Furthermore these spirals are eccentric, and their eccentricity is accounted for here.

12·2. Triangular Spirals:

The crystal which showed spiral patterns was remarkably transparent with unusually flat surfaces. Fig. 153, a positive phase-contrast photomicrograph, illustrates a triangular right-handed spiral, having only about two complete turns, which was observed on one of the minor rhombohedral faces of this crystal. Careful observation shows that it is eccentric, the initiation centre being displaced from the geometric centre. This can

easily be understood if one remembers that a rhombohedral face of a quartz crystal has no axis of three-fold symmetry and hence the rate of advance of growth layers need not necessarily be equal in all three directions normal to the growth fronts. In fact the rate of advance of growth fronts is equal for the two directions perpendicular to the vertical sides, as demanded by the plane of symmetry, but is smaller for the third direction, perpendicular to the base of the spiral pyramid. This is schematically represented in fig. 154, where the spacing between successive growth fronts is equal for the α and β directions but is smaller in the γ direction. Point B represents the centre of initiation which is eccentric; it would have been at the geometric centre A if the rate of advance had been equal in all the three directions.

Fig. 155 is a multiple beam interferogram from which the step height of the spiral shown in fig. 153 is found to be 110 Å. . In fig. 153 in addition to the spiral, a number of dislocations, each giving rise to a spiral of about half a turn, are found along the line AB, which is inclined at an angle of about 42° with the r - m edge. That the line AB is a ridge is quite evident from fig. 156 which shows fringes of equal chromatic order for this region. The Point of emergence of each screw dislocation is on this line, and so one would expect a ridge to be found here.

12·3. Closed Loops due to Frank-Read Sources:

Four rhombohedral faces, two major and two minor, of another natural quartz crystal showed clear evidence of screw dislocations.

Fig. 157, a photomicrograph, shows the formation of closed loops due to two unlike screw dislocations of equal strength emerging on a major rhombohedral face. Figs. 158 and 159 are multiple beam interferograms which illustrate the nature of the growth fronts, the former in reflection and the latter in transmission. Although the growth fronts appear to be approximately circular without clear evidence of centres of initiations, they

must not be attributed to two-dimensional nucleation growth mechanism, because close examination at a higher magnification shows clearly that they are due to screw dislocations. This is illustrated in fig. 160, where one can see clearly two pairs of black dots at the centre, which mark points of emergence of four screw dislocations in two pairs. The members of each pair are unlike in sense but equal in strength and give rise to closed loops of growth fronts. It is also clear that the shape of the growth fronts is affected when they advance and meet other weaker dislocations. Fig. 161, an interferogram for this area, shows the nature of this growth hill and the distribution of some small mole-hills which probably have a similar form of origin. The step height in this case is found to be about 600 Å. .

It should be noted that all these four faces are covered with a large number of growth pyramids, as a result of which all attempts to obtain fringes across the growth fronts failed. Geographic dispersion was therefore used, for which fringes are required to be set parallel to growth fronts. From such an interferogram the height of the growth pyramid is determined and when this is divided by the number of growth layers composing the pyramid, it gives thickness of one layer. The accuracy of the step height determined in this way will, therefore, depend upon the precision with which the fringes can be aligned and the number of growth layers counted.

Fig. 162(a), a photomicrograph of a region on a major rhombohedral face of another natural quartz crystal, shows two growth pyramids, in which some growth fronts look like half turns of spirals. This is clearer in the smaller pyramid than in the larger one. A similar case is illustrated in fig. 162(b). It is evident from these figures that the faces of this crystal are

very dirty and hence it is suggested that, in the last stage of growth, impurities in the form of an exposed edge may have acted as growth nuclei.

C H A P T E R XIII

Topography of Prism, Trigonal Bipyramidal and Trapezohedral Faces of Natural Quartz

13.1. Prism Faces:

From the examination of about a hundred prism faces it was found that they all exhibit typical horizontal striations perpendicular to the c-axis, one example of which is illustrated in fig. 163. Here, in addition to the horizontal striations some etch figures formed as a result of natural etching are also visible. Praagh and Willis (1952) have reported the presence of tetrahedral growth pyramids on prism faces of natural quartz crystals. A similar case was found on all the six prism faces of a natural quartz crystal all the faces of which were densely covered with irregular pits formed as a result of dissolution of chlorite crystals which grew along with the quartz. Fig. 164 illustrates a portion of a prism face of this crystal where some tetrahedral growth pyramids are clearly visible. Unlike those observed by Praagh and Willis (loc. cit.) growth layers in the present case are relatively thin and widely spaced so that the pyramids are low-angle type. A similar case, fig. 165, was observed on a prism face of the natural quartz on a rhombohedral face of which evidence of spiral patterns was obtained (see chapter XII). Fig. 166 illustrates the presence of twin boundaries on a prism face. These twin boundaries were formed as a result of some kind of fault during the period of growth of the crystal.

13·2. Trigonal Bipyramidal Faces:

In the present study about twelve 's' faces were found on different crystals, surface structures on which will now be described.

Fig. 167 is a photomicrograph showing an 's' face of a left-handed quartz crystal, where the line AB indicates the S - R edge to which of course the striations on this face are parallel. From this figure it is clear that the face is covered with tetrahedral growth pyramids which, it is suggested are a result of independent growth on the 's' face itself. Fig. 168 illustrates, at a higher magnification, a portion of this face, while fig. 169, a multiple-beam interferogram, shows the nature of these tetrahedral growth pyramids and the surface in between. From these interferograms it is clear that these pyramids are of different heights and have almost flat top surfaces. However, presence of small ridges on the top surfaces of some pyramids and the nature of valleys between neighbouring pyramids are made clear in fig. 170 which shows fringes of equal chromatic order. Fig. 171, a photomicrograph, illustrates a portion of an 's' face of another natural quartz crystal, where the striations are parallel to the line AB which indicates the s - R edge. Fig.172 illustrates a similar case for an 's' face of some other crystal. Although both these faces show typical striations one can readily see that both these faces are covered with natural etch pits all orientated in a direction parallel to the striations. In fig. 172, however, some etch pits are found arranged along some lines crossing the face which, it is suggested, may be due to some kind of fault surface which obviously will be the region of weakness. Fig. 173, a positive phase-contrast micrograph, illustrates one such case of etch pits along a line crossing the face.

13·3. Trapezohedral Faces:

In the present study only one natural quartz crystal showed the presence of three trapezohedral faces. The crystal was a left-handed one, surface structures on which have already been described in section 9 of chapter X. Fig. 174 is a photomicrograph showing one of these 'x' faces. Irregular pits visible in the figure were formed due to chlorite crystals which grew along with quartz and were then almost completely dissolved away. Tiny bits of undissolved chlorite crystals left in the cavities can be seen by careful inspection with a hand-lens.

P A R T VI

FUSED QUARTZ

C H A P T E R XIV

Surface Topography of Fused Quartz and Synthetic Fused Silica 'Spectrosil'

14·1. Introduction:

In this chapter a brief account is given of the study of the topography of surfaces of fused quartz. This study, it is hoped, will be in harmony with the present work on natural and synthetic quartz crystals.

Synthetic fused silica is recognised to be the purest form of fused silica available, although a precise determination of the impurity elements present has not yet been made. The purity of the material available viz. synthetic fused silica 'spectrosil' has been assessed by indirect methods such as gamma-irradiation, fluorescence at various incident wave-lengths, and resistivity of standard batches of silica grown in special crucibles (private communication, Thermal Syndicate Ltd).

Using chemical, spectrographic, and other direct methods for analysis for aluminium, boron, calcium, copper, iron, magnesium, manganese, potassium and sodium, The Thermal Syndicate (loc.citt) claims the total impurities in the samples under consideration to be less than one part per million. The aluminium content is 0·2 parts per million, with boron less than 0·5 parts per million.

It is found that after exposures to $4{\cdot}5 \times 10^{8}$ Röntgens, no colouration is produced by gamma rays or by irradiation in an atomic pile. This extreme purity is also confirmed by the complete absence of fluorescence and the very high transmittance of the material in the ultra-violet.

It is found that the synthetic fused silica is entirely homogeneous and free from granularity as compared with the various

grades of vitreosil fused quartz, made from rock quartz crystal. This type of silica is now incorporated as standard components in many instruments. It is claimed that because of the exceptional purity of this synthetic fused silica it is eminently suitable for all applications in which the slightest contamination must be avoided.

In the present work four samples have been examined. They are:

I Thermal Syndicate Ltd., Spectrosil Disc;
21 mm. thick; Optical polish.

II Corning Synthetic Silica Plate;
10 mm. thick; Optical polish.

III Corning Synthetic Silica Plate;
3 mm. thick; plate glass finish;

IV Thermal Syndicate Ltd., Spectrosil Plate;
1 mm. thick; plate glass finish.

Microscopic examination by reflection shows that the samples are transparent with apparently no grain structure in the bulk. Examination under phase contrast microscope confirms this.

Each sample was silvered and matched against an optical flat also silvered to the required percentage for good multiple beam fringes in reflection and in transmission. For each face of each sample interferograms were taken at different suitable dispersions. As explained below, these interferograms are of immense help in revealing the nature of the surfaces of these samples.

14·2. Observations:

Fig. 175 is an interferogram in reflection for one face of sample I. Fringes are reasonably smooth and fairly sharp. Other interferograms (not shown here) at different dispersions show equally smooth fringes. From these interferograms it can safely be concluded that both the surfaces of this sample are

quite smooth though not perfectly flat.

Fig. 176 is an interferogram in reflection for one surface of sample II. Fringes are remarkably straight and very smooth; dispersion is uniform and contrast is fairly good. Similar types of fringes were obtained for the other surface of this sample. These fringes amply justify the good finish of the surfaces of this sample. It is suggested that there is no granularity in the bulk, and the finish of the surfaces is, in the author's opinion, the best of the four samples examined.

Coming now to sample III, fig. 177 is a phase contrast photomicrograph of one of its surfaces and shows small specks on the surface. Fig. 178 shows multiple beam interference Fizeau fringes at low dispersion. Random irregular kinks in every part of the fringes indicate the ruggedness of the surface. It is interesting to note that even in the high dispersion region, where fringes are very irregular the fringe definition is surprisingly high and the contrast is excellent. The general roughness of the surfaces of this sample becomes more and more apparent, the higher the dispersion. This is self-explanatory from fig. 179 which is an interferogram at a very high dispersion with only two fringes in the field of view; the fringe at the left hand top corner has been purposely retained for the comparison of the high definition of this fringe on one hand, and the absolutely rugged, broad, patchy fringe (right half of fig.179) on the other. It is needless to add anything to what fig. 179 reveals itself about the very poor quality of the surface finish of this sample.

Even though Fizeau fringes in these interferograms reveal the general irregularities in the surfaces, they do not give much detail about the nature of these irregularities. Here the powerful technique of Tolansky (1948) of using fringes of equal

chromatic order, usually abbreviated to 'Feco' is most useful. Fig. 180 shows such fringes for the tip of one of the innumerable surface irregularities on this sample. The straight fringes turn, in the middle part, towards the violet end of the spectrum, indicating thereby that the feature is an elevation. It is clear that the elevation is not an abrupt step; it is a hillock gradually rising up to the peak, and then gradually falling away again. From this it is concluded that the general roughness of the surface of this sample is due to innumerable small pimple like projections ranging from a few tens to a few hundreds of Ängstroms in height.

Equally interesting results are obtained in the case of sample IV. Figs. 181 and 182 are multiple beam interferograms, the former in reflection and the latter in transmission. In fig. 181 the fringes are sharp and slightly wavy but the contrast is not so good as that obtained for sample III. In fig. 182 three mercury lines (one green and two yellow) are used as incident light and these fringes reveal the irregular wavy nature of the surface, which, it is suggested, is due to some micro-granularities on the surface. The exact nature of the features, forming surface irregularities, is surprising and is made clear by fig. 183 which shows 'feco' at a randomly selected point. It shows that the structure is a small hillock, gradually sloping, with a smooth depression at its summit. Thus 'feco' not only provides a means for determining the exact nature (hill or valley) of surface irregularities, and the exact profile of such microscopic features, with a precise evaluation of their magnitude, but also helps in bringing out at a submicroscopic scale the fine structure, if any, on such features. But this is not easily obtained; it requires vigilence and an experienced hand on the technique, because only for the correct dispersion, and

only when the fringe passes right through the summit of this very small hillock, can the sub-structure be seen. In this case, the feature is like an extinct volcano, with a crator at its top. But for 'feco' this fine sub-microscopic structure would have, in the author's opinion, escaped observation.

14·3. Discussion and Conclusion:

From the observations and interpretation thereof, given above, for sample I 'spectrosil' and sample II 'Corning Synthetic Silica', it can safely be said that if there were any granularities in the bulk they should have been observed to some extent on the surface of at least one of the samples. That it was not observed at all indicates the almost entire absence of granularity in either sample. Secondly, both these samples had the same surface finish, viz. optical polish, and since the fringes are quite smooth, the surface finishes are quite good and of similar quality.

Samples III and IV show many surface irregularities, but this does not mean that there is necessarily granularity in the bulk, because if it were so, it should have been observed on samples I and II also; both samples I and IV being 'Spectrosil' and both samples II and III being 'corning synthetic silica'. On the other hand, samples III and IV have plate glass finish as against optical polish finish for samples I and II. Obviously, therefore, the surface irregularities in samples III and IV can safely be attributed to the finishing process, viz. plate-glass finish. Furthermore, the depression in the top of the hillock is observed for sample IV only, and not in sample III, which may be accounted for by the method of preparation.

From what has been discussed above it can be concluded that none of the four samples have any granularities in the bulk, and that the optical finish is far superior to plate glass finish. Also the 'spectrosil' is perhaps better than 'corning synthetic silica'.

It was anticipated by The Thermal Syndicate (loc. cit.) that there might be an abrupt step on these samples. Careful observations have failed to reveal any such abrupt step anywhere on any face of any one of these samples. The absence of such a step is not surprising. A step is caused by external or internal stress, mechanical, thermal or otherwise, and there is no reason why there should be a stress of any kind in such specially and carefully prepared samples.

A P P E N D I X

HIGH - PRESSURE DIAMOND BOMB

A P P E N D I X

High-Pressure Diamond Bomb

A·1. Introduction:

An interesting and useful experiment on high pressure polymorphism was carried out by Jemison (1957). An approximately three carat single crystal diamond was used as a bomb in his experiment. A highly polished straight hole 0·172 inch in length was ground through the diamond having a flat surface at each end of the hole. The flat surfaces were perpendicular to the axis of the hole. The original crystal was a deformed dodecahedron with a roughly spherical exterior. A chemical substance (KI , Cd or $CaCO_3$) was placed in the hole at the centre of the body of the crystal in between two pistons and by applying a pressure of 24,000 bars on the pistons, the substance was exploded. This explosion produced a four-winged star shaped crack in the crystal. An interferometric examination has been carried out to study the effect of this explosion-produced crack on the six cut faces of the crystal and a brief report of this study is given in the present chapter. Before describing the observations it is essential to make a few remarks about the crystallographic orientation of the hole.

A·2. Crystallographic Orientation of the Hole:

(a) Morphological Considerations:

It is stated by Jemison (loc. cit.) that the hole drilled in the diamond is in the direction of one of the cubic axes. Morphologically and also with the help of X-ray photographs it is proved below that the hole is not in a direction parallel to one of the cubic axes but in a direction perpendicular to (011)

and $(0\bar{1}\bar{1})$ faces; i.e., in the direction $[011]$.

When the crystal is orientated as shown in fig. 184 so that the smallest cut faces (No. 1 and 2) are one towards and the other away from the observer, the cut face from which a bit has been chipped off is on the left, with the chipped end pointing upwards. In this case, the front face (No. 1) and the back face (No. 2) are (100) and $(\bar{1}00)$ respectively; the chipped face (No. 3) and the face (No. 4) parallel to it are $(0\bar{1}1)$ and $(01\bar{1})$ respectively, while the upper (No. 5) and the lower (No. 6) large cut faces perpendicular to the axis of the hole are (011) and $(0\bar{1}\bar{1})$. The curved natural faces are each divided into two parts and are of the form $\{hko\}$.

The reason why it is correct to take the orientation shown in fig. 184 is as follows:
If the hole is taken to be in a direction of one of the cubic axes (say vertical), as was suggested by Jemison, the crystal could be shown as in fig. 185. The small face in the centre is one of the cubic faces; PQ and SR are faces perpendicular to the hole; and PS and QR faces parallel to the hole (PS chipped). The dotted lines show how the dodecahedral faces are divided into two parts, which is not the correct way. Fig. 186 shows a dodecahedron with small cubic faces and the dotted lines indicate the way in which dodecahedral faces of a diamond are divided into two parts, which is correct. Now if fig. 185 is brought on to fig. 186 in such a way that the cube faces coincide (this can be achieved by turning fig. 185, through 45°, in the clockwise direction, about a-axis) c-axis of fig. 185 will emerge from point L in fig. 186; this indicates that c-axis is an axis of three-fold symmetry, which is absurd in the case of diamond, which belongs to the cubic system. On the other hand, in fig. 186 c-axis is an axis of four-fold symmetry which is in

harmony with the fact that diamond belonging to the cubic system should have three four-fold axes, one of which is the c-axis, the other two being a and b. Hence it is clear that the orientation in fig. 184 is correct, and that the axis of the hole is perpendicular to (011) and(0 $\bar{1}$ $\bar{1}$) faces and not parallel to a cube axis. This was also checked by X-ray methods.

(b) X-Ray Diffraction Experiments:

The crystal was set in such a way that faces No. 5 and 6 were exactly vertical. Using a cylindrical camera 15^{o} oscillation X-ray diffraction photographs were taken for these faces which are perpendicular to the hole. Figs. 187 (a) and (b) are X-ray diffraction photographs for face No. 5 and figs. 188(a) and (b) are those for face No. 6. Using Bernal chart values of Θ were found out for each spot on these photographs. Each spot was then properly indexed, and corresponding values of Φ and ρ determined. A steriogram was drawn for each of these faces, wherein with the help of a steriographic net traces of faces 5 and 6 were located. These steriograms are shown in figs. 189 and 190. These faces were found to be of the form $\{110\}$.

Observations are given below.

$$a^{x} = \frac{\lambda}{a} ; \qquad \lambda = 1{\cdot}54 \text{ Å}. ; \quad a = 3{\cdot}567 \text{ Å}. .$$

$$\therefore a^{x} = \frac{1{\cdot}54}{3{\cdot}567} = 0{\cdot}4317 \text{ Å}. ; \qquad a^{x2} = 0{\cdot}1864$$

$$d^{x2} = a^{x2} N.$$

Diamomd: Fd 3m.

cubic

P N = 1, 2, 3, 4, 5, 6, -, 8, 9, 10, 11, 12, 13, 14, - .
16, - 18, 19, 20, 21, etc., etc.

N	cubic. P. h k l	d in Å.	$d^{x2} = a^{x2}N$	$\text{Sin}\beta = \frac{\lambda^x}{2}$	θ
1	100		0·1864	0·2159	12° - 28'
2	110		0·3728	0·3053	17° - 47'
3	111	2·05	0·5592	0·3739	21° - 57'
4	200		0·7456	0·4317	25° - 35'
5	210		0·9320	0·4827	28° - 52'
6	211		1·1184	0·5285	31° - 54'
7	-	-	-	-	-
8	220	1·26	1·4912	0·6105	37° - 38'
9	300		1·6776	0·6475	40° - 21'
9	211		1·6776	0·6475	40° - 21'
10	310		1·8640	0·6825	43° - 3'
11	311	1·07	2·0504	0·7160	45° - 44'
12	222		2·2368	0·7480	48° - 26'
13	320		2·4232	0·7780	51° - 5'
14	321		2·6096	0·8075	53° - 51'
15	-	-	-	-	-
16	400	0·89	2·9824	0·8635	59° - 43'
17	410		3·1688	0·8900	62° - 53'
17	322		3·1688	0·8900	62° - 53'
18	411		3·3552	0·9160	66° - 21'
18	330		3·3552	0·9160	66° - 21'
19	331	0·82	3·5416	0·9410	70° - 13'
20	420		3·7280	0·9655	74° - 54'
21	421		3·9144	0·9890	81° - 30'

Face No. 5:

When face 5 is at 45° to the incident X-ray beam,

reading on horizontal circular scale .... 197° - 15'.

Now the crystal is turned through 45° so that the face is parallel to the incident X-ray beam;

reading on the horizontal circular scale 242° - 15'.

The crystal is now rotated through 10° so that the incident X-ray beam is at a glancing angle of 10°.

Reading on horizontal scale ..... 252° - 15'.

Fig. 187(a): 15° oscillation; 252° - 15' — 267° - 15'

Fig. 187(b): 15° " 262° - 15' — 277° - 15'.

Note: Bernel chart gives complementary angles of Φ .

Spot No.	Θ in degrees	h k l	Φ in degrees	ρ in degrees
1	22	111	90 - 17 = 73	48
2	46	311	90 - 44 = 46	71
3	46·5	311	90 - 37 = 53	74
4	22	111	90 - 9 = 81	57
5	37·5	220	90 - 50 = 40	44
6	61	400	90 - 57 = 33	88
7	38	220	90 - 13 = 77	84

In fig. 189 is shown the trace of face No. 5. It is of the form $\{110\}$.

Face No. 6:

When face No. 6 is at 45° to the incident X-ray beam,

reading on horizontal circular scale ..... 17° - 45'.

The crystal is now turned through 45° so that this face is parallel to the incident X-ray beam;

reading on circular scale ..... 62° - 45'.

The crystal is now rotated through 10° so that the incident X-ray beam is at a glancing angle of 10°.

Reading on horizontal circular scale .... 72° - 45'.
Fig. 188(a): 15° oscillation: 72° - 45' — 87° - 45'.
Fig. 188(b): 15° " 82° - 45' — 97° - 45'.

Spot No.	θ in degrees	h k l	ϕ in degrees	ρ in degrees
1	46	311	90 - 36 = 54	73
2	59	400	90 - 56 = 34	88
3	46	311	90 - 41 = 49	70
4	20	111	90 - 8 = 82	57
5	23	111	90 - 17 = 73	46
6	47·5	311	90 - 40 = 50	80
7	72·5	331	90 - 58 = 32	83
8	66	411 (330)	90 - 66 = 24	71
9	47·5	311	90 - 47 = 43	66
10	37·5	220	90 - 10 = 80	84

In fig. 190 is shown the trace of face No. 6. It is of the form $\{110\}$.
In figs. 189 and 190 the c-axis passes through the centre of the circle, is perpendicular to the plane of the figure, and its positive end points upwards.

A·3. Observations:

Face No. 1: (100) face:

Fig. 191 is an interferogram at low dispersion. At P there is a depression in the form of a V-shaped valley. It is broad and deep, about 1800 Å. at the edge of the face, while both breadth and depth fall to zero at a little distance from the edge.

Face No. 2: $(\bar{1}00)$ face:

Fig. 192 is an interferogram at very high dispersion. There is nothing significant on the face except the polish marks which are very well brought out by the fringe.

Face No. 3: $(0\bar{1}1)$ face:

Undulations in the surface flatness, probably due to polishing, are revealed by fig. 193 which shows multiple beam interference fringes at very low dispersion. The chip on this face, previously mentioned, is clearly shown.

Face No1 4: $(01\bar{1})$ face:

Fig. 194 shows good definition, low dispersion Fizeau fringes, revealing a straight valley across the face and the details of this valley are clear in fig. 195 which is an interfergram at higher dispersion.

Face No. 5: (011) face: and Face No. 6: $(0\ \bar{1}\ \bar{1})$ face:

Fig. 196 is a photomicrograph of face No. 5 showing at the centre the section of the hole and in the lower half of the figure a step PQ extending from the hole to the edge of the face. Fig. 197, a photomicrograph of face No. 6, shows the section of the hole at the centre and a similar step RS. Fig. 198 is a photomicrograph, in transmission, with the faces unsilvered. It shows the four-winged crack in the crystal and also the section of the hole. It also shows the two steps (PQ and RS) on faces 5 and 6 in strictly coincident position. The steps are a bit out of focus (one within and the other without) because the

microscope was focussed on the crack in the body of the crystal. It shows that the steps on these faces are strictly parallel to one another.

Fig. 199, an interferogram of face No. 5, shows the hole and the step. It indicates that the step is an abrupt one. Fig.200 shows fringes for half of the face including the step. It is clear from this figure that the height of the step gradually decreases from the hole to the edge of the face.

Fig. 201 is an interferogram, in reflection, for face No.6. It shows the hole and the step gradually decreasing from the hole to the edge of the face. Fig. 202 is an interferogram, in transmission, where three wave-lengths (green and yellow doublet) of mercury are used as incident light. Fringe definition is extremely good particularly when one remembers that the faint line is the unresolved yellow doublet. From measurements it is found that for face No. 5 the height of the step is 140 Å. at the hole and 60 Å. at the edge, and that for face No. 6, it is 400 Å. at the hole and 80 Å. at the edge.

That these steps are elevations is evident from figs. 203(a) and 203(b) which show fringes of equal chromatic order, for faces 5 and 6 respectively.

A·4. Discussion:

From these observations two possibilities arise:

(1) The facts

(a) That the steps on faces 5 and 6 are remarkably parallel to one another,

(b) that their heights decreases from the hole towards the edge of the face,

(c) that the wing No.1 of the crack between the steps is V shaped, the plane of V being perpendicular to the faces with steps,

(d) that the wings extend only about half way from the hole,

(e) that the wing No. 1 of the crack and the valleys on

faces 1 and 4 are in the same plane, with the broad ends of the valleys towards the end to which the wing (between the steps) points,

(f) that the steps are within a few degrees of the wing of the crack,

(g) that both the steps are elevations, implying that these faces have been pushed away from the centre of the crystal (up for the upper face and down for the lower one), and

(h) that the steps are in a plane parallel to faces $(0\bar{1}1)$ and $(01\bar{1})$, which direction is a weak cleavage direction for diamond, leading one to conclude that these steps are a result of the crack in the crystal.

(2) On the other hand, the following facts

(i) that the steps are remarkably parallel to the polish marks,

(ii) that the steps are not precisely parallel but are inclined at a few degrees to the wing (No. 1) of the crack,

(iii) that no steps are observed corresponding to the other three wings (No. 2, 3 and 4) of the crack,

(iv) that the steps are not in the cleavage plane (111) of the diamond,

lead one to conclude that the steps have nothing to do with the crack but are only due to polishing.

Unfortunately the diamond was sent to us only after and not before the high pressure experiment was carried out. If the opportunity had been given to examine the diamond also before the experiment, it would have been easy to establish the exact deformation, if any, produced by the crack.

If the results are in favour of the first set of arguments, both the high pressure experiment and the interferometric examination are interesting. If the second set of arguments are

more convincing only one conclusion may be drawn that such a high pressure does not produce any deformation in the crystal. A repeat of such an experiment and interferometric examination of the surfaces of the crystal before and after the experiment would throw a good deal of light on such bombs.

Very recently we have succeeded in obtaining one diamond on which a similar experiment will be repeated. In this case an opportunity has been given to us to examine the surfaces before the explosion is produced in the diamond. Results, if interesting, will be communicated elsewhere.

REFERENCES

Amelinckx, S. (1952 a) Nature, 169 , 841
(1952 b) Phil. Mag., 43 , 562
(1952 c) Nature, 170 , 760
(1956 a) Acta Cryst., 9 , 16
(1956 b) ibid., 9 , 217

Anderson, N.G. and Dawson, I.M. (1953) Proc. Roy. Soc., A 218 , 555 (see Mott. 1953)

Becker, R. (1929) J. Am. Electrochem. Soc., 55 , 153
(1949) Disc. Faraday Soc., No.5 (Crystal Growth), p.55
and Döring, W. (1935) Ann. Physik, 24 , 719

Bentivoglio, M. (1927) Proc. Roy. Soc., A 115 , 59

Berg, W.F. (1938) Proc. Roy. Soc., A 164 , 79

Bragg, W. H. and Gibbs, R.E. (1925) Proc. Roy. Soc., A 109 , 405

Brandes, H. (1927) Z. Physik. Chem., 126 , 196
and Volmer, M. (1931) ibid., 155 , 460

Bravais, A. (1866) A Etudes Cristallographiques, Gauthiar Villars, Paris

Brown, C.S., Kerr, R.C., Thomas L.A., Wooster, Nora. and Wooster, W.A. (1951) Nature, 167, 940

Buckley, H.E. (1951) Crystal Growth, John Wiley and Sons, Inc., New York

Buerger, M.J. (1947) Amer. Min., 32 , 593
(1951) Phase Transformations in Solids, p. 183, John Wiley and Sons, Inc., New York

Bunn, C.W. (1949) Disc. Faraday Soc., No. 5 (Crystal Growth), p. 132
and Emmett, H. (1949) ibid., p.119

Burgers, J.M. (1939) Proc. Acad. Sci. Amst., 42 , 293, 378

Burton, W.K., Cabrera, N. and Frank, F.C. (1949a) Nature, 163 , 398
(1949b) Disc. Faraday Soc., No. 5 (Crystal Growth), p.33
(1951) Phil. Trans., A243 , 299

Cabrera, N. (1953) J. Chem. Phys., 21, 1111

Cockroft, J.D. (1928) Proc. Roy. Soc., A 119 , 293

Cahn, R. W. (1954) Advances in Physics., Vol. 3, No. 12, p.363

Cottrell, A.H. (1949) 'Theory of Dislocations', Progress in Metal Physics, Vol.I, p.77, Butterworths Scientific Publications, London

Curie, P. (1885) Bull. Soc. Franc. Miner., 8 , 145

Dake, H.C., Fleener, F.L. and Wilson, B.H. (1938) Quartz Family Minerals, Mc.Graw Hill Co., London

Dale, D.R. (1948) Science, 107 , 393
(1949) Disc. Faraday Soc., No.5 (Crystal Growth), p.189, 363

Davey, W.P. (1934) A Study of Crystal Structure and its Applications, Mc.Graw Hill Book Co., Inc., New York

Dawson, I.M. (1952) Proc. Roy. Soc., A 214 , 72
and Vand, V. (1951a) Proc. Roy. Soc., A 206 , 555
(1951b) Nature, 167 , 476

Desch, C.H. (1934) Chemistry of Solids, Cornwell University Press

Eshelby, J.D. and Stroh, A.N. (1951) Phil. Mag., 42 , 1401

Forty, A.J. (1952a) Phil. Mag., 43 , 72, 949
(1952b) ibid., 43 , 72, 377
and Frank, F.C. (1953) Proc. Roy. Soc., A 217 , 262

Frank, F.C. (1949a) Disc. Faraday Soc., No.5 (Crystal Growth), p. 48
(1949b) ibid., p. 48, 67, 76, 186

(1950a) Proc. Roy. Soc., A 201 , 586
(1950b) Phil. Mag., 41 , 200
(1951a) ibid., 42 , 809
(1951b) Phil. Mag., 42 , 1014
(1951c) Acta Cryst., 4 , 497
(1952) Advances in Physics, Vol. 1 , No. 1, p.91
and Read, W.T. (1950) Phys. Rev., 79 , 723

Frankel, J. (1945) J. Phys., Moscow, 9 , 392
(1946) Kinetic Theory of Liquids, Clarendon Press, Oxford

Gibbs, J.W. (1878) Collected Works, 1928, p. 325, foot note, Longmans Green and Co., London

Gibbs, R.E. (1925) Proc. Roy. Soc., A 107 , 561
(1926) ibid., A110 , 443

Griffin, L.J. (1950a) Phil. Mag., 41 , 196
(1950b) Ph. D. Thesis, London University
(1951a) Phil. Mag., 42 , 775
(1951b) ibid., 42, 1337
(1952) ibid., 43 , 827

Hedges, J.M. and Mitchell, J.W. (1953) Phil. Mag., 44 , 223

Heising, R.A. (1945) Quartz Crystals for Electrical Circuits, D Van Nostrand Co., Inc., New York

Ichikawa, S. (1915) Amer. Journ. Sci., 39 , 455

Jemison, J.C. (1957) Journ. Geol., 65 , No. 3

(1) Kaischew, R and (1) Stranski, I.N. (1935) Physik. Z., 36 , 393

Kalb, (1930) Z. Krist., 73 , 266
(1933) ibid., 86 , 439
(1934) ibid., 89 , 400

Marcelin, A. (1918) Ann. Phys., 10 , 185
and Boudin, S. (1930) C.R. Acad. Sci., Paris,191,31

Mason, V.P. (1949) Piezolectric Crystals and their Application to Ultrasonics; D. Van Nostrand Co., Inc., New York

Menzies, A.W.C. and Sloat, C.A. (1929) Nature, 123 , 348

Mott, N.F. (1949) Disc. Faraday Soc., No. 5 (Crystal Growth), p.11

(1950a) Nature, 165 , 295

(1950b) Phil. Mag., 41 , 200

(1953) Nature, 171 , 234

and Nabarro, F.R.N. (1948) Strength of Solids (Phys. Soc.) p. 1

Nabarrow, F.R.N. (1947) Proc. Phys. Soc., 59 , 256

(1952) Advances in Physics, Vol. 1, No. 1, p.269

Noyes, A.A. and Whitney, W.R. (1897) Z. Physik. Chem., 23 , 689

Orowan, E. (1934) Z. Phys., 89 , 634

Peierls, R. (1940) Proc. Phys. Soc., 52 , 34

Polanyi, M. (1934) Z. Phys., 89 , 660

Praagh, Van. (1949) Disc. Faraday Soc., No.5 (Crystal Growth), p.338

and Willis, B.T.M. (1952) Nature, 169 , 623

Read, W.T. (1953) Dislocations in Crystals, Mc. Graw-Hill Co., Inc., New York

and Shockley, W. (1952) Imperfections in nearly perfect crystals, p.77, John Wiley and Sons, Inc., New York

Seager, A.F. (1952) Ph. D. Thesis, London University,

Seegar, A. (1953) Phil. Mag., 44 , 1 (1953) Min. Mag., Vol. 30, No. 220, pp. 1-25

Seitz, F. (1950) Phys. Rev., 79 , 723

(1952) Imperfections in nearly perfect crystals, p. 4, John Wiley and Sons Inc., New York

Smekal, A. (1933) 'Strukturempfindliche Eigenschaften der Kristalle in Geiger and Scheel'. Handb. Phys., 24 , 795

Sosman, R.B. (1927) 'The Properties of Silica', Chem. Catalog Co., Inc., New York

Spezia, G. (1905) Acad. Sci. Torino., 40 , 254
(1906) ibid., 41 , 158

Sunagawa, I. (1958) Journ. Min. Soc., Japan, 3 , 543
(1959) 'Symposium on Twinning', General Meeting, International Mineralogical Association, Zurich

Taylor, G.I. (1934) Proc. Roy. Soc., A 145 , 362

Teghtsoonnian, E. and Chalmers, B. (1951) Canad. Journ. Phys., 29 , 370

Tolansky, S. (1945) Proc. Roy. Soc. A. 184, 41.
(1948) Multiple Beam Interferometry of Surfaces and Films, Oxford, Clarendon Press
and Wilcock, W.L. (1946) Nature, 157 , 583
and Omar, M. (1952) Nature, 170 , 81
and Bhide, V.G. (1956) 6e Reunion de Chemie Physique, No.97

Vand, V. (1951a) Phil. Mag., 42 , 1384
(1951b) Nature, 168 , 783

Vigoureux, P. and Booth, C.F. (1950) Quartz Vibrators and Their Applications, His Majesty's Stationary Office, London

Verma, A.R. (1951a) Nature, 167 , 939
(1951b) Phil. Mag., 42 , 1005
(1952a) Proc. Phys. Soc., B 65 , 806
(1952b) Phil. Mag., 43 , 441
(1953) Crystal Growth and Dislocations, Butterworths Scientific Publications, London
(1955) Proc. Roy. Soc., A 228 , 34
and Reynolds, P.M. (1953) Proc. Phys. Soc., B 66 , 414, 989

Volmer, M. (1922) Z. Phys. Chem., 102 , 267
(1926) Z. F. Phys., 35 , 170
(1939) Kinetik der Phasenbildung, Steinkopff, Dresden and Leipzig
and Adhikari, G. (1926) Z. Phys. Chem., 119 , 46
and Easterman, I. (1921) Z.F. Phys., 7 , 13
and Schultze, W. (1931) Z. Phys. Chem., 156 , 1
Walker, A.C. and Buehler, E. (1950) Indus. and Eng. Chem., 42 , 1369
Wells, A.F. (1946) Chem. Soc. (London) Ann. Rep., 43 , 62
Willis, B.T.M. (1952a) Nature, 170 , 115
(1952b) Ph. D. Thesis, London University
Wooster, Nora. and Wooster, W.A. (1946) Nature, 157 , 297
Wulfe, G. (1901) Z. Krist., 34 , 449
Wyckoff, R.W.G. (see Bunn and Emmett (1949), p. 130)

A C K N O W L E D G E M E N T S

I wish to express my gratitude to Professor S. Tolansky, F.R.S. for his continued guidance, keen interest and kind encouragement throughout the course of this work.

I also wish to thank Professor J.D. Bernal, F.R.S. for permission to carry out X-ray work in his laboratory at Birkbeck College, and Dr. J.W. Jeffry for his assistance in taking and interpreting X-ray photographs.

I am very much grateful to Dr. I. Sunagawa of the Geological Survey, Japan and Dr. A.F. Seager of Birkbeck College for their interest, helpful criticisms, suggestions and discussions. In particular Dr. Sunagawa has kindly allowed the frequent use of his Olympus phase-contrast microscope.

I wish to record my sincere thanks to Mrs. Jill G. Wood, B.Sc. (Eng.) of the National Physical Laboratory, who has kindly read the manuscript.

My thanks are also due to the physics laboratory staff and in particular to Mr. A. Grant and Mr. J. Hanley of the Royal Holloway College, for their kind co-operation and help in preparing apparatus throughout this work.

I also wish to thank Dr. A.F.B. Wood of Standard Telephones and Cables Ltd., and the directors of the Clevite Corporation, Ltd. U.S.A. and the G.E.C. Laboratories, U.K. for the generous supply of many quartz crystals.

Finally, I am indebted to Charotar Vidyamandal, Vallabh Vidyanagar, (India) for the grant of study leave which enabled me to carry out this work.

MICROTOPOGRAPHICAL STUDIES

ON

NATURAL AND SYNTHETIC QUARTZ CRYSTALS

THESIS PRESENTED FOR THE DEGREE OF
DOCTOR OF PHILOSOPHY
IN THE
UNIVERSITY OF LONDON
BY

MANUBHAI SURYARAM JOSHI

NOVEMBER, 1959.

To facilitate the comparision of
the figures with the text, this thesis
has been bound in two separate volumes.
Volume I contains the text, and volume II
the figures.

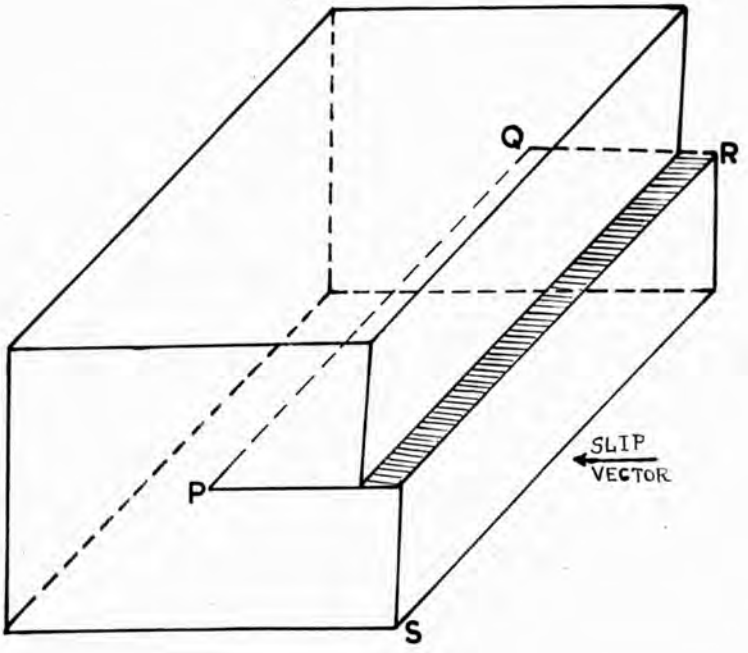

Fig. 1.

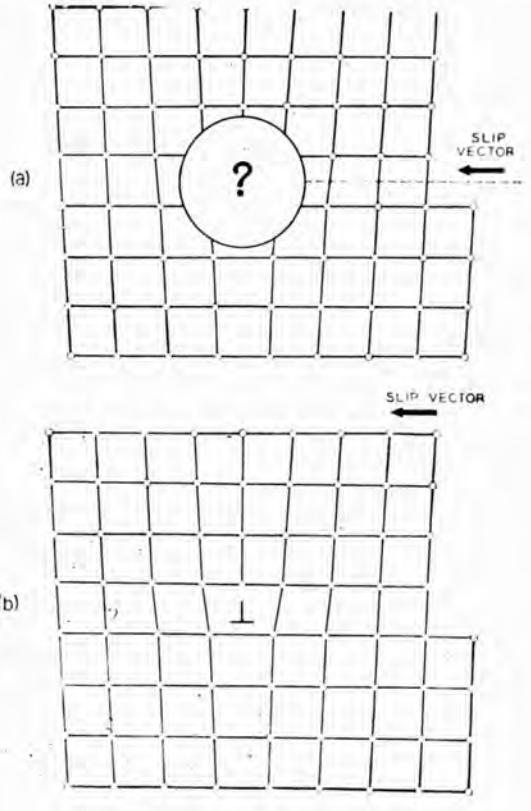

Fig. 2.

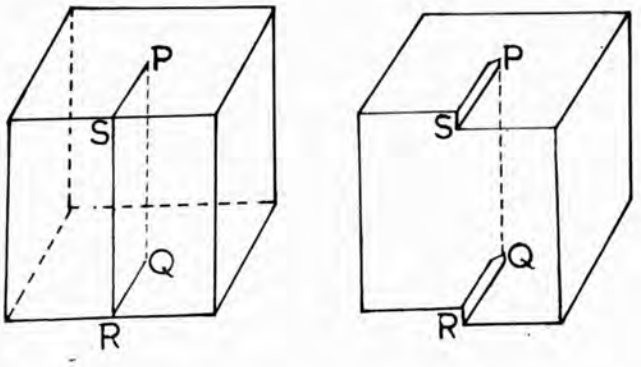

Fig. 3.

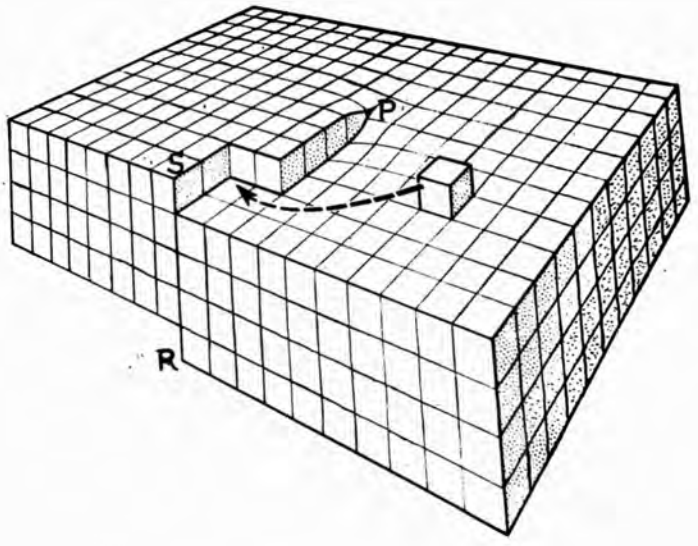

Fig. 4.

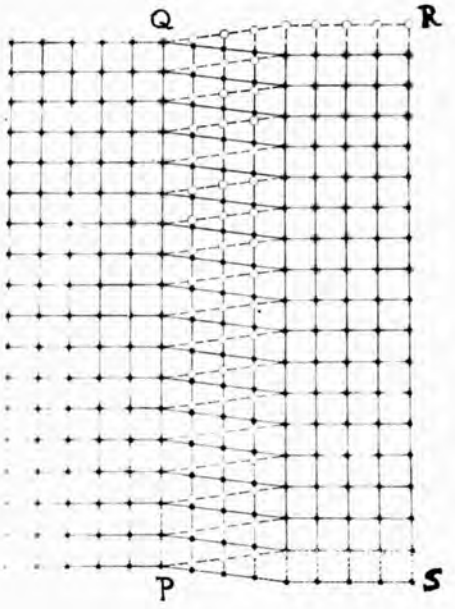

Fig. 5.

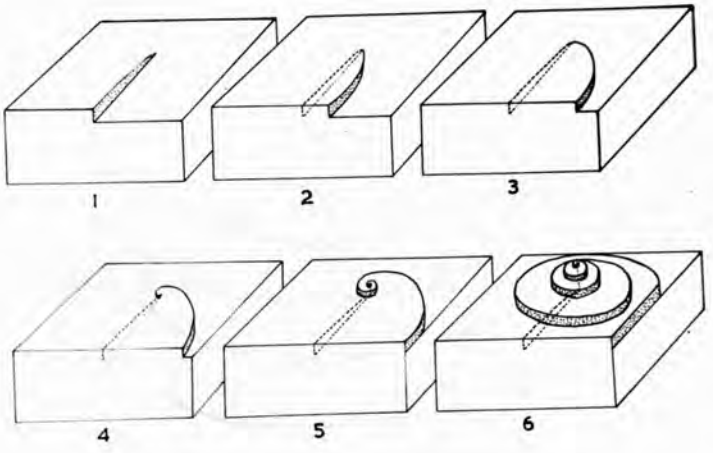

Fig. 6.

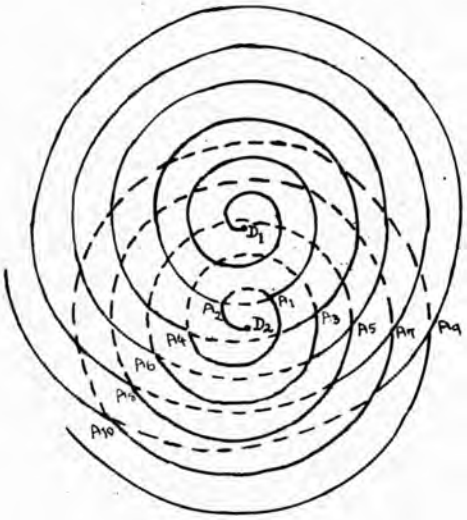
D1
D2
A1
A2
A3
A4
A5
A6
A7
A8
A9
A10

Fig. 7.

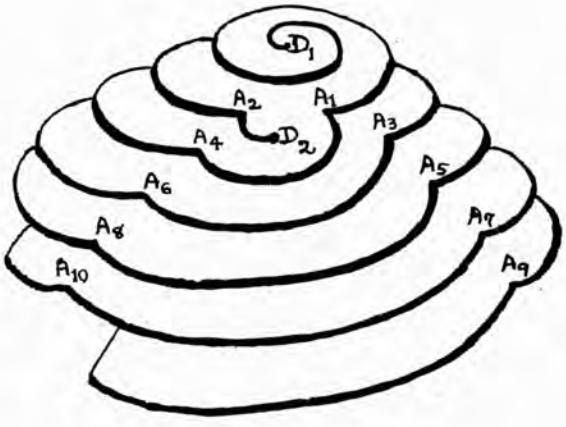
D1
D2
A1
A2
A3
A4
A5
A6
A7
A8
A9
A10

Fig. 8.

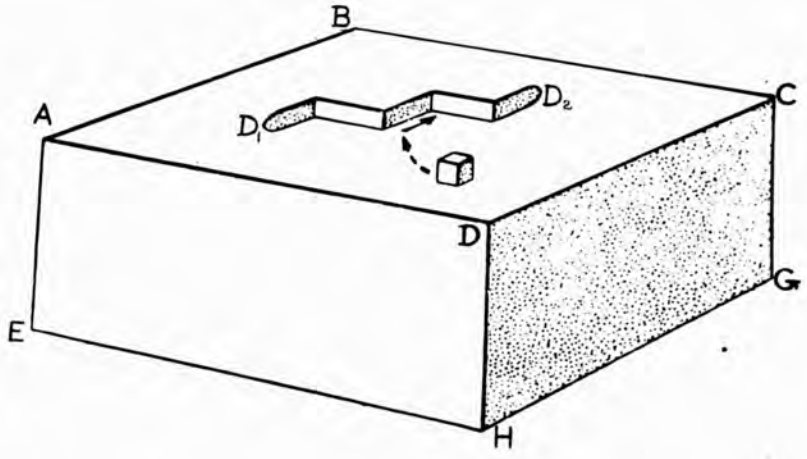

Fig. 9.

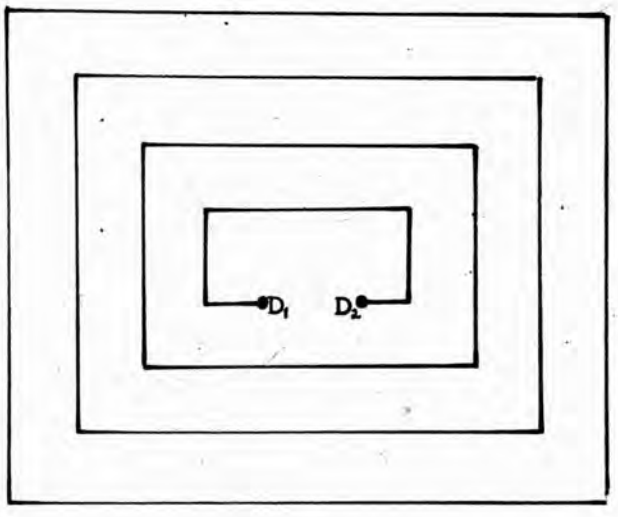

Fig. 10.

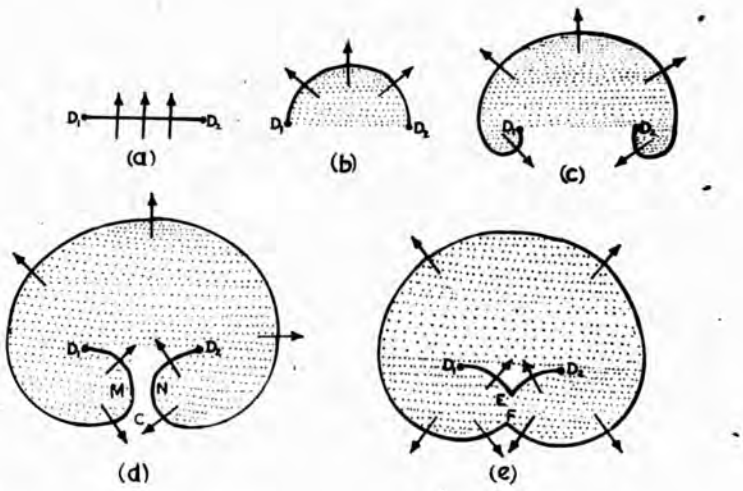

Fig. 11.

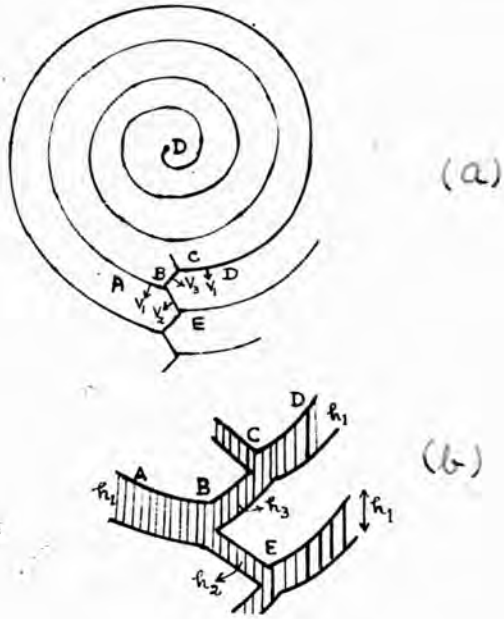

Fig. 12.

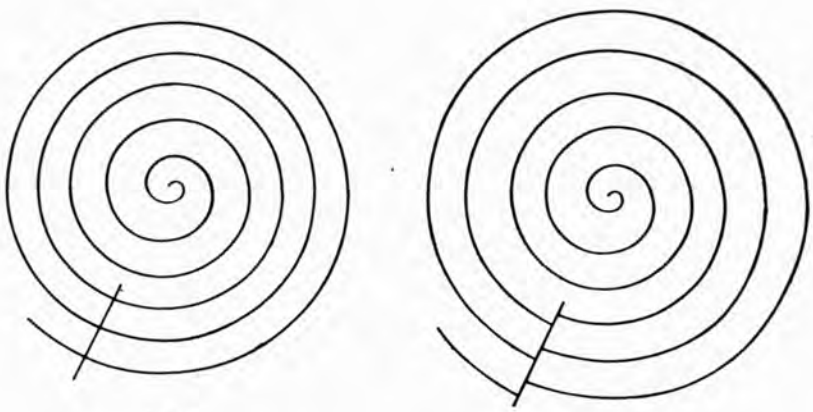

Fig. 13.

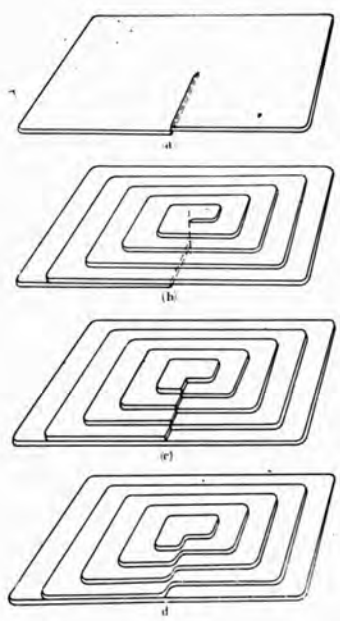

Fig. 14.

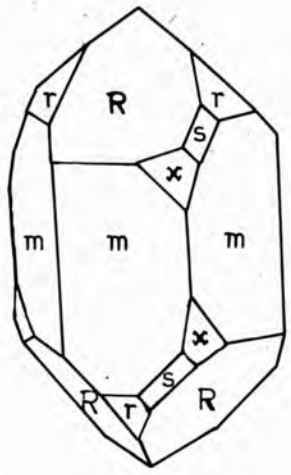

Fig. 15.

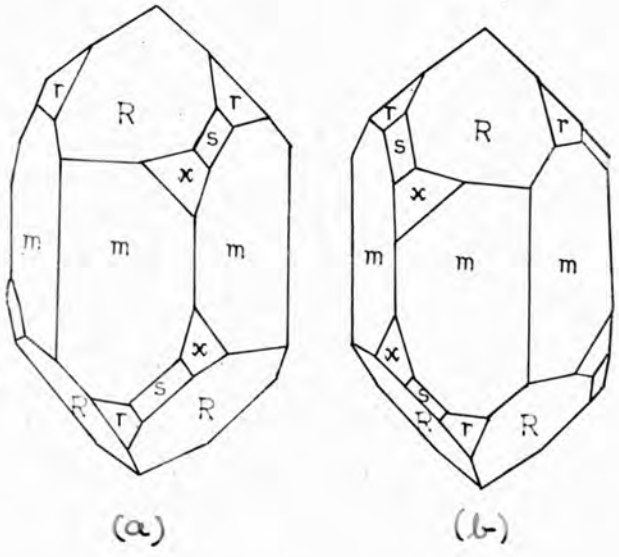

Fig. 16.

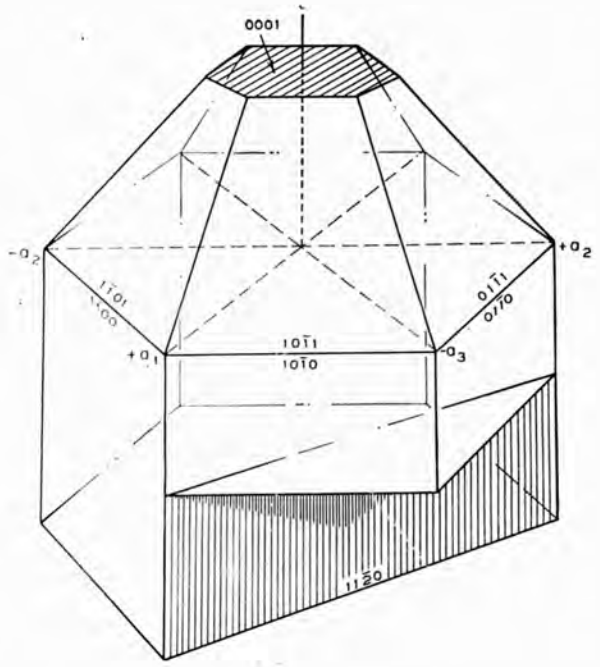
0001
$-a_2$
$+a_2$
$+a_1$
$-a_3$
$1\bar{1}01$
$1\bar{1}00$
$10\bar{1}1$
$10\bar{1}0$
$01\bar{1}1$
$01\bar{1}0$
$11\bar{2}0$

Fig. 17.

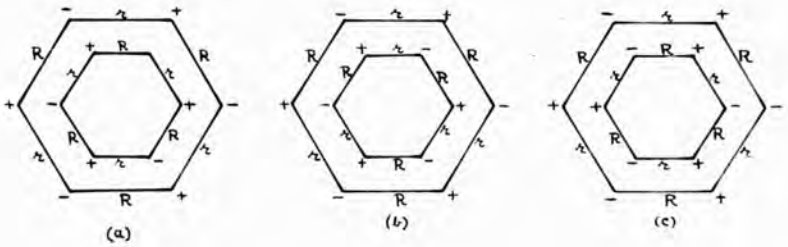
R
(a)
(b)
(c)

Fig. 18.

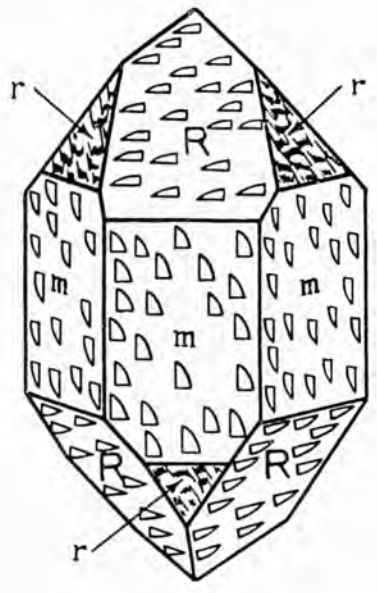
r
r
R
m
m
R
R
r

Fig. 19.

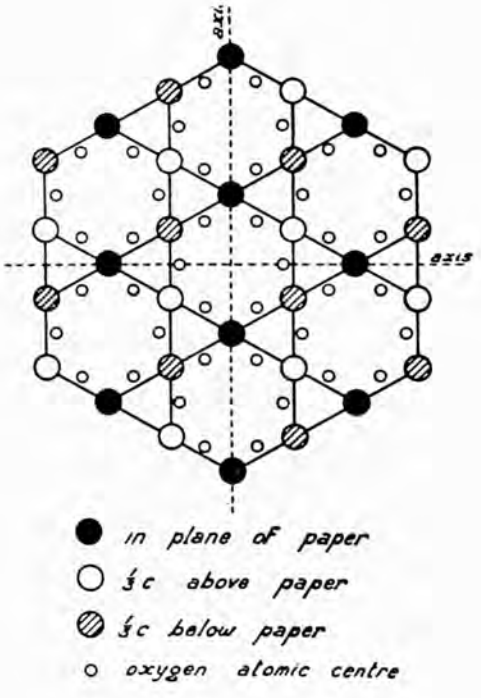
axis
axis
in plane of paper
½c above paper
½c below paper
oxygen atomic centre

Fig. 20.

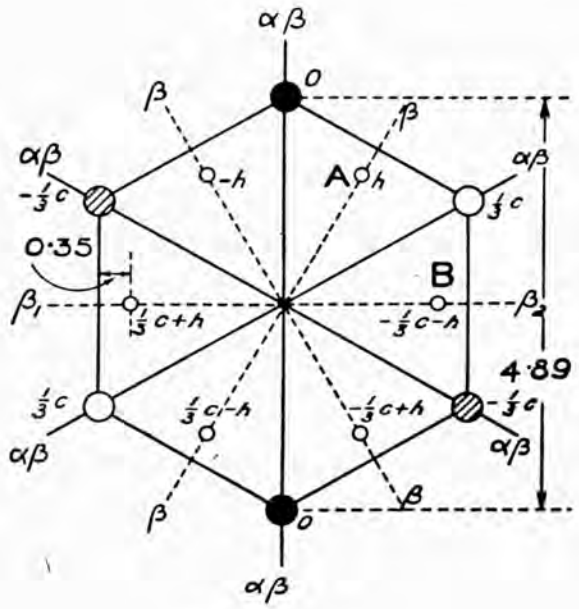
αβ
O
β
β
αβ
-⅓c
-h
A
h
⅓c
αβ
0·35
B
β₁
⅓c+h
-⅓c-h
β₂
4·89
⅓c
⅓c-h
-⅓c+h
-⅓c
αβ
αβ
β
O
β
αβ

Fig. 21.

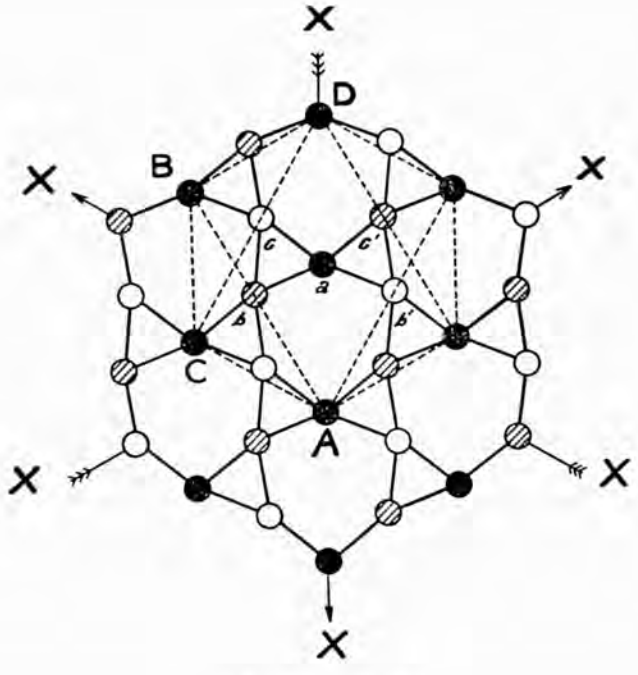
X
D
B
X
X
c
c'
a
b
b'
C
A
X
X
X

Fig. 22.

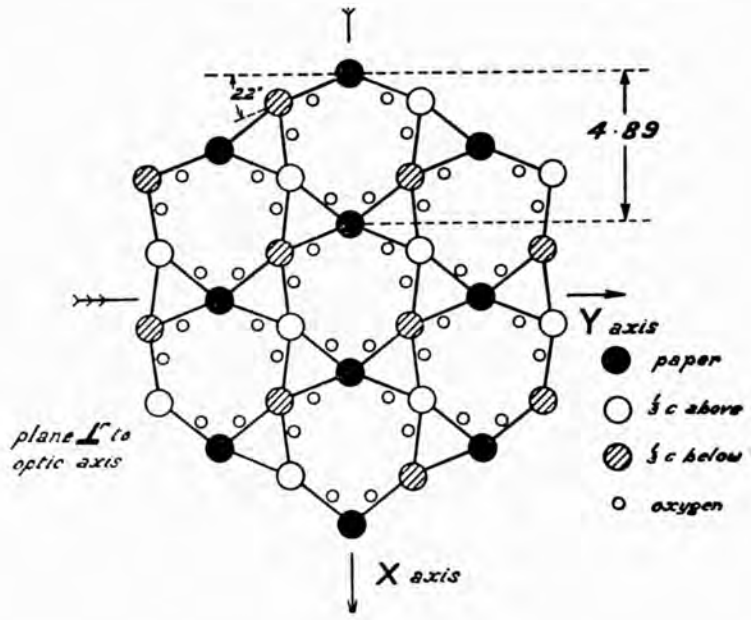
22°
4·89
Y axis
paper
½ c above
½ c below
oxygen
plane ⊥ to optic axis
X axis

Fig. 23.

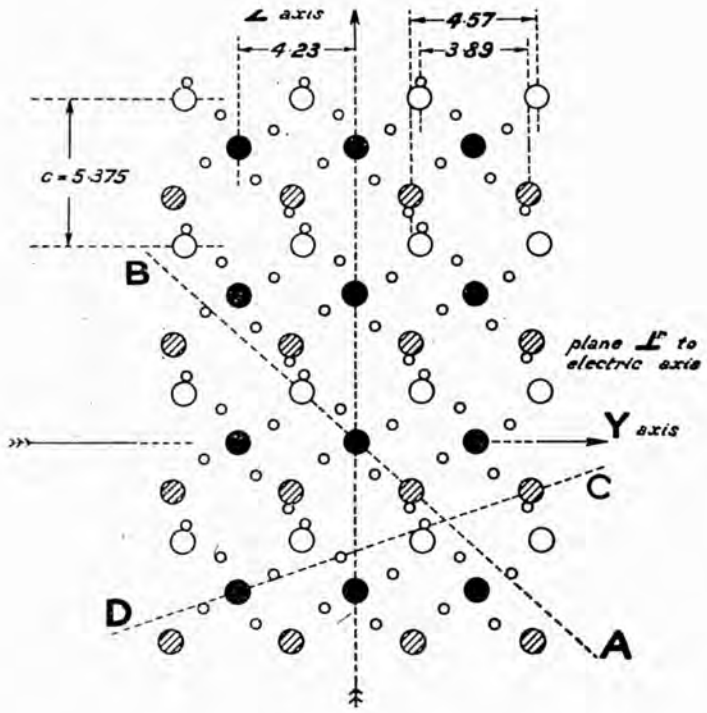
Z axis
4·23
4·57
3·89
c = 5·375
B
plane ⊥ to electric axis
Y axis
C
D
A

Fig. 24.

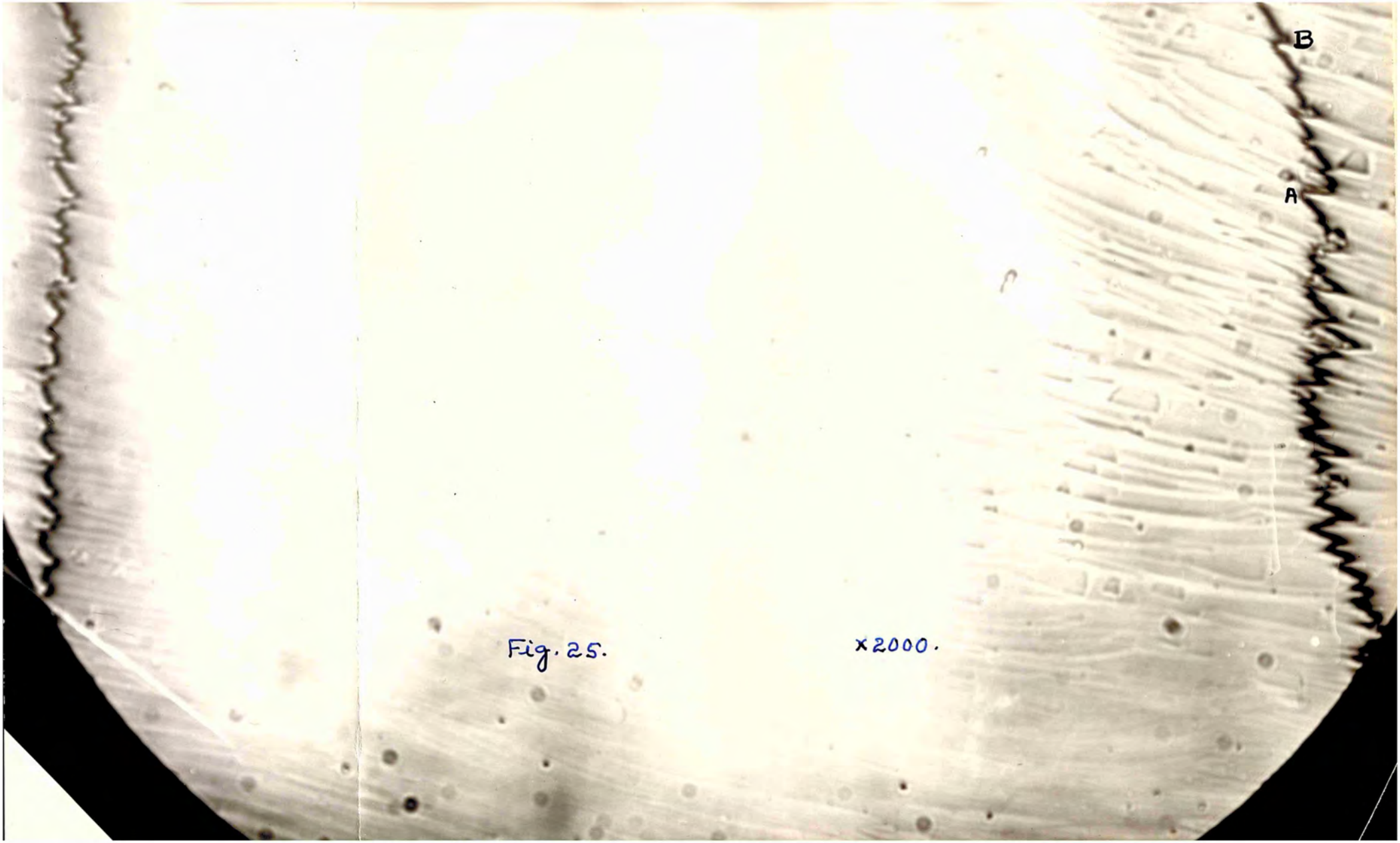

Fig. 25. ×2000.

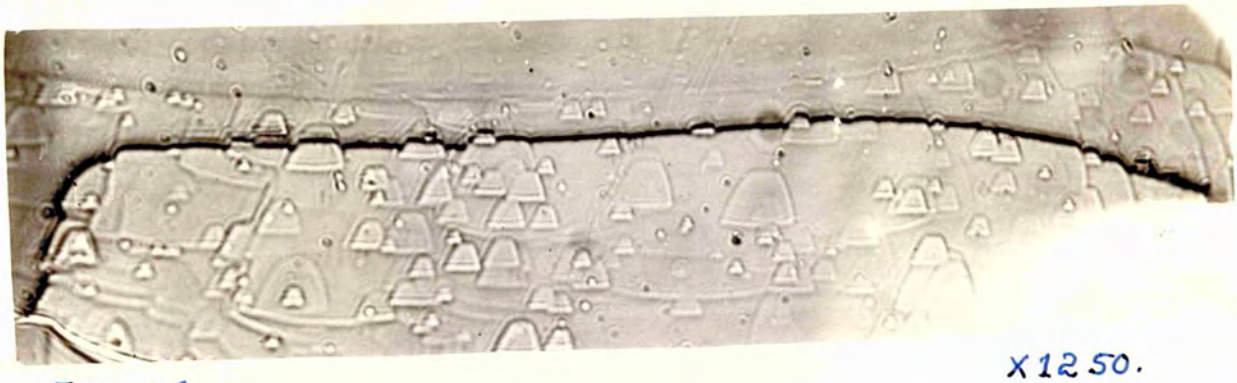

Fig. 26. X 1250.

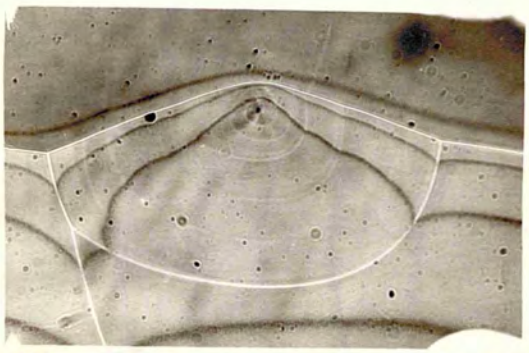

Fig. 27. X 105.

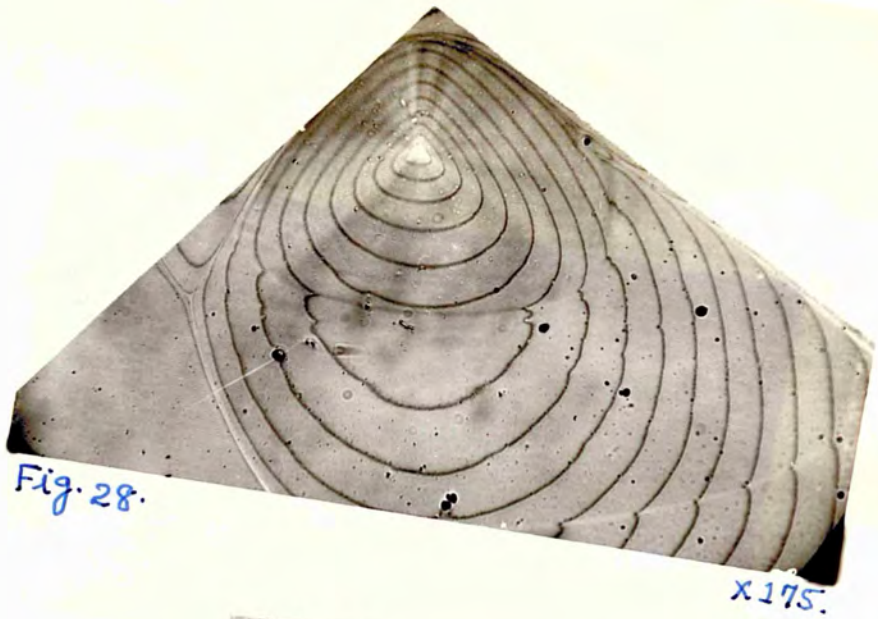

Fig. 28.

x 175.

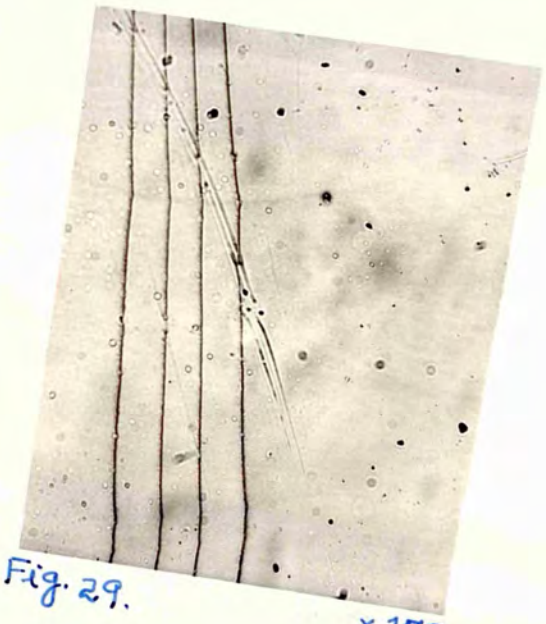

Fig. 29.

x 175.

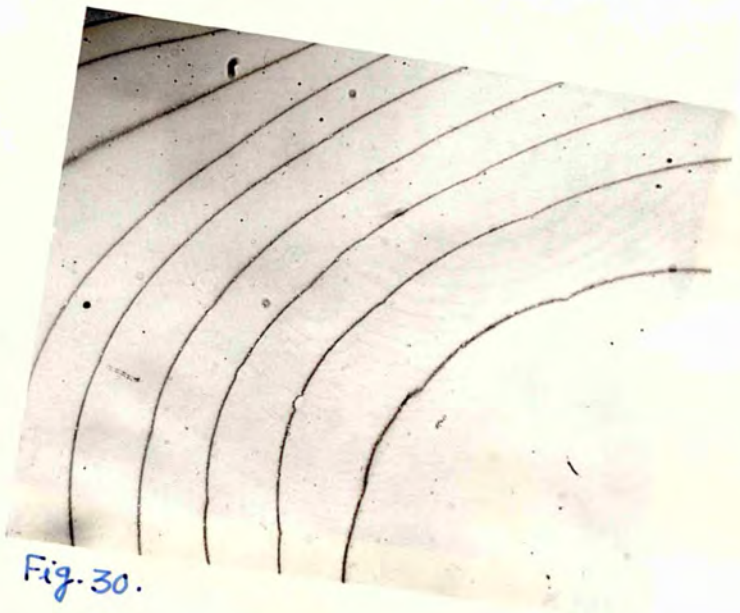

Fig. 30.

x 105.

Fig. 31. ×105.

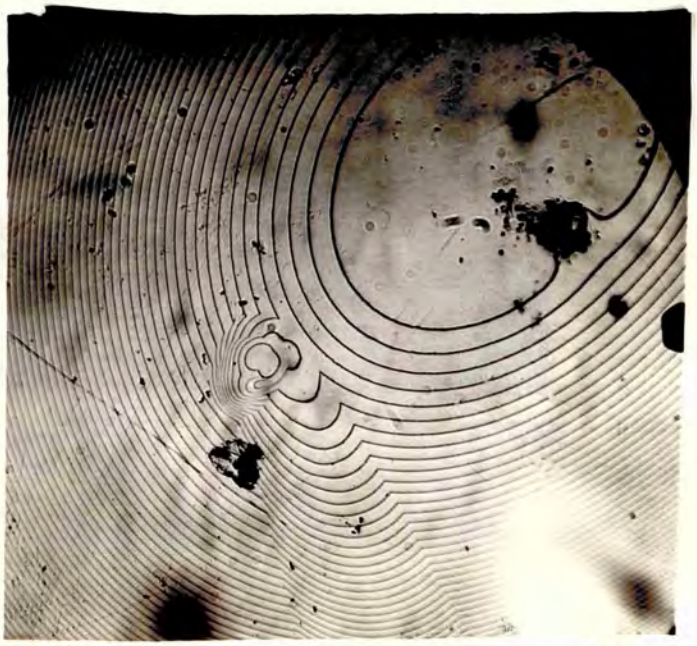

Fig. 32. ×105.

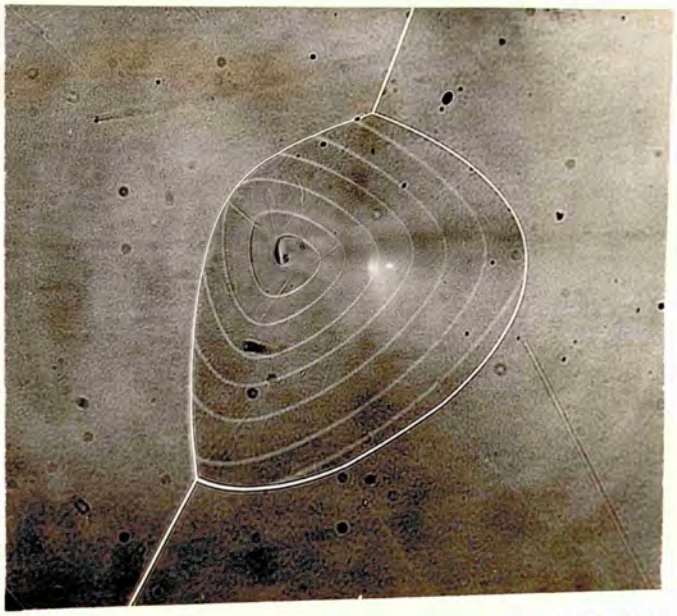

Fig. 33. ×175.

Fig. 34. ×175.

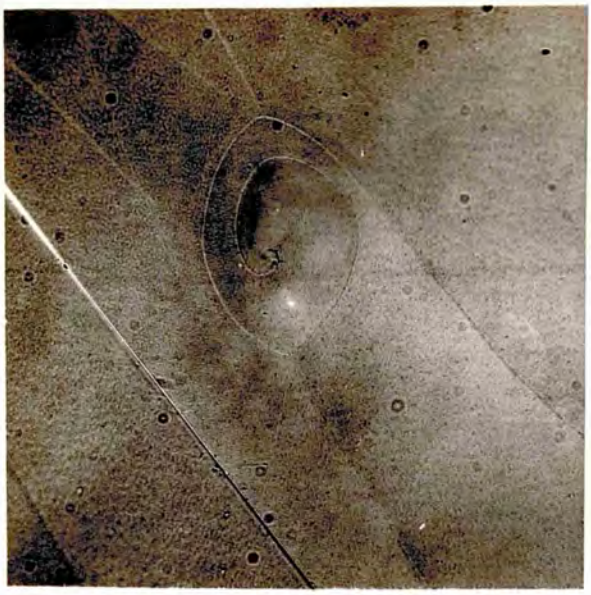

Fig. 35. x 175.

Fig. 36. x 175.

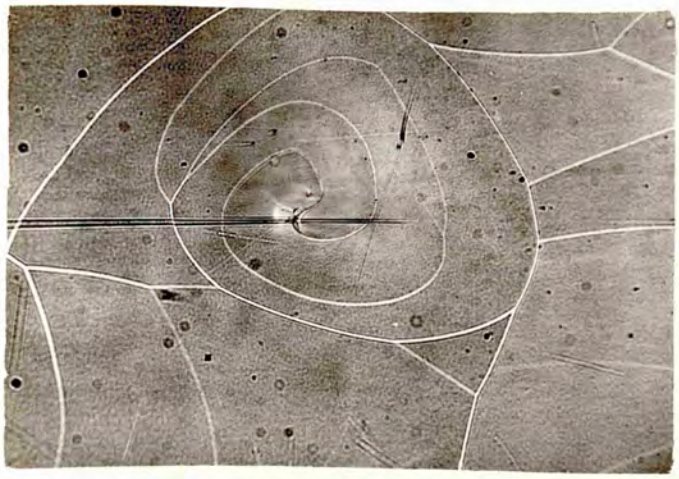

Fig. 37. ×175.

Fig. 38. ×410.

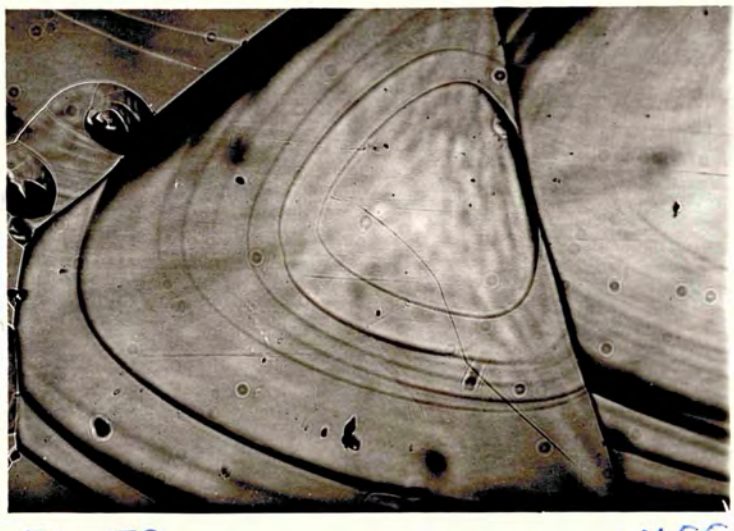

Fig. 39. x55.

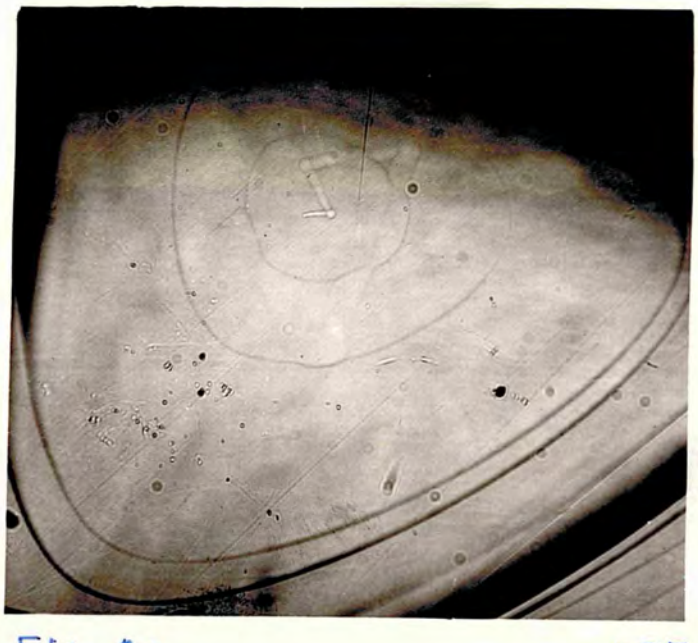

Fig. 40. x55.

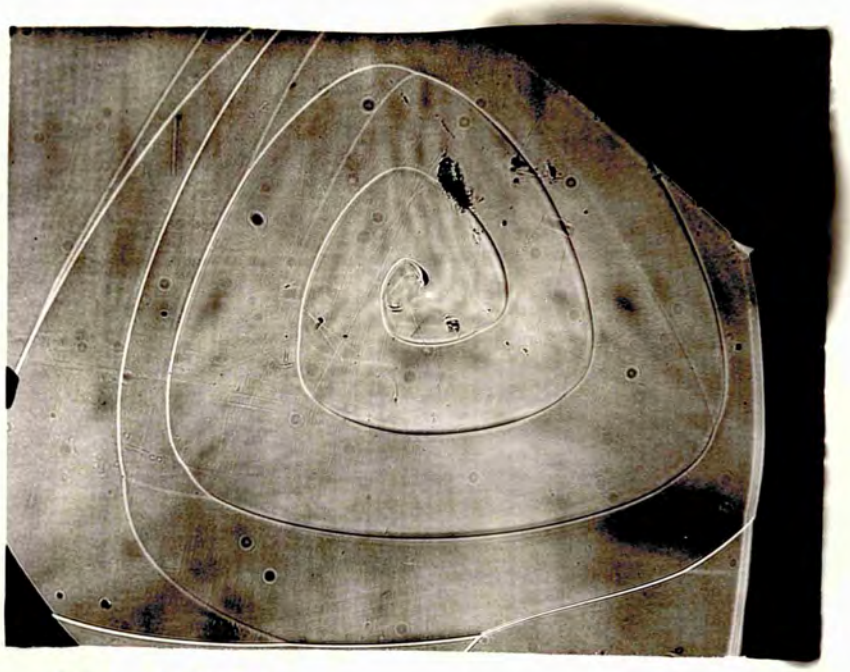

Fig. 41 (a). ×105.

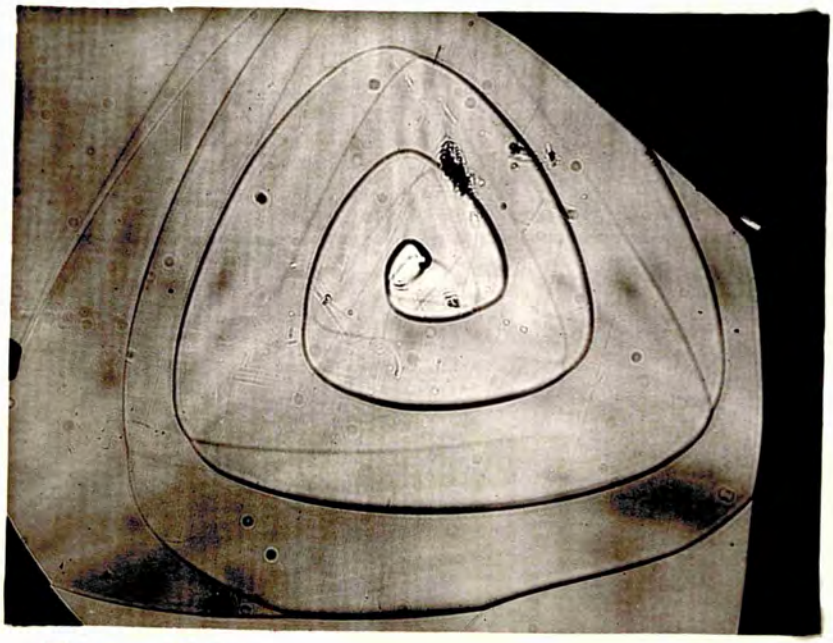

Fig. 41 (b). ×105.

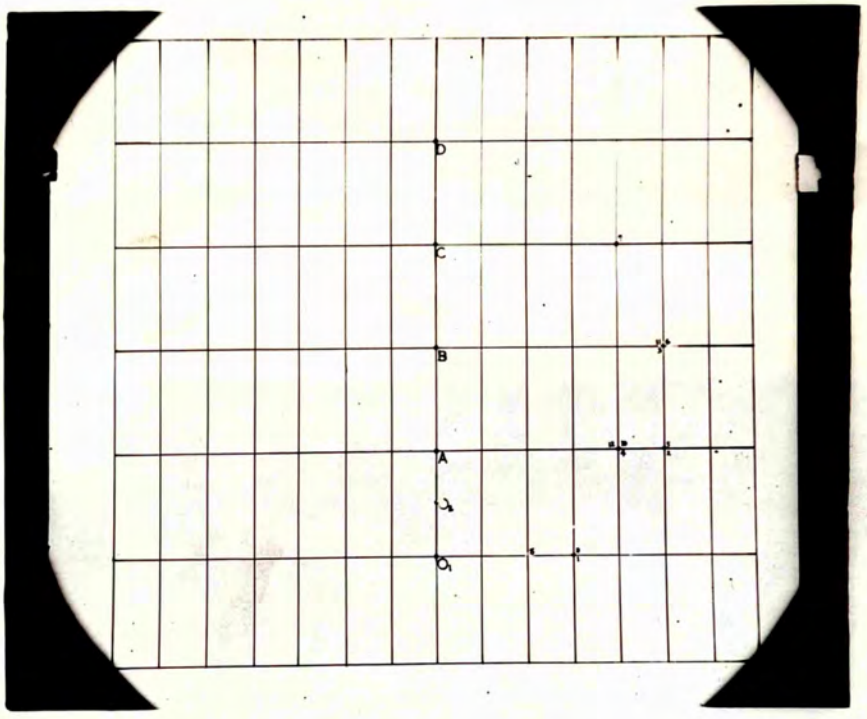

Fig. 42.

Fig. 43.

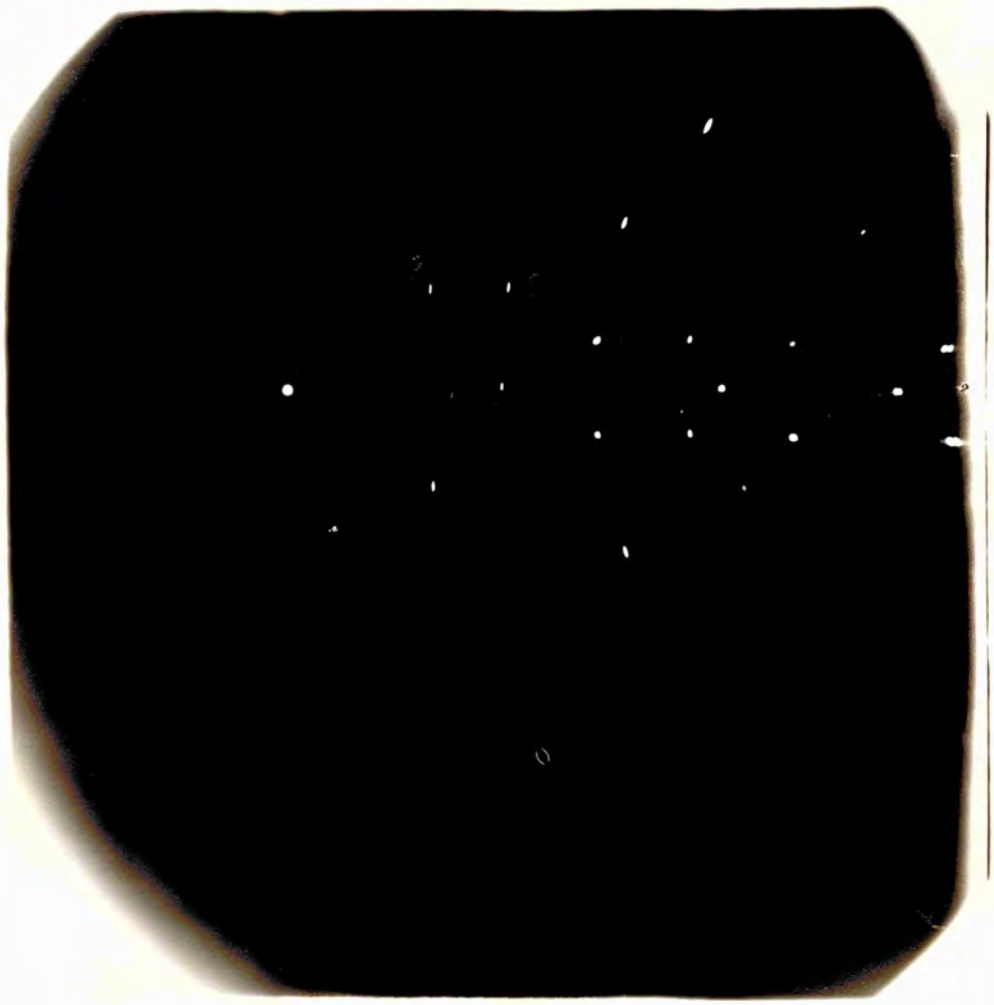

Fig. 43

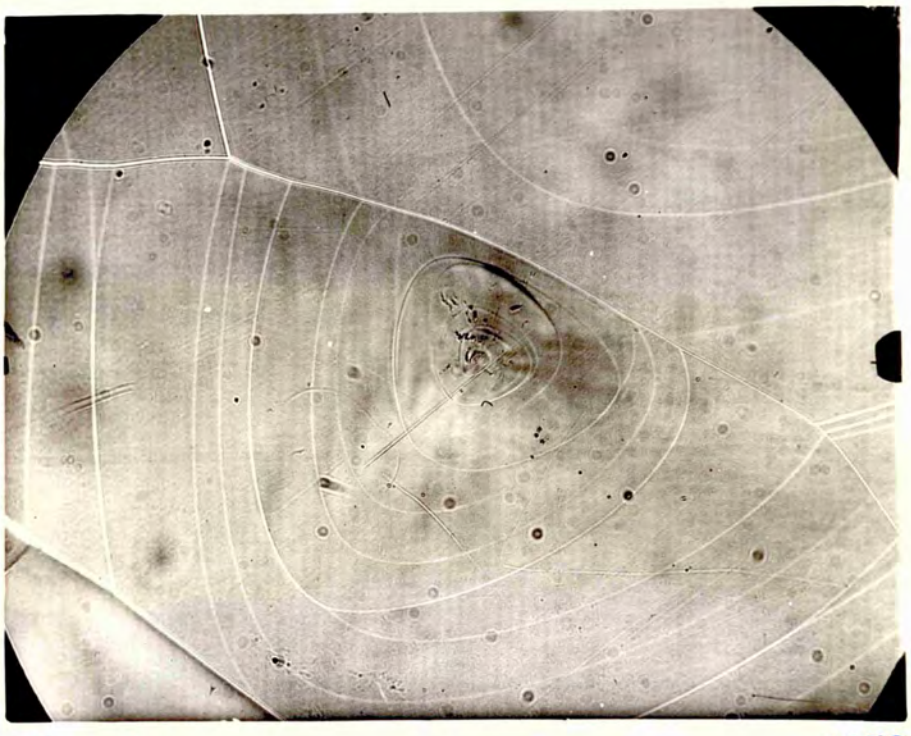

Fig. 44. x175.

Fig. 45. x 105.

Fig. 46. x 105.

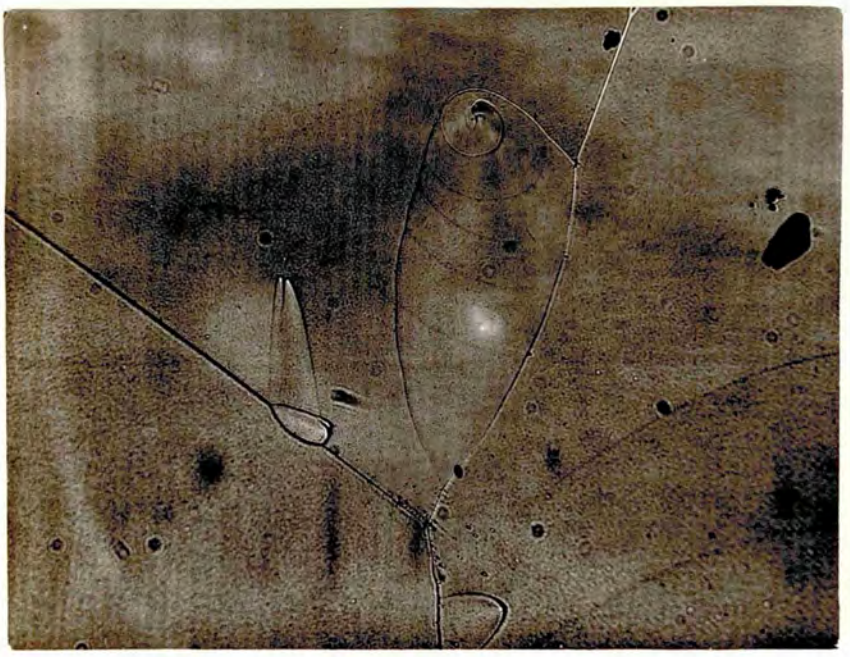

Fig. 47(a). x175.

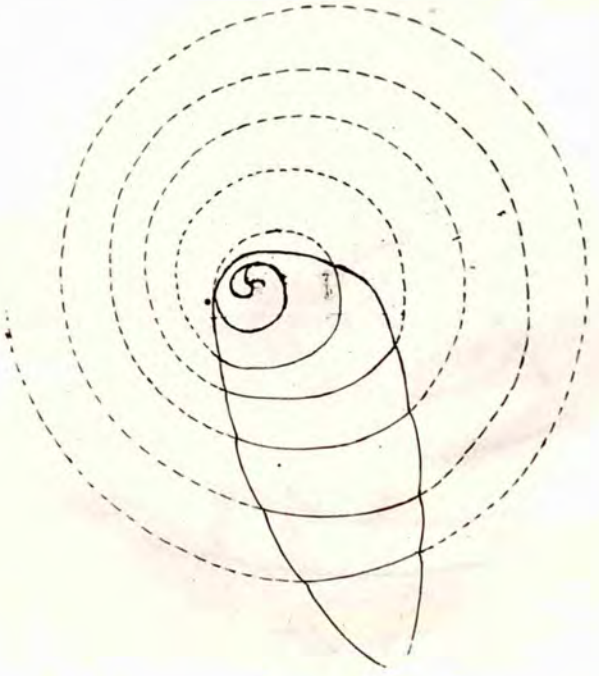

Fig. 47(b).

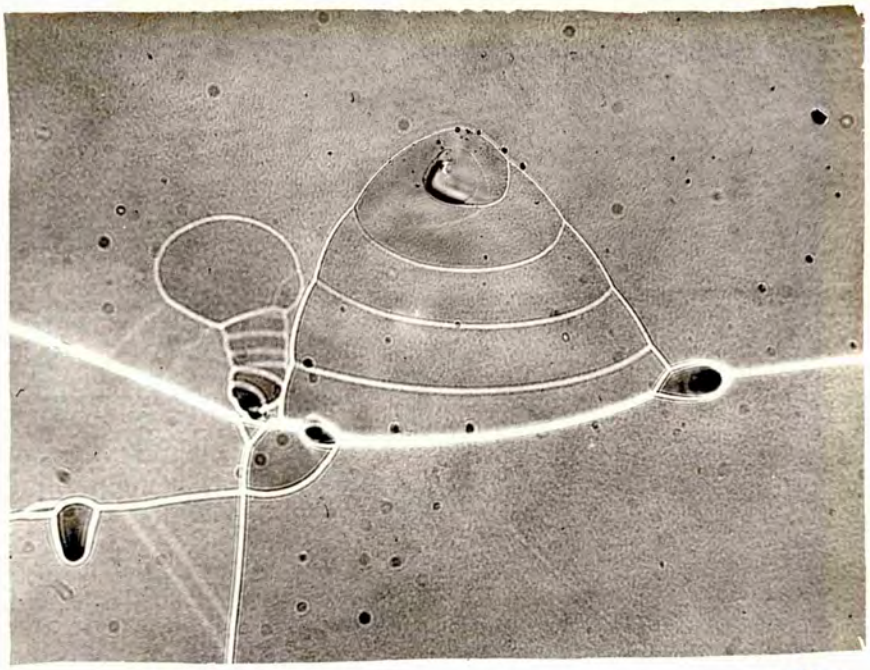

Fig. 48 (a). x 175.

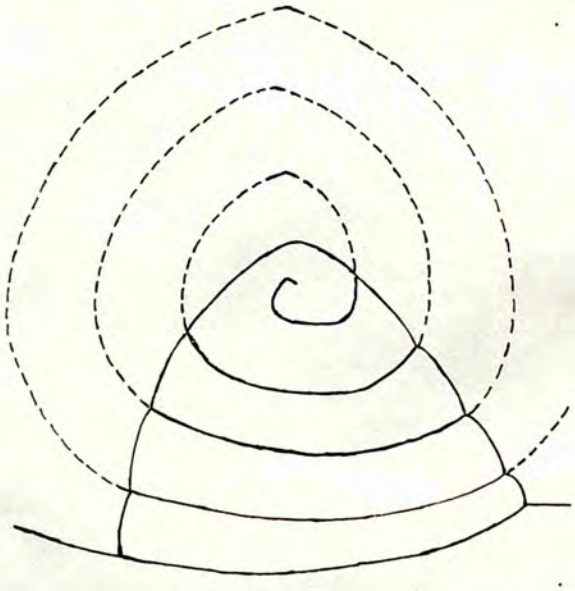

Fig. 48 (b).

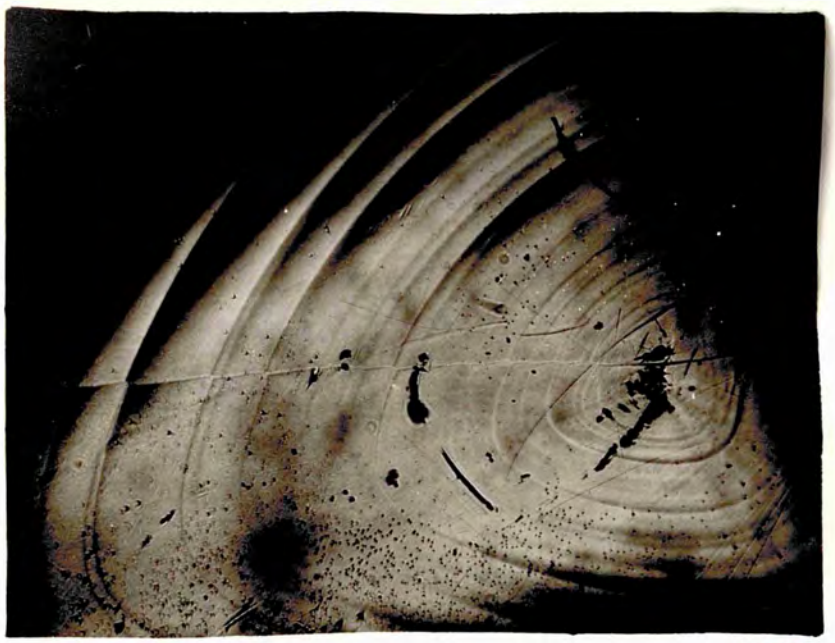

Fig. 49. X55.

Fig. 50. X55.

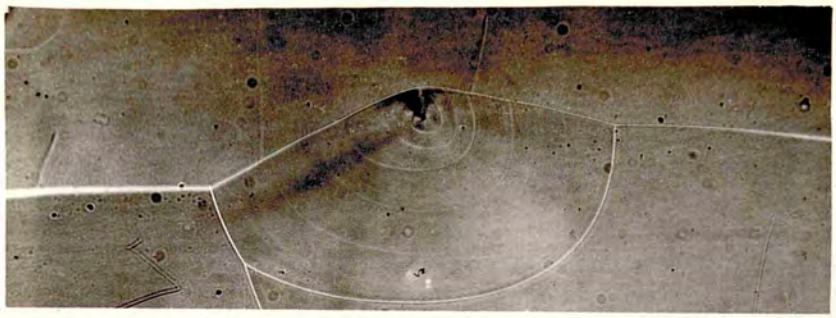

Fig. 51. x105.

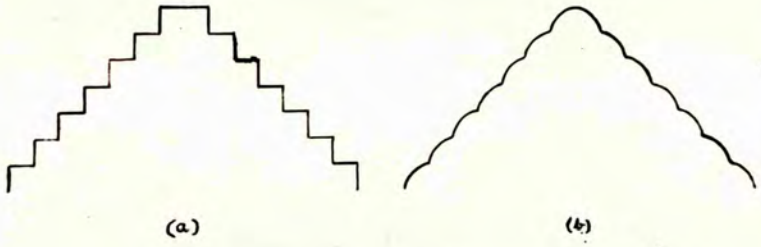

Fig. 52.

Fig. 53. x175.

Fig. 54. x55.

Fig. 55. x55.

Fig. 56. x 84.

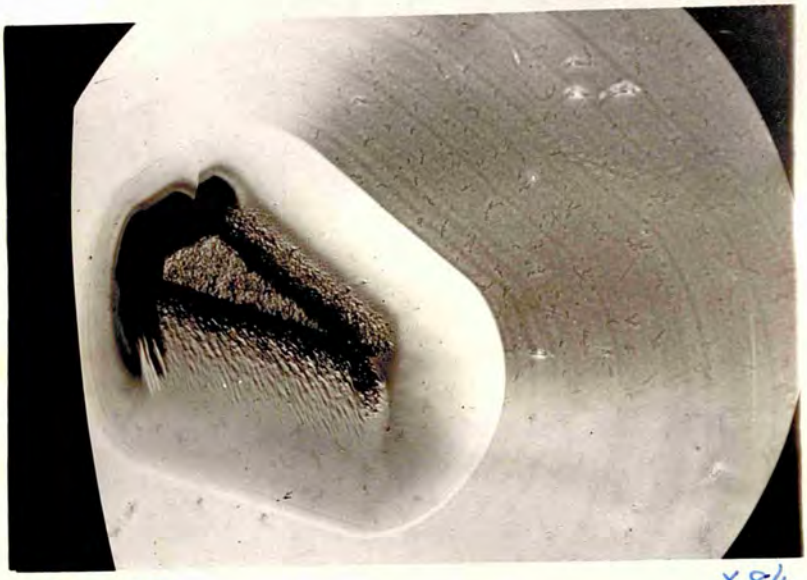

Fig. 57. x 84.

Fig. 58. x 84.

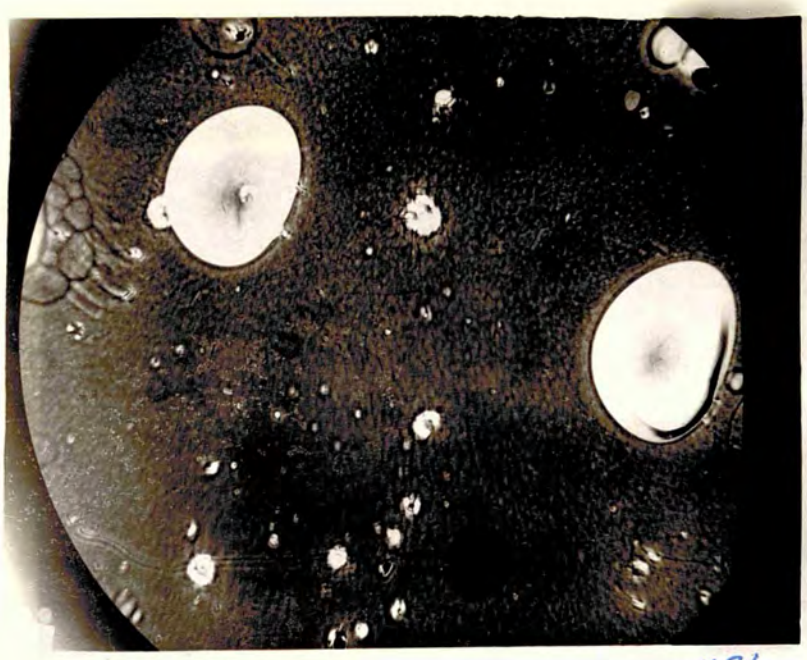

Fig. 59. ×84.

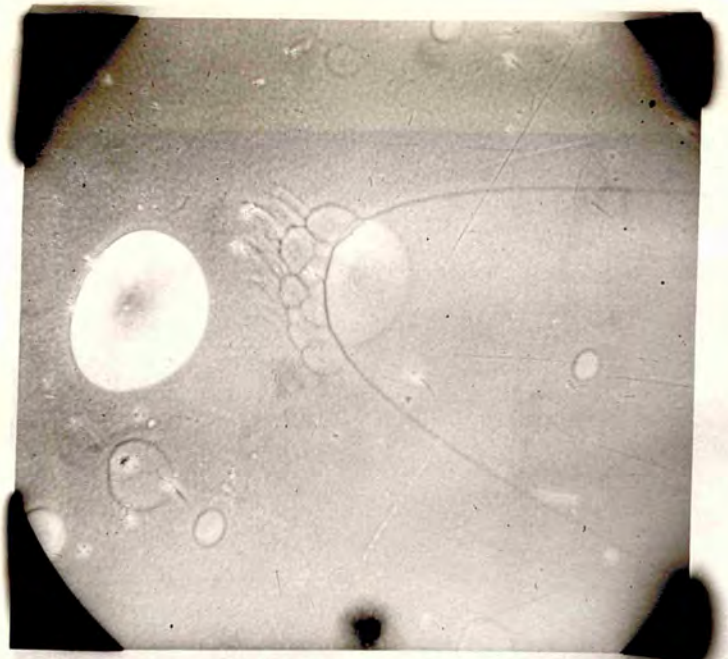

Fig. 60. ×84

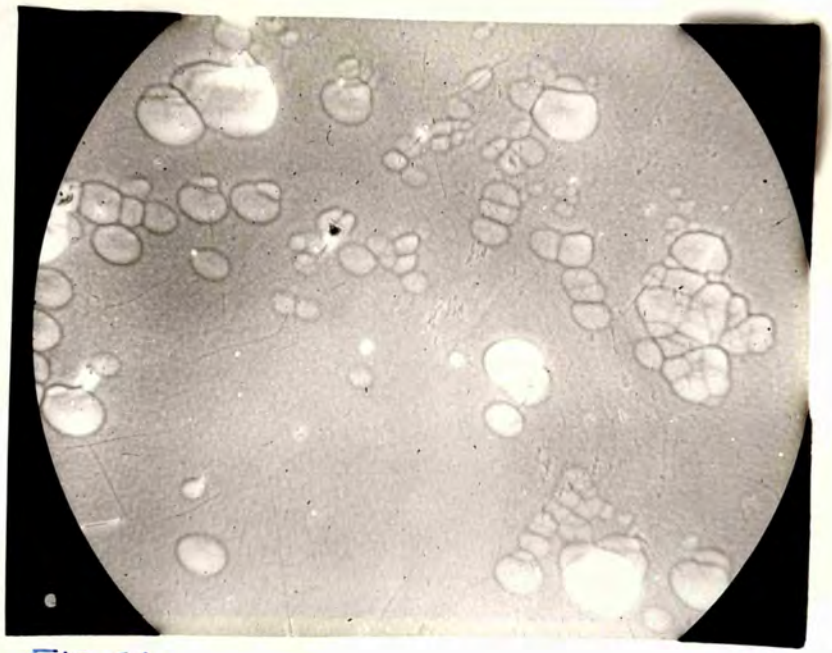

Fig. 61. x84.

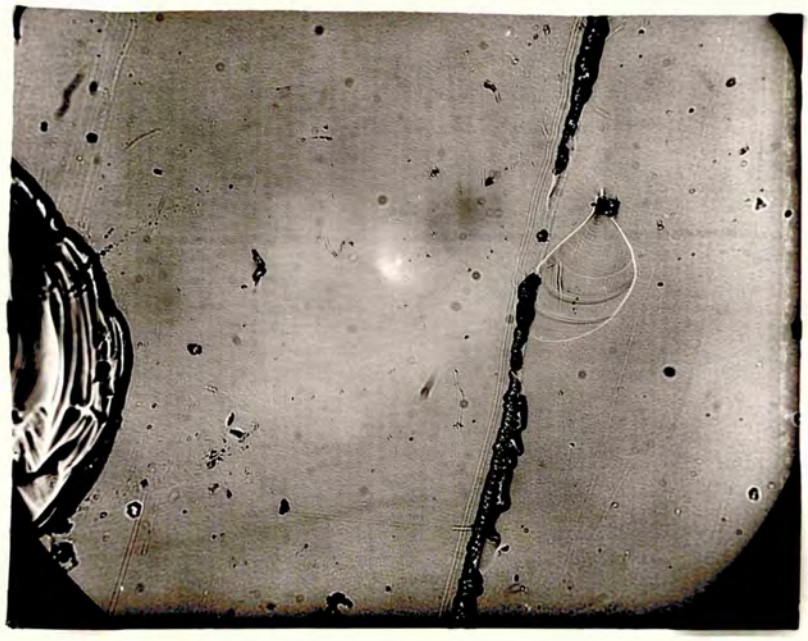

Fig. 62. x 105.

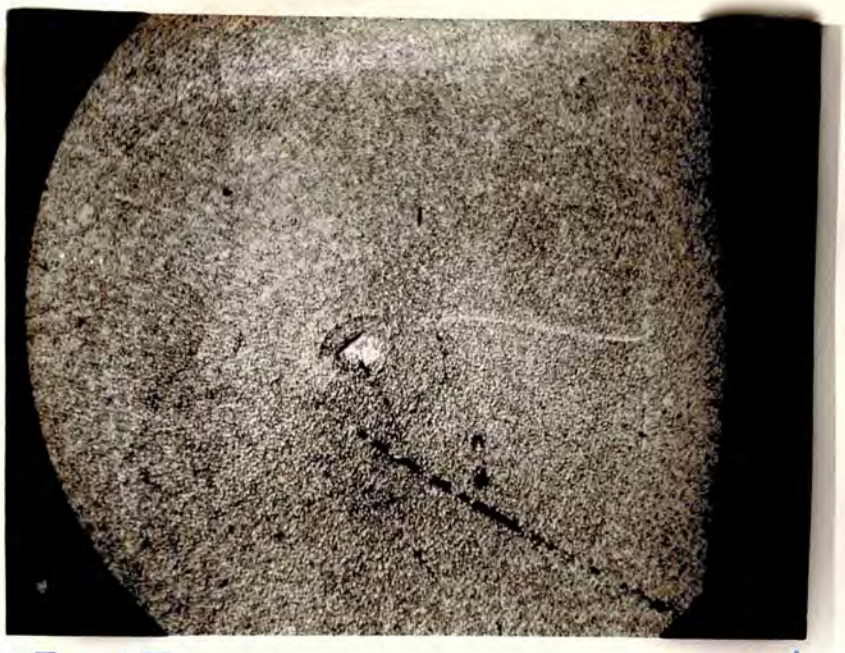

Fig. 63. x 84.

Fig. 64. x 84.

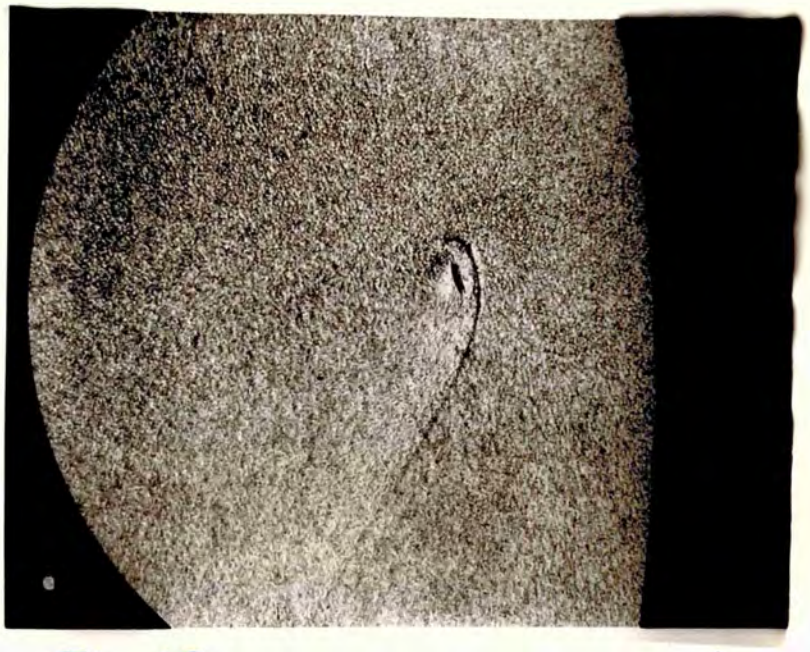

Fig. 65. x84.

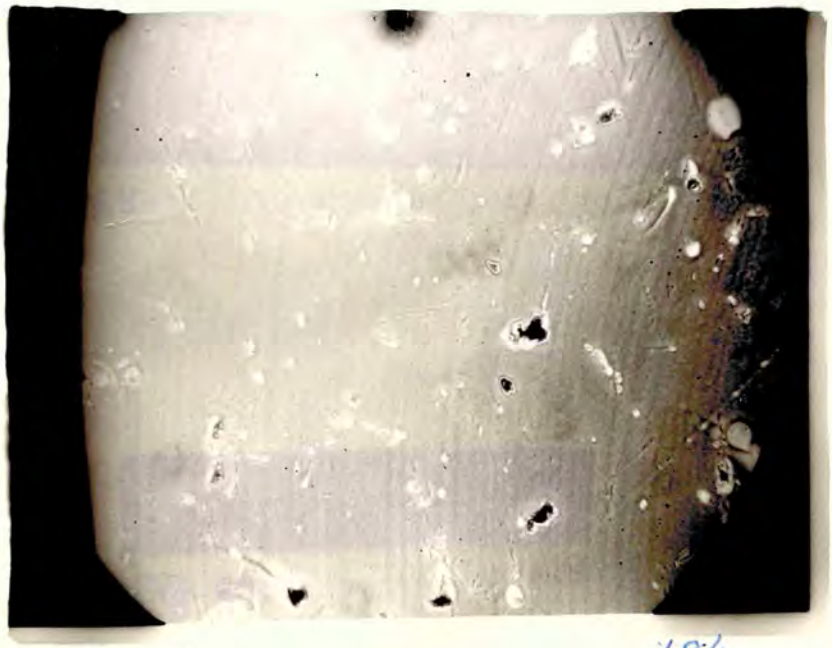

Fig. 66. x84.

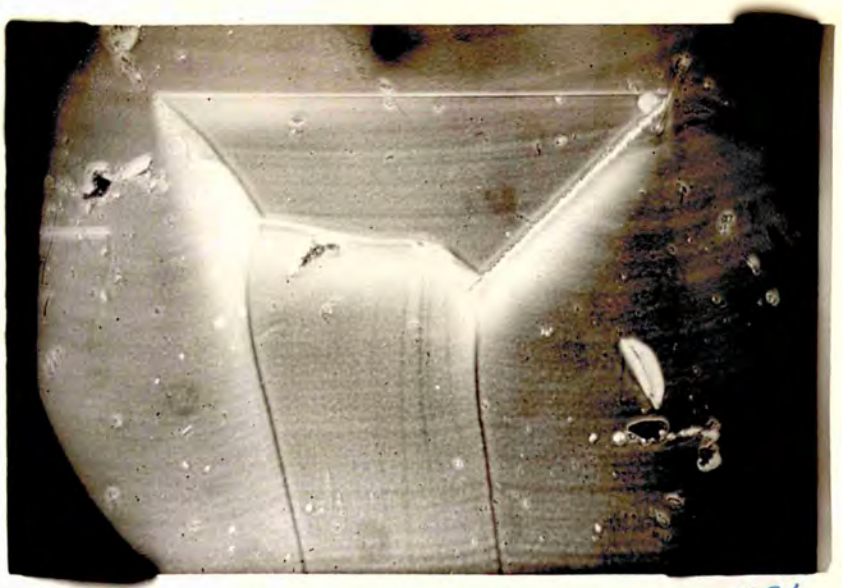

Fig. 67. x 84

Fig. 68. x 84.

Fig. 69. x 19.

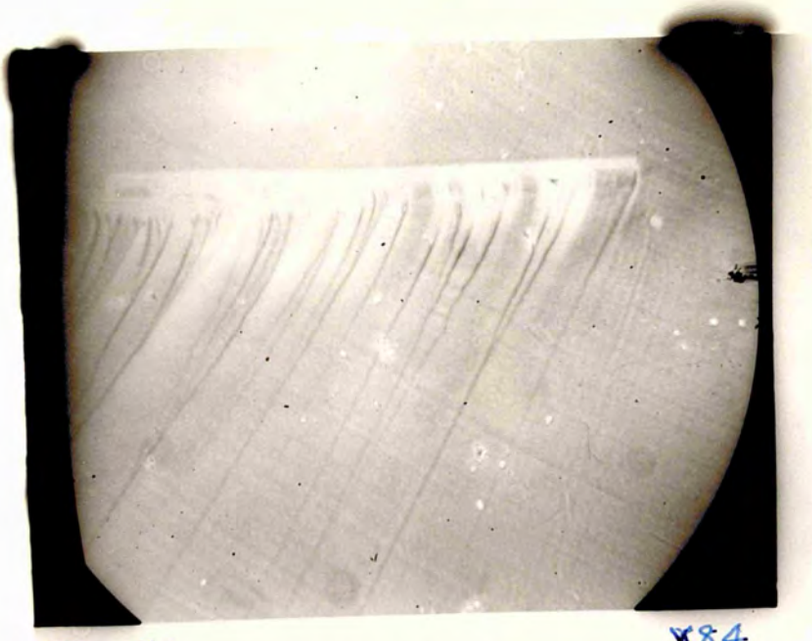

Fig. 70. ×84.

Fig. 71. ×57.

Fig. 72. x84.

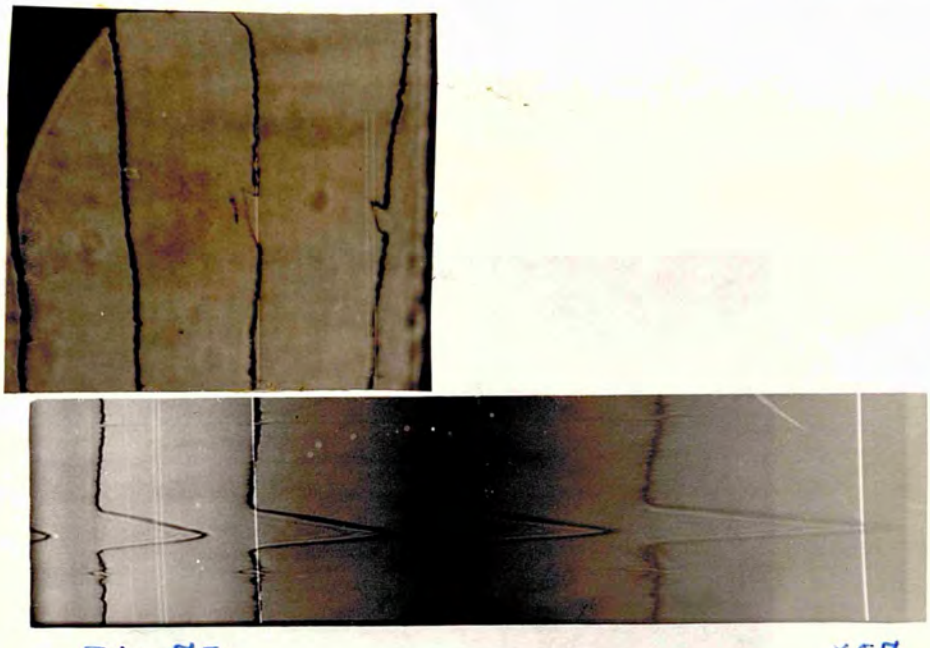

Fig. 73. x57.

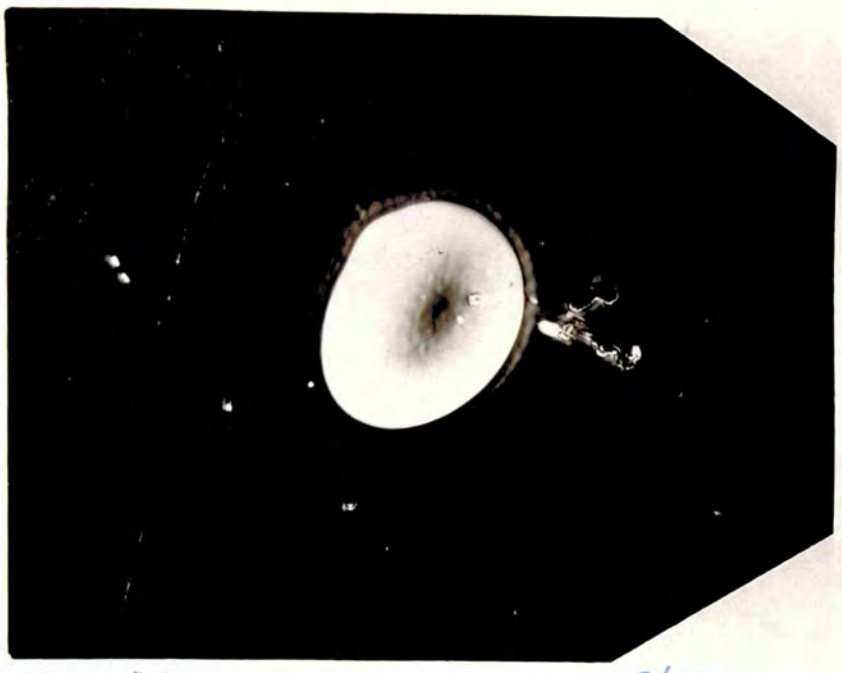

Fig. 74. ×84.

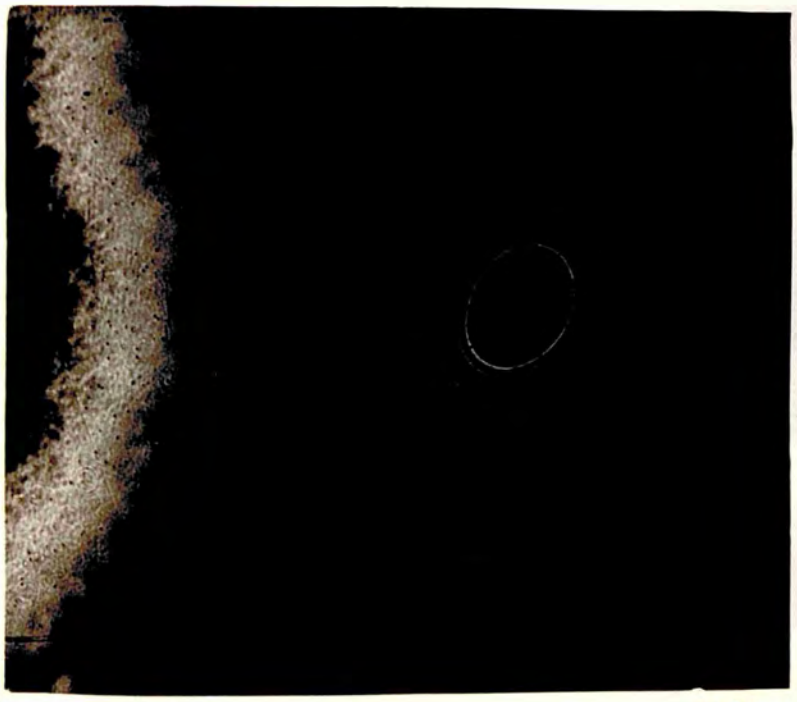

Fig. 75. ×105.

Fig. 76. x 84.

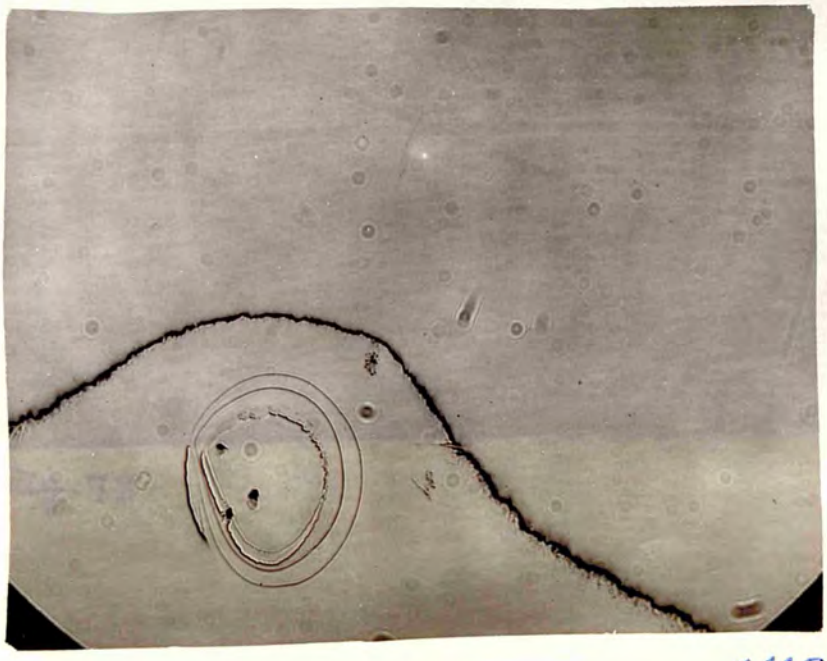

Fig. 77. x 105.

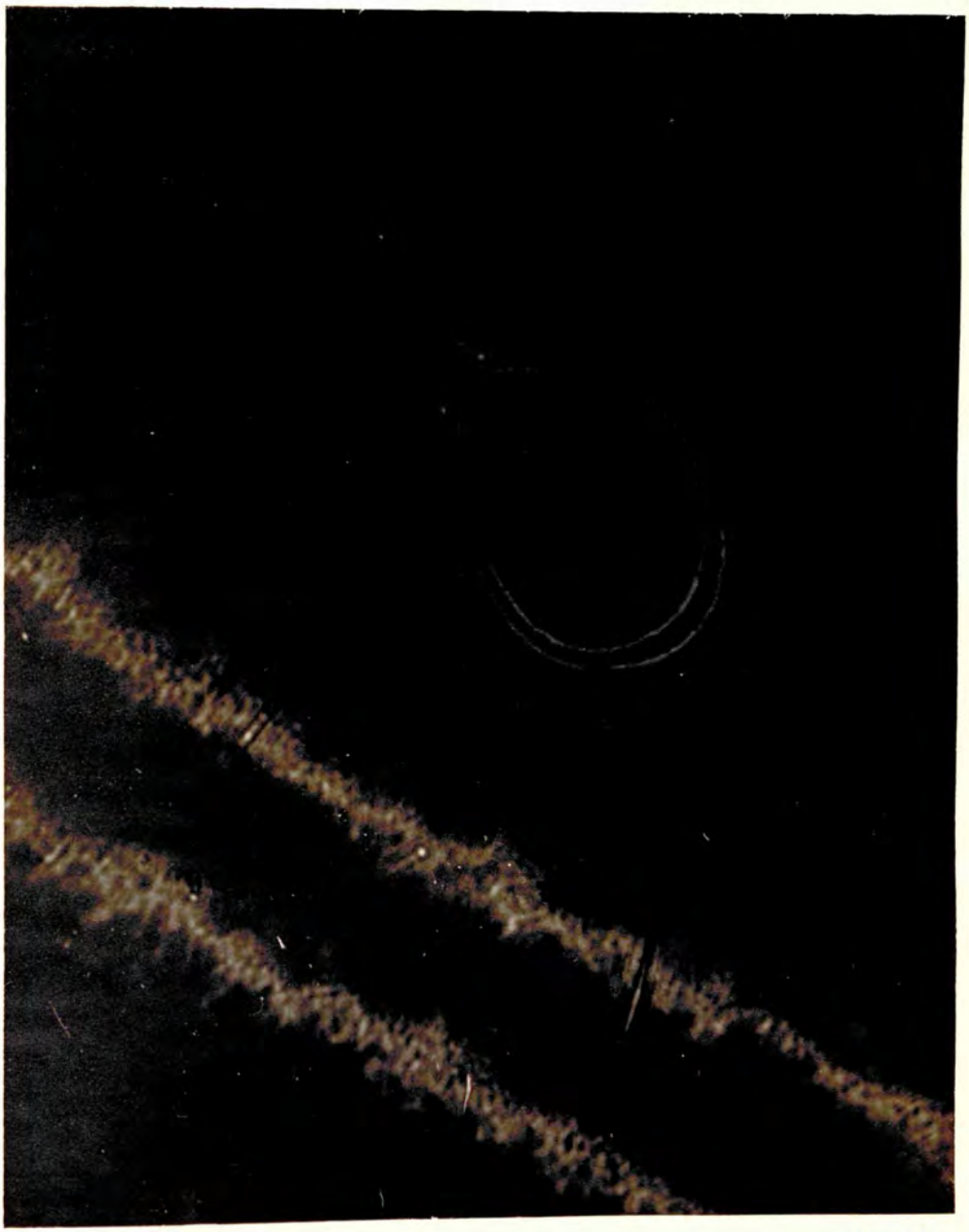

Fig. 78. X350.

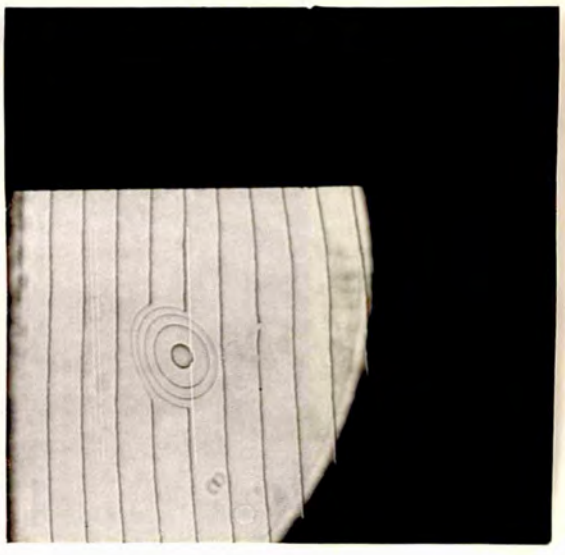

Fig. 79. X57.

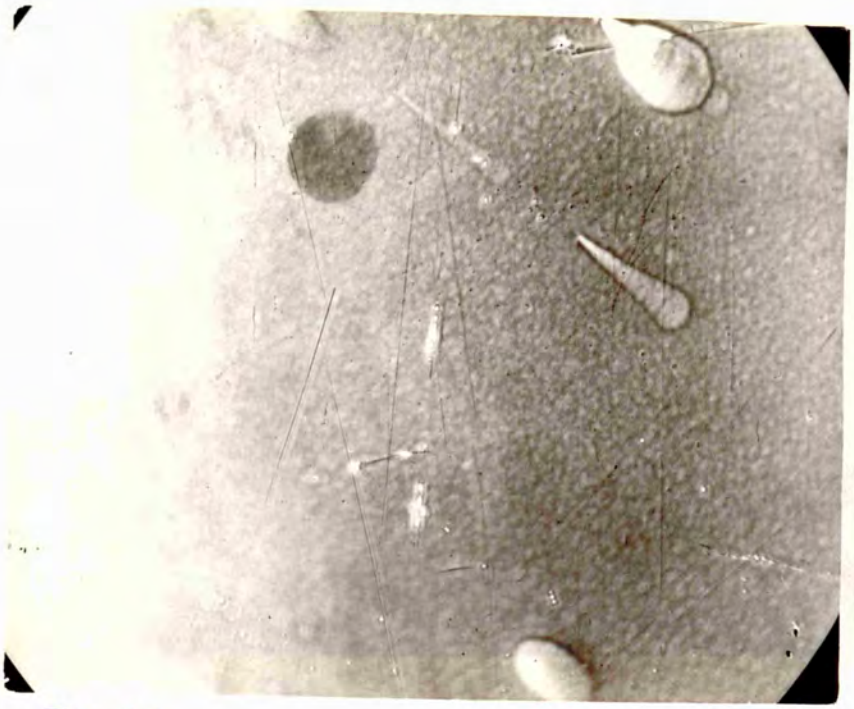

Fig. 80. x 84.

Fig. 81. x 140.

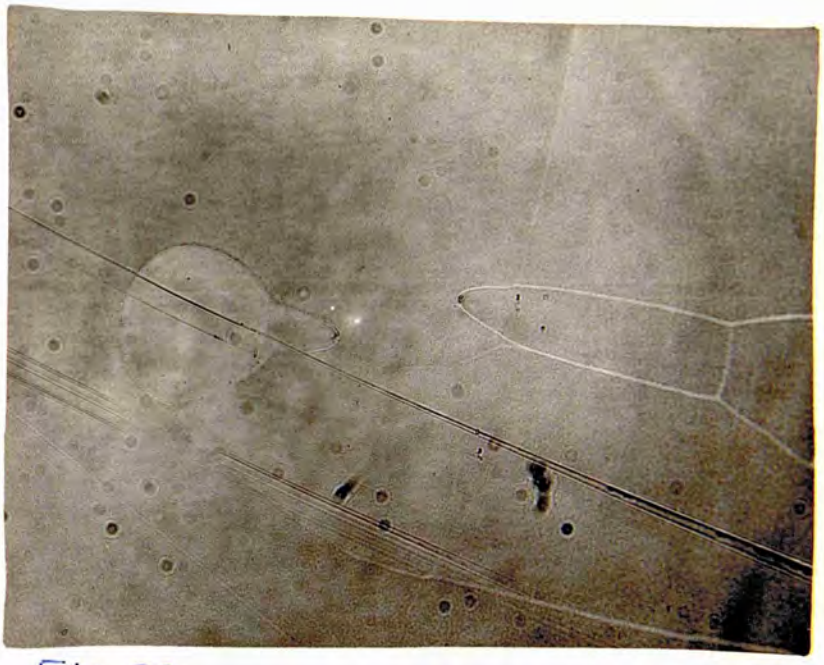

Fig. 82. x 105.

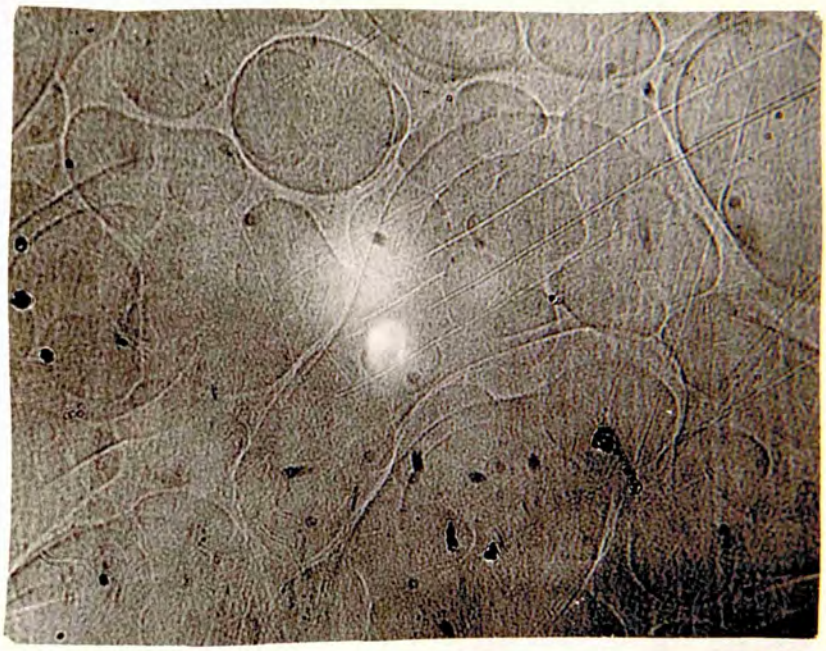

Fig. 83. x 105.

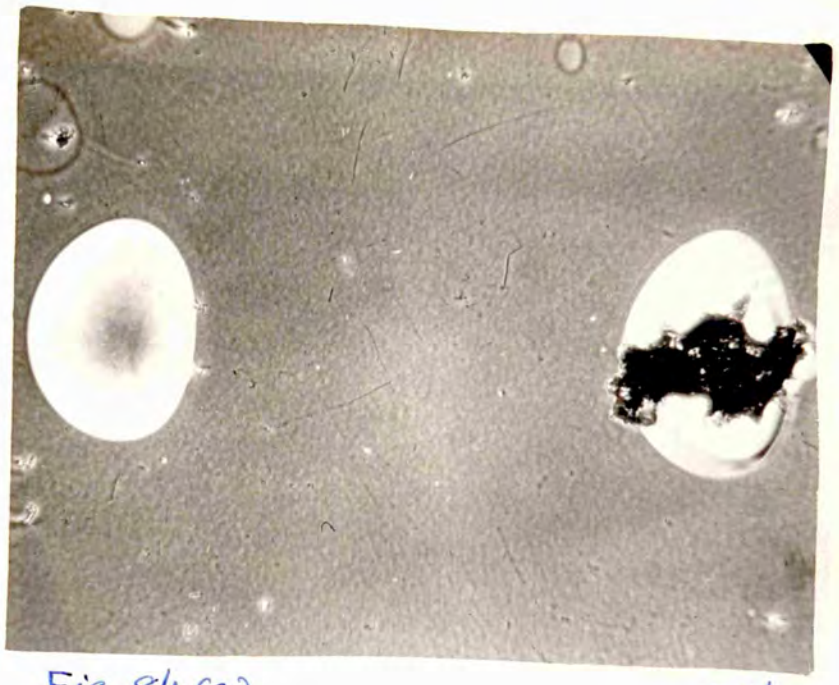

Fig. 84(a). x 84.

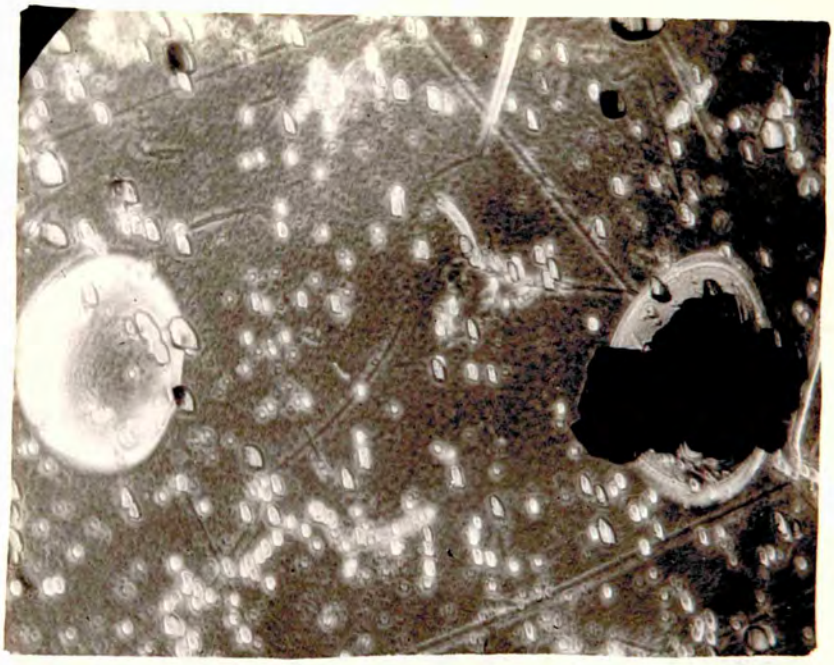

Fig. 84(b). x 84.

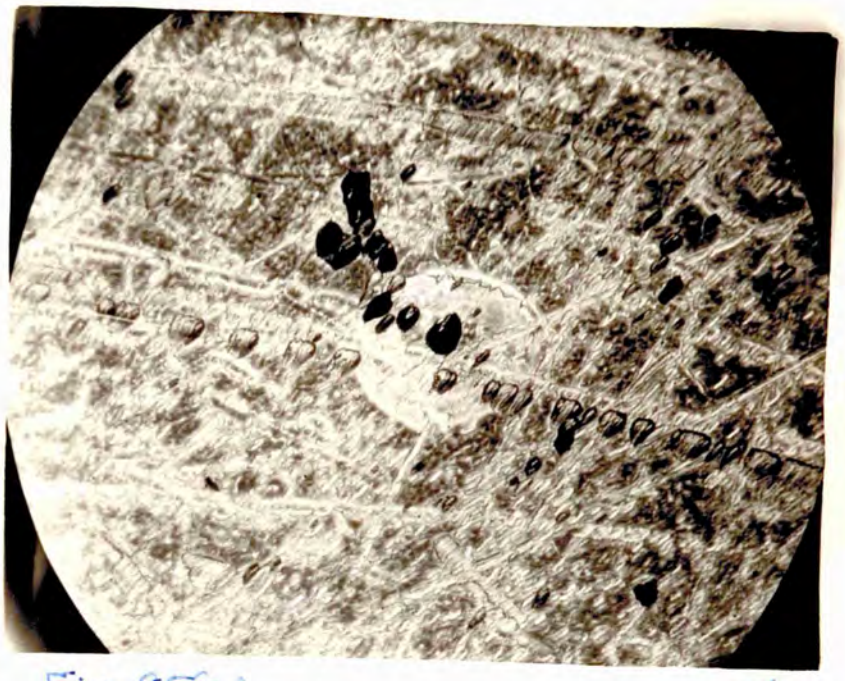

Fig. 85(a). ×84.

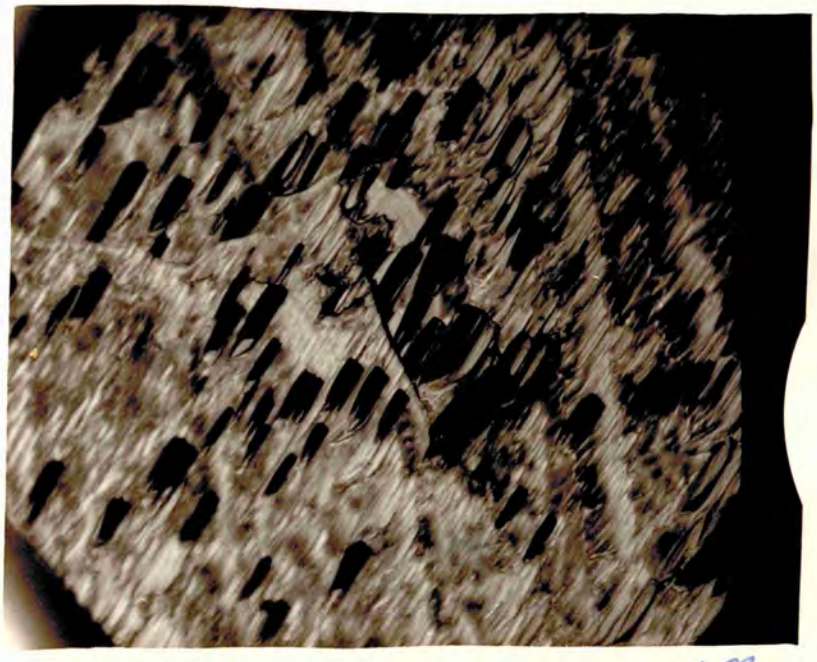

Fig. 85(b). ×84.

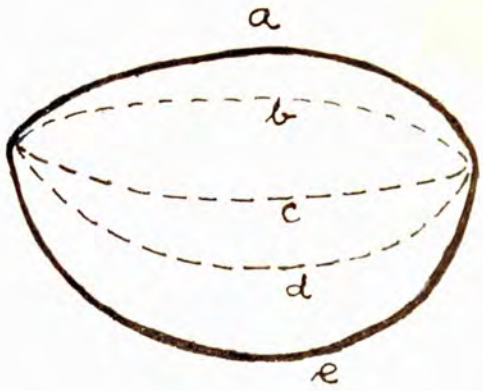

Fig. 86 (A).

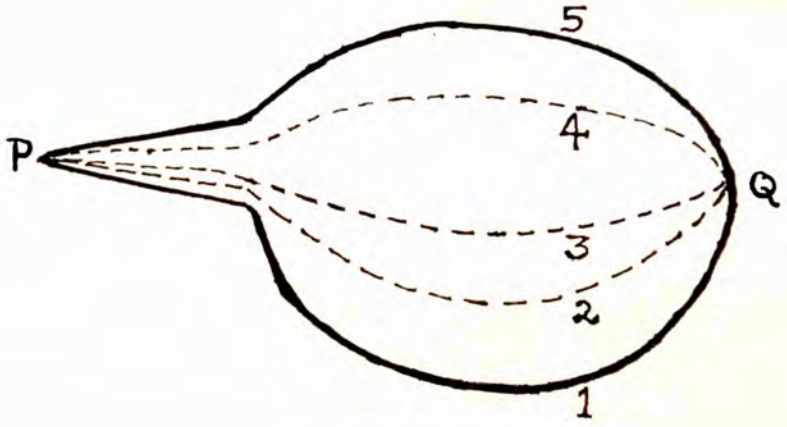

Fig. 86 (B).

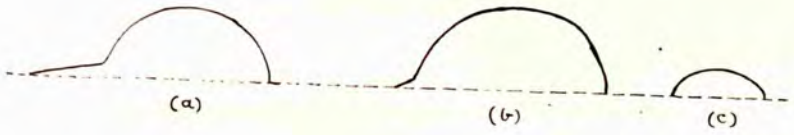

Fig. 87.

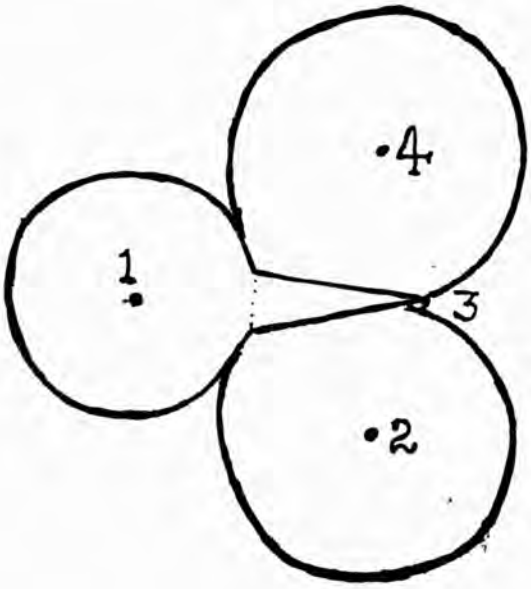

Fig. 88.

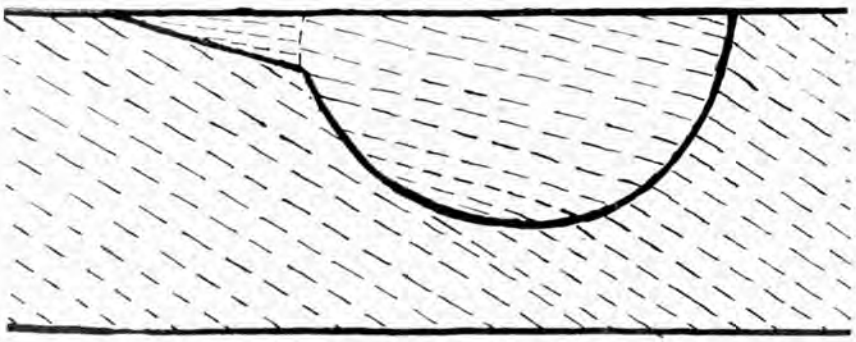

Fig. 89.

Fig. 90. x 9.

Fig. 91. x 9.

Fig. 92. x 9.

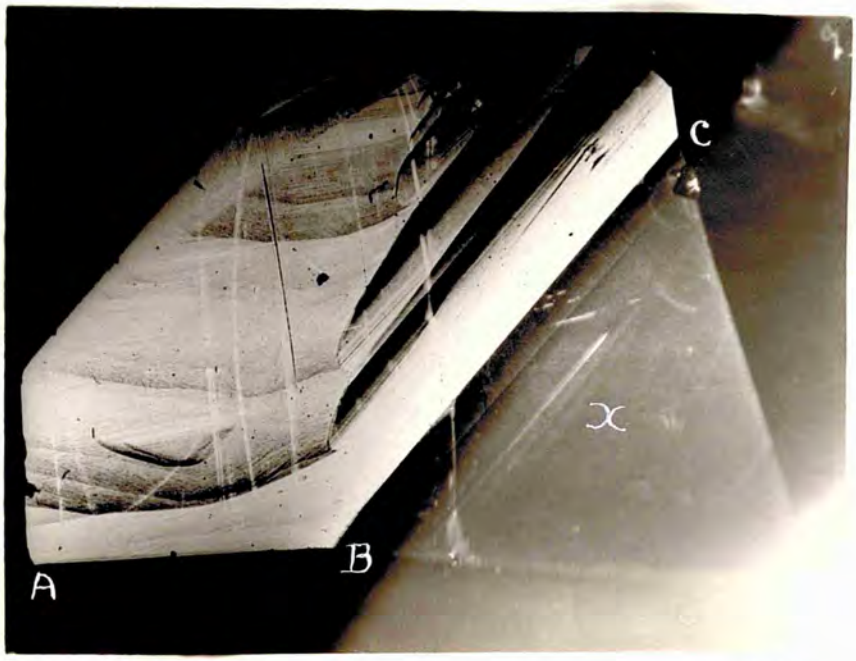

Fig. 93. ×9.

Fig. 94. ×9.

Fig. 95. X55.

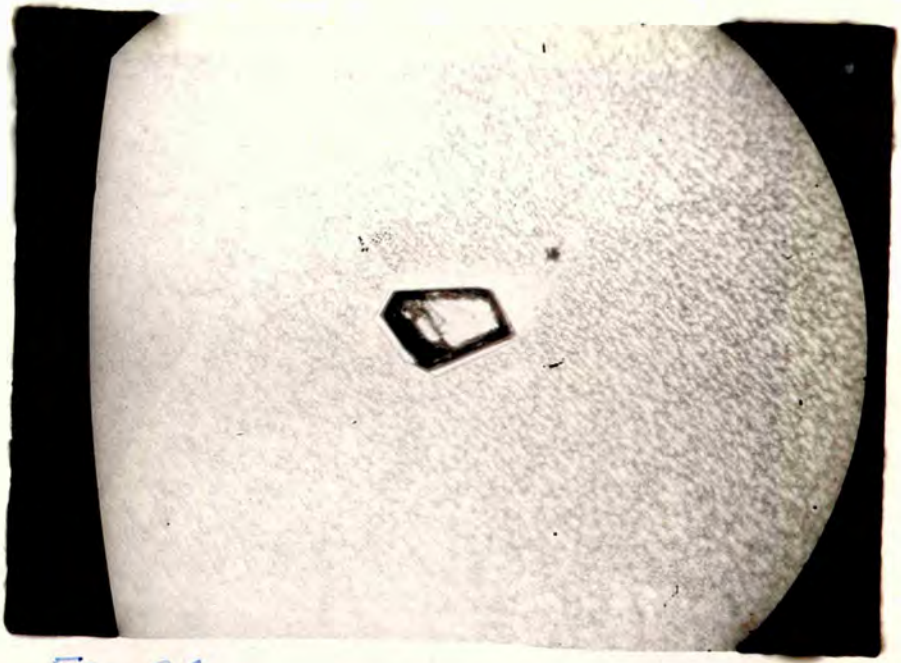

Fig. 96. X84.

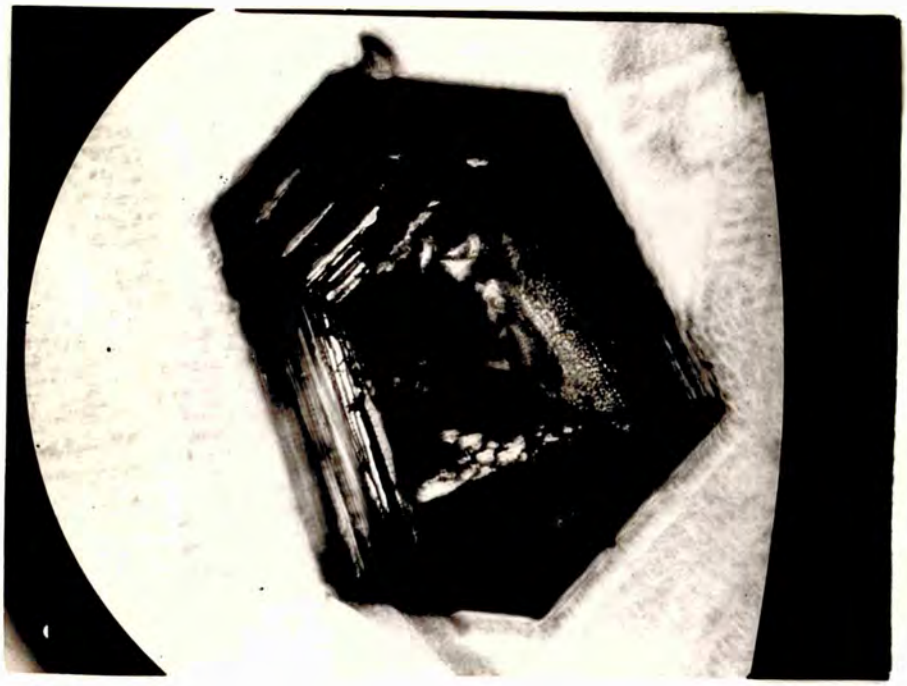

Fig. 97. x84.

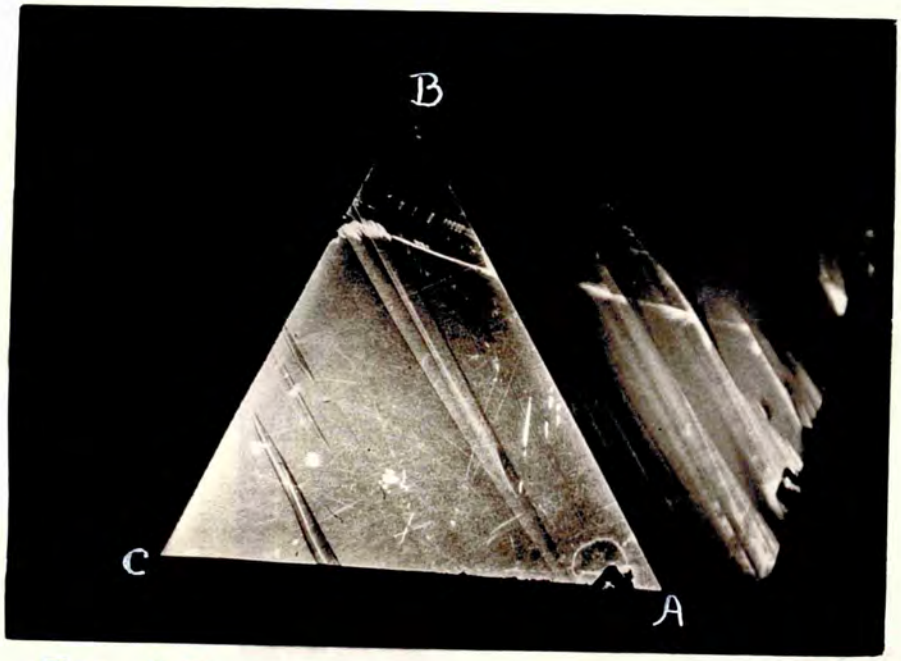

Fig. 98. x9.

Fig. 99. ×35.

Fig. 100. ×35.

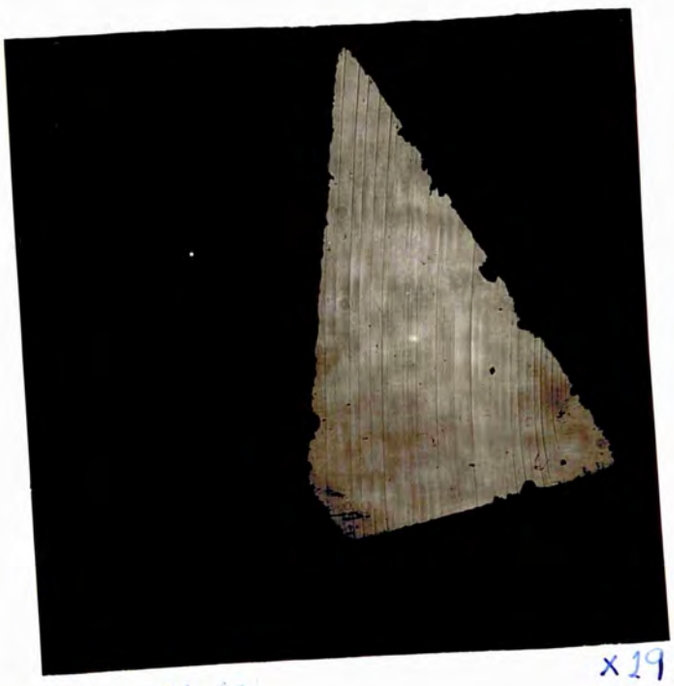

x 19.

Fig. 101. (a).

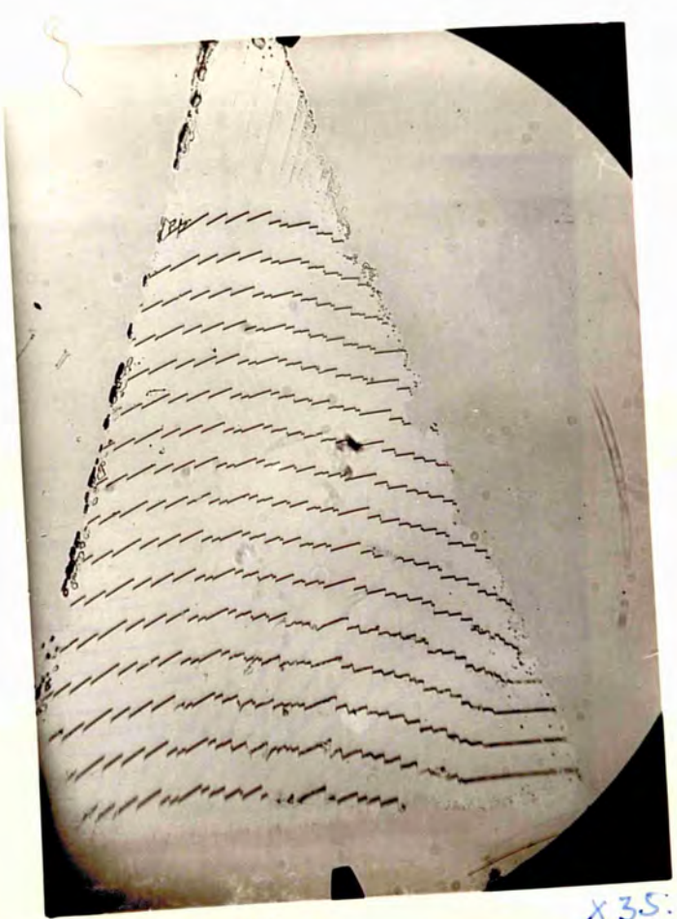

x 35.

Fig. 101 (b).

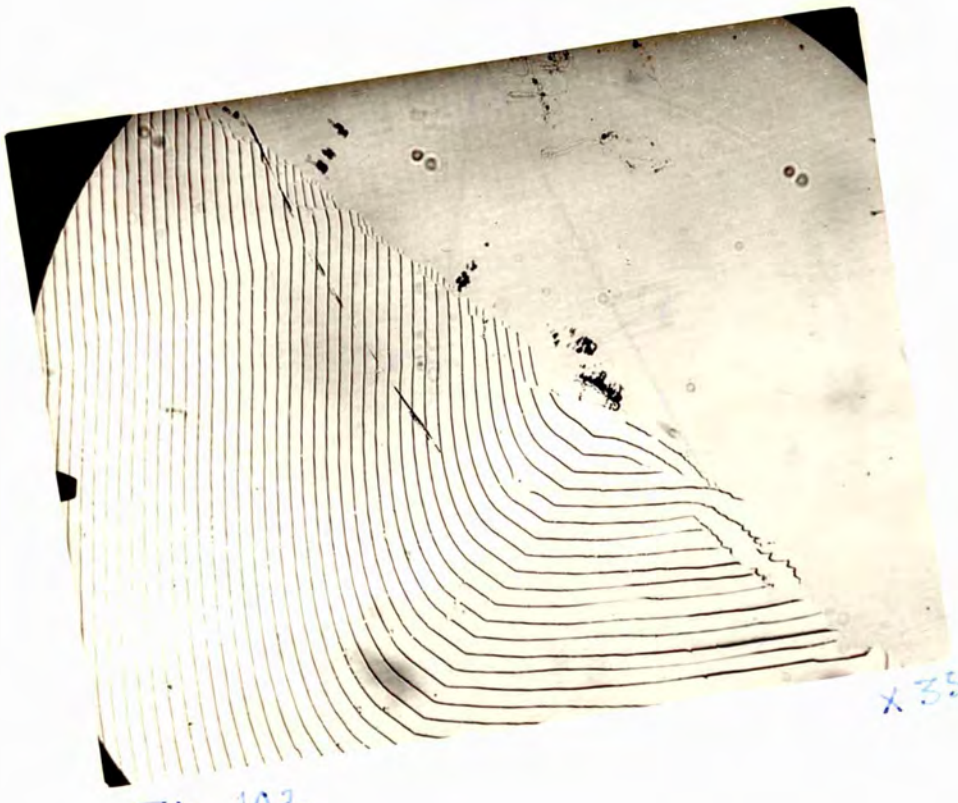

x 35.

Fig. 102.

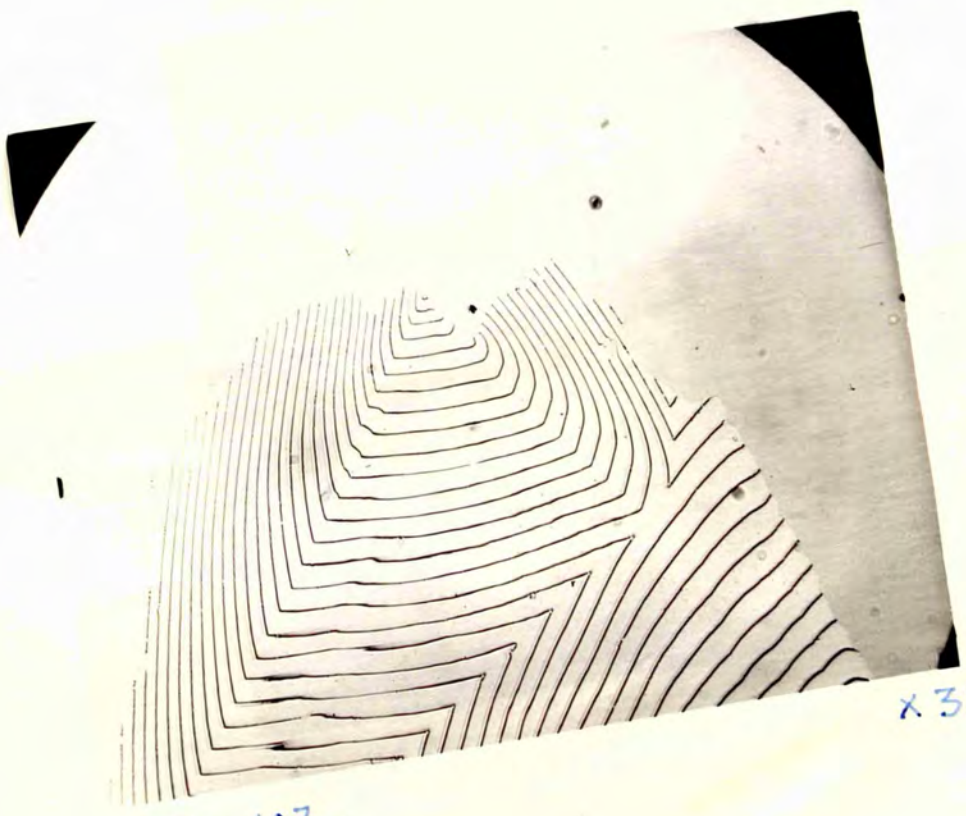

x 35.

Fig. 103.

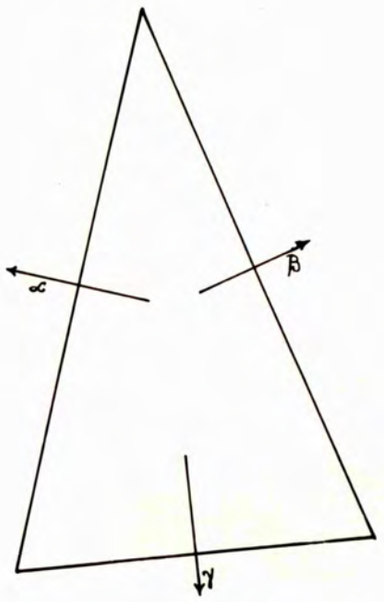

Fig. 104.

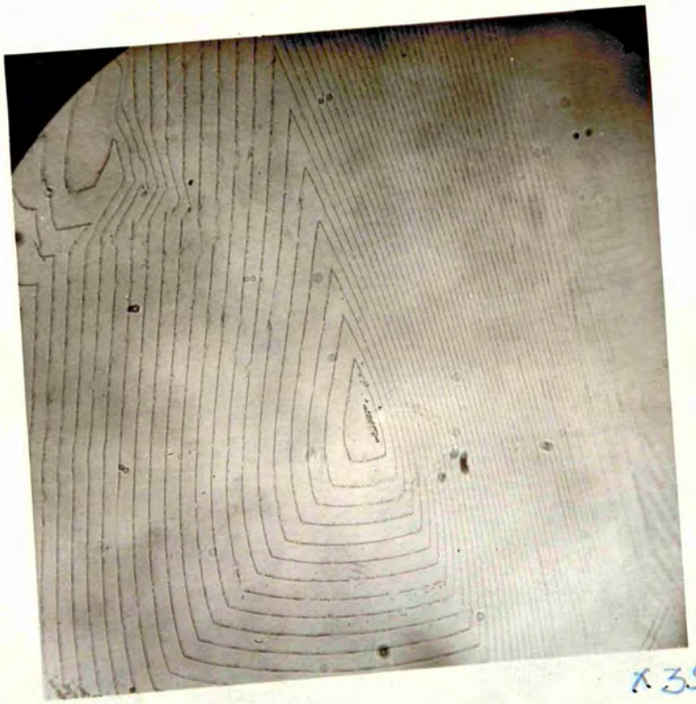

x 35.

Fig. 105.

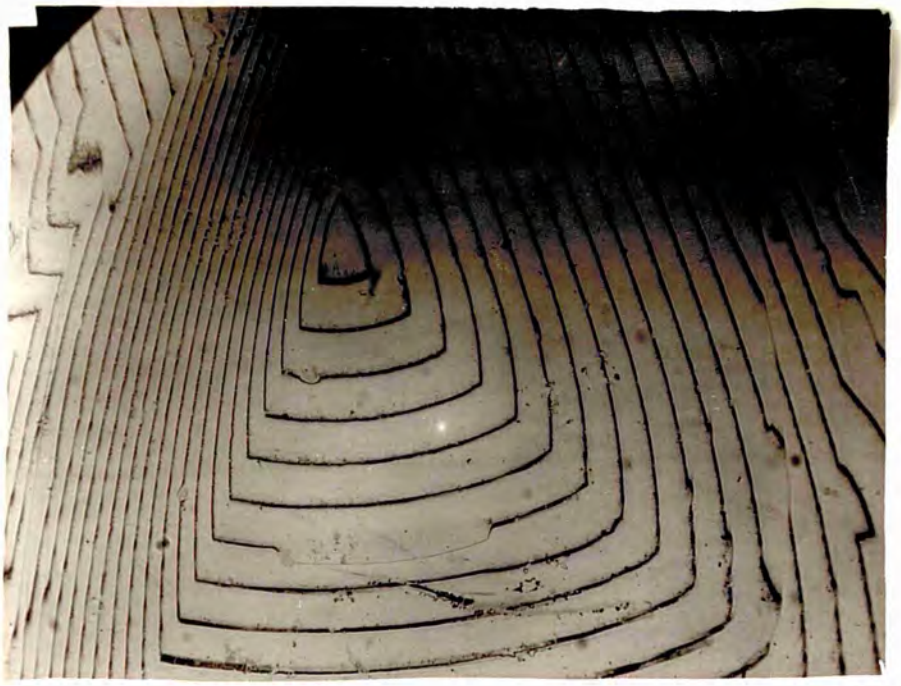

Fig. 106 (a) x 35.

Fig. 106 (b). x 9.

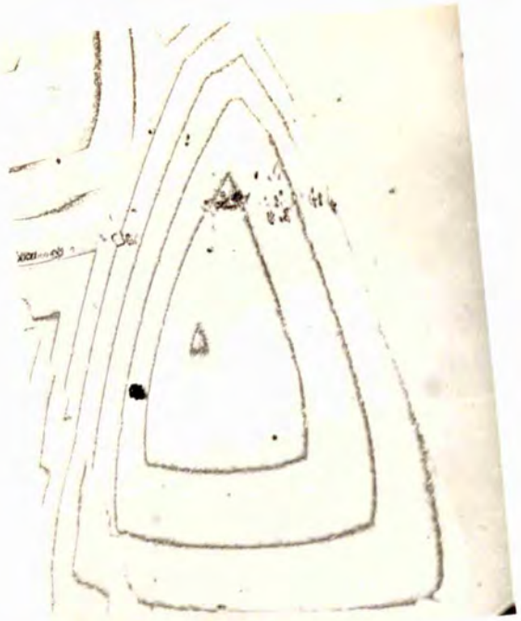

x 35.

Fig. 107.

x 35.

Fig. 108.

Fig. 109. x 27.

Fig. 110. x 19.

Fig. 111. X 35.

Fig. 114. X 19.

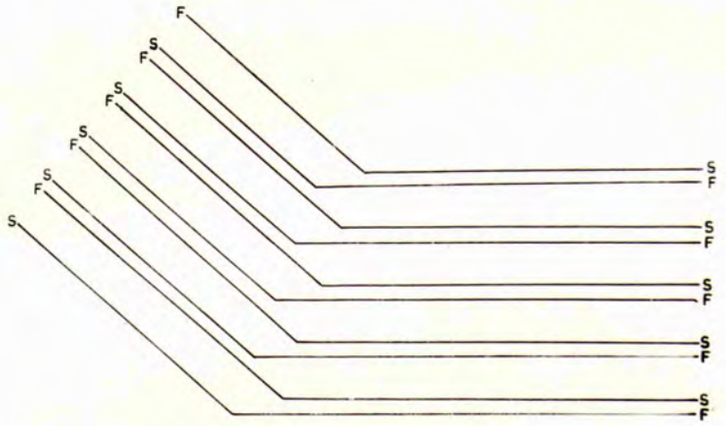

Fig. 112.

Fig. 113. X35.

Fig. 115. x 105

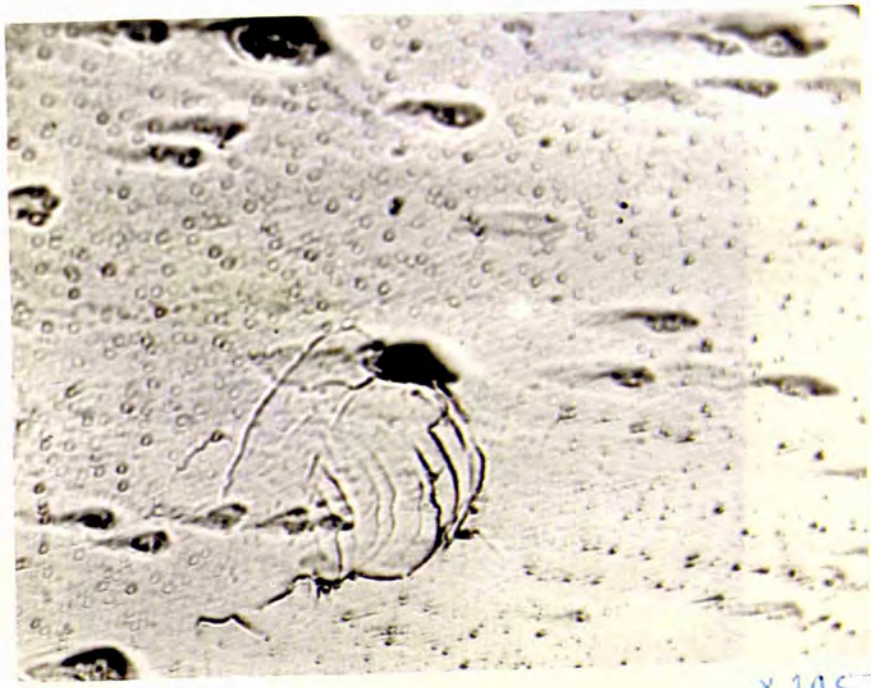

Fig. 116. x 105

Fig. 117. x 15.

Fig. 118. x 35.

× 105

Fig. 119 (a).

× 105.

Fig. 119 (b).

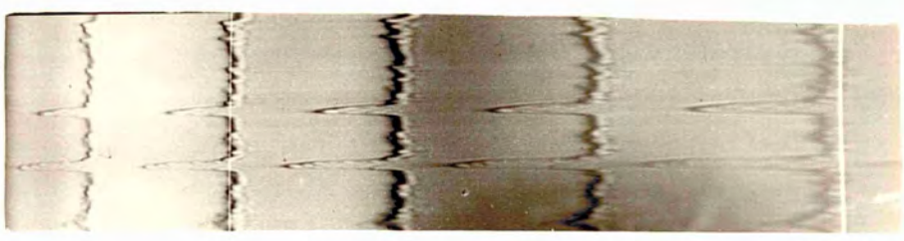

Fig. 120. ×57.

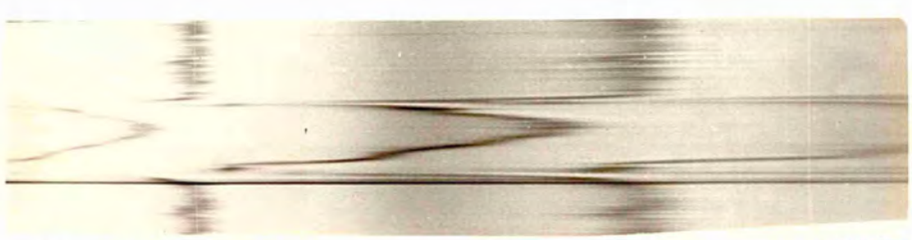

Fig. 121. ×95.

Fig. 122. X250.

Fig. 123 (a). X 105.

Fig. 123 (b). X 105.

Fig. 124. x105

Fig. 125. x53

Fig. 126(a). X 10.5

Fig. 126(b). X 10.5

Fig. 127. × 105.

Fig. 128. × 54.

Fig. 121. ×11.

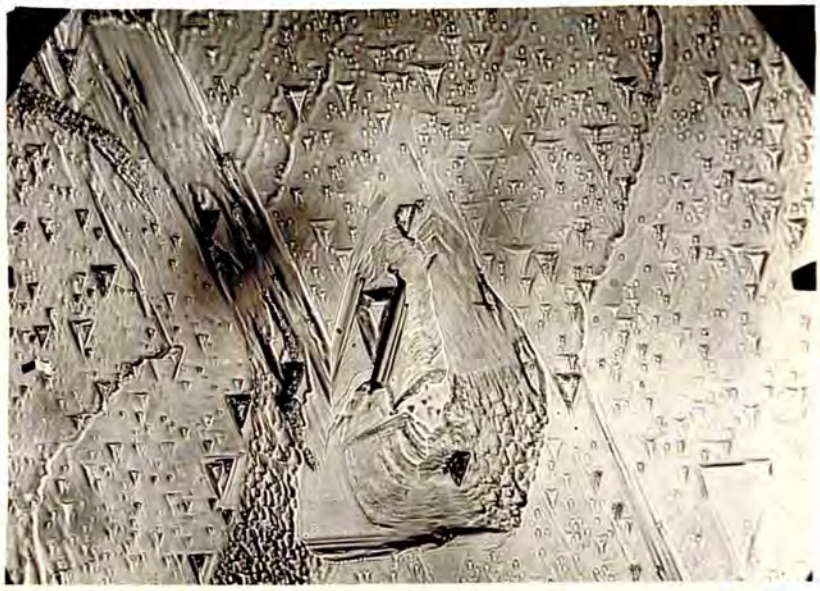

Fig. 130. ×410.

Fig. 131. ×95.

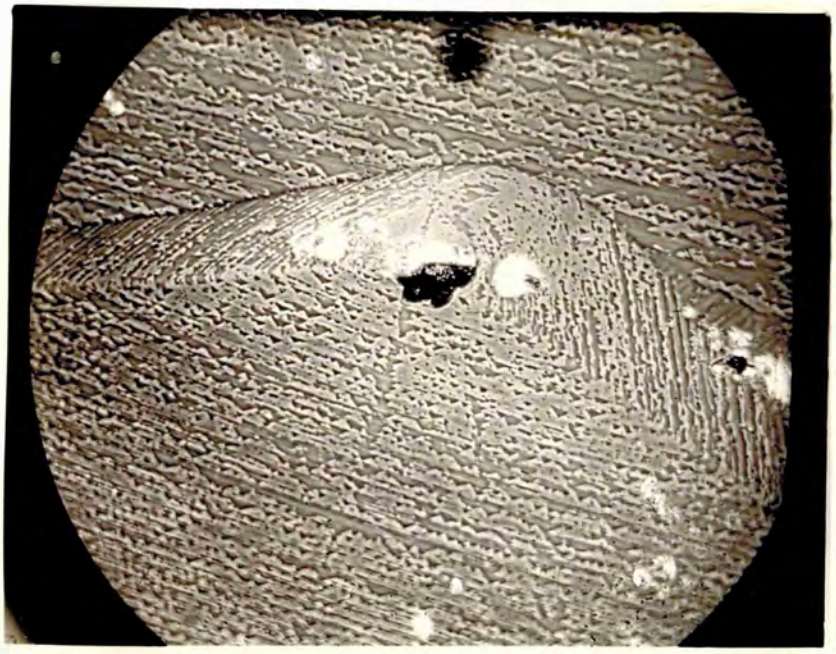

Fig. 132. ×84.

Fig. 133. ×410.

Fig. 136. ×410.

Fig. 134. x 1100.

Fig. 135. x320.

Fig. 137. x 14.

Fig. 138. x 175.

Fig. 139. x 175.

Fig. 140.

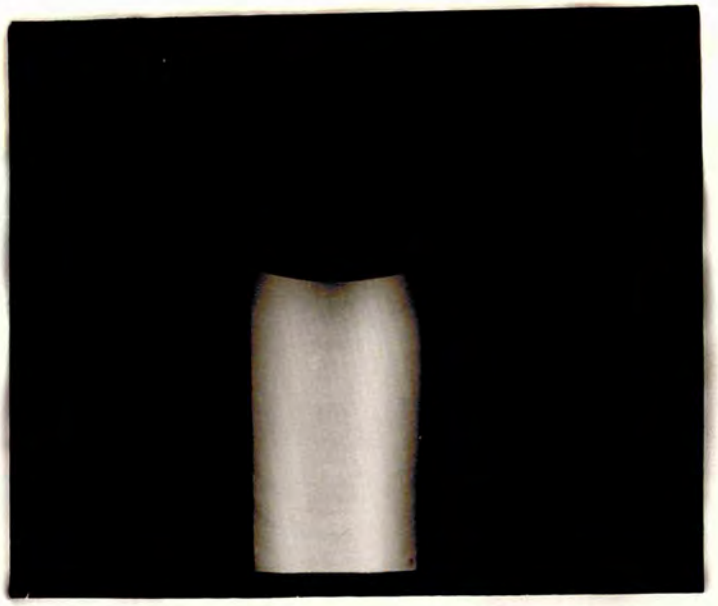

Fig. 141

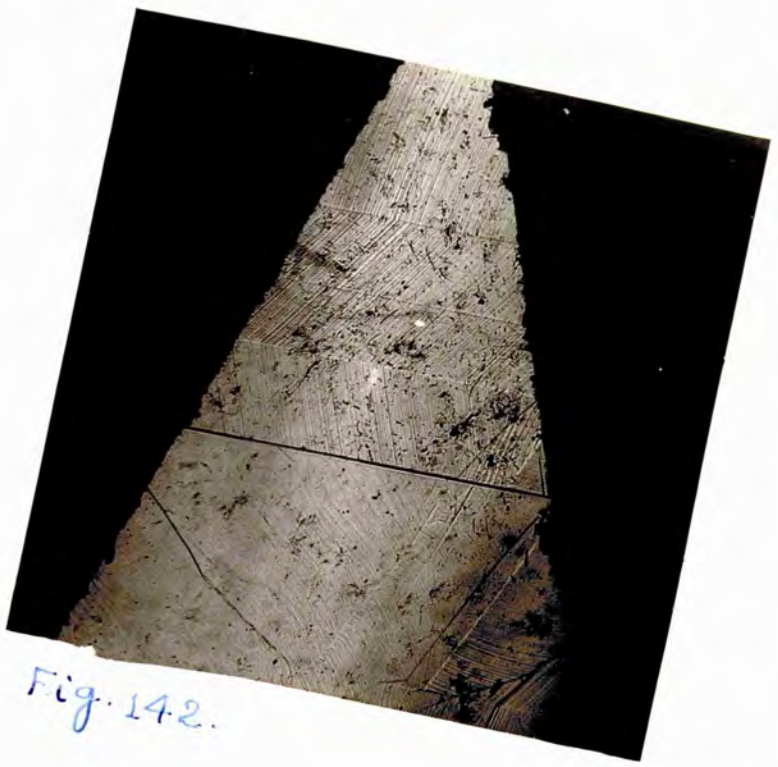

Fig. 142.

× 14.

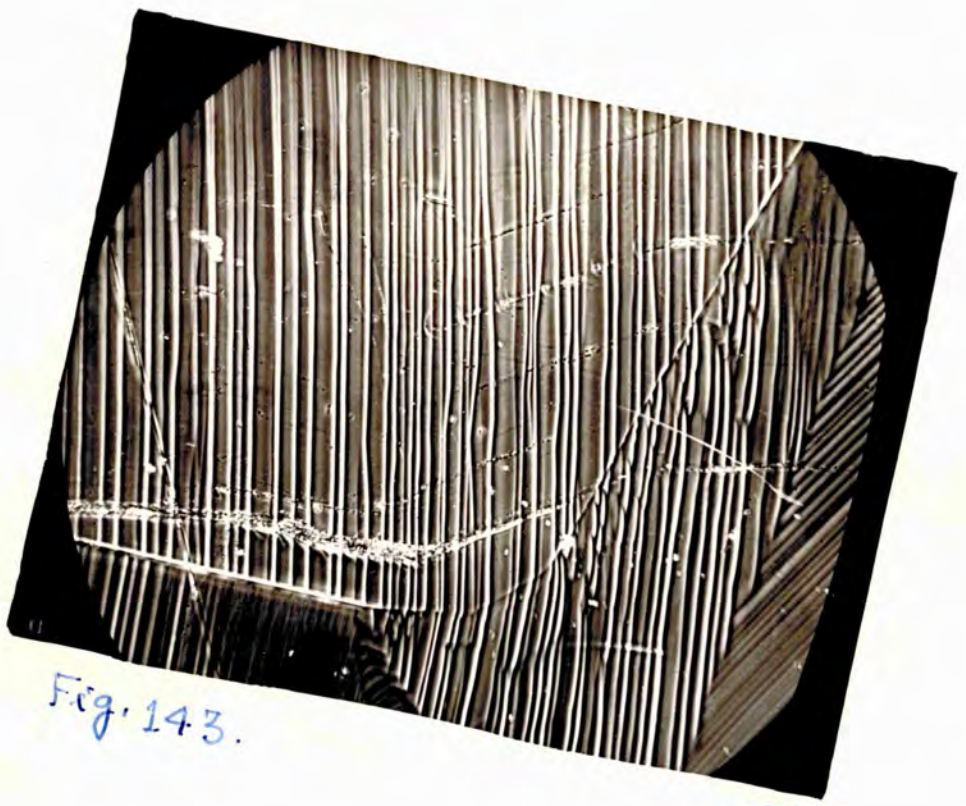

Fig. 143.

× 84.

×14.

Fig. 144(a).

×19.

Fig. 144(b).

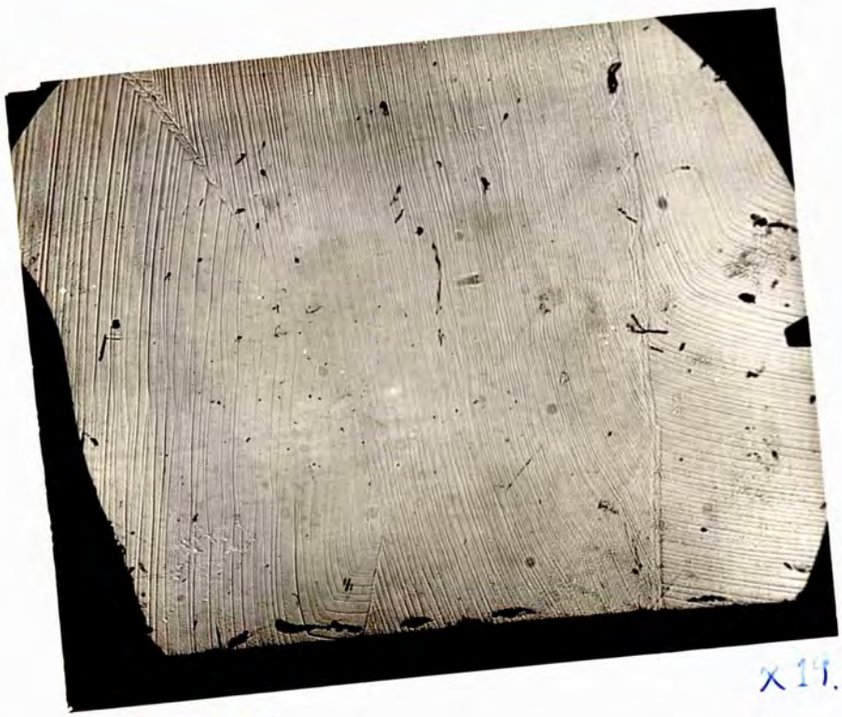

x 19.

Fig. 145.

x 19.

Fig. 146.

Fig. 147.

x 84.

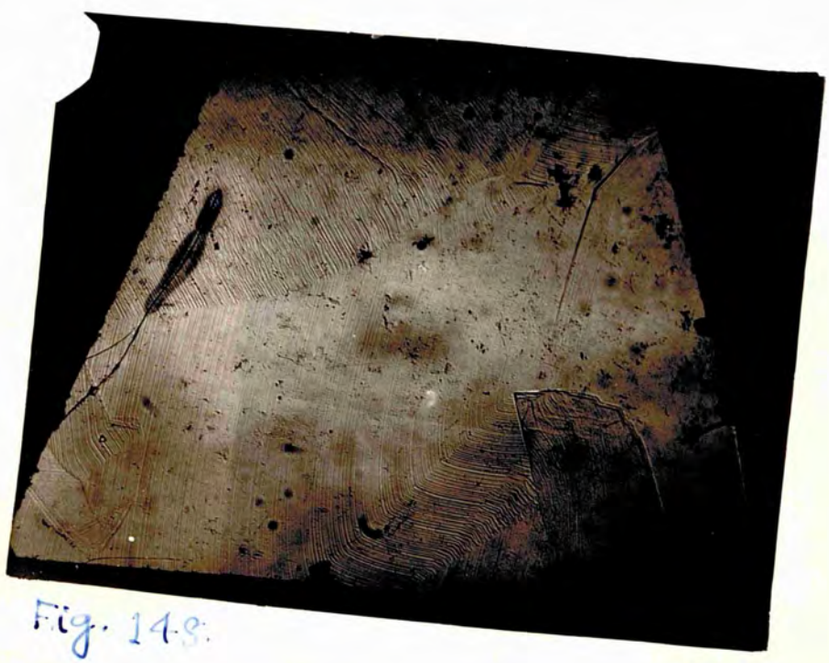

Fig. 148.

x 19.

Fig. 14.9(a) x19.

Fig. 14.9(b). x19.

Fig. 150(5). x 1).

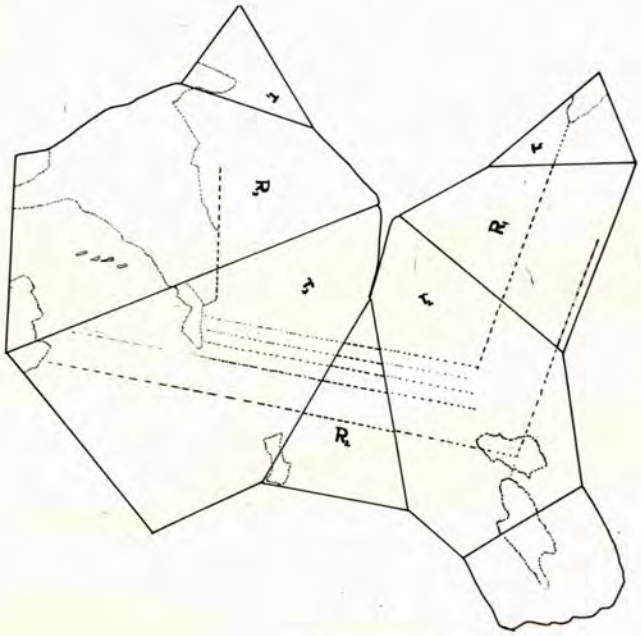

Fig. 150(6).

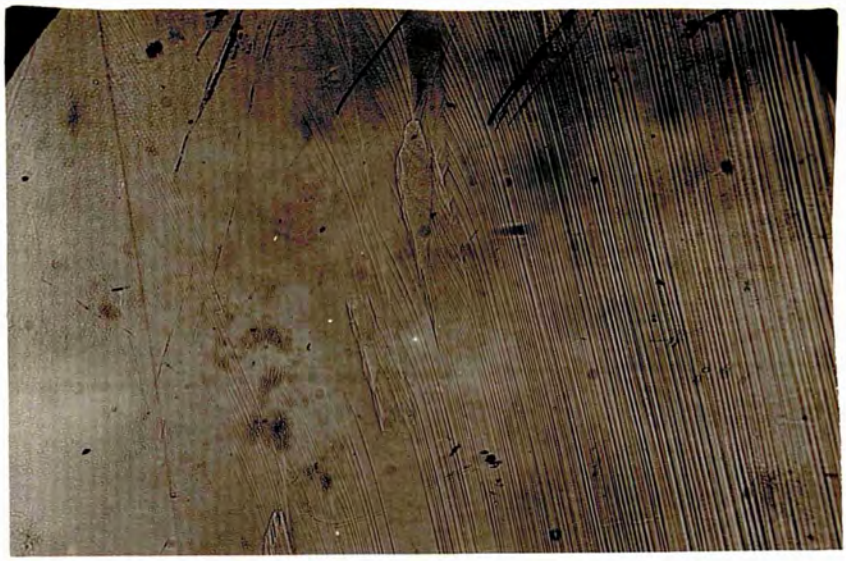

Fig. 151. × 55.

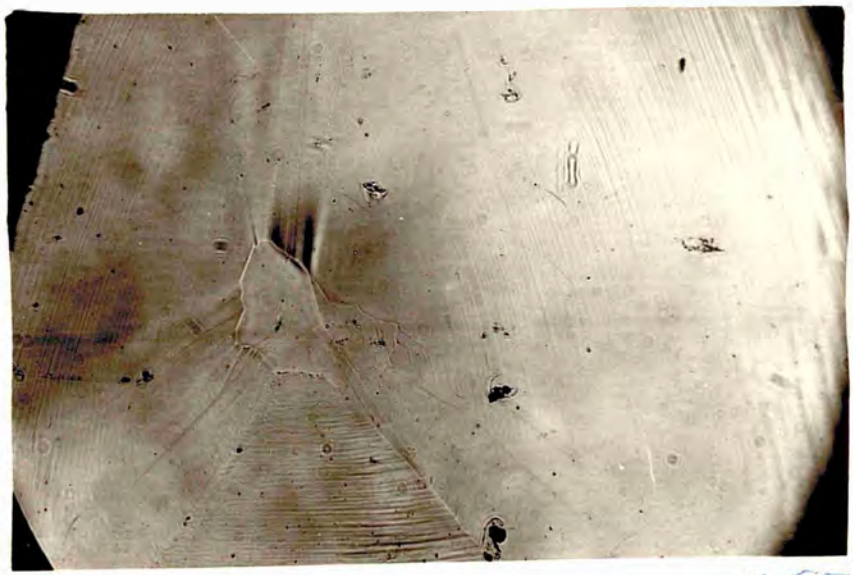

Fig. 152. × 55.

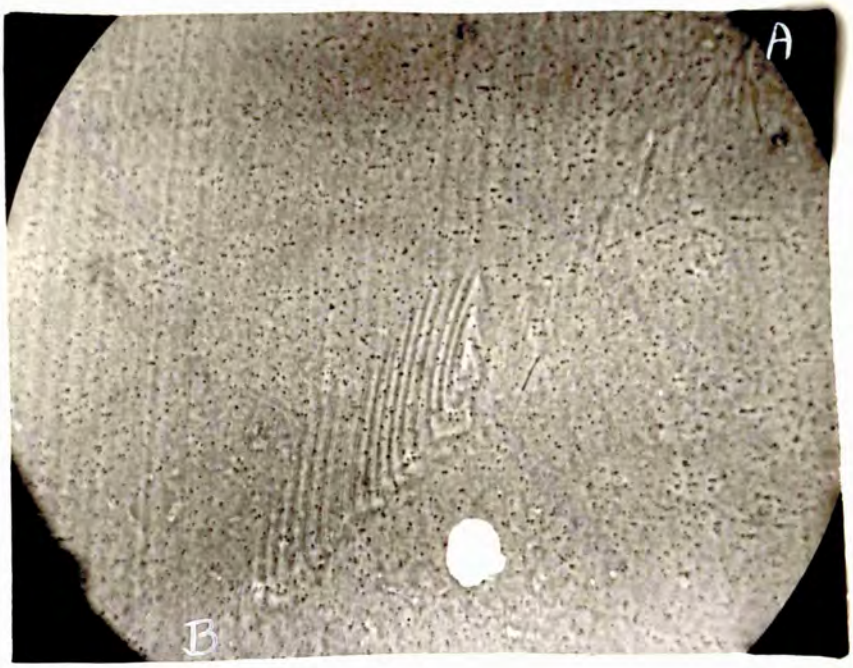

Fig. 153. × 120.

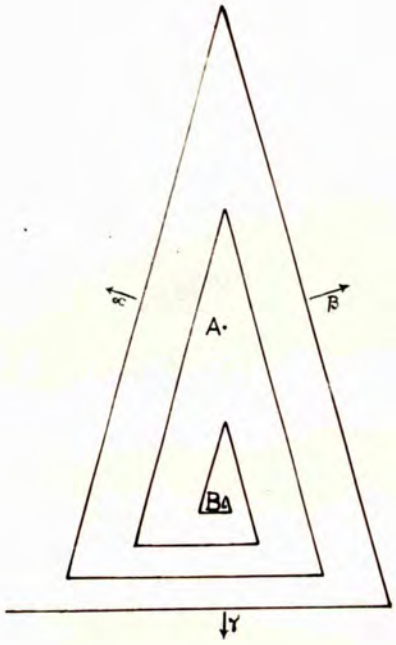

Fig. 154.

Fig. 155. ×55.

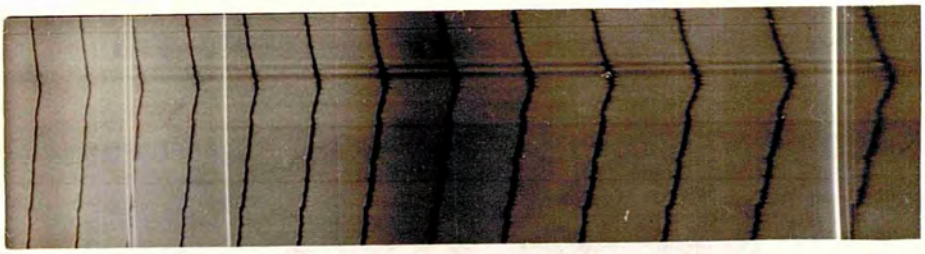

Fig. 156. ×45.

Fig. 157. x35

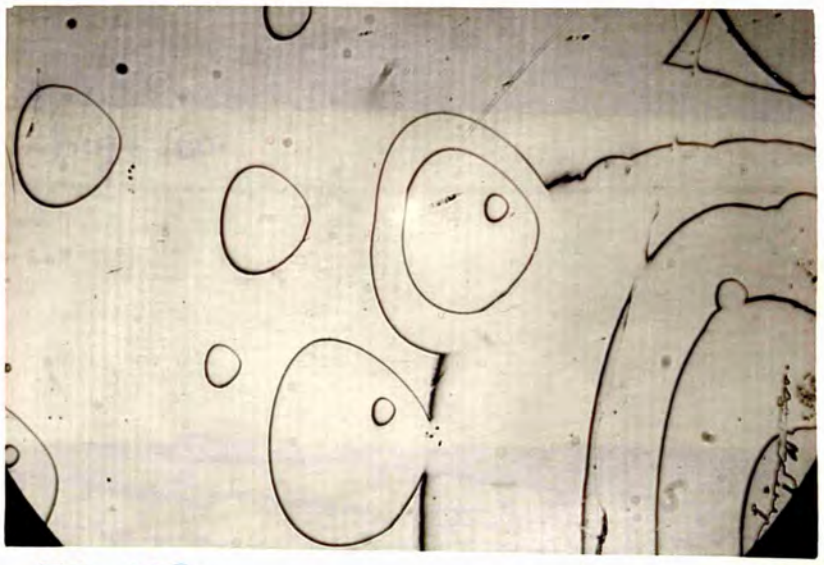

Fig. 158. x105

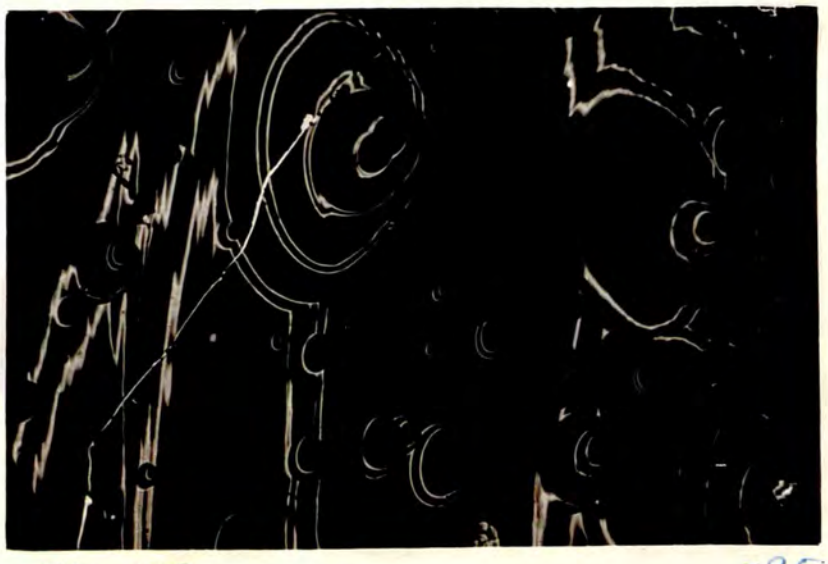

Fig. 159. x9.5

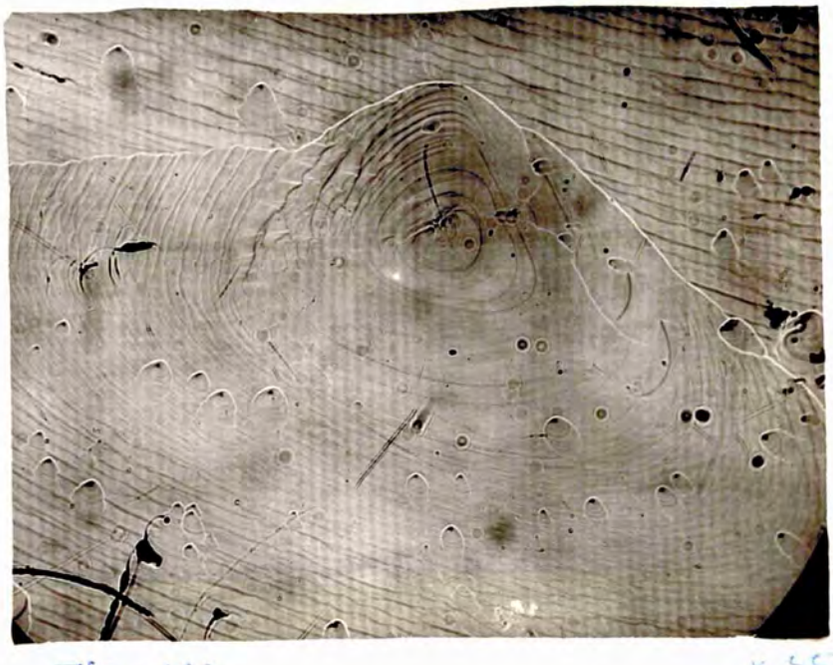

Fig. 160. x 55.

Fig. 161. x 55.

Fig. 162 (a). X 55.

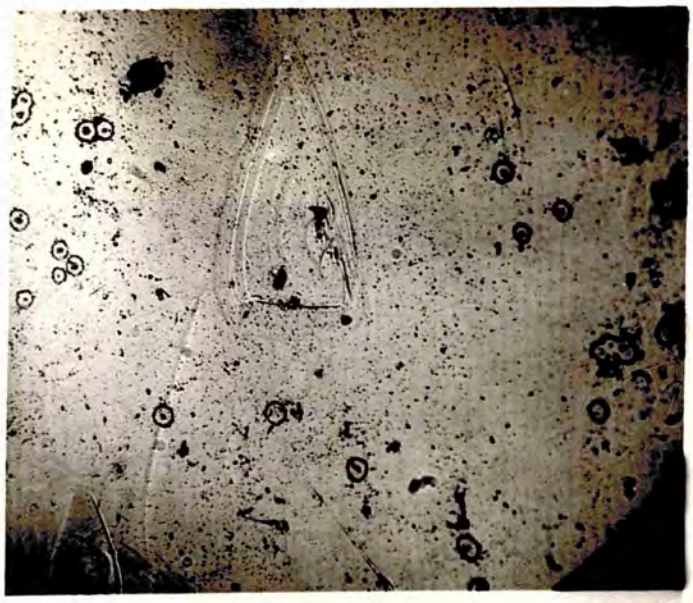

Fig. 162 (b). X 55.

Fig. 163. x 19.

Fig. 164. x 10.5

Fig. 165. x 54.

Fig. 166. x 19.

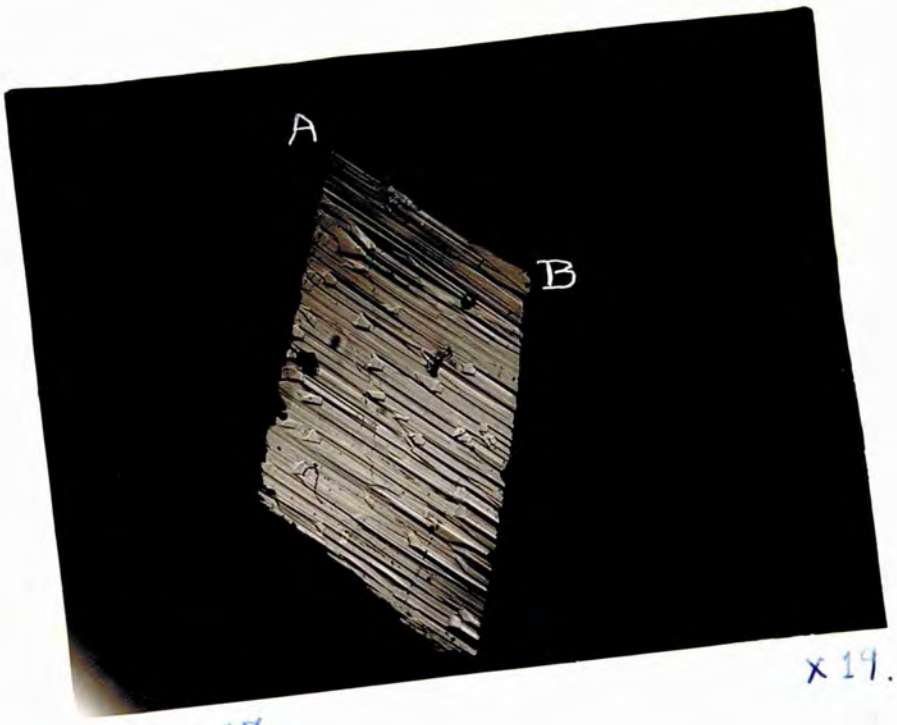

x 19.

Fig. 167.

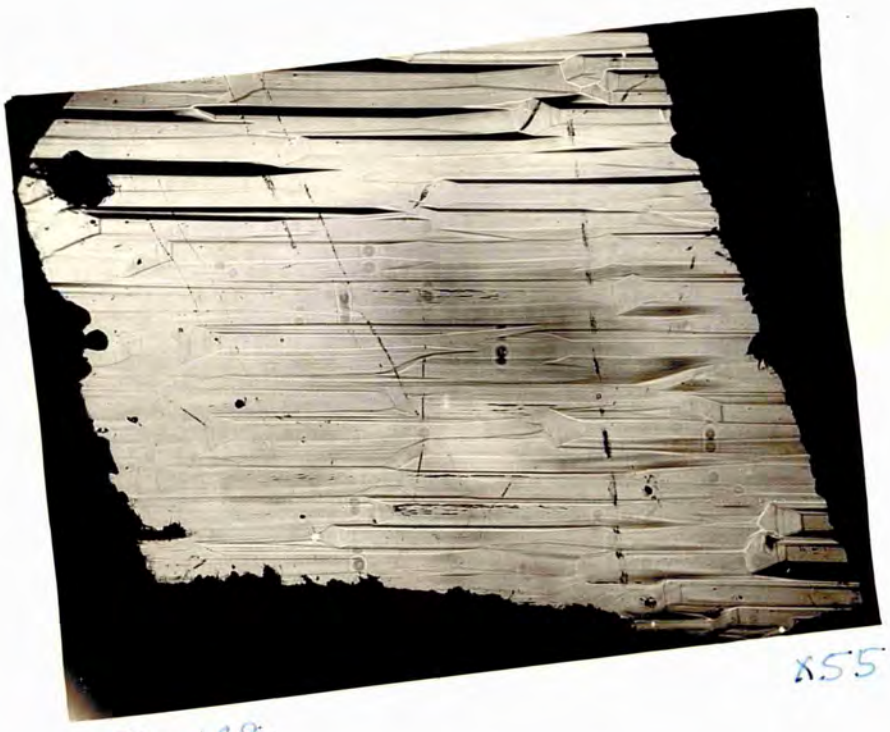

x 55.

Fig. 168.

Fig. 169. ×35.

Fig. 170. ×30

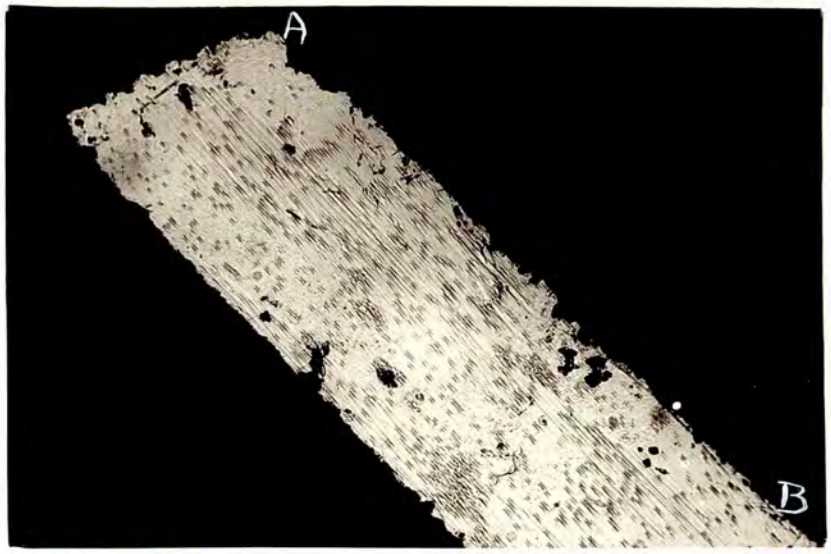

Fig. 171. x 19.

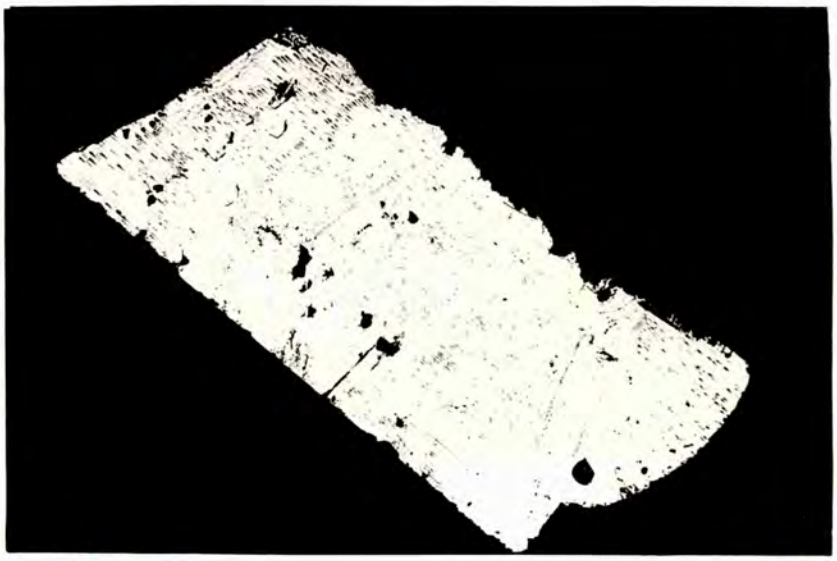

Fig. 172. x 19.

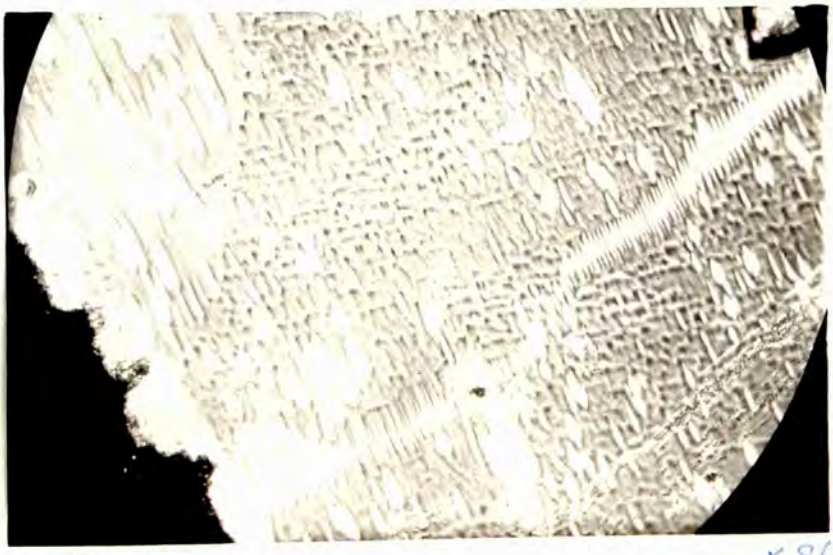

Fig. 173. x 84.

Fig. 174. x19.

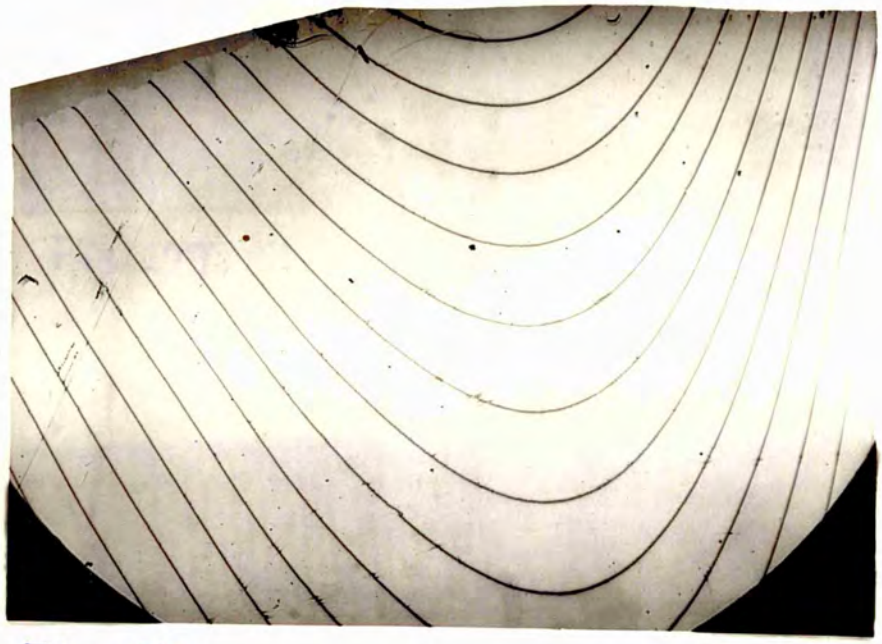

Fig. 175. X55

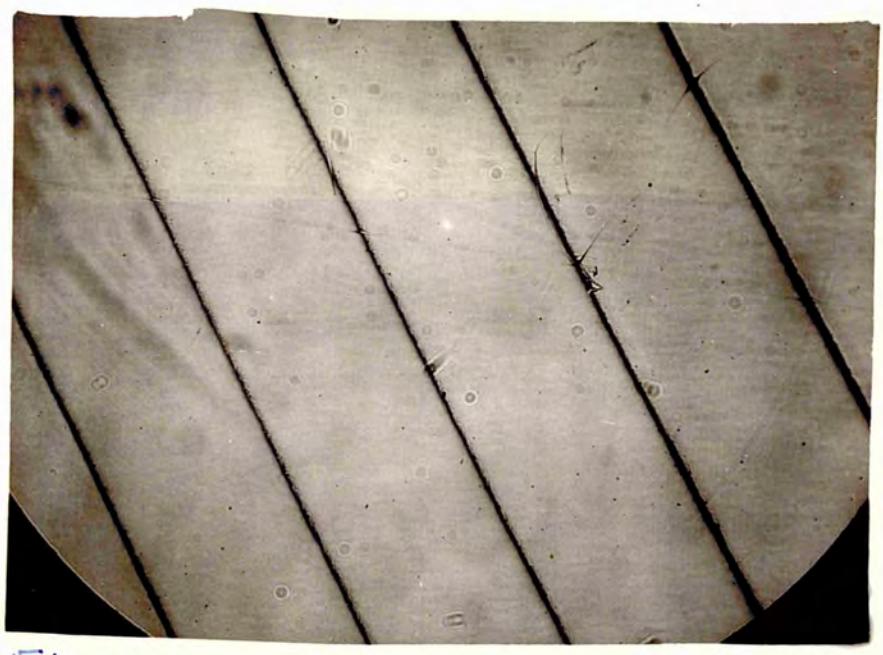

Fig. 176. X55.

Fig. 177. X 84.

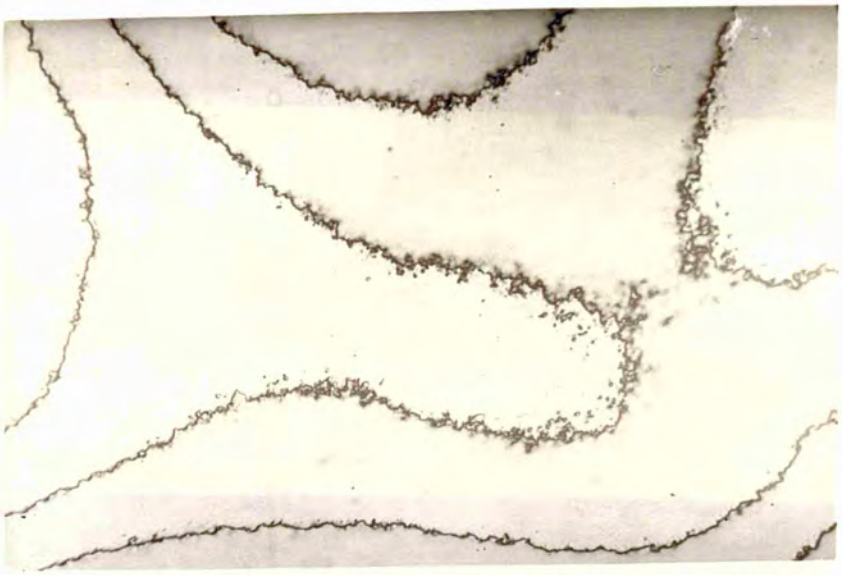

Fig. 178. X 55.

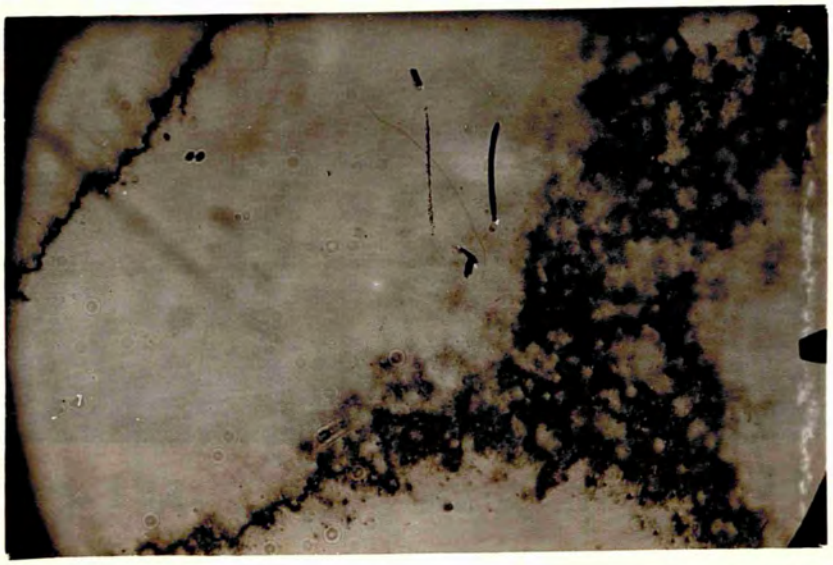

Fig. 179. X 55.

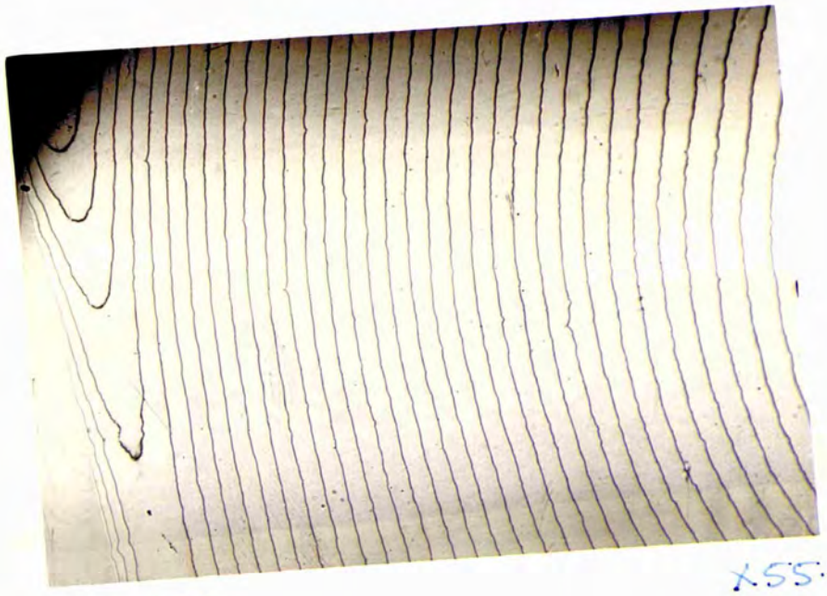

X55.

Fig. 181.

X55.

Fig. 182.

Fig. 180. X27.

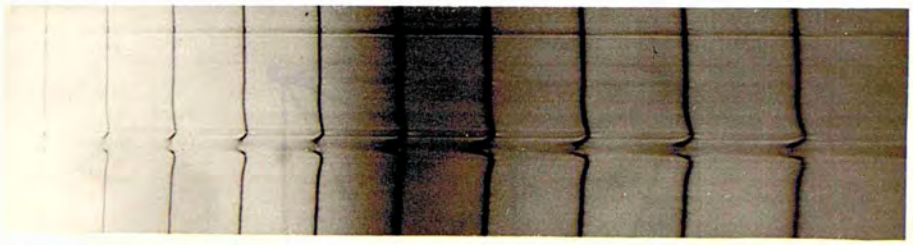

Fig. 183. X27.

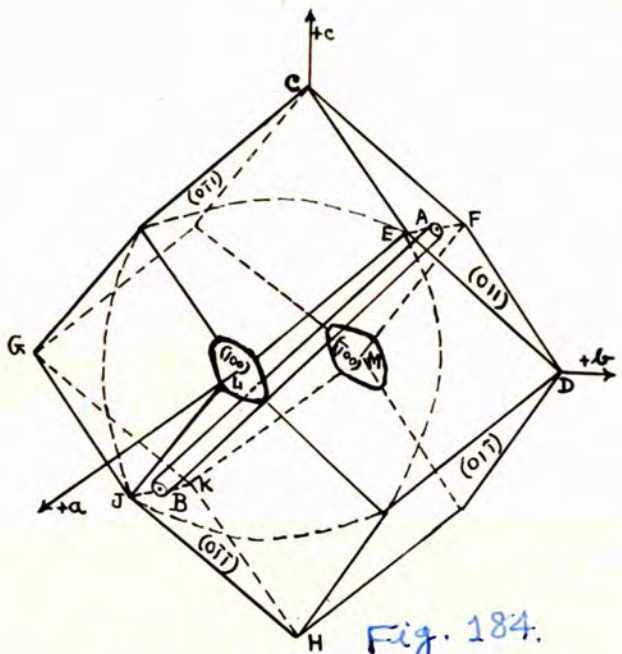

Fig. 184.

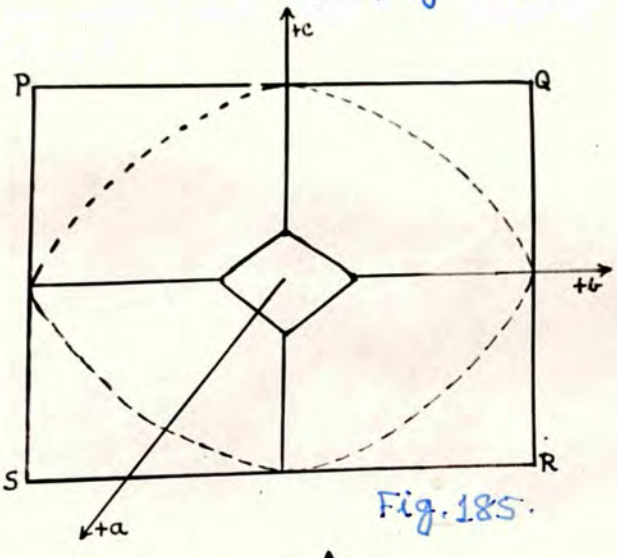

Fig. 185.

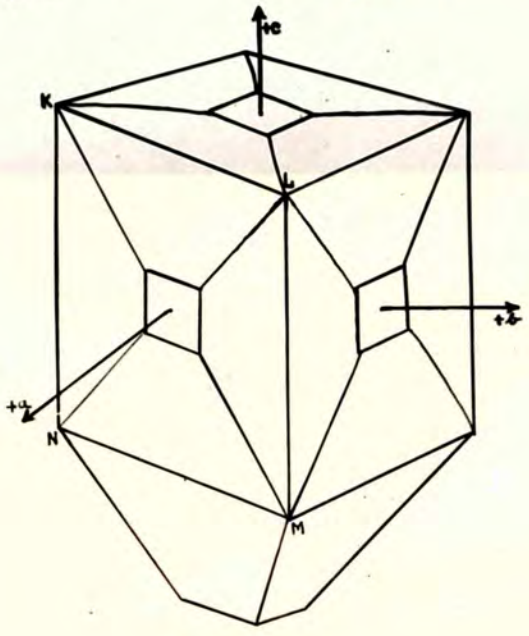

Fig. 186.

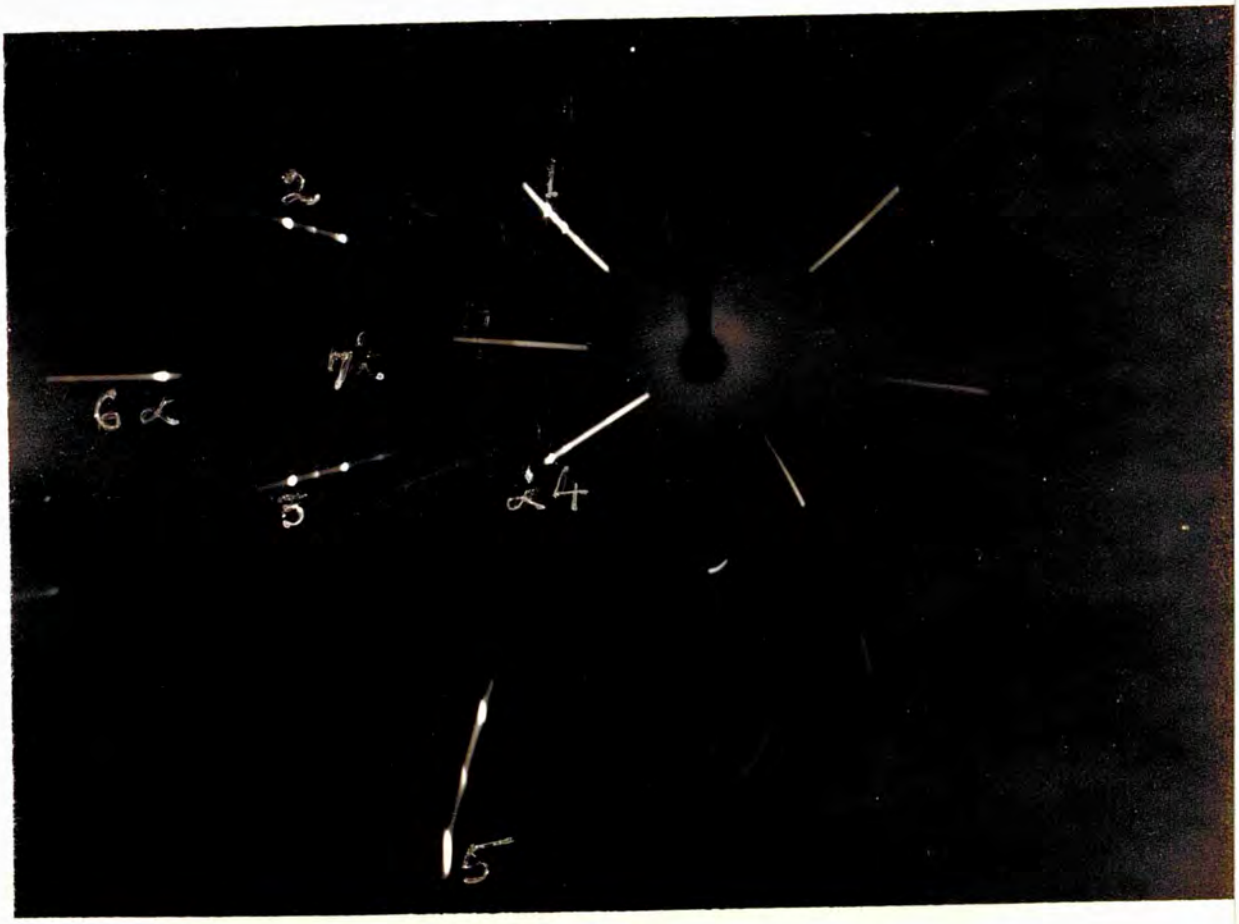

Fig. 187 (a).

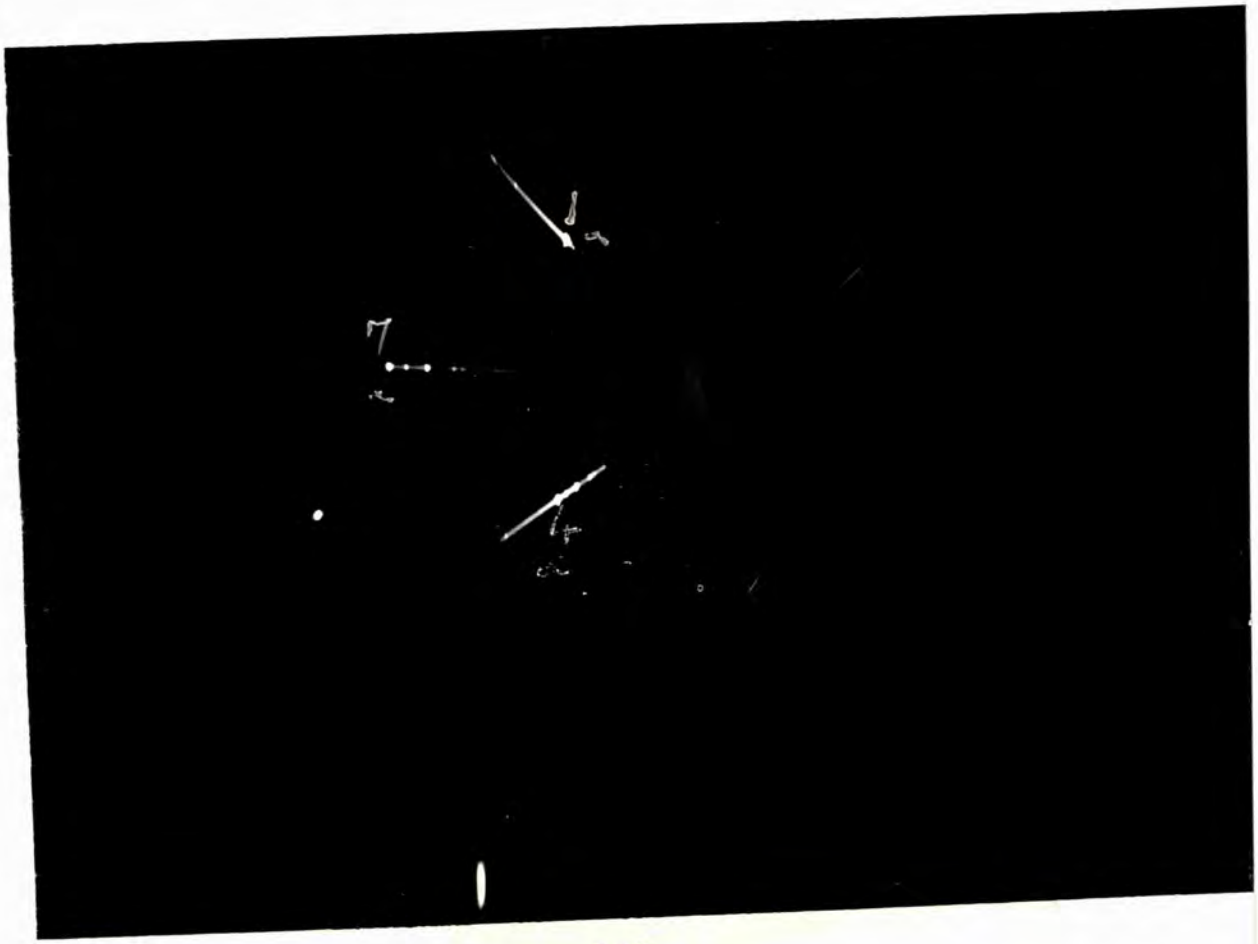

Fig. 187 (b).

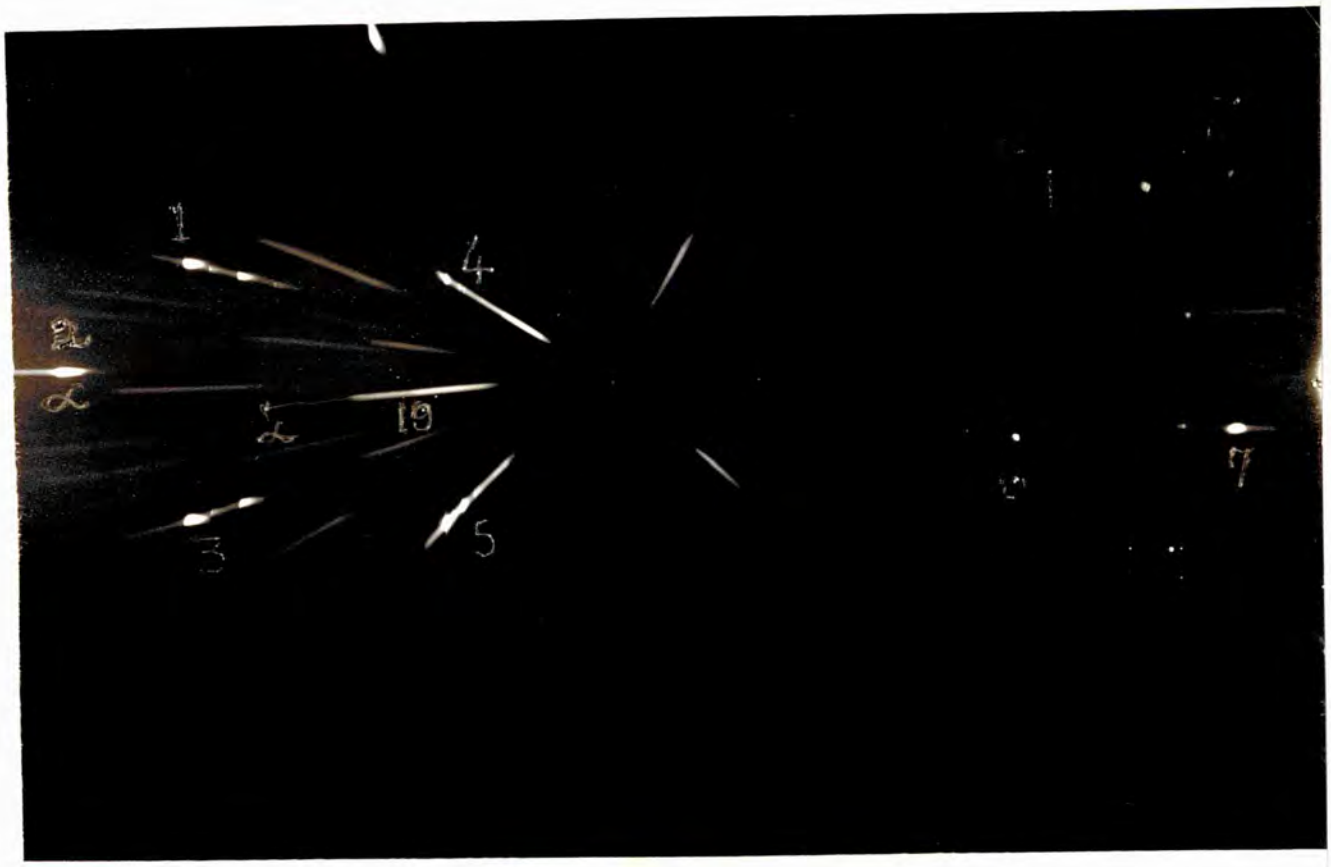

Fig. 188 (a).

Fig. 18·8(b).

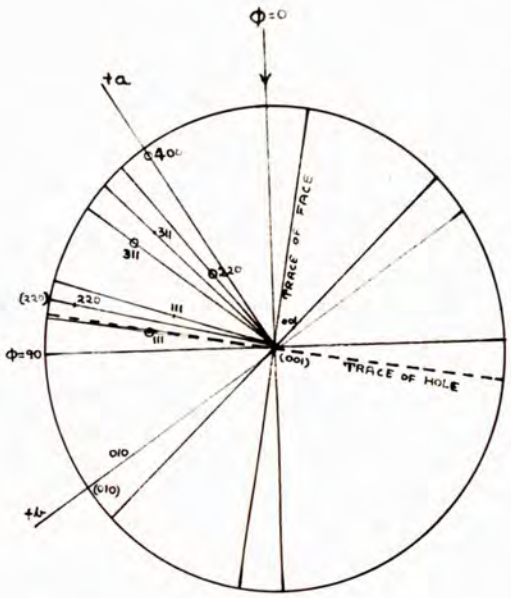

Fig. 189.

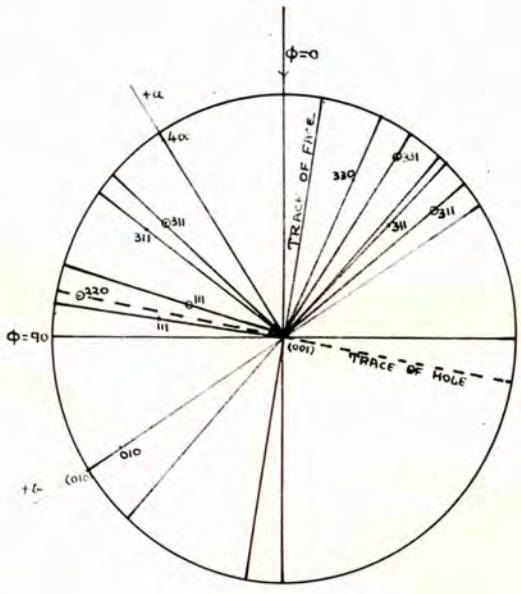

Fig. 190.

Fig. 191.

X35.

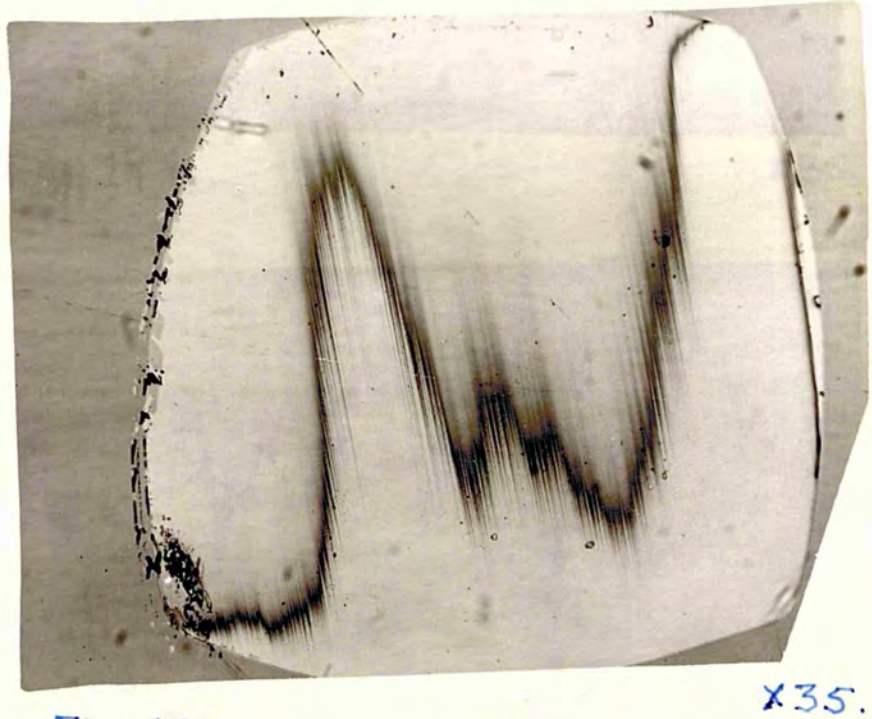

X35.

Fig. 192.

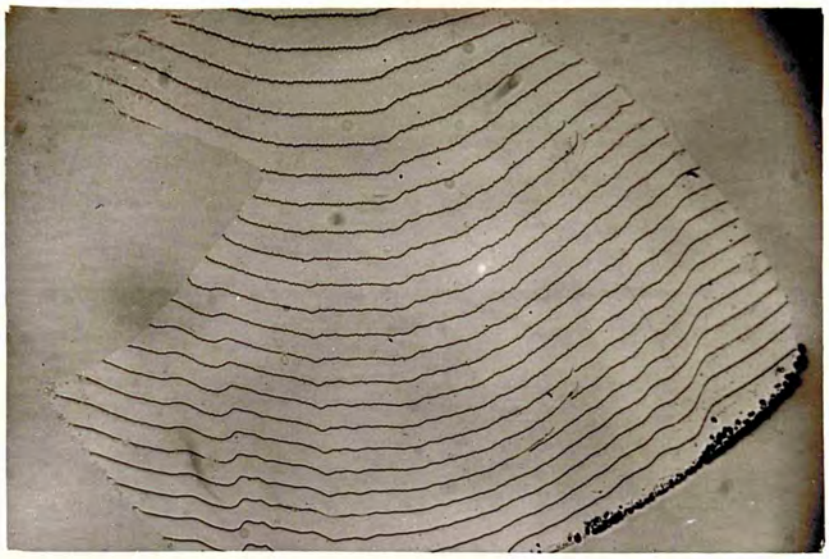

Fig. 193. x 19.

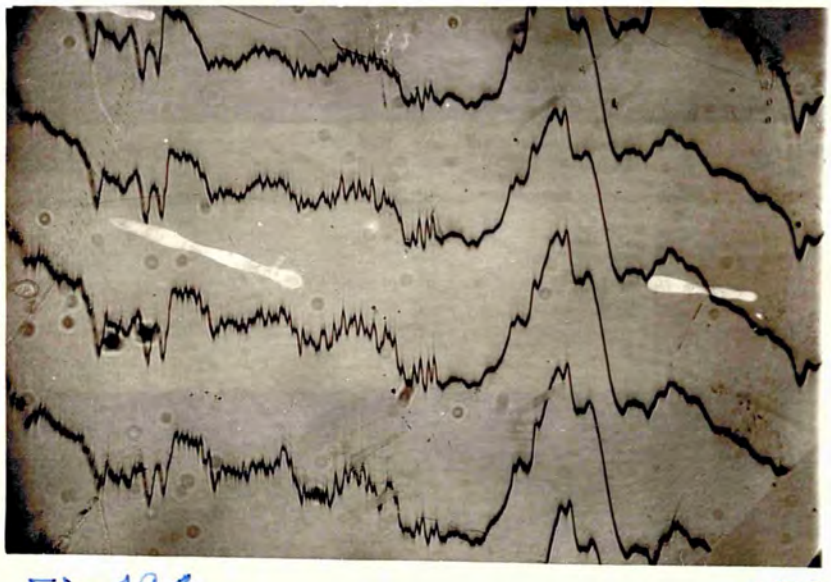

Fig. 194. x 35.

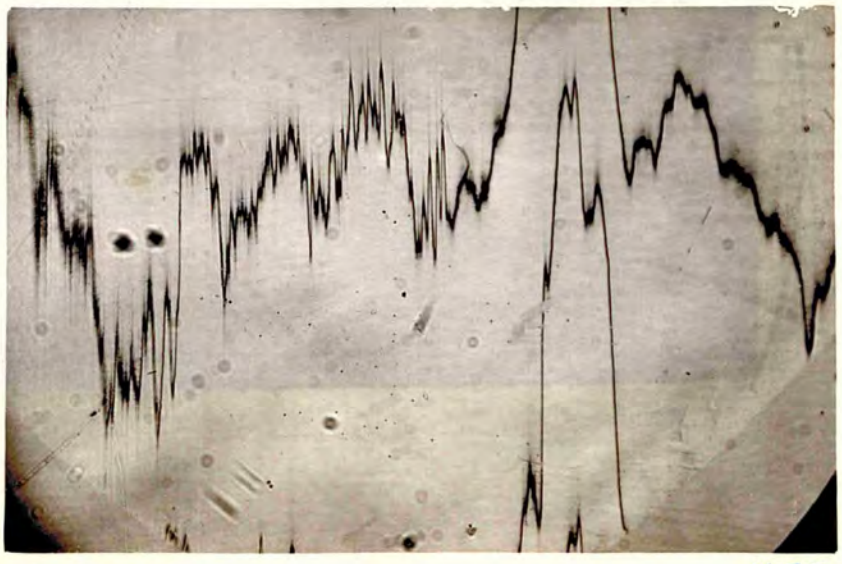

Fig. 195. x 35.

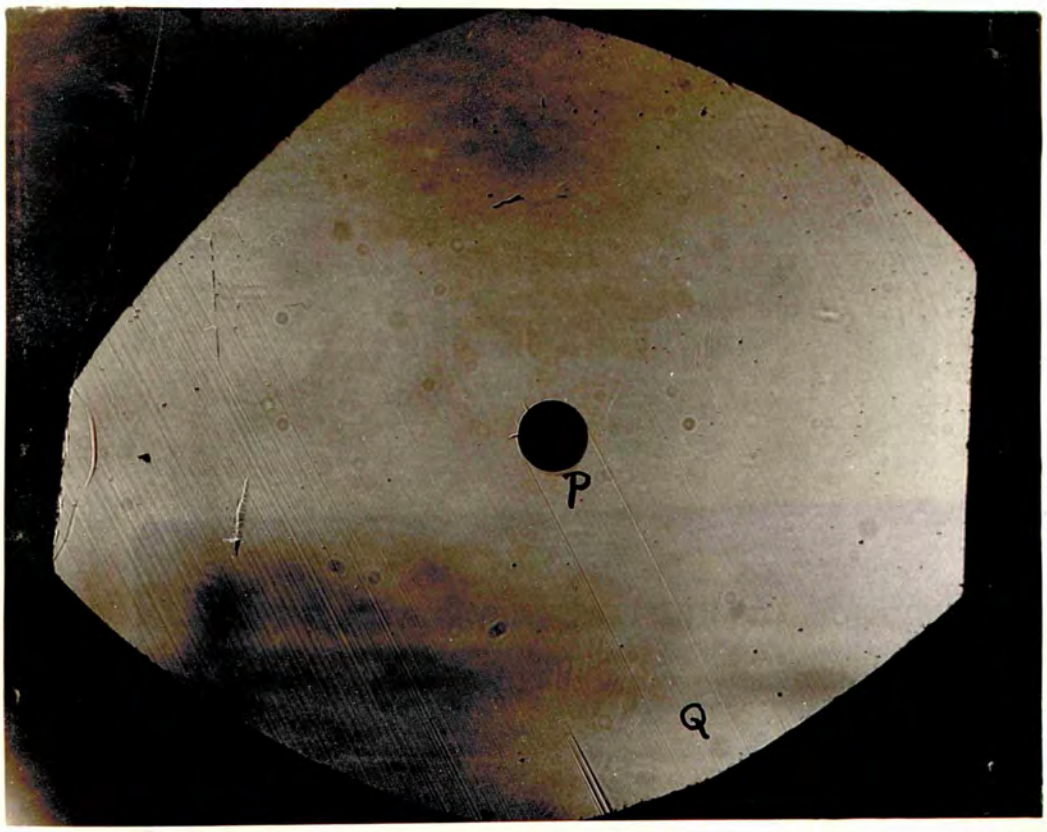

Fig. 196. x 17.

Fig. 197. x 9.

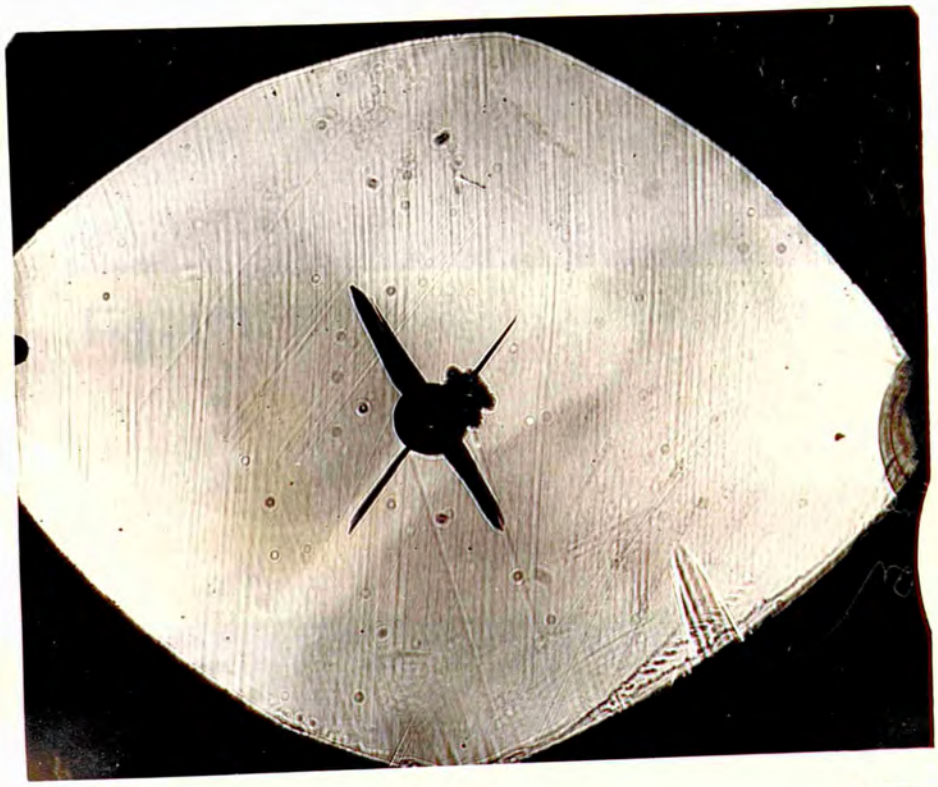

Fig. 198. × 17.

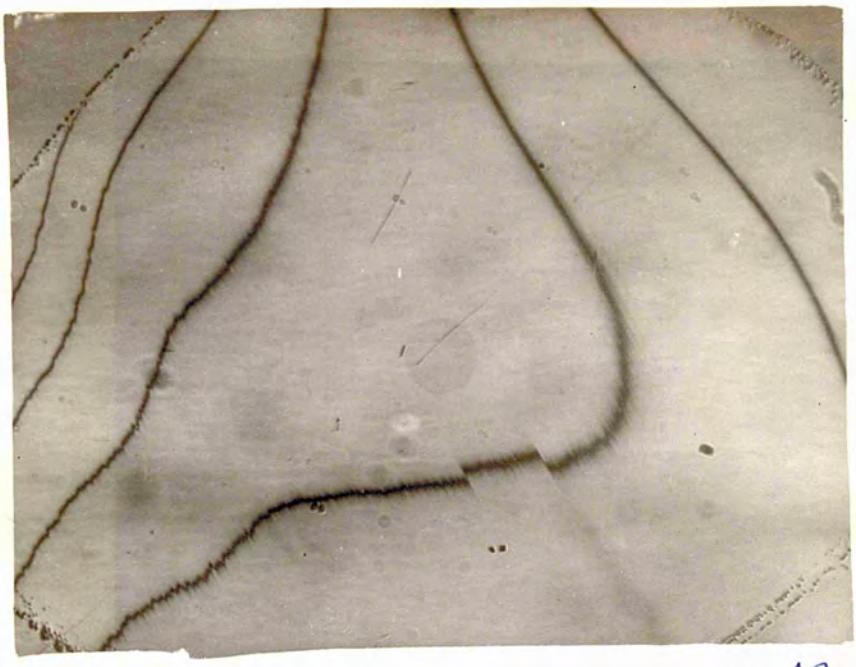

Fig. 199. x 19.

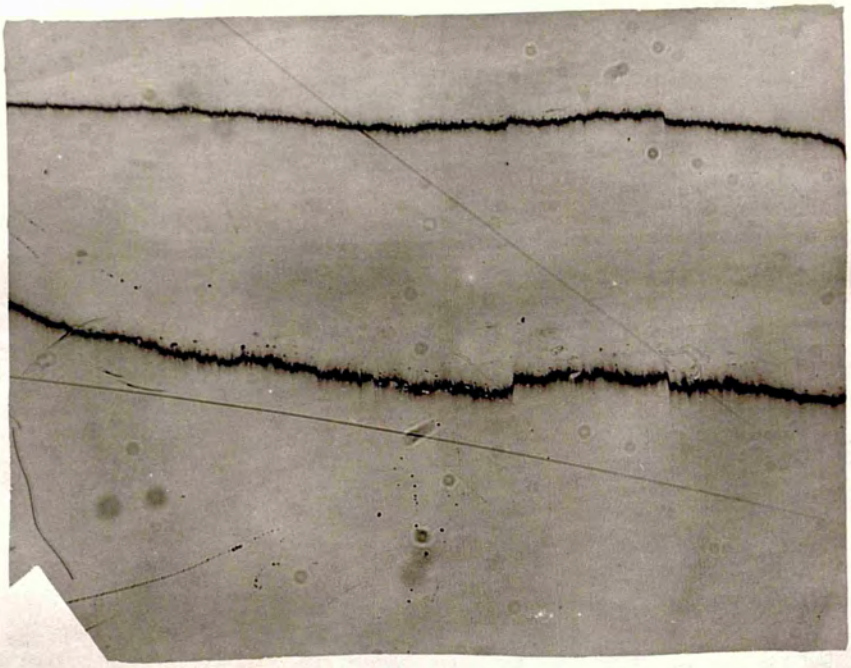

Fig. 200. x 35.

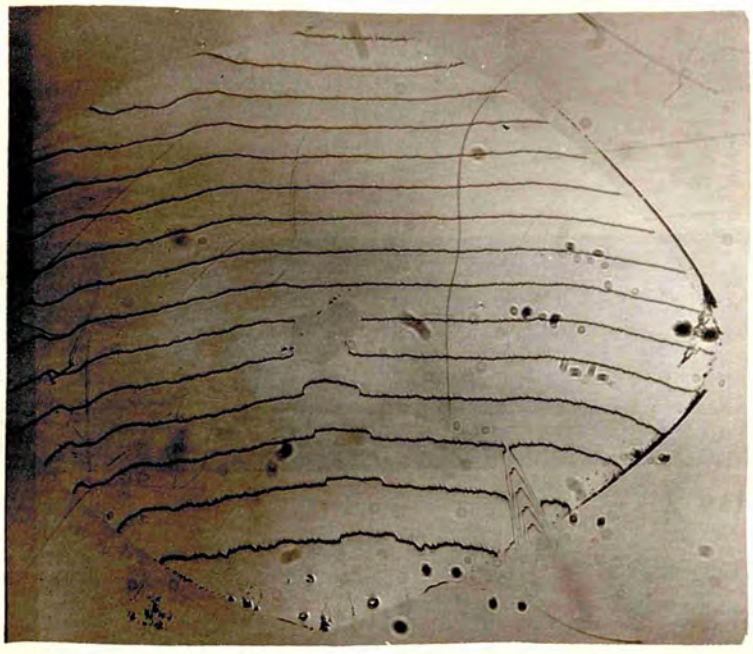

Fig. 201. x 9

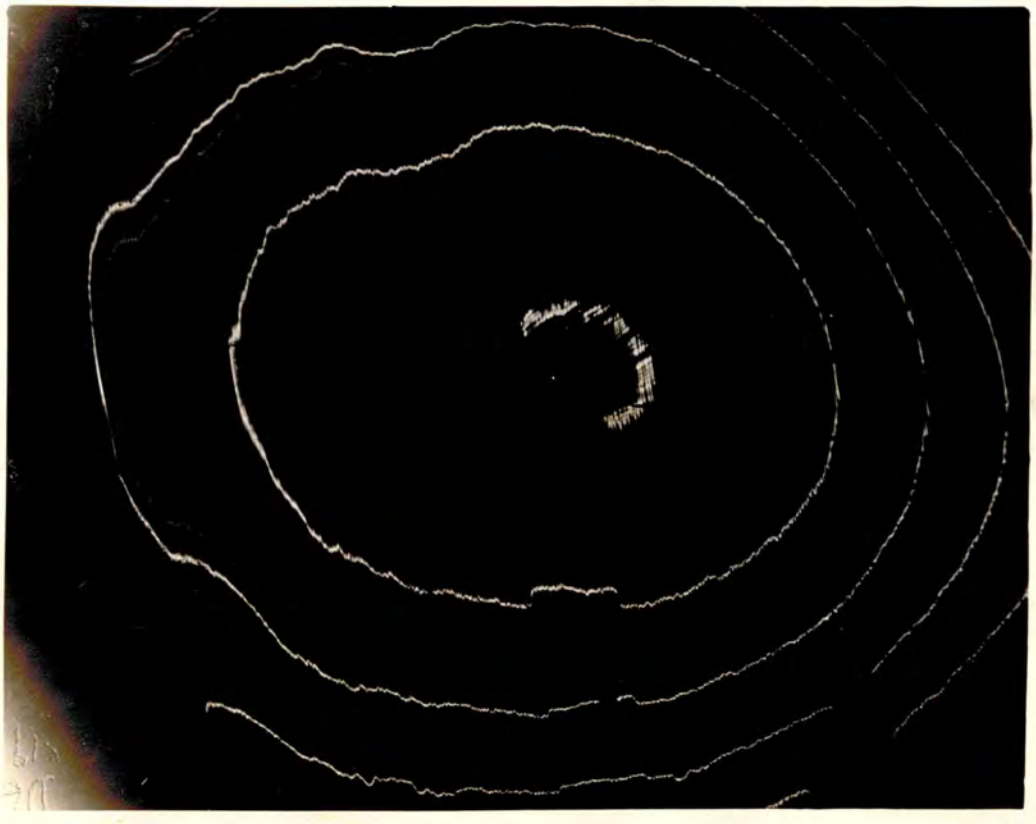

Fig. 202. x 19.

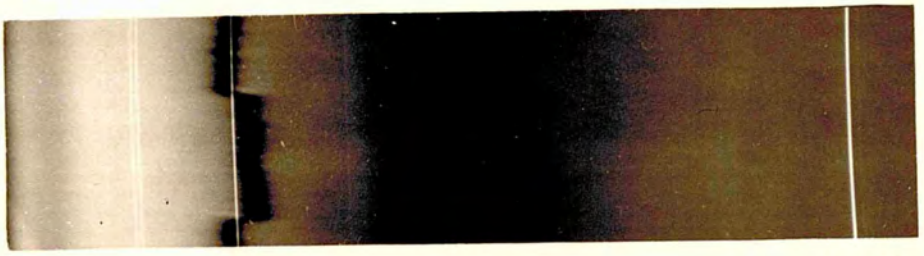

Fig. 203(a). ×27.

Fig. 203(b). ×27.